RNA import into mitochondria of human cells : large-scale identification and therapeutic applications

Damien Jeandard

UNIVERSITÉ DE STRASBOURG

ÉCOLE DOCTORALE DES SCIENCES DE LA VIE ET DE LA SANTE

UMR7156 Génétique Moléculaire Génomique Microbiologie

THÈSE présentée par :

Damien JEANDARD

soutenue le : **1 février 2019**

pour obtenir le grade de : **Docteur de l'Université de Strasbourg**
Discipline/ Spécialité : Aspects moléculaires et cellulaire de la biologie

Import d'ARN dans les mitochondries de cellules humaines : identification à grande échelle et applications thérapeutiques

THÈSE dirigée par :
Mme. ENTELIS Nina Docteur, Université de Strasbourg

RAPPORTEURS :
M. BARREY Eric Docteur, INRA, Jouy en Josas
Mme. RÖTIG Agnès Docteur, IMAGINE, Paris

AUTRE MEMBRE DU JURY :
M. GIEGE Philippe Docteur, Université de Strasbourg

INVITE :
M. SMIRNOV Alexandre Docteur, Université de Strasbourg (co-encadrant de thèse)

Remerciements

En premier lieu, je souhaite remercier les membres de mon jury, les docteurs Agnès Rötig, Eric Barrey et Philippe Giegé, pour avoir gentiment accepté d'évaluer mon travail de thèse.

Je remercie aussi toute les personnes qui m'ont aidé durant mon travail de thèse et qui ont contribué à l'accomplissement de ce manuscrit.

Je tiens tout d'abord à remercier Ivan Tarassov et Nina Entelis de m'avoir accueilli dans leur équipe, d'abord lors de mon stage de master et ensuite pour la réalisation de ce projet de thèse. Je les remercie tous deux pour leurs conseils et gentillesse. Je les remercie aussi de m'avoir fait confiance et offert si souvent l'opportunité de participer à des congrès pour présenter mes résultats.

Je remercie tout particulièrement ma directrice de thèse Nina Entelis, ainsi que Alexandre Smirnov, pour avoir guidé mon travail grâce à leurs nombreux conseils et leurs critiques constructives, pour le temps qu'ils m'ont consacré et pour leur patiente. Je les remercie aussi pour leur précieuse aide lors de la préparation de ce manuscrit. Merci pour tout ce que vous m'avez apporté et tout ce que vous m'avez appris.

Je remercie Anna pour avoir eu la gentillesse de réaliser des expériences de microscopie pour moi mais aussi pour sa sympathie et son enthousiasme. Merci aussi à Benoît pour ses questions, ses conseils et ses remarques avisées. Merci à Diana, pour nos discussions scientifiques ou non, pour ces courtes leçons de russes et à qui je souhaite bonne chance dans la poursuite de son projet.

Merci Anne-Marie pour ton aide inconditionnelle, ta bonne humeur, tes encouragements et pour avoir toujours été à l'écoute. Merci aussi d'avoir été là pour moi dans les situations les plus improbables, comme ce fameux jour sur la péniche. Je suis heureux d'avoir eu la chance de partager une place dans ton bureau et d'avoir été témoin de tes éclats de rire quotidiens.

Merci à toi Romuald, tout d'abord pour m'avoir encadré durant mon stage et ensuite pour m'avoir constamment encouragé et avoir eu confiance en mes capacité lorsque que moi-même j'en doutais. Merci aussi pour toutes nos discussions et nos réflexions. Surtout, je ne te remercierai jamais assez de m'avoir autorisé à emprunter

tes pipettes, en sachant que tu ne les reverrais peut être jamais… ;-). Mais s'il y a une chose pour laquelle je dois te remercier, c'est d'avoir été, plus qu'un collègue, un modèle.

Merci aussi à tous les stagiaires, que j'ai encadré ou non. Merci à Akira, Cyriac, Darya, Laurine, Lena, Mathilde, Michaele, Pierre, Romane et Victor pour tous ce qu'ils m'ont apporté, tant sur le plan scientifique que personnel.

Enfin, je remercie mes parents et ma sœur qui m'ont toujours soutenu dans toutes mes décisions. Merci aussi à mes amis d'avoir été la dans les moments plus difficiles. Merci notamment à Noémie, Lauriane et bien entendu Thomas.

Puisqu'il me serait difficile de remercier toute les personnes sans qui je n'aurais pu mener cette thèse à son terme, je remercie aussi ici tous ceux et celles que j'aurais pu oublier.

Table of content

List of figures

List of tables

I. Introduction

I.A. Organization and function of mitochondria

I.A.1. Mitochondria are essential organelles

I.A.1.1. Structure and dynamics of mitochondria

Mitochondria are organelles found in almost every eukaryote and commonly known as the “powerhouses of the cell” due to their major role in energy production. Under electron microscopy, they appear as round or elongated compartments delimited by two lipid bilayer membranes which delimit individual sub-compartments, the internal mitochondrial matrix and the intermembrane space (IMS). The outer mitochondrial membrane (OMM) faces the cytosol and contains specific proteins and channels to facilitate transport of diverse molecules to and from the mitochondrial matrix or membranes. The inner mitochondrial membrane (IMM) folds and protrudes into the matrix to from cristae. **(Figure 1A) (Palade, 1953; Sjostrand, 1953).**

Mitochondria are usually represented as isolated “bean-shaped” particles lying in the cytosol, however their shape, size and organization vary greatly in living cells. Mitochondria undergo frequent events of fusion and fission. They can form large dynamic interconnected networks spreading all over the cells **(figure 1B) (Westermann, 2010)**. Elongated mitochondria are often observed in metabolically active cells, since the fusion can improve the efficiency of mitochondrial functions through sharing of components and gene products. In contrast, quiescent cells present more isolated mitochondria. Fission, or division, is required for proliferation of mitochondria, quality control to eliminate non-functional organelles and mobility along cytoskeletal tracks to ensure correct distribution of mitochondria throughout the cell. Hence, the mitochondrial structure and dynamic adapt in response to changes in physiological conditions in order to maintain correct activity where it is needed, depending on cell type and developmental stages **(Scorrano, 2013).** Recent studies showed that mitochondria can even be transferred from healthy cells to injured or mitochondrially deficient cells in culture in order to compensate the loss of mitochondrial functions. **(Berridge *et al.,* 2016; Sinha *et al.,* 2016)**. However, this seems to be a rare event *in organismo* and the mechanisms allowing for such transfer are not completely understood.

A

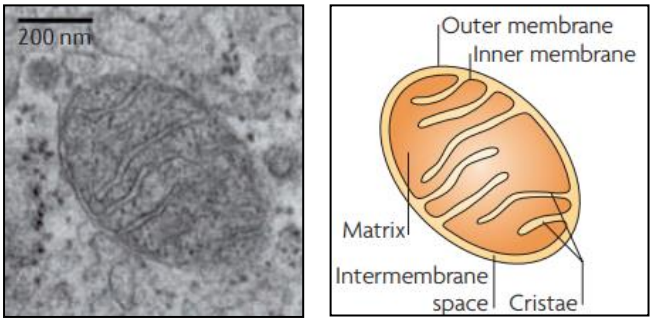

B

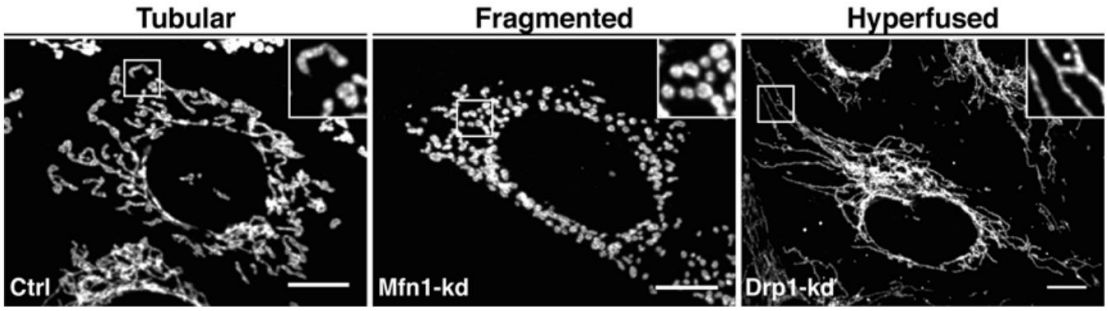

Figure 1. Mitochondrial structure and dynamic.

A) Transmission electron microscopy image of an isolated mitochondrion in ultrathin sections of human fibroblast (left) and its schematic representation (right). Adapted from **(Westermann, 2010)**. **B)** Confocal microscopy images of mousse embryonic fibroblasts labelled with an antibody against an outer-membrane protein (TOM20). Mitochondrial network in physiological conditions is usually composed of tubular mitochondria (ctrl), knockdown of a fusion protein (Mfn1-kd) induces fragmented and isolated mitochondria while knockdown of a fission protein (Drp1-kd) induces hyperfused long mitochondria. Scale bars: 10µm. Adapted from **(Tilokani *et al.*, 2018)**.

I.A.1.2. Mitochondrial functions

In most eukaryotic cells, more than 90% of energy is produced in the form of ATP during the oxidative phosphorylation taking place in mitochondria. This process relies on the “pumping” and accumulation of protons in the IMS by the electron transport chain (ETC), also known as the respiratory chain, composed of four enzymatic complexes located in the IMM. The accumulation of protons in the IMS generates an electrochemical gradient, or membrane potential, between the IMS and the matrix. Protons are then released into the matrix at the level of the F_0-F_1 ATP synthase, also located in the inner membrane and often referred to as the fifth complex of the respiratory chain **(Figure 2)**. ATP synthase uses the free energy of the proton flux to generate ATP from ADP and inorganic phosphate inside the matrix **(Rich and Marechal, 2010)**.

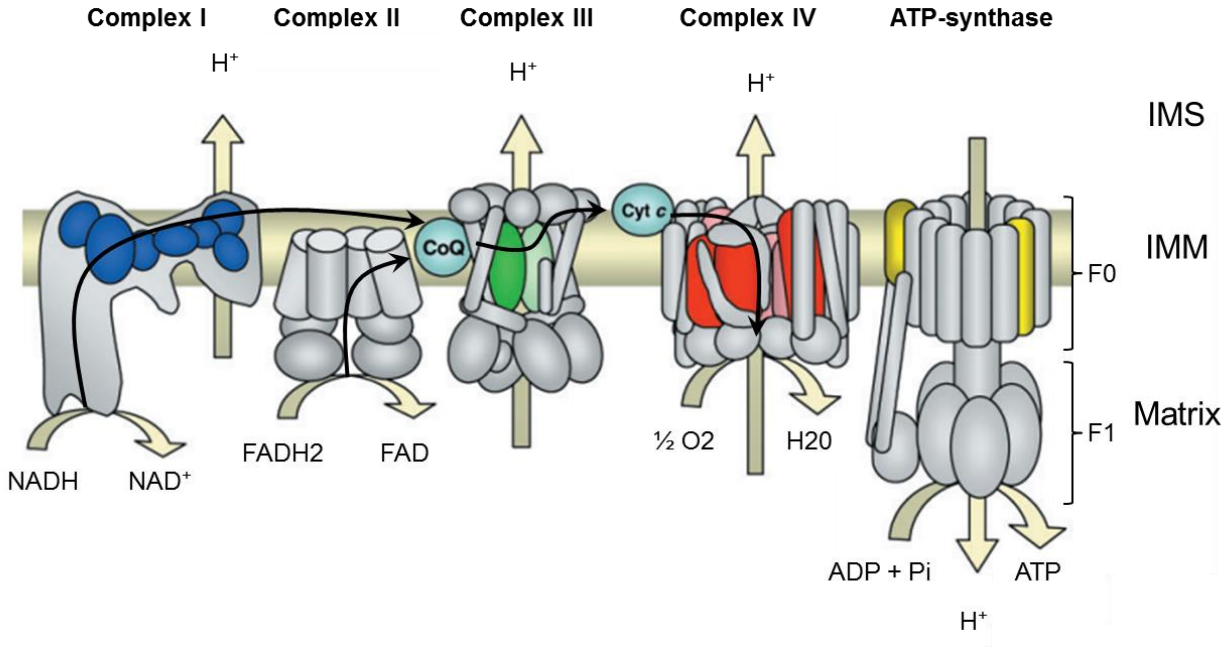

Figure 2. Respiratory chain complexes.

Schematic representation of the four respiratory chain complexes and the F_0-F_1 ATP synthase. Black arrows indicate the path of the electrons along the four complexes. Large beige arrows indicate the transfer of protons across the IMM. Subunits encoded by the mitochondrial genome are highlighted in different colors. Pi: inorganic phosphate. Cyt c: cytochrome c; CoQ: coenzyme Q;. Adapted from **(Zeviani and Di Donato, 2004)**.

Electrons are delivered to the respiratory chain during the oxidation of two electron carrier cofactors, NADH and FADH2, at the level of complex I (NADH dehydrogenase) and complex II (succinate dehydrogenase). Electrons are then transported to coenzyme Q (CoQ) by iron-sulfur clusters. Reduced CoQ can diffuse in the inner membrane to contact complex III (cytochrome c reductase) and transfer the electrons to cytochrome c in the IMS. The complex IV (cytochrome c oxidase) will ultimately use the electrons to reduce oxygen into water. The transport of electron induces the simultaneous translocation of protons across the membrane at the level of complexes I, III and IV **(Efremov *et al.*, 2010)**.

Most of the electron carrier cofactors used to power the proton pump originally come from the Krebs, or tricarboxylic acid (TCA), cycle taking place in the matrix (**Figure 3**). Through 8 enzymatic steps, oxaloacetate and acetyl-coA are converted into citrate and progressively oxidized back to oxaloacetate while electrons removed during this process are used to regenerate NADH and FADH2 **(Osellame *et al.*, 2012)**. In order to sustain the cycle, pyruvate, the product of oxidation of glucose by glycolysis, is imported from the cytosol and can be converted either into acetyl-coA

by pyruvate dehydrogenase or into oxaloacetate by pyruvate carboxylase. Acetyl-coA is also produced during the progressive cleavage of long-chain fatty acids in the process of β-oxidation similarly taking place inside mitochondria **(Eaton *et al.*, 1996)**. Finally, glutamine and branched-chain amino-acids can also be converted by different enzymes into pyruvate, acetyl-coA or other Krebs cycle intermediates **(Spinelli and Haigis, 2018)**.

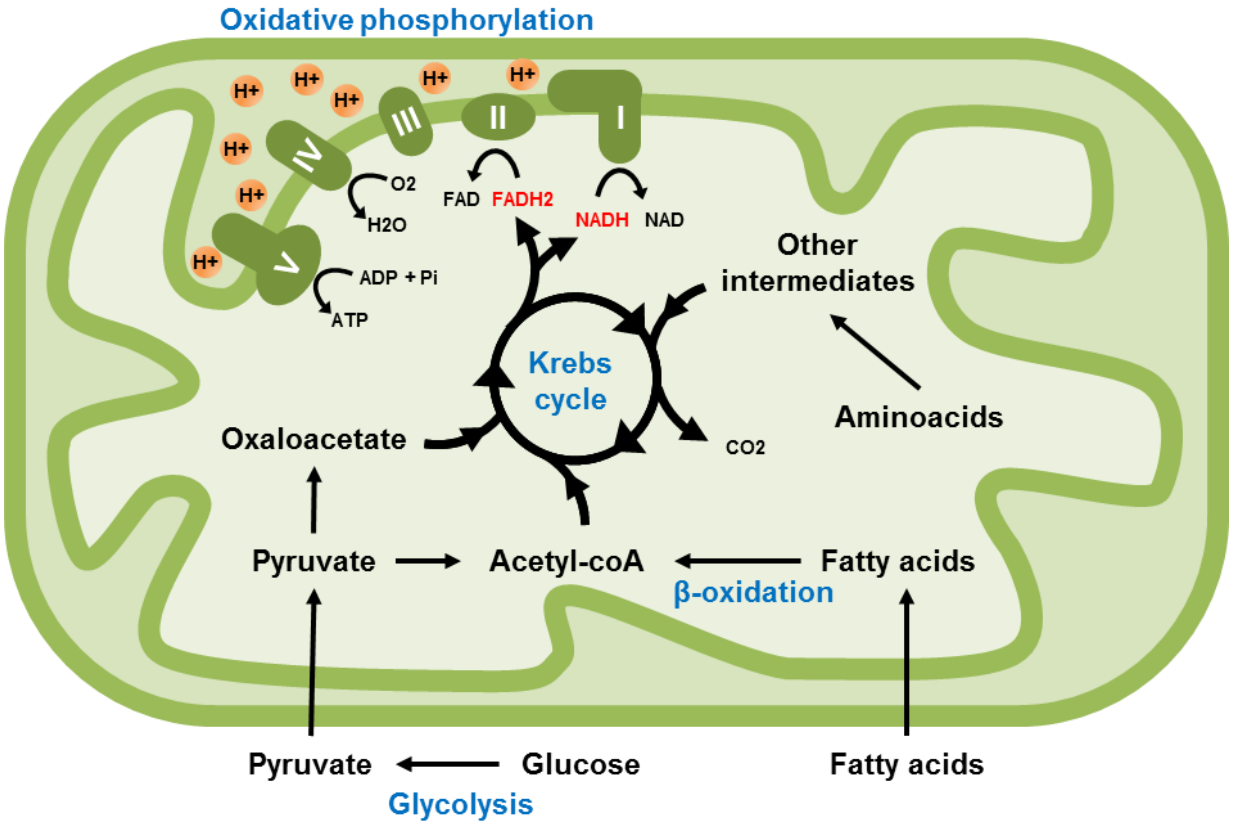

Figure 3. The Krebs cycle fuels the electron transport chain.

Most of NADH and FADH2 (red) supplying the oxidative phosphorylation in electrons comes from the Krebs cycle. Glucose, fatty acids and amino acids can be converted into Krebs cycle intermediates to sustain the cycle. NADH molecules are also product of other processes such as glycolysis and β-oxidation.

Besides their role in energy production, mitochondria are involved in many other cellular functions and the diversity of these functions varies between different eukaryotes and cell types. Mitochondria are essential for the biosynthesis of many metabolites and constituents used by the cells like nucleotides, cholesterol, fatty acids and amino acids **(Spinelli and Haigis, 2018)**. Importantly, mitochondria ensure the synthesis of iron-sulfur clusters, essential cofactors of cellular enzymes including many subunits of the respiratory chain or proteins involved in DNA maintenance and protein translation **(Lill and Muhlenhoff, 2005)**.

All eukaryotic organisms (except one isolated case **(Karnkowska *et al.,* 2016)**) appear to retain the iron-sulfur cluster biogenesis pathway, and it was suggested that in some organisms it is the main reason for keeping the organelle **(Dellibovi-Ragheb *et al.,* 2013)**.

Mitochondria play a role in other various cellular processes like apoptosis, calcium signaling, thermogenesis or removal of toxic products.

Apoptosis, or programmed cell death, is an important mechanism used to control cell proliferation or to remove defective and infected cells. Mitochondria-dependent apoptosis is initiated by the release of cytochrome c, from the IMS to the cytosol. Cytochrome c will then interact with other proteins to form the apoptosome and induce the subsequent cleavage and activation of caspases leading to apoptosis **(Estaquier *et al.,* 2012)**.

Intracellular calcium concentration governs many functions of the cells from cell proliferation to cell death and can be modulated by extracellular signals. Mitochondrial functions are also strongly regulated by calcium signaling. When cellular calcium concentration rises, it enters into mitochondria by the mitochondrial calcium uniporter (MCU) mainly at the level of specific ER-mitochondria contact sites. The increase in calcium concentration promotes the acceleration of Krebs cycle enzymes and subsequently increases ATP synthesis. Mitochondria can also serve as calcium “sink” for the regulation of physiological calcium signaling **(Contreras *et al.,* 2010).**

I.A.2. Mitochondria are chimeric organelles

Many features of mitochondria indicate that these organelles have an endosymbiotic origin **(Yang *et al.*, 1985; Gray *et al.*, 1999; Zimorski *et al.*, 2014)**. First, mitochondria ensure functions that are well conserved among eukaryotes, suggesting they appeared during the same early evolutionary event involving the last eukaryotic common ancestor (LECA). Second, contrary to most organelles, they are delimited by two different membranes: the outer membrane composition is similar to other eukaryotic membranes while the inner membrane shares physical properties and composition with bacterial plasma membranes. For example, cardiolipin is a lipid found in bacterial membranes and it also represents 20% of the IMM, where it is required for the activity and correct localization of several mitochondrial membrane proteins and participates in generation of the membrane potential **(Joshi *et al.*, 2009).** Most importantly, mitochondria contain their own genome, though encoding only between 3 and 67 proteins. Proteins encoded by the mitochondrial genome, as well as nuclear-encoded protein imported into mitochondria, share high similarity with their α-proteobacterial orthologues implying that the mitochondria had a bacterial ancestor **(Timmis *et al.*, 2004)**. These three particular features are notably shared with plants chloroplasts, likely inherited through another endosymbiotic event involving cyanobacteria.

I.A.2.1. Human mitochondrial genome

I.A.2.1.1. Organization of the mitochondrial genome

The human mitochondrial genome is a circular double-stranded DNA present in 100 to 1000 copies per cell depending of the cell type. It is relatively small and compact (16,569 bp), and encodes 13 essential subunits of the oxidative phosphorylation along with 22 tRNAs and 2 rRNAs required for their translation **(Figure 4)**. The gene repartition between the two strands is uneven. The heavy strand (H-strand), named for its high proportion of purines leading to a higher density, contains most of the protein-coding genes, 14 tRNAs as well as the two ribosomal RNAs, 12S and 16S rRNAs. The light strand (L-strand) contains only one protein-coding gene (*MT-ND6*) and a few tRNA genes. Mitochondrial RNAs are transcribed

as long polycistronic transcripts from 3 promoters, situated in the ≈1.1 kb-long non-coding region (NCR), one for the L-strand (LSP) and two for the H-strand (HSP1 and HSP2), and further processed into individual RNA species. Mitochondrial transcription will be further detailed in section I.B.2.1.

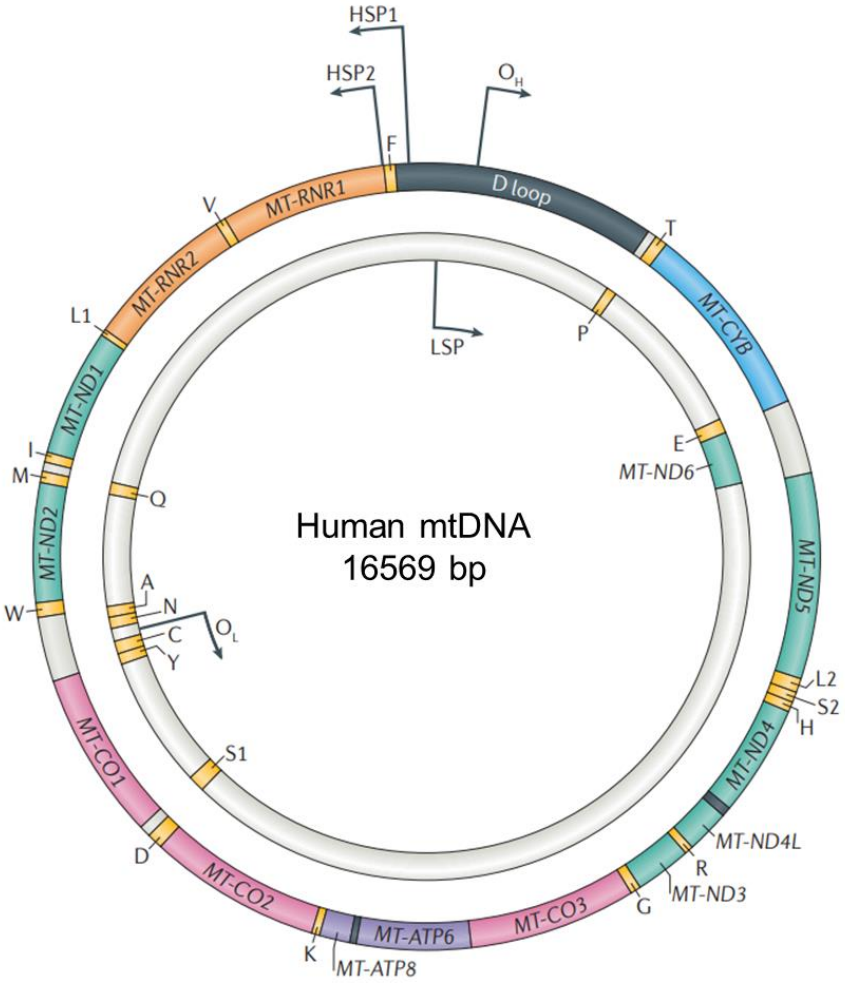

Figure 4. Map of the human mitochondrial DNA.

The H-strand (outer circle), encodes 14 tRNAs, 10 mRNAs (for 12 proteins) and the 2 ribosomal RNAs. The L-strand (inner circle) encodes 8 tRNAs and 1 mRNA. The 3 promoters for transcription (HSP1, HSP2 and LSP) as well as the 2 replication origins (O_H and O_L) are indicated by arrows. The D-loop is part of the NCR and is involved in transcription and replication regulation and mtDNA association with IMM. tRNAs are annotated by their single letter code. *Mt-RNR1*: 12S rRNA. *Mt-RNR2*: 16S rRNA. Adapted from **(Gorman *et al.*, 2016)**.

Mitochondrial DNA (mtDNA) is organized in nucleoids, structures containing 1 or more mtDNA molecules **(Cavelier *et al.,* 2000; Brown *et al.,* 2011)** which ensure DNA compaction and association with several proteins involved in its replication, expression and maintenance. These include the mitochondrial single-strand binding protein (mt-SSB) which coats and protects single-stranded DNA regions, the DNA polymerase γ (POLG), the Twinkle helicase involved in replication and transcription and translation factors such as the mitochondrial RNA polymerase (POLRMT) and some mitochondrial ribosomal proteins **(Bogenhagen, 2012).** Contrary to the nuclear genome, the compaction of mtDNA is not ensured by histone proteins. Instead, the main protein involved in nucleoid formation is the mitochondrial transcription factor A (TFAM) **(Kukat *et al.,* 2015).** TFAM covers the mtDNA, with approximately 1 subunit per every 16-17bp, and is sufficient to induce the formation of nucleoid *in vitro* **(Figure 5)**. Several studies showed that mitochondrial nucleoids are maintained close to the mitochondrial membranes by the AAA+ ATPase protein (ATAD3). This localization may compartmentalize transcriptional and translational events close to IMM in order to facilitate the incorporation of the newly synthesized proteins into the membrane **(Brown *et al.,* 2011; He *et al.,* 2012).**

The presence of a second genome in the cells implies that every DNA-related function, from replication to translation, as well as DNA maintenance and repair, must occur both in the nucleus and in mitochondria. However, the corresponding mitochondrial mechanisms often differ greatly from those used for the nuclear genome.

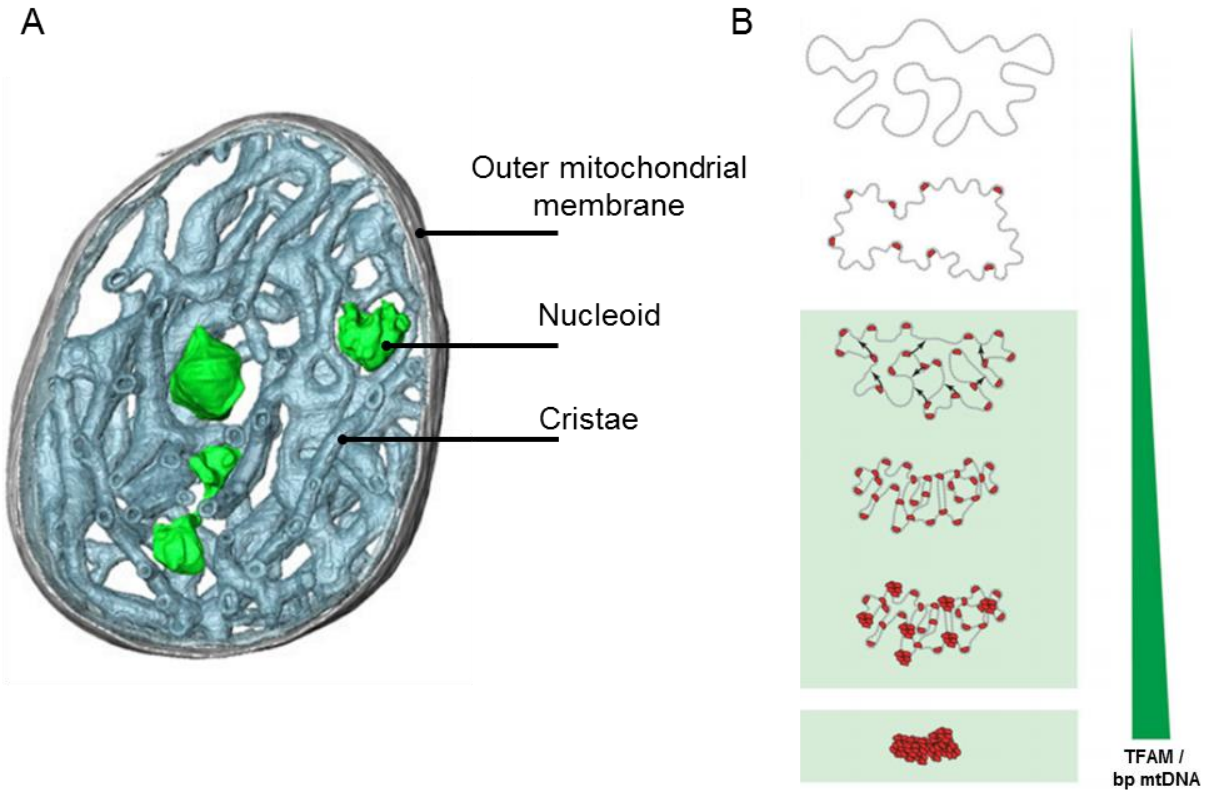

Figure 5. MtDNA is organized in nucleoids.

A) Cryo-electron tomography of a bovine heart mitochondrion. Green: compact mtDNA nucleoids; Blue: cristae; Gray: outer mitochondrial membrane. **B)** Schematic representation of how TFAM (red) covers the mtDNA in a concentration-dependent manner and induces the mitochondrial genome compaction by forming bridges between neighboring mtDNA strands (black arrows). Adapted from **(Kukat *et al.*, 2015)**

I.A.2.1.2. Mechanisms of mitochondrial DNA replication

The mitochondrial replisome contains the DNA polymerase γ, a heterotrimer composed of one catalytic subunit (POLG1) and 2 accessory subunits (POLG2) required for improved processivity and rate of replication **(Yakubovskaya *et al.*, 2006)**. Other major proteins are the helicase Twinkle, essential to unwind DNA during the progression of the replication fork and the mt-SSB protecting the parental single-stranded DNA during the replication. To initiate replication, POLG needs RNA primers created by POLRMT through aborted transcription events. These primers are subsequently removed by specific ribonucleases, including RNase H1, before the

DNA ligase III can ligate the ends of the newly synthetized DNA strands **(Al-Behadili *et al.*, 2018).**

Replication and gene expression are mainly regulated at the level of the NCR **(figure 6)** which contains 2 transcription starting sites, the light strand promoter (LSP) and the heavy strand promoter 1 (HSP1) as well as the origin of replication of the H strand (O_H). The NCR also contains a Termination Associated Sequence (TAS) ~100 nucleotides downstream of O_H which induces frequent premature arrest of the replication. This leads to the formation of a small DNA fragment named 7S DNA which hybridizes to the L strand, displacing the H strand and forming a D-loop. While the D-loop is required for replication regulation, its exact role remains unclear **(Gustafsson *et al.*, 2016)**.

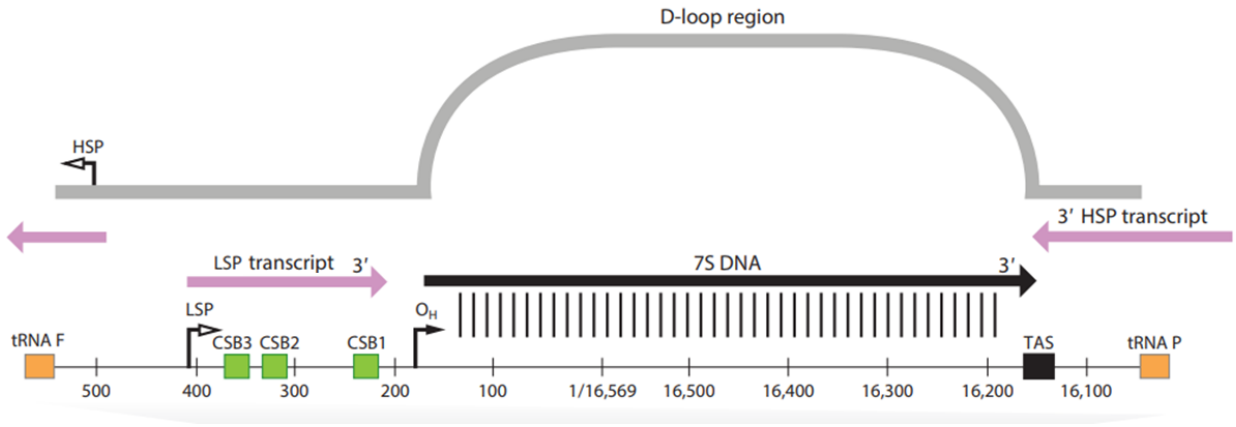

Figure 6. The non-coding region of human mtDNA.

The non-coding region, a ~1.1-kb sequence located between the genes for $tRNA^{Phe}$ and $tRNA^{Pro}$, plays a major role in regulation of replication and transcription. It contains the promoters for the H strand (HSP) and L strand (LSP) as well as the replication origin of the H strand (O_H). CSB1, CSB2 and CSB3 are conserved sequence blocks. Interruption of L strand transcription at CSB2 eventually results in formation of the RNA primer required for the replication of the H strand. The termination associated sequence (TAS) induces frequent premature arrest of the H-strand replication leading to the formation of 7S DNA. Association of 7S DNA with mtDNA results in the displacement-loop (D-loop). TAS is also involved in the transcription termination of the full length HSP transcripts. Adapted from **(Gustafsson *et al.*, 2016)**.

The mechanism by which the human mtDNA replicates is still under debate since at least three different models have been proposed **(Pohjoismaki and Goffart, 2011) (Figure 7)**. The strand-asynchronous, or strand displacement model, was the first described **(Clayton, 2003)**. In this model, the replication starts with the synthesis of the H strand from its origin of replication O_H and the replication fork moves unidirectionally. The single parental H strand is then progressively displaced and protected by mtSSB **(Miralles Fuste *et al.,* 2014).** The replication origin of the L strand (O_L) is exposed when the replication fork reaches approximately 2/3 of the mtDNA. When released, the O_L ssDNA region folds into a stem-loop structure recognized by POLRMT to produce the second RNA primer and the replication of the L-strand can start.

The second model, Ribonucleotide Incorporation ThroughOut the Lagging Strand (RITOLS), is very similar except that the displaced single-stranded DNA would be coated with RNA instead of mtSSB **(Yasukawa *et al.,* 2006)**. This model was suggested after the observation of RNA-DNA hybrids as replication intermediates.

The third model resembles the conventional strand-coupled DNA synthesis where both the lagging and the leading strands are produced simultaneously from another region, Ori Z, located between O_L and O_H. Under this model, the replication forks move bidirectionaly with the formation of Okazaki fragments on the lagging strand **(Bowmaker *et al.,* 2003)**. It is probable that different mechanisms can actually be used depending on the cell type or energetic state **(Herbers *et al.,* 2018).**

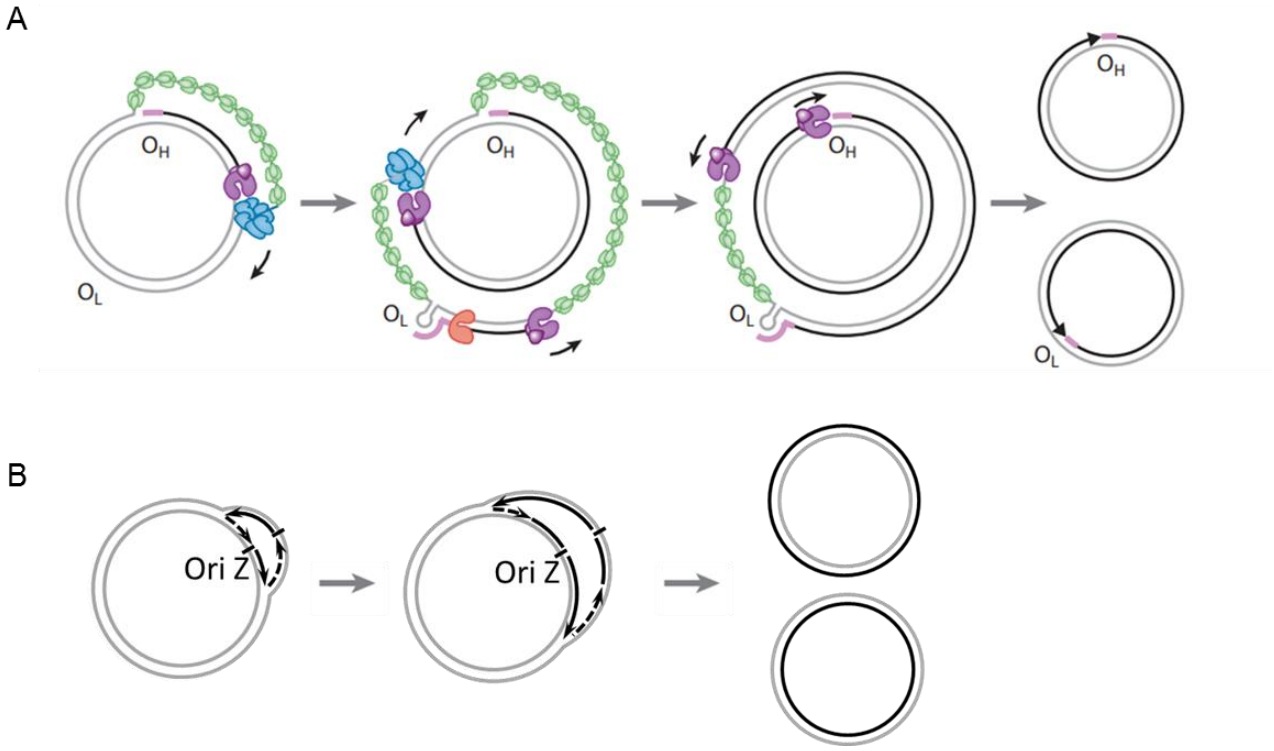

Figure 7. Mitochondrial DNA replication models.

A) Strand-displacement asynchronous model. Replication of the H strand initiates at $O_{H.}$ The TWINKLE helicase (blue) participates in the displacement of the parental strand (grey) while DNA polymerase (purple) progressively synthesizes the new strand (black). The displaced parental strand is then either protected by association with mtSSB (green) or, according to the RITOLS model, by RNA. When the H-strand replication machinery passes O_L, a stem-loop structure is formed in the displaced H-strand and the RNA polymerase (orange) synthesize the primer required to initiate the L-strand replication. Adapted from **(Gustafsson *et al.*, 2016)**. **B)** The synchronized model. The replication fork moves bidirectionally from an alternative origin of replication (Ori Z) with formation of Okazaki fragments on the lagging strands (dotted lines).

I.A.2.1.3. Mitochondrial DNA heteroplasmy, repair and elimination

Since cells contain several copies of mitochondrial genomes, one can expect that some mutations can be tolerated as long as enough wild-type molecules remain to ensure the expression of the correct genes. Indeed in human cells, mutated and wild-type mtDNA molecules can coexist, a property called heteroplasmy. The observation that mtDNA had a mutation rate 10 to 20 times higher than nuclear DNA

first lead to the hypothesis that there were very few repair systems. However, many repair pathways have been further identified in mitochondria.

First, POLG possesses an efficient 3'-to-5' exonuclease activity to correct errors during replication. The removal of altered bases by base excision repair (BER) and the repair of single-strand breaks (SSBR) have also been demonstrated **(Bohr *et al.,* 2002)**. Some actors of these pathways have been identified, such as mitochondrial DNA glycosylases required for the recognition and cleavage of the damages as well as POLG and DNA ligase III to fill-in the removed nucleotides and ligate the strands. While Microhomology Mediated End Joining (MMEJ) was proposed as the main mechanism for the repair of double-strand breaks (DSB) **(Tadi *et al.,* 2016)**, such a mechanism does not seem to be efficient and seems to be rather unfaithful by inducing small deletions of mtDNA after repair. In fact, it has been shown that DSB-containing molecules are preferentially degraded to avoid deletions **(Moretton *et al.,* 2017)**. The degradation seems to be performed, at least partially, by the exonuclease activity of the mitochondrial DNA polymerase itself **(Nissanka *et al.,* 2018).**

I.A.2.2. Cytosolic-mitochondrial transport of molecule

Many metabolites (pyruvate, nucleotides, coenzymes …) and ions must be translocated across the mitochondrial membranes. The OMM contains multiple voltage-dependent anion channels (VDAC) which make it permeable to molecules smaller than 5 KDa. On the other hand, the inner membrane is very impermeable and specific membrane mitochondrial carriers and transporters are required to allow the selective and controlled passage of molecules such as ADP-ATP carrier **(Palmieri and Pierri, 2010)**.

In all groups of eukaryotes, some RNAs are also imported in the mitochondria and usually participate in the mitochondrial genome expression **(Sieber *et al.,* 2011a)**. However, contrary to protein mitochondrial import (see below), the mechanisms involved in RNA import in human mitochondria are less understood and will be discussed more in detail in section I.B.3.

Most mitochondrial genes have been progressively transferred to the nuclear genome since the original endosymbiosis **(Timmis *et al.,* 2004)** and human mtDNA retained only a few genes required for the synthesis of respiratory chain subunits.

However, mitochondria require more than 1500 proteins to ensure all their functions. Those proteins need to be imported inside mitochondria through different complexes present in both the outer and inner membranes. Moreover, cytosolic mRNAs encoding mitochondrial proteins may be translated in the vicinity of OMM to facilitate their import **(Matsumoto *et al.,* 2012; Williams *et al.,* 2014)**.

Five different pathways contribute to the import of nuclear-encoded mitochondrial proteins **(Figure 8)**. Each of them recognizes a different targeting signal present in the protein and can target it to specific mitochondrial localization. The complex of the translocase of the outer membrane (TOM) is the “entry gate” for four of the five pathways. It is composed of several receptor proteins that identify the targeting signal and a β-barrel protein of the VDAC family which form a channel for the passage of the proteins across the outer membrane. After being recognized by TOM, the proteins are redirected to other complexes according to their final destination **(Wiedemann and Pfanner, 2017)**.

The main import pathway requires a pre-sequence targeting signal of 15 to 70 aminoacids. This sequence, usually found on the N-terminus, forms an amphiphilic helix and is present in the majority of pre-proteins destined for the matrix and in many inner-membrane proteins **(Vogtle *et al.,* 2009)**. After the recognition of the hydrophobic surface of the pre-sequence helix and the passage through the TOM complex, proteins are delivered to the translocase of the inner membrane 23 (TIM23). The binding of the pre-sequence activates the TIM23 channel by a conformational change dependent of the membrane potential **(van der Laan *et al.,* 2007)**. From there, the translocation into the matrix is driven by the pre-sequence translocase-associated motor (PAM) located on the matrix side of the inner membrane, consuming ATP in the process. If the protein contains an additional hydrophobic sorting signal, the translocation will stop inside TIM23 and the protein will be laterally released in IMM. In the end, the pre-sequence is cleaved by the mitochondrial processing peptidase (MPP) present in the matrix and, in some cases, the pre-proteins are further processed by mitochondrial intermediate peptidases (MIPs).

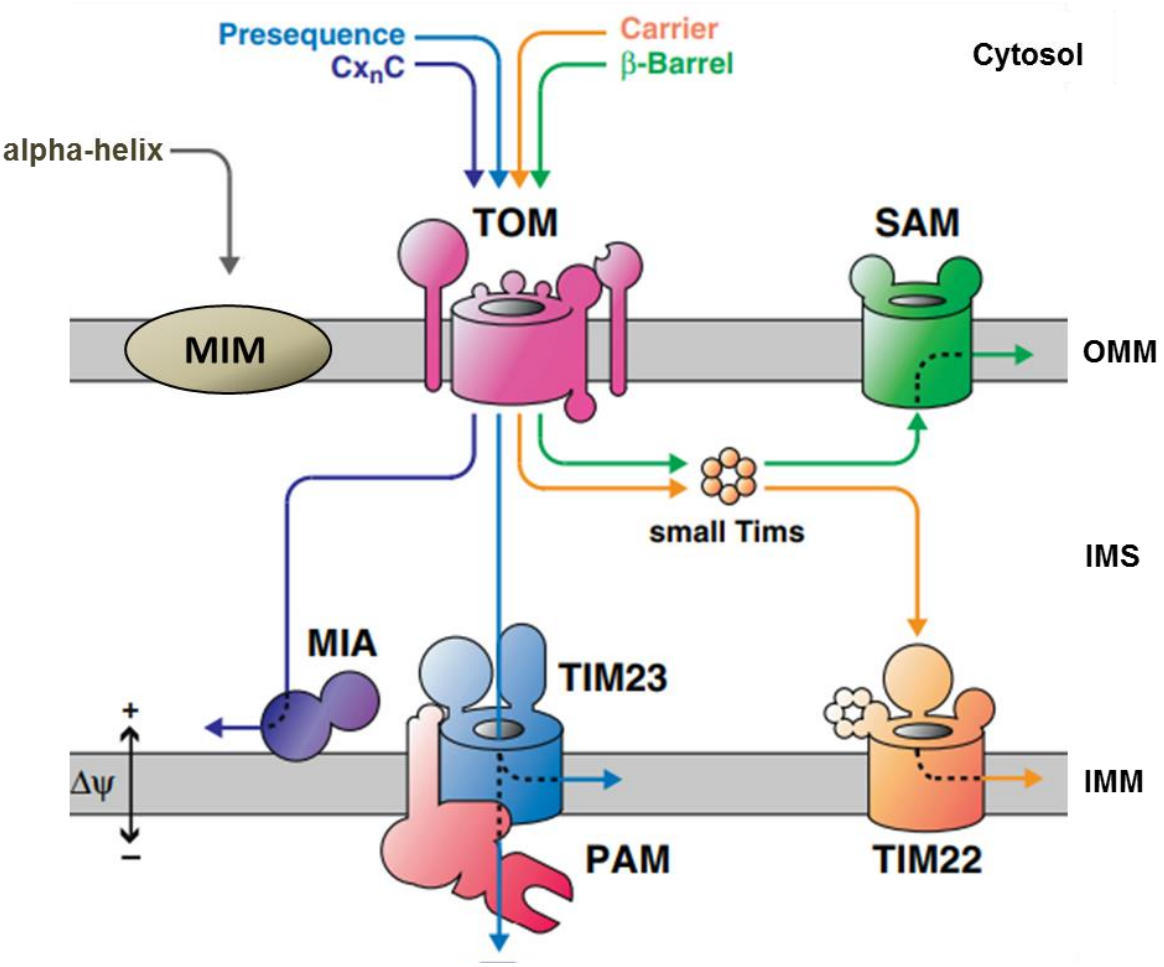

Figure 8. Mitochondrial protein import pathways.

Schematic representation of mitochondrial protein import pathways. Different targeting signals direct nuclear encoded precursor proteins on specific routes to their final mitochondrial locations. The translocase of the outer membrane (TOM) is the main complex for protein translocation through OMM. Pre-sequence-containing proteins will be targeted to TIM23 and either inserted in IMM or translocated in the matrix. The pre-sequence is then cleaved by the mitochondrial processing peptidase (MPP). Carrier proteins of IMM are transported with the help of the small TIMs to TIM22 and inserted in IMM. Proteins with a cysteine motif (CxnC) are taken in charge by the mitochondrial import and assembly (MIA) machinery and released in IMS. β-barrel-containing proteins will be inserted in OMM by the sorting and assembly machinery (SAM). Finally, proteins with α-helical transmembrane segments or a single N-terminal α-helix are directly inserted in OMM by the mitochondrial import (MIM) complex. ΔΨ : Membrane potential across IMM. Adapted from **(Dudek *et al.*, 2013)**

Other proteins destined for the inner membrane are mainly mitochondrial carriers and proteins with several transmembrane domains that do not contain a pre-sequence. Instead they harbor internal import signals recognized by TOM receptors. These proteins being highly hydrophobic, their redirection through the hydrophilic inter-membrane space to the specialized TIM22 complex is mediated by chaperone proteins called small TIM chaperones **(Koehler *et al.,* 1998)**. Similar to TIM23-directed proteins, the lateral release of proteins in IMM by the TIM22 channel requires the mitochondrial membrane potential.

Most proteins destined for the IMS harbor characteristic motifs containing cysteine residues. After their passage through the TOM complex, the mitochondrial import and assembly (MIA) machinery present in the IMS catalyzes the formation of intramolecular disulfide bonds between the cysteines. This promotes the conformational stabilization of the proteins and release in IMS. **(Wrobel *et al.,* 2013; Longen *et al.,* 2014).**

Finally, proteins can be inserted in OMM by two different pathways. The TOM complex recognizes a C-terminal structure in β-barrel-containing proteins and translocates them in IMS where they are handed over to the small TIM chaperones. The incorporation into the membrane is achieved by the sorting and assembly machinery (SAM) located in OMM **(Kutik *et al.,* 2008).** Proteins with α-helical transmembrane segments or a single N-terminal helix are taken in charge by the mitochondrial import (MIM) complex. The mechanisms of this pathway are not fully understood, but TOM complex does not seem to play a decisive role here, and it was even postulated that some proteins do not require any complexes to be inserted in OMM **(Wiedemann and Pfanner, 2017).** Moreover, some mRNAs are targeted to the mitochondrial surface and the involvement of TOM and MIM complexes in the co-translational translocation of the corresponding proteins remains unclear **(Eliyahu *et al.,* 2010)**.

I.A.2.3. Mitochondrial pathologies

I.A.2.3.1. Mitochondria are involved in diverse cellular disorders

Mitochondria are involved in many essential metabolic pathways and their dysfunctions can lead to the development of diverse human pathologies.

Mitochondrial disorders are particularly challenging because they can result from mutations of either the nuclear or the mitochondrial genome **(Filosto and Mancuso, 2007)**. Since mtDNA encodes 13 proteins of the electron transport chain and the RNAs required for their synthesis, mtDNA mutations usually induce defects of the respiratory chain function and impaired energy production. Typical symptoms of mitochondrial diseases are myopathy, neurodegeneration, lactic acidosis, gastrointestinal impairments, deafness and blindness and the most frequent pathologies are neuromuscular syndromes because of the high energy requirement of neuronal and muscular tissues **(DiMauro and Schon, 2003)**. Mutations of nuclear genes encoding other respiratory chain subunits or cyto-mitochondrial transport machineries may also induce respiratory chain defects. Moreover, nuclear mutations can affect genes involved in the mitochondrial genome stability, replication and expression **(Rusecka *et al.,* 2018)**. Although the term “mitochondrial disease” often implies only the impairment of the respiratory chain, some neurodegenerative pathologies have been linked to mutations in nuclear genes encoding mitochondrial proteins that are not directly related to respiration **(Filosto *et al.,* 2011)**. For example, mutations in the *PINK1* gene, encoding a kinase participating in regulation of mitochondrial quality control of IMM, affect the PINK1/Parkin pathway involved in mitochondrial dynamics and lead to Parkinson’s disease. Similarly, mutations in the *FXN* gene encoding the mitochondrial protein frataxin, involved in the assembly of iron-sulfur clusters, are responsible for Friedreich’s ataxia. Mitochondrial dysfunctions or deregulations in general have been also associated with other human disorders, such as the metabolic defect **(Auger *et al.,* 2015)**, self-immune diseases **(Walker *et al.,* 2014)**, aging **(Bratic and Larsson, 2013)** and cancer **(Zong *et al.,* 2016)**.

I.A.2.3.2. Pathologies linked to mtDNA mutations

More than 300 different mtDNA pathogenic mutations, affecting about 1 in 10,000 people, have been reported to date **(Gorman *et al.,* 2015)**. Since paternal mtDNA is eliminated during fertilization, mutation inheritance follows a non-mendelian pattern where only maternal mtDNA is transmitted to the child **(Zhou *et al.,* 2016),** except some recently reported cases **(Luo *et al.,* 2018a)**. Symptoms usually appear early in life, with a progressive aggravation which often leads to death. They may be

manifested in a tissue-specific manner but are generally multi-systemic with neuronal and muscular tissues frequently affected.

While some mtDNA mutations are often associated with specific syndromes **(Filosto and Mancuso, 2007)**, the same genetic alteration may results in various phenotypes in different individuals. Indeed, most mutations are recessive and usually heteroplasmic (see section I.A.2.1.3) with a mixture of both mutant and wild-type mtDNA in the same cells. Symptoms often appear when the level of heteroplasmy reaches a pathological threshold, usually 60-90% of mutated mtDNA depending on the mutation, the tissue and the age of the patient **(figure 9)**. Higher levels of mutant mtDNA are often associated with more severe symptoms and different levels of heteroplasmy for the same mutation may lead to various phenotypes **(Picard *et al.,* 2014)**. In addition, heteroplasmy levels may change over time due to random segregation of mitochondrial genomes during mitosis, resulting in daughter cells containing different mtDNA mutation levels **(Craven *et al.,* 2017)**. This mechanism is supposedly at the origin of the radical difference in heteroplasmy that may be observed between a mother and a child. In the germ line, cells divide rapidly inducing a reduction of mtDNA copy number per cells which is not compensated by mtDNA replication. This genetic “bottleneck” associated with random distribution of mtDNA produces cells with relatively few mtDNA molecules and, consequently, highly variable levels of heteroplasmy **(Cree *et al.,* 2008)**.

Alternatively, since the mitochondrial genome normally replicates even in non-mitotic cells, other theories suggest that a replicative advantage of mutated DNA may be involved in increasing heteroplasmy over time, although the mechanisms thereof are not completely understood. For example, smaller mtDNA molecules formed after big deletion events are expected to replicate faster than wild-type mtDNA molecules **(Bradshaw *et al.,* 2017)**.

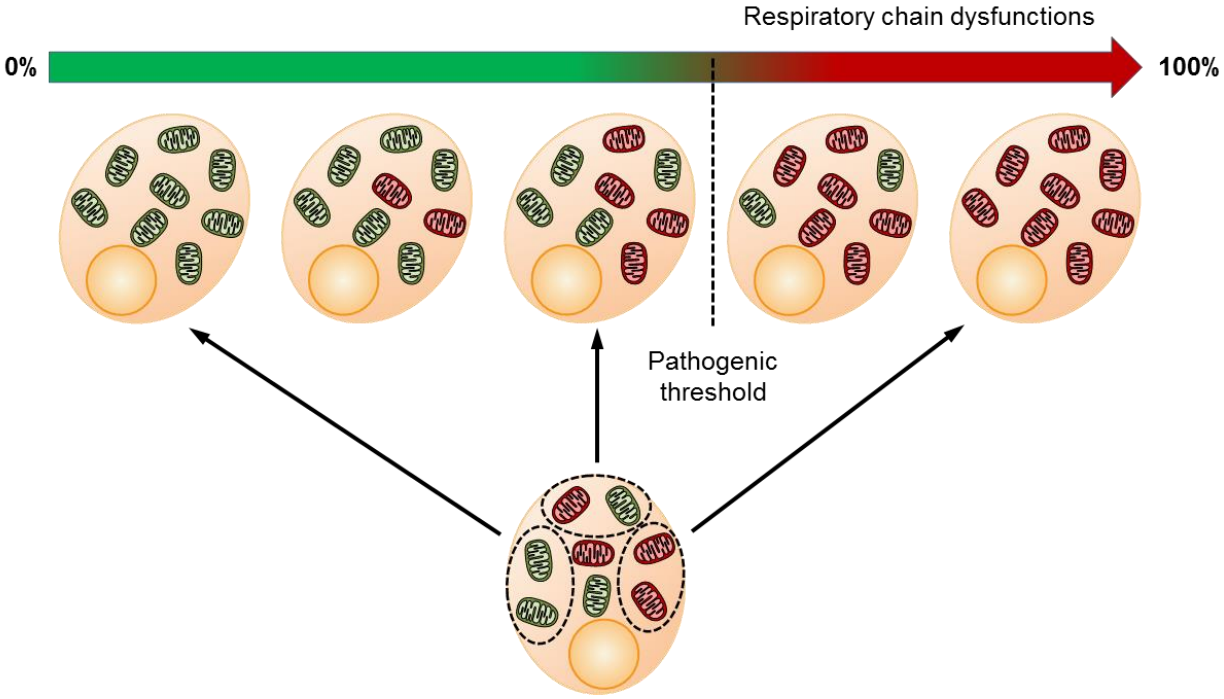

Figure 9. Mitochondrial heteroplasmy.

Within a cell, mutated (red mitochondria) and wild type (green mitochondria) mtDNA molecules can coexist, a property called heteroplasmy. Low levels of heteroplasmy (*i.e*. low proportion of mutated genomes) are usually tolerated. Respiratory chain defects appear when the proportion of mutant mtDNA molecules reaches the pathogenic threshold. Importantly, random segregation of mtDNA during mitosis can lead to modification of the heteroplasmy level in daughter cells in both directions.

I.A.2.3.3. Therapies for mitochondrial pathologies

So far, there is no effective treatment to cure mitochondrial diseases. In the majority of cases, therapies are limited to palliative treatment, though many different approaches are currently used and under development **(Gorman *et al.*, 2016)**. Nutritional supplement cocktails of anti-oxidants and vitamins are frequently administered to increase mitochondrial functions or biogenesis and relieve metabolic stress. In some mitochondrial diseases caused by enzyme deficiency, symptoms can be attenuated by administration of the deficient enzyme, enzyme product or co-enzyme **(Repp *et al.*, 2018)**. In some cases, organ transplantation can be performed but is only temporarily effective due to the multi-systemic nature of most mitochondrial diseases and their rapid progression.

Stimulation of mitochondrial biogenesis, mitochondrial oxidative phosphorylation and even reduction of heteroplasmy seem to be also achievable with specific diets, like high-fat or ketogenic diets, and physical exercise **(Taivassalo and Haller, 2005; Ahola-Erkkila *et al.,* 2010; Frey *et al.,* 2017)**. Those methods seem to be somewhat effective and improve patient conditions, or at least delay the progression of the disease. Recent studies suggest that hypoxia (11% of O_2 instead of approximatively 21% in the atmosphere) may also alleviate the symptoms of mitochondrial disorders linked to the respiratory chain, as it was shown for a mouse model of Leigh syndrome. How hypoxia is beneficial remains unclear but it may trigger a cellular adaptive pathway and prevent damages caused by extensive use of the defective ETC **(Jain *et al.,* 2016)**.

None of the strategies cited previously can remove the primary cause of the mitochondrial disease, i.e. mutation. Extensive research is conducted to develop gene therapies to cure mitochondrial diseases. However, most tools developed for the editing of the nuclear genome are not suitable for the mitochondrial genome, mainly because DNA cannot be efficiently addressed to the mammalian mitochondria. Up to date, possible gene therapy strategies addressing mtDNA mutations can be organized in 3 main categories **(Figure 10)**. The allotopic strategy aims to express the wild-type product of the corresponding mutated mitochondrial gene in the nucleus and then to target it inside mitochondria. The anti-genomic and anti-replicative strategies, on the other hand, tend to specifically eliminate the mutated mtDNAs. All those strategies face the same challenge to import macromolecules inside mitochondria.

Allotopic strategy:

Many attempts have been made to express mitochondrial-encoded proteins from nuclear genes and import them inside mitochondria. Mitochondrial-encoded proteins are believed to be so hydrophobic that their genes could not be transferred to the nuclear genome because they would preferentially be targeted to the endoplasmic reticulum **(Bjorkholm *et al.,* 2017)**. Thus, the allotopic approach remains challenging because of the high hydrophobicity of the mitochondrial-encoded proteins which generally do not reach their expected mitochondrial destination. Nevertheless, this approach was successfully applied to target into mitochondria ATP8 and ATP6 proteins fused to a pre-sequence signal resulting in

rescue of the phenotype due to mutation affecting these two overlapping genes **(Boominathan *et al.*, 2016)**.

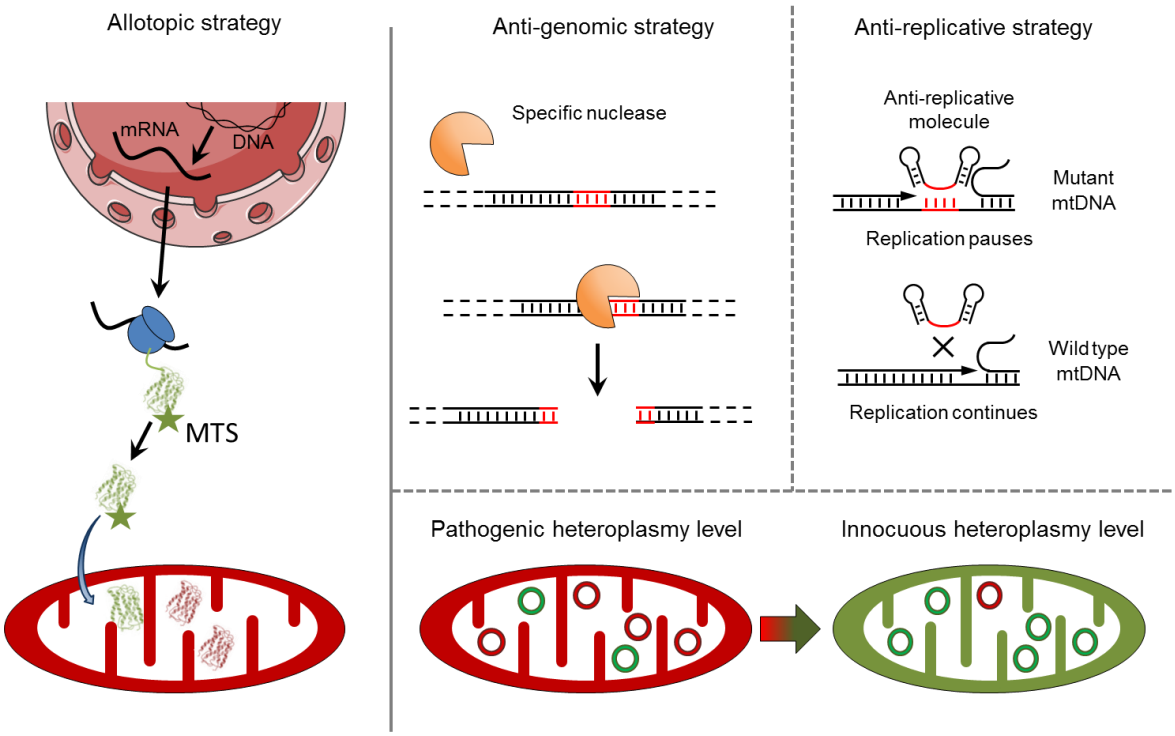

Figure 10. Different gene therapy strategies to cure mitochondrial diseases.

The allotopic strategy aims to re-express the wild-type variant of a mutated mtDNA-encoded protein or RNA from the nucleus and target it to the mitochondria to compensate the defect due to the mutation. This strategy however does not remove the mutation responsible for the pathology. Both the anti-genomic and anti-replicative strategies aim to reduce the level of heteroplasmy below the pathogenic threshold. While the anti-genomic strategy uses nucleases to cut specifically the mutated mtDNA, the anti-replicative strategy targets to mitochondria a molecule that can specifically anneal to the mutated mtDNA and slow down its replication. This confers a replicative advantage to wild-type mtDNA. MTS: Mitochondrial targeting sequence.

Mutations in mitochondrial tRNA genes can also be the cause of pathologies. For example, the G-to-A substitution at the position 3243 of the mitochondrial genome (m.3243A>G) affects the $tRNA^{Leu(UUR)}$ and represents one of the most common pathogenic mtDNA mutations, usually leading to MELAS (myopathy, encephalopathy, lactic acidosis and stroke-like episodes) syndrome **(Manwaring *et al.,* 2007; Gorman *et al.,* 2015)** and mutation in position 8344A>G of $tRNA^{Lys}$ cause a mutation leading to MERRF (myoclonic epilepsy and ragged-red fibers) syndrome. Our team demonstrated that yeast $tRNA^{Lys}_{CUU}$ (tRK1) can be imported into human mitochondria (see section I.B.3) and rescue a defect in human $tRNA^{Lys}$ caused by a mutation leading to MERRF syndrome **(Kolesnikova *et al.,* 2004)**. Similarly, when tRK1 was modified to gain the identity determinant of $tRNA^{Leu(UUR)}$, it could partially rescue the defect due to the common m.3243A>G mutation **(Karicheva *et al.,* 2011).**

Anti-genomic strategy:

The anti-genomic strategy aims to cleave specifically the mutated genomes with nucleases in order to eliminate the mutated mtDNA or at least reduce the level of heteroplasmy below the pathogenic threshold. The main challenge of this strategy resides in the design of nucleases that can recognize specifically the mutant mtDNA. Initially, this strategy was developed with restriction nucleases and proved to be effective to reduce the heteroplasmy levels for mutations generating specific restriction sites **(Tanaka *et al.,* 2002)**. However those enzymes lack the possibility to be adapted for various mtDNA mutations. In this regard, nuclease domains have been fused to protein motifs that can recognize specific nucleotides, as transcription activator-like effector nucleases (TALENs) and zinc-finger nucleases (ZFNs). Those motifs can be organized in order to target specific DNA sequences and this approach has been successfully used to reduce the heteroplasmy levels of mtDNA mutations *in vivo* **(Bacman *et al.,* 2018; Gammage *et al.,* 2018)**. TALENs and ZFNs grant more flexibility than restriction nucleases but their design is relatively complex and time consuming.

To date, the CRISPR/Cas9 technology is the easiest and fastest tool used for nuclear genome editing **(Jinek *et al.,* 2012)**. This technology relies on a ribonucleic complex composed of the endonuclease Cas9 associated with an easily designed short single guide RNA (sgRNA) leading the recognition and cleavage of specific

DNA sequences. While CRISPR/Cas9 is widely used for the nuclear genome, it is yet to be successfully applied for mitochondrial mutations **(Jo *et al.,* 2015; Gammage *et al.,* 2017)**. Recent data obtained by our team showed that both the protein and RNA can be imported in mitochondria and the complex can cleave mtDNA **(Loutre *et al.,* 2018b)**. This raises the possibility of future utilization of Crispr/Cas9 to edit the mitochondrial genome, although it would require additional adaptation and optimization of the system **(Verechshagina *et al.,* 2018)**.

Anti-replicative strategy:

The anti-genomic strategies may result in considerable off-target cleavage and/or induce drastic diminution of the mtDNA copy number which, in a prospect of therapeutic application, can be detrimental for the patient with already defective mitochondria. In that regard, anti-replicative strategies may be another approach to reduce the level of heteroplasmy. The idea is to target to mitochondria molecules that will specifically anneal to mutant mtDNA and interfere with its replication, giving a replicative advantage to the wild-type genome. Our team worked on the mechanisms of import of small non-coding RNAs in mitochondria (the only nucleic acid naturally targeted into mitochondria) and identified the import determinants of tRK1 and 5S rRNA (see section I.B.3.2 and **Figure 16**) **(Smirnov *et al.,* 2008; Kolesnikova *et al.,* 2010).** Interestingly, the tRK1 import determinants can be added to small RNA molecules in order to target them into mitochondria. Similarly, part of 5S rRNA, the β-domain, can be replaced by another RNA sequence without disturbing its import. By using these import determinants to target into mitochondria anti-replicative RNA sequences, our team was able to induce mild heteroplasmy shifts (around 20%) in human cells heteroplasmic for either a point mutation in the *MT-ND5* gene (m.13514A>G) leading to MELAS syndrome or a large deletion (nt 8363 to 15438) associated with Kearns Sayre Syndrome (KSS) **(Comte *et al.,* 2013; Tonin *et al.,* 2014)** In the first part of my thesis, I contributed to the optimization of the anti-replicative strategy using the 5S rRNA import determinants (see section II.A).

For the development of other therapeutic strategies against mitochondrial diseases the complete knowledge of RNA species located inside mitochondria can be crucial. Mitochondrial RNome comprises the mtDNA transcripts (transcriptome) and RNA species imported from the cytosol (importome).

I.B. Human Mitochondrial RNome

I.B.1. Importance of sub-cellular RNA compartmentalization

Eukaryotes have developed a complex and effective internal organization composed of enclosed compartments, or organelles, delimited by intracellular membranes **(Diekmann and Pereira-Leal, 2013)**. Those compartments provide functionally specialized area, physically separate cellular processes to prevent interference from other pathways, serve for transport of molecules and isolate degradation processes and toxic components from the rest of the cell. Through local modification of intracellular composition and volume reduction, they also sustain high-rate enzymatic reactions. For example, the nucleus contains the main genome and the machinery needed for its maintenance. It separates the RNA transcription and maturation processes from translation in the cytosol, allowing fine regulation and quality control **(Martin and Koonin, 2006)**. The endoplasmic reticulum and the Golgi apparatus are hubs of protein translation, maturation and transport processes. Mitochondria ensure the production of the energy through oxidative phosphorylation as well as many other essential functions. Such an organization, however, requires efficient targeting pathways to ensure the proper localization of the molecules within the cell **(Rothman and Wieland, 1996; Kim and Hwang, 2013)**.

RNA molecules are involved in many key cellular functions from protein translation with messenger RNAs (mRNAs) and ribosomes to many aspects of gene regulation ensured by non-coding RNAs (ncRNAs). Similarly to proteins, the functions and the regulation of RNAs depend on their specific subcellular localization. Asymmetric spatial distribution of mRNAs was first observed for large or polarized cells, like neurons and oocytes, as a way to locally synthesize proteins and spatially restrict translation **(Bashirullah *et al.,* 1998)**. The localized translation ensures that the proteins are synthesized where they are required, preventing their unwanted activity in other parts of the cell. It also promotes the association of proteins translated in the same region to form larger complexes and facilitates the regulation of gene expression.

This mechanism was initially shown to be crucial during embryogenesis and early development **(Jung *et al.,* 2014)** but the improvement of cellular fractionation methods, organelle purification and microscopy techniques revealed that RNA targeting to subcellular locations is a prevalent feature among eukaryotes in all cell types and stages of life **(Cody *et al.,* 2013)**. For instance, it has been known for a long time that some mRNAs are targeted to the endoplasmic reticulum (ER) together with ribosomes and with help of the signal recognition particle (SRP) **(Walter and Blobel, 1982; Grudnik *et al.,* 2009)** in order to couple the translation with the transport of the nascent proteins into the ER lumen or membrane **(Reid and Nicchitta, 2015)**. mRNAs are also targeted to other organelles like nucleus, peroxisomes or mitochondria **(Weis *et al.,* 2013)** as it has been observed for mRNAs translated by ribosomes bound to the mitochondrial outer membrane to promote the import of nascent proteins into mitochondria **(Figure 11) (Matsumoto *et al.,* 2012; Gold *et al.,* 2017)**.

Besides its necessity for localized translation, the subcellular RNA localization plays a major role in the regulation of RNA biogenesis and gene expression. In the nucleus, long non-coding RNAs (lncRNA) act as regulators of transcription through remodeling of chromatin organization, histone modifications and alternative splicing. Cytosolic ncRNAs interact with mRNAs and proteins to influence mRNAs stability and promote or repress translation. **(Geisler and Coller, 2013; Rinn and Guttman, 2014).** Membrane-less particles composed of RNAs associated with RNA-binding proteins (located in the cytosol as P-bodies and stress granules) are involved in mRNA storage, decay and translation regulation, although the exact extent of their function remains unclear and it is still an active field of research **(Luo *et al.,* 2018b)**.

Recent studies showed that mitochondrial surface can serve as a platform for some post-transcriptional RNA processing and maturation steps. The best studied example of this pathway is pre-transfer RNA (pre-tRNA) maturation in yeast **(Chatterjee *et al.,* 2018)**. Some pre-tRNAs are exported in the cytosol and addressed to mitochondrial surface to undergo splicing and modification **(figure 11)**. The resulting tRNAs are then imported back to the nucleus to complete maturation. Re-import in the nucleus is a feature found in many eukaryotes and may be involved in tRNA quality control or translation regulation by temporary depleting the pool of tRNAs available in the cytosol. Fully matured and functional tRNAs can then be re-exported in the cytosol to participate in translation **(Hopper *et al.,* 2010)**. In

mammals, pre-tRNAs are transcribed, spliced and modified to yield functional tRNAs in the nucleus before they are exported in the cytosol **(Rubio and Hopper, 2011)**.

Besides being a meeting point where RNAs are addressed to undergo translation or post-transcriptional maturation, mitochondria also possess their own genome producing a few RNAs required for mitochondrial functions **(Anderson *et al.*, 1981)**. Moreover, some RNAs encoded in the nucleus have been reported to be imported inside mitochondria **(Sieber *et al.*, 2011a)**. Thus, mitochondrion is a particularly interesting model to study the sub-cellular localization of RNA **(Figure 11)**.

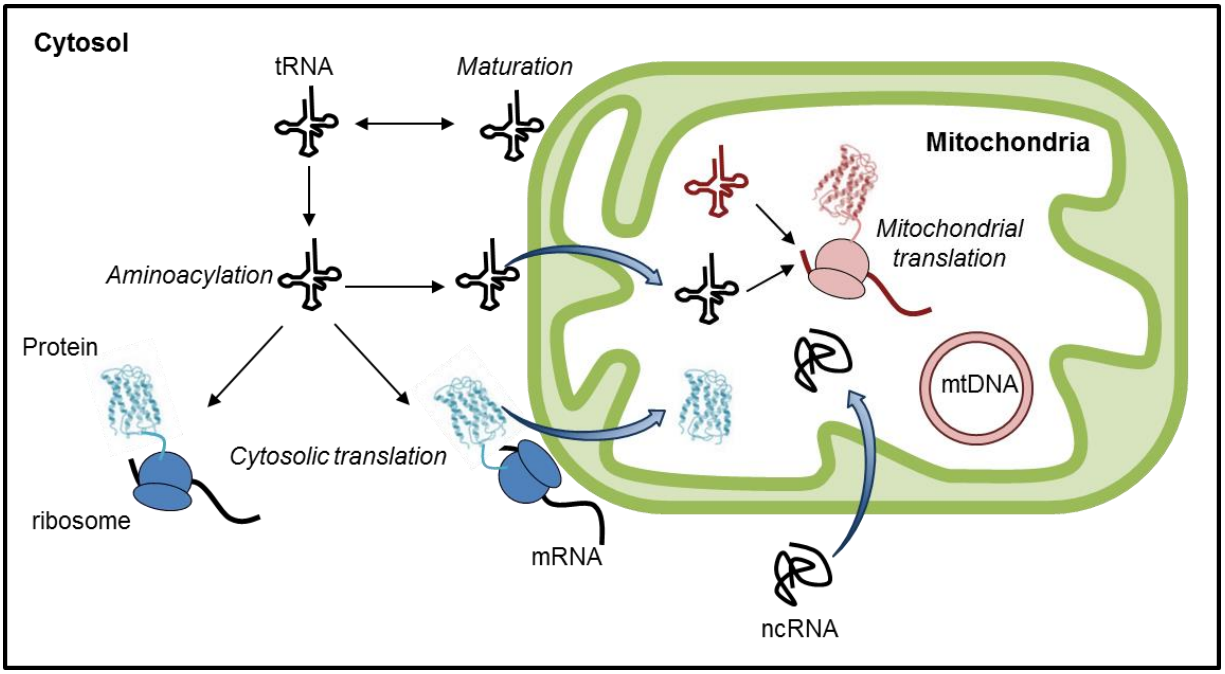

Figure 11. A generalized view of RNA localization to mitochondria.

Cytosolic tRNAs can localize to the mitochondrial surface for maturation or, along with mRNAs and ribosomes, to participate in translation of proteins destined for mitochondria. Some tRNAs and other ncRNAs may also be translocated into mitochondria were they often participate, in translation of mitochondrial mRNAs or regulation of gene expression. Note that all these mechanisms are not necessary present in every eukaryote.

I.B.2. Mitochondrial Transcriptome

I.B.2.1. Mitochondrial-encoded RNA biogenesis

I.B.2.1.1. Mechanisms of mitochondrial transcription

MtDNA is transcribed as polycistronic transcripts from three different promoters **(Montoya *et al.,* 1982) (Figure 12A).** Transcription from LSP, located in the non-coding region, produces long RNA containing 8 tRNAs and the ORF of NADH dehydrogenase subunit 6 (*MT-ND6*). H strand transcription can be initiated either at the level of HSP1, also in the non-coding region, or HSP2, located within the $tRNA^{Phe}$ gene, near the 5' extremity of the 12S rRNA gene. The initiation at the level of HSP2 has been largely debated **(Litonin *et al.,* 2010)**, mainly because *in vitro* data on the HSP2-derived transcript were confounded by the overlap with the HSP1 transcription, and the HSP2 transcription seems to require supercoiling of mtDNA, not obtained with the linearized DNA substrate used *in vitro*. Moreover, initiation at the level of HSP2 may require more factors than for HSP1 **(Zollo *et al.,* 2012; Zollo and Sondheimer, 2017)**. It has been suggested that HSP2 initiates the transcription of a long polycistronic RNA containing all the genes of the H strand, except for $tRNA^{Phe}$ (2 rRNAs, 13 tRNAs and 10 ORFs) while initiation at HSP1 produces a shorter transcript containing only $tRNA^{Phe}$, $tRNA^{Val}$ and the two rRNAs, leading to a higher amount of these RNAs in comparison to the rest of the transcriptome **(Chang and Clayton, 1984) (Figure 12B)**.

Mitochondrial transcription is carried out by a single-subunit DNA-dependent RNA polymerase (POLRMT). Two additional proteins, the mitochondrial transcription factor B2 (TFB2M), and the mitochondrial transcription factor A (TFAM) participate in the initiation of the transcription **(Falkenberg *et al.,* 2002; Shi *et al.,* 2012)**. TFAM binds to a region upstream of the transcription start positions and induces the bending of mtDNA **(Malarkey *et al.,* 2012)**. This allows the recruitment of POLRMT by direct interaction with TFAM and mtDNA. The initiation complex is then completed through the recruitment of TFB2M which performs the unwinding of the promoter region to initiate the mitochondrial RNA synthesis **(Hillen *et al.,* 2018).** Then, TFB2M disassociates from the complex and the transcription can continue **(Sologub *et al.,* 2009) (Figure 13)**. TFAM may not be strictly required for transcription since *in vitro* experiments showed that initiation can happen in the absence of TFAM **(Zollo *et al.,***

2012), although at a very low level. Low concentrations of TFAM increase the level of transcription while high concentrations repress it (Lodeiro *et al.*, 2012), indicating that TFAM may play a role as a modulator of transcription efficiency.

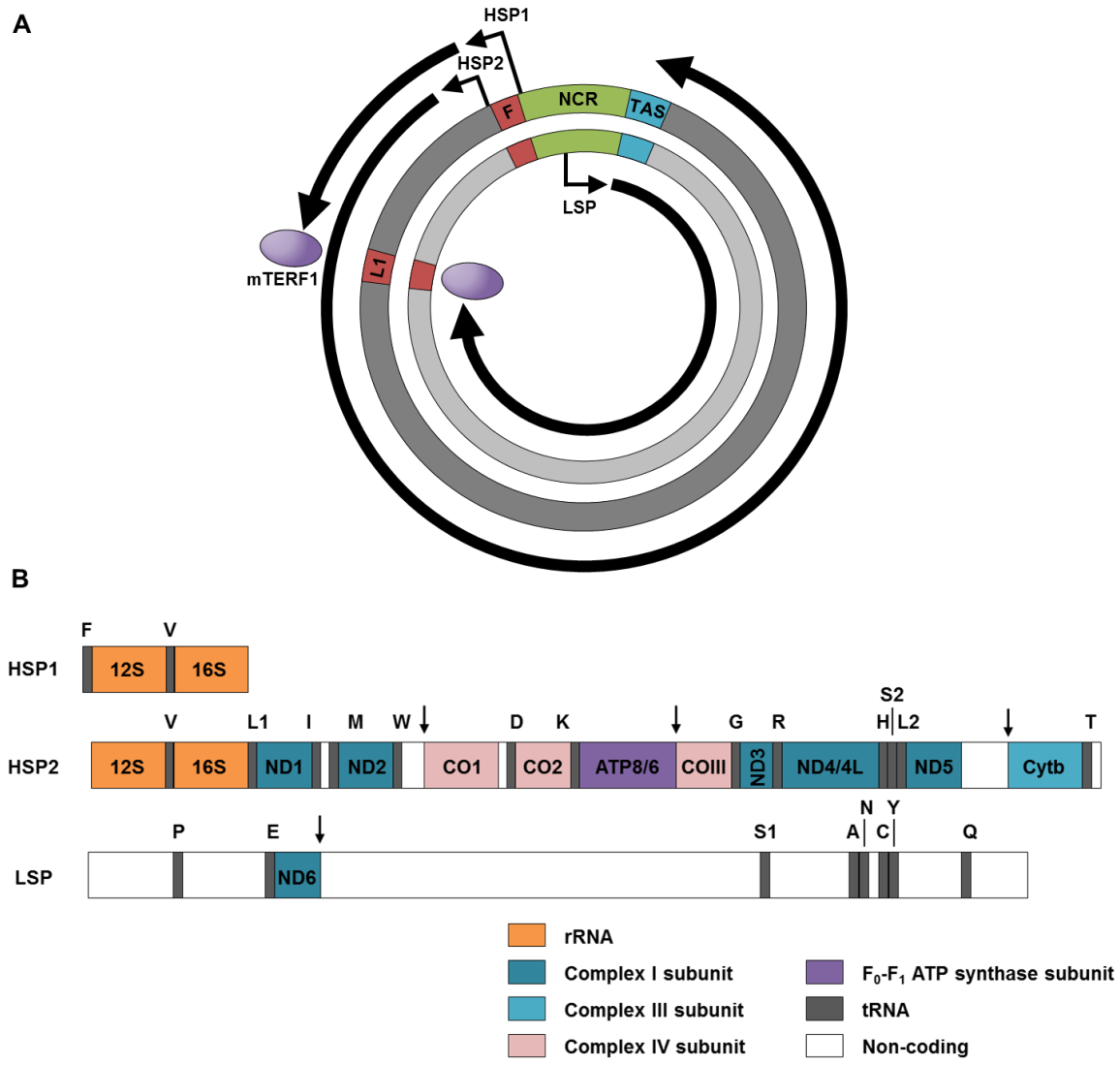

Figure 12. Human mitochondrial transcription units.

A) mtDNA is transcribed as three polycistronic RNAs. Transcription from HSP1 and LSP promoters ends in the region of the $tRNA^{Leu(UUR)}$ gene, probably mediated by the protein mTERF1. Transcription from HSP2 ends at the termination associated sequence (TAS) located in the NCR. **B)** The transcript from LSP contains only the coding sequence for the ND6 subunit of complex I and 8 mt-tRNAs. HSP1- and HSP2-derived transcripts overlap and both produce the ribosomal RNAs, but only transcription from HSP2 is believed to result in transcription of all H-strand genes. The release of individual RNAs is mediated by processing of tRNAs according to the tRNA punctuation model. Processing at non-canonical (tRNA-less) sites, indicated with black arrows, is, however, not well understood. tRNAs are annotated by their single letter code. S1: $tRNA^{ser(UCN)}$; S2: $tRNA^{ser(AGY)}$; L1: $tRNA^{Leu(UUR)}$; L2: $tRNA^{Leu(CUN)}$.

Transcription initiated at LSP often terminates prematurely at the conserved sequence block CSBII in the non-coding region due to the formation of a G-quadruplex in the nascent RNA **(Wanrooij *et al.*, 2010)**. This structure is formed by the stacking of planar guanine quartets one onto another and is stable enough to weaken the association of POLRMT with the RNA and stimulate transcription termination. The small RNA, named 7S RNA, released from this abortive transcription event can serve as primer for the replication of the H strand of mtDNA **(Agaronyan *et al.*, 2015)**. The mitochondrial transcription elongation factor (TEFM) can associate with POLRMT in order to increase the processivity of the transcription machinery and avoid the premature termination at CSBII, thus leading to the synthesis of the long polycistronic RNA **(Posse *et al.*, 2015)**.

Mitochondrial transcription termination remains poorly understood. The mitochondrial termination factor 1 (MTERF1) is the only factor involved in termination that has been identified so far. Its binding to mtDNA can mediate termination by interfering with the transcription elongation machinery. MTERF1 induces termination of the transcription of the L strand as well as short H strand transcripts. Its binding site has been localized within the $tRNA^{Leu(UUR)}$ gene **(Kruse *et al.*, 1989; Terzioglu *et al.*, 2013)**. Termination for the long H-strand transcript happens somewhere in the non-coding region, probably at the level of TAS and may involve so-far unidentified protein factors **(Figure 12A)**.

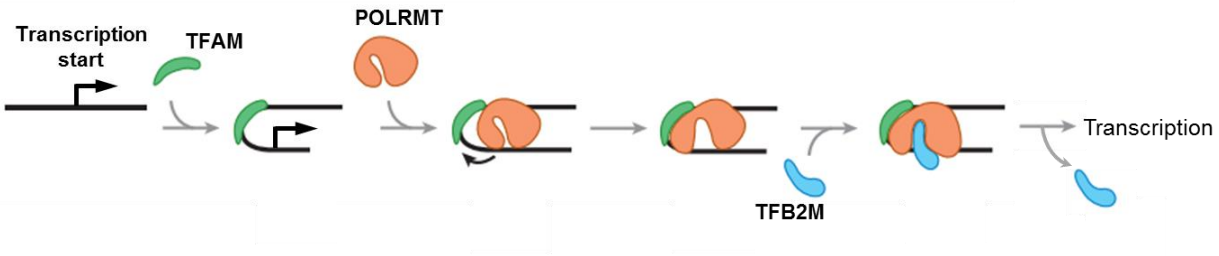

Figure 13. Initiation of the mitochondrial transcription.

TFAM induces the bending of mtDNA and POLRMT is further recruited to the transcription start site. The initiation complex is completed with the interaction of TFB2M to initiate RNA synthesis. TFB2M then disassociates from the complex so the transcription can progress. Adapted from **(Gustafsson *et al.*, 2016)**.

I.B.2.1.2. Maturation and fate of mitochondrial-encoded RNAs

Mitochondrial encoded RNAs arise from the same three polycistronic precursor transcripts which are then processed into individual RNA molecules. Despite this, individual RNAs show a large variation in steady-state expression levels which cannot be imputed to transcription regulation alone **(Mercer *et al.,* 2011)**. This suggests that mt-RNA abundance is mainly regulated by post-transcriptional mechanisms affecting transcript stability.

Most of the mitochondrial RNA processing proteins are clustered in distinct foci called mitochondrial RNA granules (MRG), formed in close proximity of nucleoids **(Antonicka and Shoubridge, 2015)**.

Since tRNA genes often flank rRNA and protein-coding genes, most individual transcripts are released according to the "tRNA punctuation model" **(Ojala *et al.,* 1981b) (Figure 12B, Figure 14)**. The cloverleaf structures of tRNAs are specifically recognized and excised at 5' by the enzyme RNase P **(Rossmanith *et al.,* 1995)** composed of 3 protein subunits (MRPP1, MRPP2 and MRPP3) and in 3' by the mitochondrial RNase Z, ELAC2 **(Brzezniak *et al.,* 2011)**. However the "tRNA punctuation model" is not sufficient for the complete release of all individual transcripts since some mRNAs are not flanked by tRNAs on both sides **(Figure 12B)**. The mechanisms of cleavage at the sites that cannot be processed by RNase P and ELACZ remain unclear, however, some factors have been identified. For example Fas-Activated Serine/Threonine Kinase 2 (FASTK2) is required for the maturation of the *MT-ND6* transcript, flanked by mt-tRNA^{Glu} only on its 5'-terminus **(Popow *et al.,* 2015)**, The pentatricopeptide repeat domain protein 2 (PTCD2) is involved in the cleavage between the *MT-ND5* and *MT-CYB* ORFs **(Xu *et al.,* 2008)** and the G-rich Sequence Factor 1 protein (GRSF1) co-localized with RNA granules, interacts with RNase P and may participate in the processing of several mtRNAs, including *MT-ATP6/ATP8-MT-CO3* precursor **(Jourdain *et al.,* 2013)**.

Human mtDNA is very compact. RNAs do not contain any introns and don't need to be spliced. However other maturation events are required to obtain functional mt-RNAs. mt-tRNA genes do not encode the 3' terminal CCA, which is, consequently, added later on by the ATP(CTP):tRNA nucleotidyltransferase 1 (TRNT1) **(Nagaike *et al.,* 2001)**. Interestingly, the mitochondrial tRNA^{Tyr} also lacks a 3' terminal A73 discriminator nucleotide, preventing the addition of the CCA

trinucleotide by TRNT1. This single A is provided by the addition of a polyadenylic acid (poly(A)) tail to the tRNA by the mitochondrial poly(A) polymerase (mtPAP), which is further processed by the 3' phosphodiesterase exonuclease 12 (PDE12) **(Fiedler *et al.,* 2015).** Similarly, 7 of 11 mRNAs do not possess a complete stop codon and contain only U or UA at their 3' termini after processing. For these mRNAs, the completion of the termination codon UAA is also ensured through the addition of a poly(A) tail by mtPAP. Except for *MT-ND6* mRNA, all mt-mRNAs are polyadenylated **(Hallberg and Larsson, 2014).** In the eukaryotic cytosol, poly(A) tails confer stability and promote initiation of translation while in bacteria, it stimulates RNA degradation. In mitochondria, the role of poly(A) tails on mRNA turnover seems to depend on their length, regulated by the actions of both mtPAP and PDE12, and vary greatly for each RNA **(Temperley *et al.,* 2010b; Rorbach *et al.,* 2011)**. A recent study showed that abnormal mt-tRNAs can also undergo extensive polyadenylation and are then degraded by the mitochondrial degradosome **(Toompuu *et al.,* 2018).**

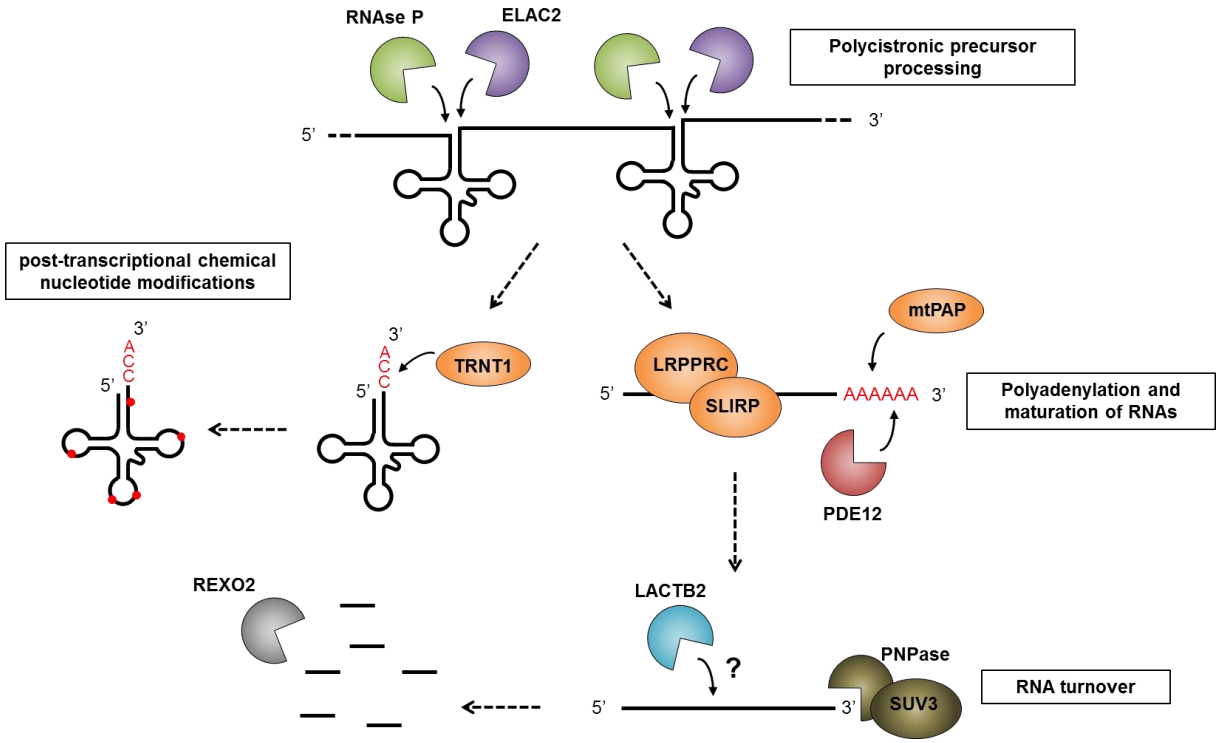

Figure 14. Maturation and degradation of mitochondrial RNAs

MtDNA is transcribed as polycistronic RNAs, individual transcripts are released according to the "tRNA punctuation model" through the cleavage of tRNAs at 5' by RNase P and at 3' by ELAC2. The 3' terminal CCA of the tRNAs is added by TRNT1, and chemical nucleotide modifications, important for the tRNA stability and decoding ability, are introduced by several specific enzymes. mtPAP adds 3' poly(A) tails to mtRNAs and the lengh of the tail is regulated by the action of PDE12. LRPPRC/SLIRP complex promotes mRNA stability and facilitates RNA polyadenylation and translation. The first step of mitochondrial RNA degradation may be induced by LACTB2 endonucleolytic cleavage and RNAs are further degraded by the mitochondrial degradosome composed of PNPase and SUV3. REXO2 eliminates the short oligonucleotides produced by the degradosome.

Contrary to nuclear-encoded mRNAs, mt-mRNAs do not possess a 5' 7-methylguanosine cap involved in mRNA stability and translation **(Montoya *et al.*, 1981)**. The stability of mitochondrial mRNAs is regulated by the leucine-rich pentatricopeptide repeat-containing (LRPPRC) protein which associates with the stem-loop-interacting RNA-binding protein (SLIRP) to facilitate RNA polyadenylation and translation and protect mt-mRNA from degradation **(Chujo *et al.*, 2012)**. To date the main candidate for the mitochondrial degradosome is the trimeric 3'-5' exoribonuclease polynucleotide phosphorylase (PNPase) in complex with the DNA/RNA helicase SUV3 **(Borowski *et al.*, 2013).** However, different functions and mitochondrial sublocalization have been reported for PNPase, resulting in some

controversy about its role in the organelle. PNPase has been observed in the matrix and/or in IMS **(Chen *et al.,* 2006; Borowski *et al.,* 2013).** In the matrix, PNPase was suggested to be involved in RNA decay but also processing and stabilization of RNA transcripts **(Nagaike *et al.,* 2005; Wang *et al.,* 2014).** In IMS it is believed to be a central factor for the nuclear-encoded RNA import inside mitochondria **(Wang *et al.,* 2010)** and may, upon release in the cytosol, also play a role in apoptosis **(Liu *et al.,* 2018)**. However, all those functions are not necessary exclusive. The PNPase-SUV3 complex can only degrade RNA to 4-nt-long oligonucleotides. At least one other nuclease is required to complete the degradation of the short oligonucleotides and it has been suggested that this was performed by the exonuclease REXO2 **(Bruni *et al.,* 2017) (Figure 14)**. Finally, the metallo-β-lacatmase protein LACTB2 is an endoribonuclease identified recently and may perform the initial endonucleolytic cleavage of mRNA to facilitate the degradation by the mitochondrial degradosome **(Levy *et al.,* 2016).** L-strand transcripts containing G-quadruplex structures can be efficiently degraded only in presence of the GRSF1 proteins which melts quadruplexes to facilitate the degradation by the degradosome complex ***(Pietras et al., 2018)***.

Notably, mt-tRNAs contain modified nucleosides which are important for their stability and decoding ability. For instance, N^1-methylation of adenine or guanine at position 9 of tRNAs (m^1R9) is present in most tRNAs and prevents the alternative base-pairing interactions to allow the correct folding of tRNAs. This modification is introduced in the precursor transcript by a subcomplex of RNase P composed of MRPP1 and MRPP2 **(Reinhard *et al.,* 2017)**. The third subunit (MRPP3) of RNase P is then recruited to cut the 5' end of the tRNA. Conversion of uridine into pseudouridine is another common nucleoside modification stabilizing the structure of tRNAs at different position and is performed by several mitochondrial pseudouridine synthases, depending of the position **(Bohnsack and Sloan, 2018).** Modification of U34, althought often present in cytosolic tRNA, is absent in many mt-tRNAs recognizing 4 codons families (see next section).

Position 37 downstream of the anticodon is also frequently modified in order to facilitate stable codon-anticodon interactions. For example, the enzymes TRIT1 and CDK5RAP1 are responsible for the modification of adenine with a 2-methylthio-N6-isopentenyl group ($ms2i^6A_{37}$) leading to accurate decoding and increased translation efficiency. $ms2i^6A_{37}$ is a specific feature of mitochondrial tRNAs and is not found in

nuclear-encoded tRNAs **(Yarham *et al.,* 2014; Fakruddin *et al.,* 2017)**. Ribosomal 16S and 12S rRNAs also require post-transcriptional modification of nucleosides, such as methylation and pseudouridynylation, for the assembly of the mitochondrial ribosomes **(Bohnsack and Sloan, 2018)**. Similarly to mt-tRNAs, the number of modifications found to date in mt-rRNAs is less than for cytosolic rRNAs.

I.B.2.2. Mitochondrial transcripts

I.B.2.2.1. Translation related RNAs : mRNAs, tRNAs and rRNAs

<u>mRNAs :</u>

mt-mRNAs do not contain any introns, Shine-Dalgarno sequences, 5' cap and have no or very short untranslated regions (UTR) **(Temperley *et al.,* 2010b)**. The *MT-CO1*, *MT-ND6* and *MT-ND5* mRNAs contain longer 3' UTRs covering the neighbor open reading frame (ORF) or tRNA in the antisense direction; they are currently of unknown function. Interestingly, the *MT-ND6 and MT-ND5* 3' UTRs were also observed as stand-alone long non-coding RNAs **(AP, Rackham *et al.,* 2011)**. The *MT-ND4L/ND4* and *MT-ATP8/ATP6* mRNAs are bicistronic as their ORFs are overlapping by 7 and 46 bp, respectively. How the translation of both polypeptides for each bicistronic RNA is performed remains unclear. Either the ribosome repositions itself after the translation termination on the first ORF to restart the translation on the second one, or the upstream ORF serves as 5' UTR for the correct positioning of ribosomes on the downstream ORF **(Gao *et al.,* 2017)**. The absence of long UTRs in human mitochondrial genome may suggest that regulation of gene expression is performed directly through protein binding in the ORF.

Human mitochondrial genetic code differs slightly from the nuclear one **(Table 1) (Anderson *et al.,* 1981)**. First, all NADH dehydrogenase subunit mt-mRNAs (except for the *MT-ND4/4L* mRNA) contain non-conventional initiating codons, AUU or AUA, encoding isoleucine in the cytosol **(Fearnley and Walker, 1987)**. Notably, human mitochondria contain only one $tRNA^{Met}$ which participates in both initiation and elongation and recognizes up to three different codons (AUG used both in initiation and elongation, and AUA and AUU exclusively employed in initiation of select mt-mRNAs). NSUN3 and ABH1 are the two enzymes involved in the modification of the position 34 of this unique $tRNA^{Met}$, producing m^5C_{34} and f^5C_{34}, respectively **(Haag *et al.,* 2016)**. The UGA stop codon actually encodes tryptophan in the mitochondria,

and the AGA and AGG codons, coding for arginine in the nuclear genetic code, are mitochondrial stop codons used in the *MT-CO1* and *MT-ND6* transcripts. AGA and AGG mitochondrial stop codons are so-called hungry codons since neither a tRNA nor a termination factor correspond to them. This situation may induce a -1 frameshift leading to conventional UAG stop codon translation termination **(Temperley *et al.*, 2010a).** This makes a total of 4 different stop codons in mitochondrial genetic code **(Table 1).**

Codon	Universal genetic code	Mitochondrial genetic code
UGA	STOP	Trp
AUA	Ile	Met
AUU	Ile	Met
AGA	Arg	STOP
AGG	Arg	STOP

Table 1. Differences between the mammalian mitochondrial and the universal genetic codes

tRNAs :

Human mitochondrial genome codes for a set of 22 tRNAs, this is a minimal number of tRNAs sufficient to decode all the amino-acids. In mammalian mitochondria, nine four-codon families are decoded by only one tRNA bearing unmodified U in the wobble position (first position of the anticodon) and only two tRNAs ($tRNA^{Leu}$ and $tRNA^{ser}$) have two isoacceptor forms **(Szymanski and Barciszewski, 2007).** Moreover, there are no tRNAs AAG and AGG codons and only one methionine tRNA which can function both for transaltion elongation and initiation.

Mt-tRNAs are characterized by a rather high adenine and uracil content and some tRNAs have non-canonical secondary structure **(Suzuki *et al.*, 2011)**. For example, mt-$tRNA^{ser(AGY)}$ lacks the entire D-arm preventing the folding into the canonical cloverleaf structu re; mt-$tRNA^{Asp}$ and mt-$tRNA^{Phe}$ lack the conventional D-loop/T-loop stabilizing interactions. The unusual features of mt-tRNAs, and the

reduction of the set of mt-tRNA genes seem to be a consequence of the size reduction of the mitochondrial genome

rRNAs :

12S rRNA and 16S rRNA of the human mitochondrial ribosome are encoded by mtDNA. All ribosomal proteins are, however, encoded by the nuclear genome and imported inside human mitochondria. 16S rRNA and over 80 mitoribosomal proteins (MRPLs) assemble to form the large ribosomal subunit (mt-LSU, 39S), while 12S rRNA and 30 mitoribosomal proteins (MRPSs) assemble into the small ribosomal subunit (mt-SSU, 28S). Both subunits form together the complete 55S mitochondrial ribosome. **(Bogenhagen *et al.,* 2014)**. Mammalian mitochondrial ribosomes have a higher protein/RNA mass ratio (1:2) than cytosolic ribosomes (2:1) **(Agrawal and Sharma, 2012)**. Indeed, recent structural analysis of mammalian mitochondrial ribosome showed that it only contains three RNAs: the two canonical large rRNAs and, surprisingly, the mt-tRNA^{Val} in human or the mt-tRNA^{Phe} in porcine and bovine **(Greber *et al.,* 2015; Rorbach *et al.,* 2016)**. The tRNAs were discovered in the central protuberance of the ribosome, where 5S rRNA is usually found. The function of these tRNAs is still unclear, but the presence of mt-tRNA^{Val} and mt-tRNA^{Phe} as structural elements is most likely related to the position of the genes in the mammalian mitochondrial genome **(Figure 4)**. This gives a spatial proximity as well as stoichiometry for the assembly of ribosomes.

I.B.2.2.2. Other non-coding RNAs

lncND5, lncND6 and lncCytb :

The light strand polycistronic transcript spans almost the entire length of the mitochondrial DNA while it only encodes 8 tRNAs and the *MT-ND6* ORF separated by long stretches of non-coding sequences. Similarly, the H-strand polycistronic transcript contains short regions of non-coding sequence, especially at the level of the genes present in the L- strand **(Figure 12B)**. It is important to note that detection of non-coding RNAs is easily confounded by the presence of partially processed mRNA precursors and RNA turnover products **(Mercer *et al.,* 2011; Kuznetsova *et al.,* 2017)**. Strand-specific deep sequencing revealed three abundant RNA transcripts corresponding in anti-sense to the *MT-ND5*, *MT-ND6* and *MT-CYB* genes

accordingly named lncND5, lncND6 and lncCytb **(Rackham *et al.,* 2011)**. LncND5 and lncND6 are found as individual transcripts but also as *MT-ND6* and *MT-ND5* mRNA 3'UTRs, respectively. The function of the three lncRNAs remains elusive, but they have been suggested to either stabilize or regulate the expression of their anti-sense counterparts by forming intermolecular duplex structures.

7S RNA and LC-RNA :

7S RNA is a non-coding polyadenlyated RNA of about 200 nt transcribed from LSP promoter **(Ojala *et al.,* 1981a)**. This RNA spans the proximal region of the origin of replication O_H in the non-coding mtDNA region and its 3' end map to the CSB1 region **(Figure 6)**. However from the same promoter another ncRNA, named LC-RNA (light strand coding region RNA) can be transcribed. It was suggested that 7S RNA acts as a primer for the mtDNA replication from O_H ***(Jemt et al., 2015; Kuhl et al., 2016)***. LC-RNA is rather involved in the formation of an R-loop by hybridization with mtDNA in the NCR and may participate in mitochondrial DNA segregation **(Akman *et al.,* 2016)**.

Chimeric transcripts :

SncmtRNAs is a long chimeric transcript which contains a hairpin structure comprising the 16S rRNA sequence fused to a sequence derived from the complementary strand **(Villegas *et al.,* 2007; Yang *et al.,* 2013)**. Other RNAs, named ASncmtRNAs were found to combine the antisense sequence of the 16S rRNA fused to either 310 (ASncmtRNA-1) or 545 (ASncmtRNA-2) nucleotides of the sense strand. These RNAs supposedly form long and stable double-stranded structures. Their origin and role remains unclear, however these chimeric RNAs were characterized by different expression in highly proliferating normal and tumor cells **(Burzio *et al.,* 2009)**. Surprisingly, these RNAs were also detected in the nucleus which suggests their export from mitochondria through an unknown mechanism **(Landerer *et al.,* 2011).**

Another chimeric RNA encoded by the mitochondrial DNA, called LIPCAR (long intergenic noncoding RNA predicting cardiac remodeling) was detected in the plasma of patients suffering from chronic heart failure. LIPCAR is composed of sequences of *MT-CO2* and *MT-CYB* genes and its expression was upregulated at the late stage of the left ventricular remodeling and in cases of chronic heart failure.

Its function is unknown but its presence in plasma of patients is used as a biomarker of cardiovascular pathologies **(Kumarswamy *et al.,* 2014)**

I.B.3. Mitochondrial RNA Importome

The organization of the mitochondrial genome and the corresponding transcripts are well conserved in mammals but vary in other species. Notably, in some species, tRNAs for select amino acids are not encoded by the mitochondrial genome and must be imported from the cytosol. This range from few tRNAs in plants to the complete set of tRNA in protists such as T. *brucei* **(Hancock and Hajduk, 1990)** and L. *tarentolae* **(Simpson and Shaw, 1989)** lacking all mitochondrial tRNA genes. Even in species with a complete set of tRNAs encoded by the mitochondrial genome, tRNA import from the cytosol was observed, such as in baker yeast *S. cerevisiae* **(Martin *et al.,* 1979).** In this case it was demonstrated that the nuclear-encoded $tRNA^{Lys}_{CUU}$ (tRK1) imported into yeast mitochondria becomes essential for mitochondrial translation under stress conditions where its organellar counterparts fail to function **(Kamenski *et al.,* 2007).** Thus, in apparently all eukaryotes (animals, plants, fungi and protists), some nuclear-encoded RNAs are imported into the organelle.

Import of other noncoding RNAs was also reported in mammalian cells **(Wang *et al.,* 2010; Kim *et al.,* 2017)**. In this section I will present the RNAs reported to be imported in human mitochondria **(Table 2)** and what is known on their import mechanisms.

I.B.3.1. RNA imported into human mitochondria

<u>tRNAs :</u>

Human mtDNA encodes an apparently complete set of tRNAs required for the translation of mitochondrial proteins (see section I.B.2.2.1). Thus, it is not surprising that tRNAs do not seem to be the main type of imported RNAs in human

mitochondria. However, similarly to other organisms, some tRNAs were reported to be imported even though their mitochondrial counterpart already exist in the organelles.

In yeast S. *cerevisiae*, $tRNA^{Lys}_{CUU}$ (tRK1), one of the 2 nuclear encoded $tRNA^{Lys}$, is partially redirected to mitochondria while the mitochondrial genome already encodes a $tRNA^{Lys}$ (tRK3) able to decode both mitochondrial lysine codons **(Martin *et al.,* 1979)**, AAA and AAG. It was later demonstrated that tRK3 requires the 2-thio modification of the wobble position U34 to AAG codon, and that the wobble position was hypomodifed at 37°C, leading to a codon recognition defect. Thus import of tRK1, although dispensable at 30°C, becomes essential for AAG codons translation at 37°C **(Kamenski *et al.,* 2007)**. Interestingly, yeast tRK1 was shown to be also imported in human mitochondria when artificially introduced in the cells **(Kolesnikova *et al.,* 2000)**. While such a situation is unnatural, it proves that an undiscovered tRNA import pathway exists in human and suggests that some nuclear-encoded human tRNAs may *a priori* be imported in human mitochondria **(Kolesnikova *et al.,* 2004)**.

Indeed, $tRNA^{Gln}_{CUG}$ and $tRNA^{Gln}_{UUG}$ were reported to be imported inside mammalian mitochondria **(Rubio *et al.,* 2008)** and that this import could provide efficient mitochondrial translation in the case where the decoding of the GAG glutamine codon is compromised, for example if the wobble position of mt-$tRNA^{Gln}$ is not correctly modified. However it is important to note that this hypothesis was not verified. An RNA-seq study based on the analysis of RNA enrichment in RNase-treated mitoplasts (mitochondria devoid of the outer membrane) in comparison to crude mitochondria also identified some nuclear-encoded tRNA, including $tRNA^{Gln}_{UUG}$, within human mitochondria **(Mercer *et al.,* 2011)**. The same study also highlyted the mitochondrial enrichement of several other nuclear tRNAs.

5S rRNAs :

5S ribosomal RNA (5S rRNA) is a component of the LSU of most organisms, although often absent in the mitochondrial ribosomes of unicellular eukaryotes **(Greber and Ban, 2016)**. It plays a structural role, acting as a scaffold interconnecting the LSU and the SSU. **(Bogdanov *et al.,* 1995; Kouvela *et al.,* 2007; Amunts *et al.,* 2015)**. 5S rRNA is not encoded by the mammalian

mitochondrial genome but was found present in abundance in mammalian mitochondria by several teams **(Yoshionari *et al.,* 1994; Magalhaes *et al.,* 1998; Entelis *et al.,* 2001; Smirnov *et al.,* 2011; Autour *et al.,* 2018)**. For a long time, it was believed that 5S rRNA mitochondrial import was required for its incorporation in the mitochondrial ribosome. However, as mentioned previously, recent studies showed that mammalian mitochondrial ribosomes do not contain stably integrated 5S rRNA and instead contain mitochondrially encoded tRNAs **(Greber *et al.,* 2015; Rorbach *et al.,* 2016),** leaving a question mark on the mitochondrial function of 5S rRNA. Nevertheless, even though 5S rRNA is not an integral component of the mitochondrial ribosome, our laboratory showed that knockdown of the rhodanese protein, involved in 5S rRNA import in human, leads to decrease of the mitochondrial protein synthesis **(Smirnov *et al.,* 2010).** This suggests that 5S rRNA is required for the mitochondrial protein synthesis and may be involved in regulation of mitochondrial translation or the assembly of mitochondrial ribosomes.

RNase P RNA component (H1 RNA) :

The RNase P activity is found in all living organisms where its main function is to remove the 5' leader sequence from tRNA precursors. As mentioned in section I.B.2.1.2, this activity is also critical for the processing of mitochondrial polycistronic transcripts in the tRNA punctuation model **(Ojala *et al.,* 1981b).** Two types of RNase P can be found in different organisms: RNase P ribonucleoproteins, composed of a catalytic RNA components (H1 RNA) and protein factors and protein-only RNases P (PRORP) **(Klemm *et al.,* 2016)**. Interestingly, in human mitochondria, the RNase P activity is ensured by a proteinaceous complex composed of three subunits, MRPP1, MRPP2 and MRPP3 **(Holzmann *et al.,* 2008).** However, a 340-nt RNA corresponding to the nuclear H1 RNA was also detected in mitochondria **(Bartkiewicz *et al.,* 1989; Puranam and Attardi, 2001),** although, its function appears to be redundant. It is important to note that some bacteria and archaea encode both RNA-based and protein-only RNases P **(Nickel *et al.,* 2017)**, and a similar situation may be possible in mitochondria, taking into account that RNase P activity is not always limited to tRNA maturation and different RNases P may have different substrate specificities **(Klemm *et al.,* 2016).**

MRP RNA (RMRP) :

In the nucleus, MRP RNA (RMRP) is the catalytic component of the mitochondrial RNA processing (MRP) complex involved in the 5' end maturation of 5.8S rRNA **(Schmitt and Clayton, 1993).** RMRP was also reported to play a role in the cell cycle regulation **(Gill *et al.,* 2004)** and to associate with the telomerase reverse transcriptase (TERT) for the synthesis of double-stranded RNA further processed into short interfering RNAs (siRNAs) **(Maida *et al.,* 2009)**. However, while RMRP mainly localizes in the nucleus, part of RMRP is found in mitochondria and its function was initially studied in isolated mouse mitochondria **(Chang and Clayton, 1987, 1989)**. It was proposed to be involved in mitochondrial RNA processing as well as in the cleavage of the transcripts complementary to the origin of replication O_H, forming the RNA primer for the leading strand of mitochondrial DNA replication. However, further studies showed that the transcription-replication switch did not seem to require a nuclease activity since the RNA primer formation is a consequence of a premature arrest of the mitochondrial RNA polymerase (see section I.A.2.1.2) **(Agaronyan *et al.,* 2015)**. Moreover, it was shown that only the 3' region (about 130 nt) of the nuclear RMRP was imported inside mitochondria, the RNA being somehow processed upon or during the mitochondrial import **(Chang and Clayton, 1987; Noh *et al.,* 2016),** likely leading to the loss of catalytic activity. Recent studies showed that RMRP in mitochondria interacts with GRSF1, a component of mitochondrial RNA granules, and contributes to the mitochondrial function and metabolism **(Jourdain *et al.,* 2013).** Interestingly RMRP and H1 RNA are structurally and evolutionary related **(Esakova and Krasilnikov, 2010),** suggesting that their import could be directed by similar mechanisms. Indeed, a short hairpin structure necessary for mitochondrial import (import determinant) has been identified in both RNAs **(Wang *et al.,* 2010)**.

RNA	Cytosolic function	Putative mitochondrial function	Comments	References
5S rRNA	Component of the cytosolic ribosome	Regulation of mt-translation and/or mt-ribosome assembly	Absent from mt-ribosomes	**(Yoshionari *et al.*, 1994)** **(Magalhaes *et al.*, 1998)** **(Entelis *et al.*, 2001)**
H1 RNA	Pre-tRNA processing	Processing of polycistronic RNA precursors	A protein-only RNase P is already present in mitochondria	**(Bartkiewicz *et al.*, 1989)** **(Puranam and Attardi, 2001)** **(Wang *et al.*, 2010)**
hTERC	RNA component of telomerase	Mitochondria-cytosol communication	Not yet confirmed by other studies	**(Cheng *et al.*, 2018)**
miRNAs	Gene expression regulation	Gene expression regulation	Different studies disagree on the identity of mitochondria localized miRNAs	**(Geiger and Dalgaard, 2017)**
RMRP	5.8S rRNA maturation	Mitochondrial RNA processing and formation of replication RNA primer	RMRP is cleaved upon import	**(Chang and Clayton, 1987)** **(Noh *et al.*, 2016)**
SAMMSON lncRNA	Facilitate the import of p32 protein into mitochondria	Required for increased mitochondrial protein synthesis in highly dividing melanoma cells	No direct evidence of its presence inside mitochondria	**(Leucci *et al.*, 2016)** **(Vendramin *et al.*, 2018)**
tRK1	Participates in translation	Participates in translation	Artificial system	**(Kolesnikova *et al.*, 2000)**
$tRNA^{Gln}_{CUG}$ **$tRNA^{Gln}_{UUG}$**	Participate in translation	Participate in translation to compensate for post-transcriptional incorrect modification of $mt\text{-}tRNA^{Gln}$	Only one report, not yet confirmed by other studies	**(Rubio *et al.*, 2008)**

Table 2. Human mitochondrial imported RNAs.

SAMMSON lncRNA :

SAMMSON is a lncRNA that predominantly localizes to the cytoplasm of human melanoblasts and melanoma cells **(Leucci *et al.,* 2016; Vendramin *et al.,* 2018)**. SAMMSON interacts with the protein p32, involved in the regulation of the mitoribosome assembly in mitochondria. The knockdown of *SAMMSON* impairs the p32 targeting to mitochondria and causes mitochondrial protein synthesis defects, thus, SAMMSON seems to be required for increased mitochondrial protein synthesis in highly dividing melanoma cells. Since SAMMSON associated with mitochondria, it has been suggested that its role in p32 addressing to mitochondria could be linked to its own mitochondrial import. However, the SAMMSON lncRNA import has not been demonstrated yet.

hTERC :

Recently, the RNA component of the human telomerase, hTERC, encoding the sequence of the simple repeats added to the ends of DNA (telomere) **(Gall, 1990)**, was also identified as imported into mitochondria **(Cheng *et al.,* 2018)**. In this study, the hTERC import was initially suspected by the identification of a region similar to that of the H1 RNA import determinant **(Wang *et al.,* 2010)**. Surprisingly, deletion of this sequence in hTERC significantly increased the import efficiency instead of abolishing it. Similarly to RMRP, hTERC was observed to be processed upon mitochondrial import into a shorter 195 nt RNA. Since the processed version of hTERC was detected mostly in the cytosol, the authors suggested the mitochondrial re-export of the processed RNA. According to their hypothesis, the mitochondrial import-processing-reexport pathway of hTERC would relay the functional state of mitochondria to the nucleus and other cellular compartments. However, the evidence is lacking that the hTERC processing indeed occurs within the mitochondrial matrix and not simply at the mitochondrial surface.

microRNAs :

Small non-coding RNAs are ubiquitously found in organisms and often play a role in gene expression regulation **(Rother and Meister, 2011)**. Deep-sequencing of

mitochondrial RNAs allowed the detection of many small RNAs in mitochondria. **(Mercer *et al.,* 2011; Sripada *et al.,* 2012)**. Of those, more than 150 micro-RNAs (miRNAs) were detected in mitochondria and were subsequently called “mitomiRs”. miRNAs are small noncoding RNA molecules of about 22 nucleotides that target and repress mRNAs at the level of stability and/or translation through the recruitment of the RNA-induced silencing complex (RISC) **(Fabian *et al.,* 2010; Huntzinger and Izaurralde, 2011)**. They are transcribed as primary microRNAs (pri-miRNAs) which are processed in the nucleus by the DROSHA/DGCR8 complex into precursor (pre)microRNAs, exported to the cytoplasm and further processed by DICER1 into mature miRNAs. Then, they associate with the RNA-binding protein Argonaute 2 (AGO2), a component of RISC, and bring the complex to the target mRNA, usually by annealing to a specific region in the 3’ UTR.

While most of them seems to be nuclear-encoded and imported inside mitochondria or associated with OMM, a few miRNAs were also identified as probably mitochondrially encoded **(Bandiera *et al.,* 2011; Barrey *et al.,* 2011; Sripada *et al.,* 2012).** For example ASncmtRNA-2, a chimeric transcript combining sense and anti-sense sequences of the mitochondrially encoded 16S rRNA supposedly characterized by different expression in highly proliferating normal and tumor cells **(Burzio *et al.,* 2009)** may function as miRNA precursor involved in cell cycle regulation **(Bianchessi *et al.,* 2015)**.

In silico analysis revealed multiple putative miRNA-binding sites on the mitochondrial DNA **(Barrey *et al.,* 2011)**. However, mitochondrial mRNAs contain no or small 3’ UTR regions and only some components of RISC, such as AGO2, seems to localize to the mitochondrial matrix **(Bandiera *et al.,* 2011; Zhang *et al.,* 2014; Geiger and Dalgaard, 2017)**, suggesting that mitomiRs may have other mechanisms of action in mitochondria. Indeed, some mitochondrial microRNAs were shown to enhance transcription instead of inhibiting it. miR-1, for example, is able to stimulate the translation of multiple mtDNA-encoded transcripts, while repressing some nuclear DNA-encoded mRNAs in the cytosol **(Zhang *et al.,* 2014).** miR-181c was also shown to regulate mitochondrial genome expression in the heart **(Das *et al.,* 2012)**. Other non-canonical functions of mitochondrial miRNAs can be expected and many hypotheses have been proposed. Besides roles in regulation of mitochondrial gene expression, it was also suggested that imported miRNAs could undergo post-transcriptional modifications in mitochondria leading to structural changes, adjusting

their RNA or protein interaction specificity, before to be exported back to the cytosol **(Geiger and Dalgaard, 2017)**. To date, the function of most mitochondrial miRNAs remains unknown, but they have been suggested to play roles in cell survival, cell division and energy metabolism as well as in diseases like cancer **(Duarte *et al.,* 2014; Sripada *et al.,* 2017)**. It is important to keep in mind that only 7 miRNAs localized to the mitochondria were identified in at least 3 different studies while most mitochondrial miRNAs were identified in only 1 or 2 studies **(Geiger and Dalgaard, 2017)**.

Many other types of small non-coding RNAs have been detected in mitochondria, ranging from small nuclear or nucleolar RNAs (sn and snoRNAs) and piRNAs to tRNA fragments **(Mercer *et al.,* 2011; Sripada *et al.,* 2012).** To demonstrate whether those small RNAs are indeed located inside the mitochondria or represent the cytosolic contaminants, new experimental approaches should be developed.

I.B.3.2. Mechanisms of import

Although the mitochondrial RNA import is ubiquitously found among eukaryotes, the mechanisms that direct the mitochondrial targeting and transfer of RNAs into the mitochondrial matrix seem to differ greatly between organisms **(Figure 15) (Schneider, 2011; Salinas-Giege *et al.,* 2015)**. In a general manner, the mitochondrial RNA import answers three criteria: 1) the presence of selective signals, or import determinants, within the imported RNA, 2) the existence of a mechanism to deviate the RNA from its cytosolic function and redirect it to the mitochondrial surface, and 3) the use of a translocation pathway to transfer the RNA across the mitochondrial membranes. In most cases, targeting signals within RNAs can be found but seem to differ between RNAs and species **(Duchene *et al.,* 2009).**

Mechanisms of RNA import in plant mitochondria remain elusive. *In vitro* import tests suggest that the tRNA import does not require cytosolic factors, however, mutations disrupting aminoacylation of tRNAs prevent their import *in vivo* and addition of protein factors improves tRNA import rates *in vitro*. This indicates a potential involvement of aminoacyl-tRNA synthetases as carrier proteins to direct tRNA to mitochondria **(Sieber *et al.,* 2011b; Salinas-Giege *et al.,* 2015),** although

other unidentified factors may participate in this process. The mitochondrial tRNA transport across the membranes is ATP-dependent and requires the presence of the membrane potential **(Delage *et al.*, 2003)**. VDAC was identified as the main channel for translocation of tRNAs across the outer mitochondrial membrane, with the participation of complexes of the protein import machinery (Tom20 and Tom40) **(Salinas *et al.*, 2006; Salinas *et al.*, 2018)**. However, the mechanism of translocation through the inner membrane is still unknown **(figure 15A)**.

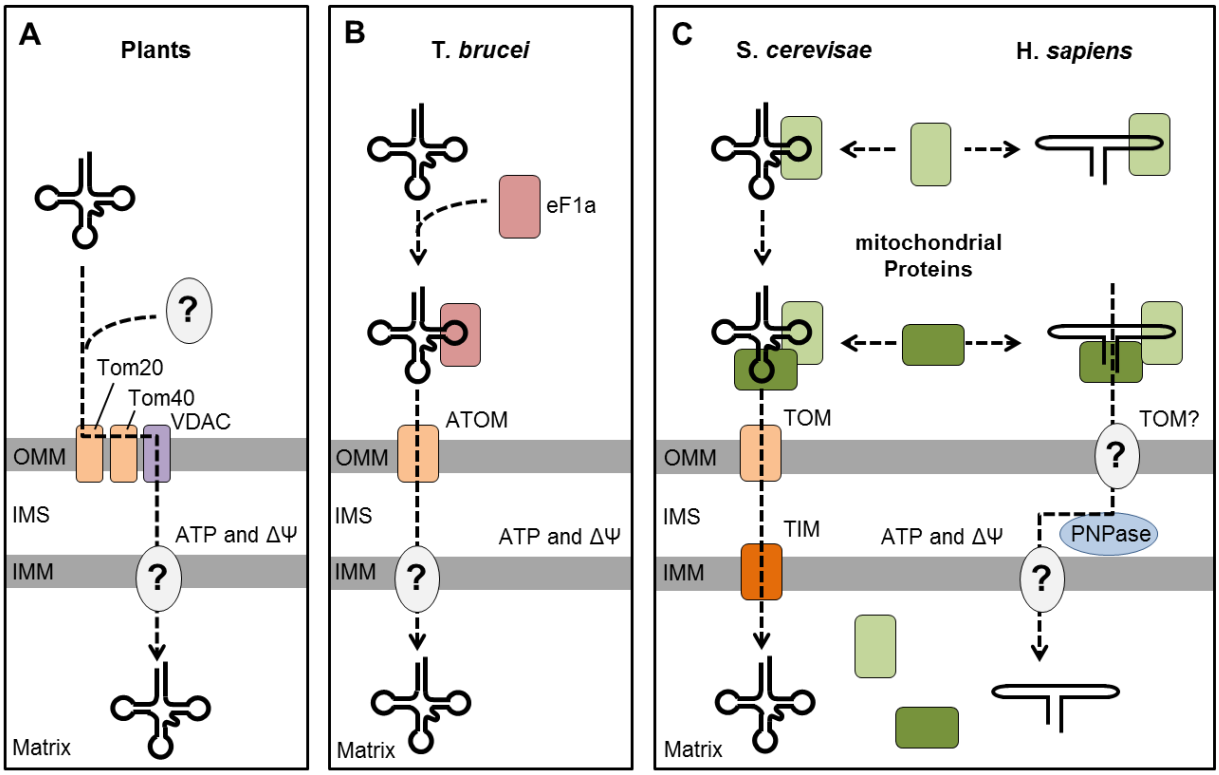

Figure 15. Mitochondrial RNA import pathways in different organisms

A) Mitochondrial RNA import in plants. The targeting of RNA to mitochondria may not require cytosolic factors. Translocation across OMM requires Tom20, Tom40 and the VDAC channel. Mechanisms of translocation across IMM are unknown. **B)** Mitochondrial RNA import in *T. brucei*. tRNAs are directed to the mitochondrial import by the translation elongation factor eEF1α and the ATOM complex mediates the translocation though OMM. **C)** Mitochondrial RNA import in *S.* cerevisiae and human. RNAs are targeted to mitochondria by the association with various nuclear-encoded proteins normally localized inside or in the vicinity of mitochondria. Translocation into the mitochondrial matrix is mediated by the protein import machinery in *S. cerevisiae* (TOM and TIM). In human, the translocation mechanism is unknown but seems to require the protein PNPase located in IMS. ΔΨ: membrane potential

The mitochondrial tRNA targeting to mitochondria in *T. brucei* seems specified by a signal in the T-loop of tRNAs recognized by the cytosolic elongation factor eEF1α **(Crausaz Esseiva *et al.,* 2004)**. The translocation into the mitochondrial matrix is also ATP-dependent but, contrary to plants, does not require VDAC and only requires components of the protein import apparatus ATOM (archaic translocase of the outer membrane) complex **(Figure 15B) (Bouzaidi-Tiali *et al.,* 2007; Niemann *et al.,* 2017)**.

The *S. cerevisiae* and human RNA import pathways seem to share similar features, although not fully understood. Studies performed on some imported RNAs, such as tRK1 and 5S rRNA, shed light on how the import may occur and uncovered general rules that may be similar for most imported RNAs, although the involved factors may differ depending on the RNA **(Figure 15C)**. For instance, imported RNAs should contain specific import determinants recognized by protein factors ensuring the deviation of a part of the RNA pool from its cytosolic pathway to mitochondria **(Kazakova *et al.,* 1999; Smirnov *et al.,* 2008; Gowher *et al.,* 2013)**. In yeast, translocation in the mitochondrial matrix is then performed by the import protein machinery, while in human, translocation through the membranes remains elusive but seems to require the protein PNPase **(Wang *et al.,* 2010)**. For both organisms, another pathway independent of any cytosolic factors **(Rinehart *et al.,* 2005; Rubio *et al.,* 2008)** has been demonstrated by *in vitro* experiments, suggesting that different RNAs might take different routes to be imported inside mitochondria.

Below I will discuss two main steps of RNA import into human mitochondria: 1) targeting of selected RNAs to mitochondria and 2) their translocation through the mitochondrial membranes.

I.B.3.2.1. RNA targeting to human mitochondria

Up to date, import of two RNAs into human mitochondria had been studied in details: endogeneous 5S rRNA and yeast $tRNA^{Lys}_{CUU}$ (tRK1). Our research team first studied the import of tRK1 into yeast S. cerevisiae mitochondria. It was demonstrated that the glycolytic enzyme enolase (Eno2p) binds to tRK1 to form a complex that is directed to the mitochondrial surface **(Entelis *et al.,* 2006)**. Interaction of Eno2 with tRK1 induces a conformational change of the tRNA which is then handed over to the precursor of the mitochondrial lysyl-tRNA synthetase (preMSK). Then, it was shown

that tRK1 can be targeted to human mitochondria if expressed or introduced into human cells **(Kolesnikova *et al.,* 2004)**. Proteins implicated in this pathway seem to be similar to those identified in yeast (human enolase and preKARS2)**(Gowher *et al.,* 2013; Baleva *et al.,* 2015)**

Import determinant of tRK1 were identified as being the CUU anticodon, specifically the 34 position, and nucleotides of the acceptor arm **(Kazakova *et al.,* 1999)**. Those determinants are responsible for the conformational change of TKR1 upon binding to each carrier protein **(Kamenski *et al.,* 2010; Kolesnikova *et al.,* 2010)**. Upon biding with enolase, tRK1 adopts an "F-structure" composed of 3 stem-loops. The 3' extremity of the tRNA interacts with the 3' part of the T-loop to form a new arm called F-stem loop (**Figure 16A)**. The change of conformation also induces rearrangement within the anti-codon arm and variable region while the D-loop is conserved. F-loop and D-loop were further identified as being the essential import determinant, sufficient to induce mitochondrial import of small synthetic RNAs (FD-RNA) **(Kolesnikova *et al.,* 2010).**

Upon binding with enolase, tRK1 adopts an alternative secondary structure named "F-structure" composed of three stem-loops **(Kazakova *et al.,* 1999; Kamenski *et al.,* 2010; Kolesnikova *et al.,* 2010)**. The 3' extremity of the tRNA interacts with the 3' side of the T-arm to form a new arm called the F-stem-loop (**Figure 16A)**. The change of conformation includes also a rearrangement within the anti-codon arm and the variable region while the D-arm is preserved. The F- and D-stem-loops were further identified as being the essential import determinants. Fused to an oligoribonucleotide of 20-25 bases, these hairpin structures can induce mitochondrial import of the resulting small synthetic RNA **(Kolesnikova *et al.,* 2010; Comte *et al.,* 2013; Tonin *et al.,* 2014; Dovydenko *et al.,* 2015)**

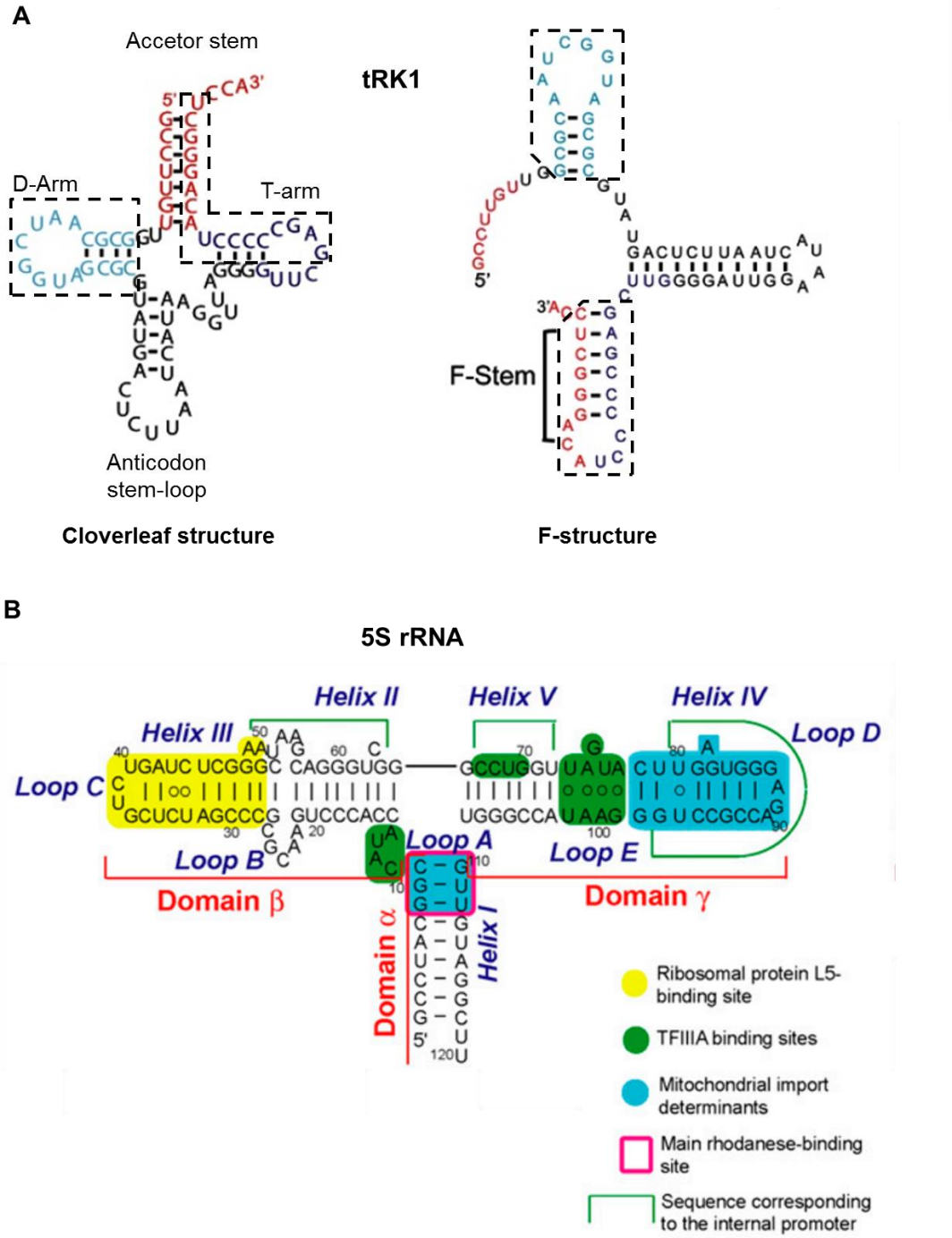

Figure 16. Import determinants of tRK1 and 5S rRNA.

A) Left: the cloverleaf secondary structure of $tRNA^{Lys}_{CUU}$ (tRK1) of *S. cerevisiae*. Right: the F-structure of tRK1 adopted upon binding with enolase. The 3' part of the acceptor stem interacts with the 3' side of the T-arm to form a new arm (F-stem). The import determinants (shown as boxes) form two stem loops in the F-structured RNA Blue : D-arm, Red : acceptor stem. Adapted from **(Gowher *et al.*, 2013)**. **B)** 5S rRNA is a 120-nt-long RNA structured in three domains (α, β and γ). The interaction with TFIIIA (binding site highlighted in green) is required for 5S rDNA transcription and the nuclear export of 5S rRNA. The interaction with the cytosolic ribosomal protein L5 (in yellow) directs its nuclear re-import and incorporation in the cytosolic ribosome. The interaction with the precursor of the mitochondrial ribosomal protein MRP-L18 and the enzyme rhodanese at the level of the import determinants (in blue) specifies the 5S rRNA import into mitochondria. Adapted from **(Smirnov *et al.*, 2011)**

The 5S rRNA import in human mitochondria follows a similar pattern and the import determinants were also identified **(Figure 16B) (Smirnov *et al.,* 2008)**. 5S rRNA is a highly structured RNA of about 120 nucleotide composed of three domains, namely α, β and γ, and transcribed by RNA polymerase III with the help of the transcription factor IIIA (TFIIIA) in the nucleus. It is believed to be exported to the cytosol in complex with TFIIIA where it interacts, through its β-domain, with the cytosolic ribosomal protein L5 **(Steitz *et al.,* 1988).** 5S rRNA is then imported back in the nucleus to be integrated in the cytosolic ribosome. In the cytosol, 5S rRNA can also interact, through its γ-domain, with the precursor of the mitochondrial ribosomal protein L18 (pre-MRPL18) and be redirected to the mitochondria **(Smirnov *et al.,* 2011)**. Similarly to tRK1 and enolase, the interaction with pre-MRP-L18 induces a change in conformation of the 5S rRNA molecule and allows the interaction of the 5S rRNA α-domain with the second carrier, the rhodanese protein (thiosulfate sulfurtransferase) and ultimately import into the mitochondrial matrix **(Smirnov *et al.,* 2010; Autour *et al.,* 2018)**. The α and γ domains are essential for the mitochondrial targeting of 5S rRNA, whereas the β-domain is only involved in the 5S rRNA incorporation in the cytosolic ribosome. Not surprisingly, the removal of the β-domain or its substitution with a short RNA sequence does not alter the import of 5S rRNA and may even increase its targeting to mitochondria **(Smirnov *et al.,* 2008).**

The mechanisms of mitochondrial targeting of other RNAs are less studied but it is probable that other protein factors destined for the mitochondrial matrix are involved. For example, a recent study showed that the RMRP export from the nucleus was mediated by the protein HuR and, once in mitochondria, this RNA interacts with GRSF1 **(Noh *et al.,* 2016).** One of the two proteins may be responsible for the targeting of the RNA to the mitochondrial surface. Similarly, the main candidate for the mitochondrial targeting of miRNAs is the RISC component AGO2, also detected inside mitochondria. However further studies should be performed to validate this hypothesis.

I.B.3.2.2. Translocation through the mitochondrial membranes

Compare to protein import pathways (section I.A.2.2), mechanisms for RNA translocation across the mitochondrial membranes in human are not well understood. It was shown that the process was ATP-dependent, required the presence of the

membrane potential and might involve the protein import apparatus, as it was observed in yeast **(Tarassov *et al.,* 1995; Entelis *et al.,* 2001)**. RNA translocation through OMM can be mediated by TOM complex and/or VDAC channel (I. Tarassov, unpublished results).

Up to date, the protein PNPase is a major candidate possibly involved in RNA translocation through IMM **(Figure 15C) (Wang *et al.,* 2010)**. PNPase is an evolutionarily conserved 3' to 5' exoribonuclease encoded by the nuclear gene *PNPT1*. It was found to possess a mitochondrial localization pre-sequence at its N-terminus and localized both in mitochondrial IMS and the matrix **(Chen *et al.,* 2006; Borowski *et al.,* 2013)**. On the one hand, as discussed previously (section I.B.2.1.2), PNPase is a major component of the RNA degradosome and is involved in mtRNA processing and turnover **(Nagaike *et al.,* 2005; Borowski *et al.,* 2013; Wang *et al.,* 2014).** On the other hand, PNPase was shown to modulate the import level of several RNAs **(Wang *et al.,* 2010)**. Mutations in human PNPase are linked to mitochondrial diseases characterized by respiratory chain defects, associated with both mitochondrial RNA processing defects and altered RNA import **(Vedrenne *et al.,* 2012; von Ameln *et al.,* 2012; Matilainen *et al.,* 2017)**

Since PNPase is a nuclease, the mechanism by which it is involved in RNA import remains puzzling. It was postulated that PNPase can recognize small stem-loop structures within RNAs acting as import determinants. Such structures are parts of import determinants found for 5S rRNA and tRK1 **(Figure 16)** but were also identified in H1 RNA and RMRP **(Wang *et al.,* 2010)**. Precursors of miRNAs are also known to adopt stable stem-loop structures that could be recognized for RNA import by PNPase.

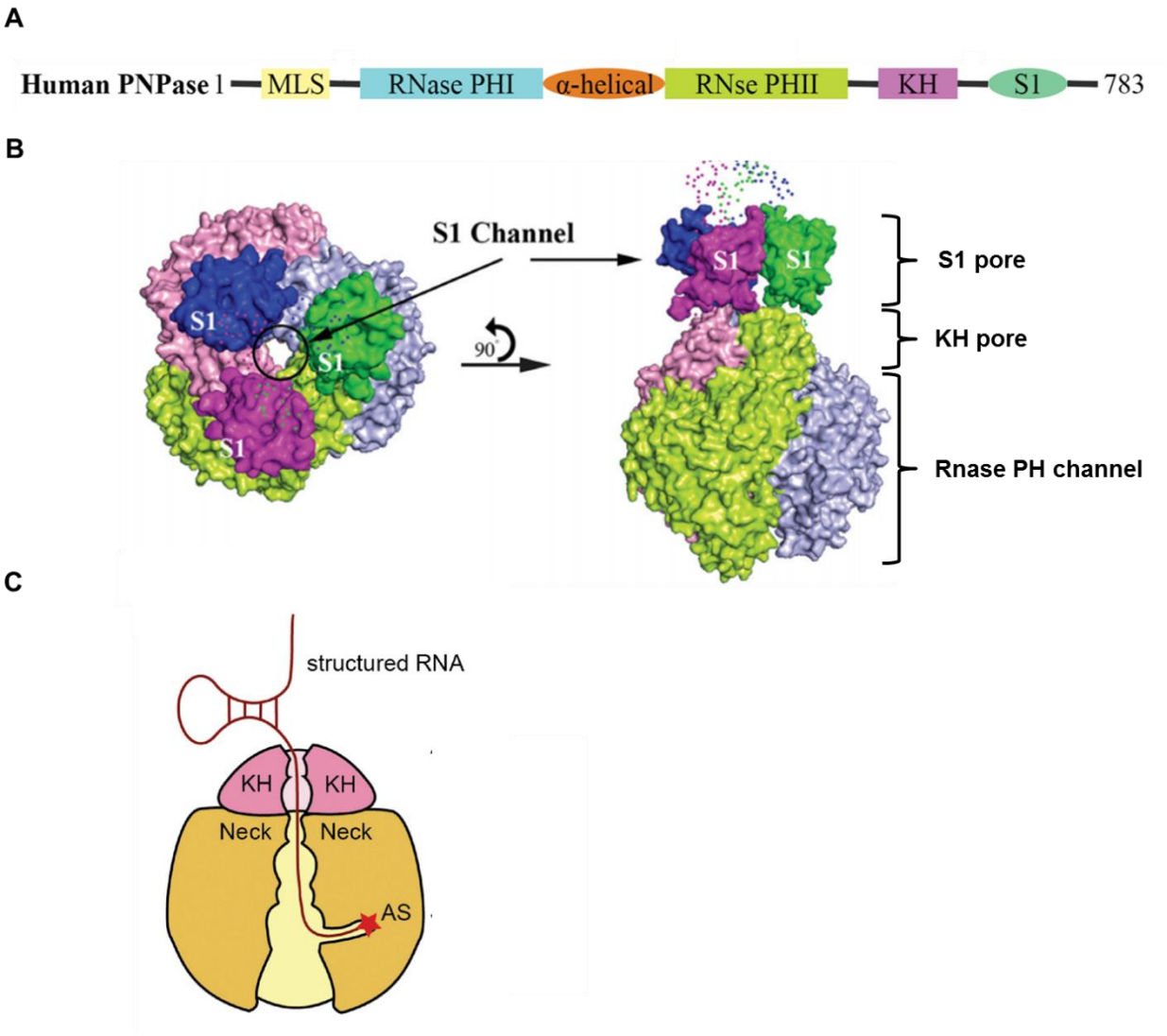

Figure 17. Structure of the human polynucleotide phosphorylase

A) Domain organization of human PNPase. **B)** Structure of human PNPase revealed by small-angle X-ray scattering (SAXS). PNPase assembles into a homotrimer, the S1 and KH domain form two pores one onto the other at the entry of the RNase PH channel containing the active site. Each PNPase monomer is represented with a different color. Adapted from **(Golzarroshan *et al.*, 2018)** **C)** Schematic model of PNPase bound to RNA (the S1 pore is not shown for simplicity). If the 3' overhang is long enough, the RNA can access the active site (AS) and be degraded. However, structured RNAs cannot enter in the KH pore. Many mitochondrially imported RNAs contain structured import determinants preventing their degradation. Adapted from **(Lin *et al.*, 2012)**.

The structure studies start to reveal how the selection for RNA mitochondrial import may occur at the level of PNPase **(Lin *et al.*, 2012)**. A PNPase monomer consists of two RNase PH domains (PHI and PHII), a so-called α-helical domain, and two RNA-binding domains, KH S1 **(Figure 17A).** Three monomers assemble into a

“doughnut”-shaped homotrimer with a central channel formed by the six RNase PH domains, where the catalytic site is located **(Figure 17B)**. The KH domains were shown to be important for single-stranded RNA binding and degradation. They form a “pore” at the entry of the PH channel through which the 3’ end of a single-stranded RNA enters and subsequently interacts with the catalytic site **(Lin *et al.*, 2012)**. However, the pore is too narrow to allow the passage of a structured RNA. A recent study proposed that it is the S1 domains, also forming a pore on top of the KH domains, which interact with structured double-stranded RNAs **(Golzarroshan *et al.*, 2018).** If the length of the 3’ overhang of the bound RNA is too short, it will prevent the entry of the RNA into the KH pore and the PH channel, protecting it from degradation **(Figure 17C) (Wang *et al.*, 2010; Lin *et al.*, 2012)**. Still, this hypothesis should be experimentally validated.

How the RNA translocation to the mitochondrial matrix can occur after the interaction with PNPase, remains unknown. In any case, PNPase cannot form a transmembrane channel; therefore, it can be implicated in the selection of imported RNA molecules and their targeting to an IMM channel which has not been identified up to date.

I.B.4. Identification of Imported RNAs

While the mitochondrial transcriptome is relatively well established the diversity of nuclear-encoded RNAs addressed to mitochondria and their functions remain largely unknown. The absence of an RNA gene in the mitochondrial genome when the gene product is required for mitochondrial functions is the first indication of mitochondrial RNA import and was particularly obvious in the case of tRNAs in some protists as Kinetoplastida **(Simpson and Shaw, 1989; Hancock and Hajduk, 1990).** However, adequate experimental techniques to detect and confirm the import of RNA in the organelles are essential, and many strategies have been employed over the years.

I.B.4.1. Classical cellular fractionation

Isolation of mitochondria :

Methods to validate the import of a candidate RNA are usually based on cellular fractionation to isolate mitochondria **(Figure 18) (Claude, 1946)**. Isolation of mitochondria requires an initial step of cell homogenization in conditions that maintain the mitochondrial integrity, usually followed by differential centrifugations. Low-speed centrifugation allows the removal of cellular debris and nuclei while mitochondria remain in the supernatant. Mitochondria are then recovered by high-speed centrifugations and can be used for *in vitro* import tests.

For this, a radiolabeled RNA transcript is added to the isolated mitochondria with or without cytosolic protein factors facilitating import, as well as ATP and ATP-regeneration system. Upon incubation, a ribonuclease treatment is performed to degrade the RNAs outside the mitochondria. The RNAs present in the mitochondrial matrix are protected from the RNase degradation by mitochondrial membranes. Isolated RNAs are separated by polyacrylamide gel electrophoresis (PAGE), and the presence of the candidate RNA at the end of the procedure is assessed by autoradiography. Examples of mitochondrial isolation and *in vitro* import test procedure are provided in **(Mager-Heckel *et al.,* 2007; Wang *et al.,* 2015).**

A slightly different experiment can be performed to check the *in vivo* import of the endogenous RNA **(figure 18)**. In this case, RNAs are directly extracted from the isolated mitochondria to analyze the mitochondrial RNA composition. However, more stringent purification steps are required to avoid cytosolic contamination. This may include, for example, an additional sucrose or Percoll gradient centrifugation step to eliminate other membrane-bounded organelles. However, differential centrifugation usually fails to eliminate efficiently all the cytosolic components tightly associated with mitochondria. To improve the purity of the mitochondrial sample, the outer membrane of mitochondria is usually removed. The generation of mitoplasts (mitochondria without the outer membrane) can be achieved by two different approaches: either with detergents such as digitonine, which preferentially permeabilize cholesterol-rich membranes such as OMM, or by inducing slight swelling of mitochondria and rupture of the mitochondrial membrane by osmotic shock **(Petit *et al.,* 1998; Zischka *et al.,* 2008)**.

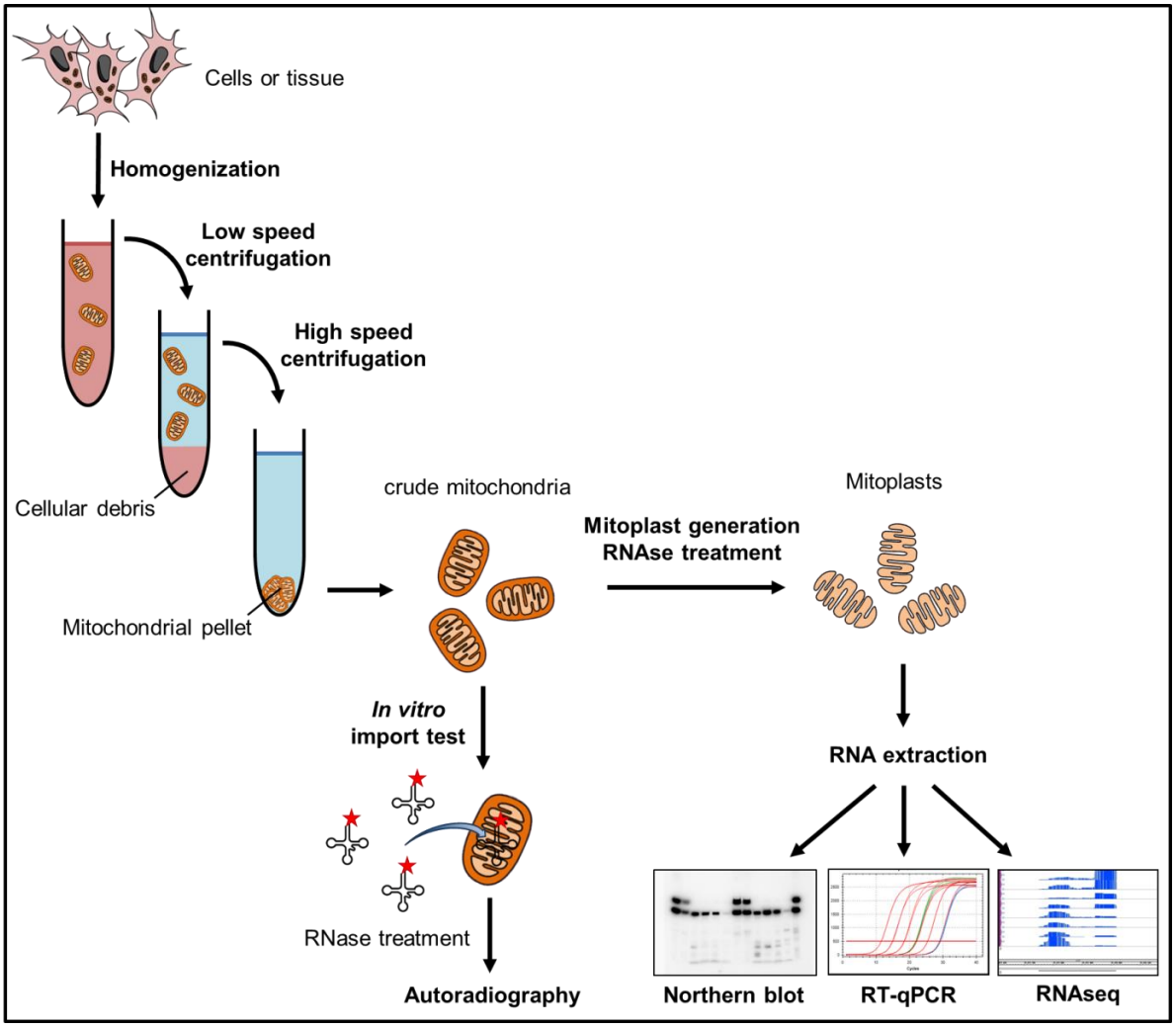

Figure 18. Analysis of mitochondrial RNA import by cellular fractionation.

Schematic representation of the experimental procedure for isolation of mitochondria and RNA import analysis. Isolated mitochondria are retrieved by cellular homogenization followed by differential centrifugation. Crude mitochondria can be used for *in vitro* import tests with radiolabeled RNA transcripts. RNase treatment eliminates RNAs outside the mitochondria, and the imported radiolabeled RNAs can be detected by autoradiography. In order to analyze endogenous mitochondrial RNAs, cytosolic RNA contaminants can be eliminated by the removal of OMM (mitoplast generation) followed by RNase treatment. Then extracted RNAs can be detected by various methods.

Since conditions of treatment are always in balance between the removal of the mitochondrial outer membrane and preservation of the inner membrane **(Cannon *et al.*, 2015)**, moderate treatments are preferred, albeit they can only partially remove the outer membrane in a population of mitochondria **(Fuller and Arriaga, 2004; Zischka *et al.*, 2008)**. Mitoplasts are also usually treated with ribonucleases, unable

to cross IMM, to digest remaining cytosolic RNA contaminants. RNA extraction can then be performed to analyze the mitochondrial RNA composition.

Analysis of the samples :

Mitochondria always interact with other cellular components like the endoplasmic reticulum **(Marchi *et al.,* 2014)**, Golgi, endosomes, some RNA-containing organelles such as P-bodies **(Huang *et al.,* 2011)**, stress granules, RNA granules **(Cande *et al.,* 2004; Aravin and Chan, 2011)** and, of course, the cytosolic ribosomes engaged in translation at the surface of OMM **(Matsumoto *et al.,* 2012; Gold *et al.,* 2017).** Hence, caution should be taken when analyzing mitochondrial RNA samples, since cytosolic contaminant RNAs have variable susceptibility to purification treatments **(Cannon *et al.,* 2015)**.

Northern blotting and RT-qPCR are routinely performed to detect RNAs in samples of isolated mitochondria. However, for both methods the identity and sequence of the candidate RNA must be known and only a limited number of RNAs can be analyzed. This also implies that only a few cytosolic control RNAs can be examined to estimate the purity of the mitochondrial samples. On the contrary, next-generation sequencing (RNA-seq) offers the possibility of large scale analysis of mitochondrial RNA import and detection of unsuspected imported RNAs. The experimental design of RNA-seq and the analysis procedure may vary greatly according to the analyzed system and the biological question. The sequencing of RNA itself may exploit completely different methodologies, depending on the commercial instrument used **(Hrdlickova *et al.,* 2017)**.

In a general manner, RNA-seq consists first in the reverse transcription of the RNAs to creation a complementary DNA (cDNA) library because most sequencing instruments are designed for DNA sequencing. However, some recently developed instrument such as Nanopore technology allows the direct sequencing of RNA molecules **(Garalde *et al.,* 2018)**. For this, adapter sequences must be ligated to the cDNA extremities, which are also required for both PCR amplification and sequencing. In the end, the sequence reads obtained virtually represent the complete RNome and can be mapped onto a reference genome, or assembled together to reconstitute the sequence of the corresponding transcripts. It is important to note that the diversity of approaches that can be used for RNA-sequencing, including removal

of some RNA species (rRNA depletion), differences in equipment and reagents and sensitivity complicates the comparison of data obtained by different laboratories.

Large-scale analyses of mitochondrial RNA samples by RNA-seq have been attempted by several laboratories **(Bandiera *et al.,* 2011; Mercer *et al.,* 2011; Sripada *et al.,* 2012; Rackham and Filipovska, 2014)**. However, in most cases it remains unclear to what extent the analyzed RNA samples contain cytosolic RNA contaminants. Indeed, RNA-seq provides high detection sensitivity capable to reveal trace amounts of contaminant RNA and it appears practically impossible to obtain completely pure mitochondria by conventional isolation methods. Moreover, standard approaches of purification of mitochondria are based on nuclease degradation of cytosolic contaminants, and laboratories often fail to provide clear controls to demonstrate that RNAs are protected from the nuclease treatment by mitochondrial membranes and not by other factors **(Cannon *et al.,* 2015)**. In fact, most published studies aimed to investigate mtDNA-encoded transcripts rather than mitochondrial RNA import, so the elimination of contaminating cytosolic RNAs during mitochondrial isolation was not of critical importance. Consequently, the procedures were successful to investigate the mitochondrial transcriptome **(Mercer *et al.,* 2011)** but were often indecisive and sometimes even contradictory in what concerns the nuclear-encoded RNAs residing in the organelles.

Altogether, RNA-seq studies of mitochondrial RNome failed to give a clear view of the mitochondrial RNA importome. However, to date, RNA-seq remains the only convenient strategy for large-scale analysis of RNomes. Thus, the methodology must be adapted in order to draw an accurate list of mitochondrially imported RNAs. The second part of my thesis consisted in the development of a new approach allowing the RNA-seq-mediated detection of nuclear-encoded RNAs in mitochondria while taking into account the inevitable presence of cytosolic RNA contaminants. The principle of this method and the results I have obtained are presented in the second part of this manuscript.

I.B.4.2. In situ detection of RNA by microscopy

Any results generated by genome-wide approaches such as RNA-seq need to be validated with orthogonal techniques. Convincing evidence of the mitochondrial import of a specific RNA in mitochondria can be obtained by direct observation of the

RNAs inside the mitochondrial matrix by microscopy imaging methods. Various approaches have been developed to this end, either by incorporating exogenous RNA aptamers binding a fluorescent substrate to the candidate RNA **(Dolgosheina and Unrau, 2016)**, or by direct observation of the endogenous RNA by fluorescence *in situ* hybridization (FISH).

Fluorescent RNA aptamers

Contrary to some proteins, RNAs cannot produce intrinsic fluorescent signal. Thus, fluorescent tools that had already been successfully used to study cellular proteins, such as the green fluorescent protein (GFP), had to be adapted to image RNAs in cells. MS2 tagging was the first system to provide GFP-mediated imaging of RNA localization (Bertrand *et al.,* 1998). The bacteriophage MS2 coat-protein, which can be fused to GFP, is specifically recruited to a short RNA element consisting of two hairpins (MS2 aptamer) that can be inserted into the RNA of interest. However, unbound GFP leads to high background levels that can mask the specific fluorescence signal. In order to increase the signal to background ratio, several repeats of the MS2 aptamer must be incorporated in the RNA, leading to long insertions of hundreds of nucleotides.

Improvement of the technique was achieved with the development of a series of RNA aptamers that can capture specific fluorophores and become fluorescent. Unbound fluorophores are poorly fluorescent and become highly fluorescent only when bound by the aptamer. (Babendure *et al.,* 2003; Huang *et al.,* 2014). Several aptamers were successfully developed, including Spinach, Broccoli and Mango **(Paige *et al.,* 2011; Filonov *et al.,* 2014; Autour *et al.,* 2018)**, with each generation providing a better affinity for the fluorophore, higher fluorescence and better resistance to photo-bleaching. Latest improvement of the RNA aptamer-based fluorescent systems allowed for the detection of the first RNA localized to mitochondria, 5S rRNA **(Autour *et al.,* 2018)**. It is important to note that, even if RNA aptamers are relatively small (40 to 100nt), their presence modifies the intrinsic structure of the concerned RNA, leading to a potential loss of RNA function or proper localisation, which is particularly relevant for short RNAs. Therefore, detection of endogenous RNAs looks especially appealing as it minimally disturbs the system,

avoiding the disruption of the RNA structure or mis-localization due to tagging or overexpression of an exogenous molecule.

Microscopy imaging of endogenous RNA molecules

Detection of specific nucleic acids in the cell can be performed by fluorescence *in situ* hybridization (FISH) **(Lecuyer *et al.,* 2007).** In FISH, specially designed nucleic acid probes coupled with fluorophores specifically hybridize with DNA or RNA molecules inside fixed cells. This technique was used to detect the mitochondrial localization of RNAs, such as microRNAs **(Barrey *et al.,* 2011)**. However, simple FISH Initially lack sensitivity since probes usually provide weak signals. Many efforts were made to improve FISH methodology aiming to easily detect signals obtained from a single molecule (smFISH). For example, the branched DNA technology increases the signal-to-background ratio by use specific DNA probes, annealing to a target RNA molecule and ultimately serving as platform for the binding of numerous fluorophore-labelled oligonucleotides **(Player *et al.,* 2001)**. However, conventional fluorescence microscopy is limited by relatively low spatial resolution because of the diffraction of light. This diffraction limit is about 200–300 nm in the lateral direction and 500–700 nm in the axial direction **(Huang *et al.,* 2009)** and correspond to the same order of size than isolated mitochondria (diameter of 300–500 nm). Thus, it is impossible to clearly distinguish between RNAs present inside the mitochondrial matrix or simply co-localized with the mitochondrial surface.

Since several years, super-resolution microscopy allows for images to be taken at a resolution up to 10 fold higher than the one imposed by the diffraction limit, which may prove useful to detect candidate transcripts inside organelles **(Brown *et al.,* 2011; Kuzmenko *et al.,* 2011; Jakobs and Wurm, 2014).** Super-resolution microscopy may in principle also determine the sub-mitochondrial localization of RNAs and glean additional information on their functions within the organelle **(Antonicka and Shoubridge, 2015)**

I.B.4.3. Mitochondrial RNA capture methods

A common view is that RNAs are never “naked” within the cell, and constantly interact with proteins. Based on this, numerous methods have been developed to

detect RNA-protein interactions and identify specific RNA-binding proteins and their ligands. Mainly, cross-linking immunoprecipitation coupled with deep sequencing (CLIP-seq) permits the identification of RNAs associated with a specific RNA-binding protein **(Ule *et al.,* 2003)**. In CLIP-seq, RNAs and proteins in direct contact with each other are covalently crosslinked together and the bait protein is then immunoprecipitated under stringent conditions. The crosslinked RNAs attached to the protein can then be sequenced. In recent years, those methods were adapted to detect localization of RNAs for example, by co-immunoprecipitation of the RNA partners of proteins with characteristic subcellular localization. Since usually only one protein is immunoprecipitated, these methods can only provide a partial view of a subcellular RNome.

A recent study provided a more comprehensive approach based on a methodology initially developed for proteome charting **(Kaewsapsak *et al.,* 2017; Fazal, 2018)**. First, an ascorbate peroxidase (APEX) that can oxidize biotin-phenol (BP) had been targeted to a specific cellular sub-localization **(Rhee *et al.,* 2013)**. The BP oxidation by H_2O_2 then created radicals covalently attached onto protein residues thus leading to the biotinylation of proteins in a close radius (< 20 nm) from APEX and allowing their subsequent enrichment by streptavidine affinity purification (APEX-RIP). Since phenoxyl radicals can also react with electron-rich nucleobases such as guanine, leading to the biotinylation of RNA species, this approach can also be used to profile sub-cellular RNome by RNA-seq (APEX-seq). The APEX methodology proved to be effective in membrane-enclosed compartments such as mitochondria and was used to profile mRNAs revealing the absence of nuclear-encoded mRNAs in the mitochondrial matrix **(Fazal, 2018)**. However, the method remains to be applied for small non-coding RNAs since they constitute most of the RNAs identified or suggested to be imported into mitochondria.

Another study proposed a similar approach based on the oxidation of guanosine induced by the accumulation of singlet oxygen generated from spatially confined fluorophores, but this system remains to be applied to mitochondria **(Li *et al.,* 2017; Li *et al.,* 2018).**

II. Experimental Results

II.A. 5S rRNA mediated anti-replicative strategy

During my thesis, I worked on two major projects related to mitochondrial RNA import. The first project was in continuity of the research performed by the laboratory on the development of an anti-replicative strategy targeting pathogenic mitochondrial DNA mutations.

Symptoms of mitochondrial pathologies due to mitochondrial genome mutations usually correlate with high mtDNA heteroplasmy level. One therapy approach would be to reduce the heteroplasmy level below the pathogenic threshold. Our laboratory previously identified import determinants required for 5S rRNA targeting into mitochondria **(figure 16)** and showed that the β-domain could be replaced by another RNA sequence without affecting the import ability **(Smirnov *et al.,* 2008)**. It has been demonstrated that mitochondrial targeting of recombinant 5S rRNA (rec.5S rRNA) harboring a RNA sequence complementary to mutated mtDNA region can induce a shift of heteroplasmy level in human *trans*mitochondrial cybrid cells. The results obtained with this anti-replicative strategy were promising, although efficiency of cellular expression of the rec.5S rRNA molecules remained very low **(Comte *et al.,* 2013)**. The first part of my thesis consisted in the pursuit of this work with the purpose to increase the cellular expression of the anti-replicative molecules and thus enhance the heteroplasmy shift. In this regard, my objectives were to:

i) Generate heteroplasmic cell lines stably expressing different anti-replicative rec.5S rRNAs molecules
ii) Estimate rec.5S rRNAs mitochondrial import *in vivo*
iii) Measure the effect of rec.5S rRNAs on heteroplasmy level in different cell growth conditions.
iv) Extend this anti-replicative approach to a point mutation of mtDNA.

II.A.1. Model of study

Previous work was focused on a large deletion of 7075bp (nt 8363 to 15438) of the mitochondrial genome associated with Kearn Sayre Syndrome (KSS). This deletion causes the disappearing of 9 protein encoding genes and 6 tRNA genes **(Comte *et al.*, 2013).** The team also developed the anti-replicative strategy for a point mutation in the *MT-ND5* gene (13514 A>G) associated with MELAS-like syndrome **(Tonin *et al.*, 2014) (Figure 19)**. The deletion in mtDNA causes the apparition of a new DNA sequence formed at the boundaries junction which highly differs from that of wild-type mtDNA. This facilitates the design of RNA molecules able to specifically discriminate mutant and wild-type mtDNA molecules. On the contrary, mtDNA bearing the point mutation only differs from wild-type mtDNA by one nucleotide, increasing the challenge to design specific anti-replicative molecules.

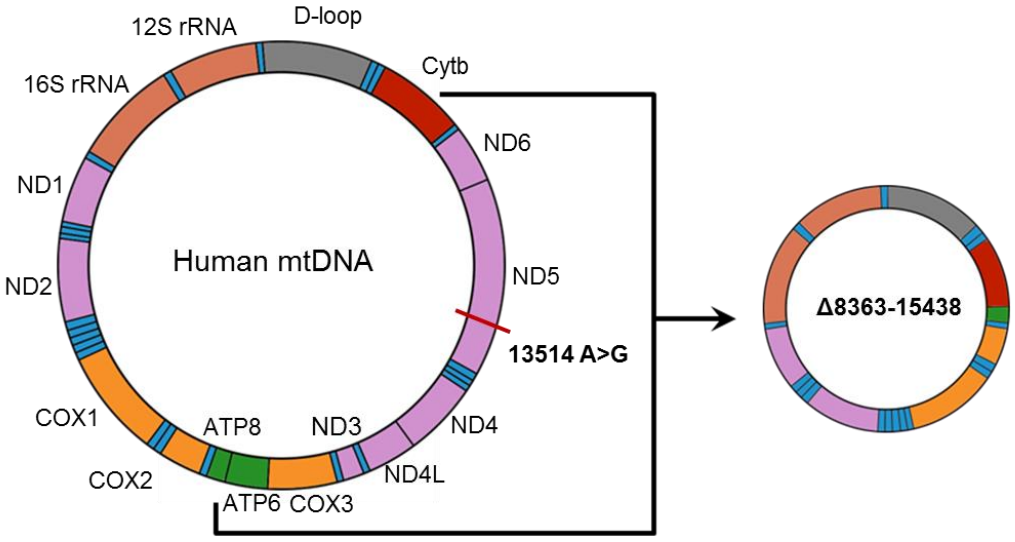

L strand 5′ …TTCTACTCCAAAGGCCACATCATCGAA… 3′
H strand 3′ …AAGATGAGGTTTCCGGTGTAGTAGCTT… 5′

L strand 5′ …CTCTTTACAGTGCTTACTTCTCTT… 3′
H strand 3′ …GAGAAATGTCACGAATGAAGAGAA… 5′

Figure 19. The two mtDNA mutations used as models for the anti-replicative strategy.

For each mutation, a part of the nucleotide sequence is presented. KSS deletion Δ8363-15438 causes the loss of 15 genes and creates a new sequence formed at the boundaries junction. The *MT-ND5* point mutation (13514 A>G) is highlighted in red.

Since no technology allows a direct modification of mtDNA, the only way to obtain immortalized cells containing heteroplasmic population of mutant and wild-type mtDNA consists in the generation of cybrid *trans*mitochondrial cell lines. Since these cells can be cultivated virtually indefinitely, they are a common model used for mtDNA studies. Cybrid (cytoplasmic hybrid) cells are created from the fusion of enucleated patients cells bearing mutation in mtDNA with immortalized cells deprived of mtDNA (ρ_0 cells) **(Figure 20A)**. Cybrid cell lines used in the work described here, were obtained by the fusion of patient's cytoplasts bearing either KSS deletion or the *MT-ND5* point mutation and the nuclei of immortalized ρ_0 osteosarcoma 143B cells **(Corona *et al.*, 2001; Comte *et al.*, 2013)**.

Previous work performed by our laboratory with stably expressed rec.5S rRNA molecules targeting the KSS deletion provided data on a decrease of heteroplasmy levels in several clones of cells. However plasmids bearing the gene of the anti-replicative molecules were inserted randomly into the genome of cybrid cells leading to relatively weak expression (about 30±5 rec.5S rRNA molecules/cell). Moreover, the different clones also harbored variable expression due to the insertion of the genes in different region of the nuclear genome, complicating the comparison of the effect of the different anti-replicative rec.5S rRNA. My work aimed to obtain increased and homogeneous expression levels of the rec.5S rRNA genes to enhance the heteroplasmy shift in the cybrid cell lines harboring either the KSS deletion or the *MT-ND5* point mutation. For this I used the Flp-In™ T-rex™ system **(Figure 20B)** which allows the integration of genes in transcriptionally active region of the nuclear genome. The first step consisted in the random integration of the Flp Recombination Target (FRT) site along with the LacZ-Zeocin fusion gene. By measuring the β-lactosidase activity provided by the fusion gene, we selected Zeocin-resistant clones were the FRT site was integrated in a transcriptionally active region of the nuclear genome. The selected clones were then transfected with pcDNATM5/FRT/TO plasmids containing different rec.5S rRNA genes. Co-transfection with the pOG44 plasmid expressing the Flp recombinase ensured the integration of the gene at the level of the FRT sites and thus provided a guaranty that the integration of the different rec.5S rRNA genes occurred in the same chromosome region.

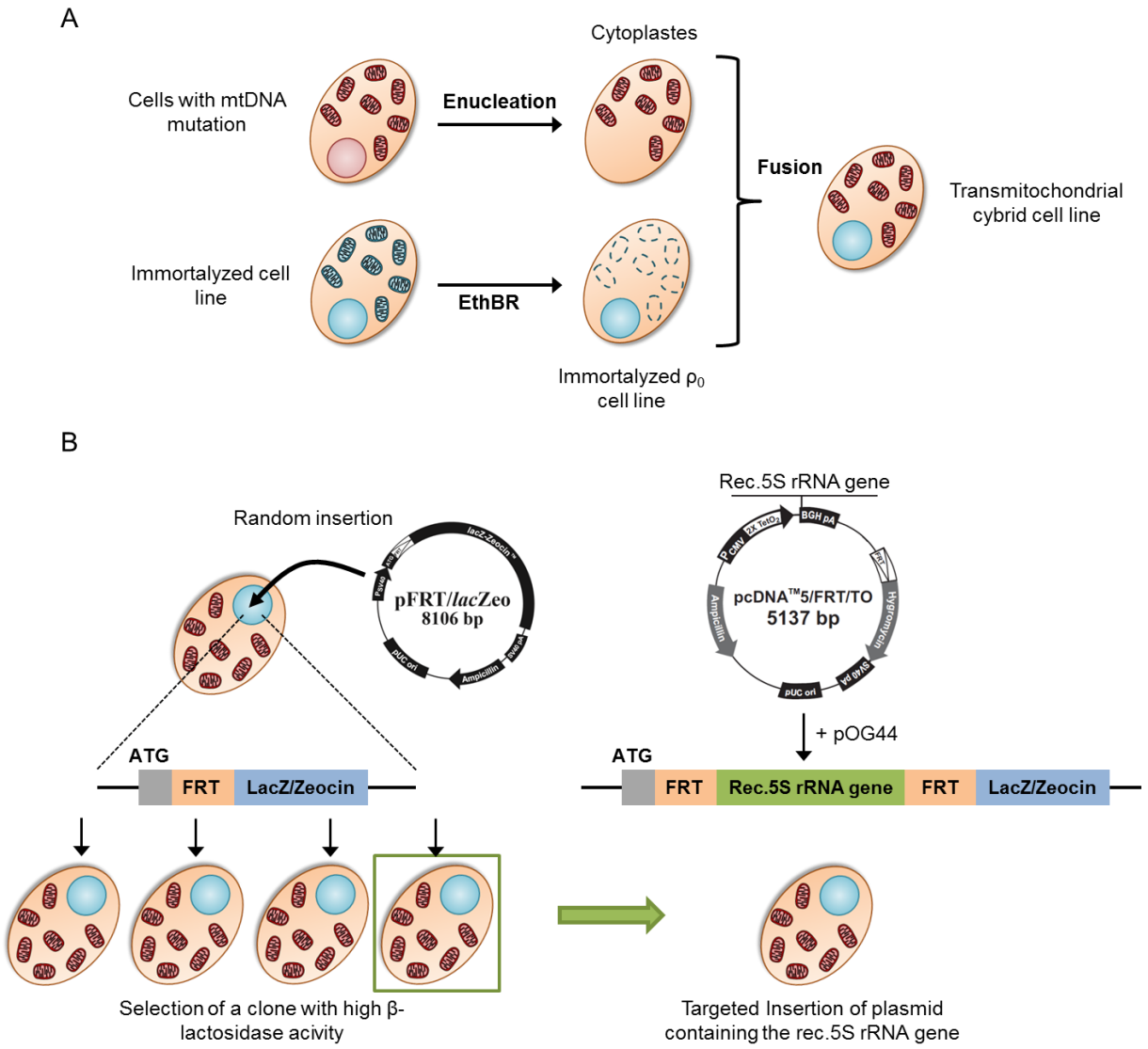

Figure 20. Targeted insertion of rec.5S rRNA molecules in *trans*mitochondrial cybrid cellular model using Flp-In™ T-REx™ system.

A) Generation of *trans*mitochondrial cybrid cell line. Cybrid cell lineS are generated by the fusion of immortalyzed ρ_0 cells (blue) and cytoplasts from patient harboring a mutation in mtDNA (red). Removal of mtDNA to generate ρ_0 cells is usually achieved by ethidium bromide (EthBr) treatment which intercalates in DNA and alters mitochondrial replication. **B)** The Flp-In™ T-rex™ system. Using Flp-In™ T-REx™ Core Kit, a recombination FRT site and the LacZ-Zeocin fusion gene are inserted randomly in the genome of cybrid cells bearing either the ND5 13514 A>G mutation or the KSS deletion. This allows the selection of zeocin-resistant transfected cells and the estimation of the transcription activity by measuring β-lactosidase activity. The selected clone is then co-transfected with the plasmid containing the rec.5S rRNA genes and the plasmid pOG44 expressing the Flp recombinase directing the insertion at the level of the FRT site.

II.A.2. KSS mutation heteroplasmy shift is modulated by cell growth conditions

The Flp-In^{TM} T-rex^{TM} system was first applied for the anti-replicative strategy targeting the KSS mutation in human cybrid cells aiming to increase the expression level of the anti-replicative rec.5S rRNAs compared to random insertion of the plasmids **(Comte *et al.*, 2013)**. Several clones of *trans*mitochondrial cybrid cells bearing the KSS deletion and containing an FRT sites (KSS-FRT-clone) were generated and selected by their β-galactosidase activity. Rec.5S rRNA molecules containing an insertion sequence targeting the KSS deletion were designed *in silico* in a way that the secondary structure of the 5S rRNA was retained and were selected based on their melting temperature prediction and ability to specifically hybridize to mutant mtDNA *in vitro*.

After introduction of the plasmid DNA bearing the selected rec.5S rRNA genes in the genome of the KSS-FRT-clone, the expression of the rec.5S rRNA molecules was measured by semi-quantitative RT-PCR, and the *in vivo* import inside mitochondria was assessed by Northern blot hybridization. The Flp-In^{TM} T-rex^{TM} system allowed an improvement of rec.5S rRNAs expression compared to the previous study (up to ≈ 2000 molecules per cell), although expression levels still varied between the cell lines. The effect of the rec.5S rRNA molecules on the KSS heteroplasmy was estimated by quantifying mutant and wild-type mtDNA molecules by qPCR. Of note, shifts in heteroplasmy levels were detected only for rec.5S rRNA versions targeting the L-strand of mtDNA. The decrease of the heteroplasmy was also dependent on the expression level of the rec.5S rRNA since lower expression of a same molecule did not impact the heteroplasmy level. The effect of the cell growth conditions on the heteroplasmy shift induced by the rec.5S rRNA molecules was also investigated. Applying selective conditions favorable for the cells where the mutant mtDNA proportion had been successfully decreased, id est in absence of glucose in the medium, improved the detection of the heteroplasmy shifts (for discussion of these data, see also section III.A).

In conclusion, the improved expression of the anti-replicative molecules based on 5S rRNA structure in human cybrid cells induced a stable shift in the heteroplasmy level of a large mtDNA deletion. This shift was dependent on the mtDNA strand targeted by the rec.5S rRNA and was increased for higher expression level of the

anti-replicative molecules. Moreover, the observed impact on heteroplasmy can be modulated by cell growth conditions. The results are presented in the recent publication **(Loutre *et al.*, 2018a)**

Publication : Loutre, R., Heckel, A.M., Jeandard, D., Tarassov, I., and Entelis, N. (2018a). Anti-replicative recombinant 5S rRNA molecules can modulate the mtDNA heteroplasmy in a glucose-dependent manner. PloS one *13*, e0199258.

PLOS ONE

RESEARCH ARTICLE

Anti-replicative recombinant 5S rRNA molecules can modulate the mtDNA heteroplasmy in a glucose-dependent manner

Romuald Loutre☯, Anne-Marie Heckel☯, Damien Jeandard☯, Ivan Tarassov, Nina Entelis*

UMR 7156 Génétique Moléculaire, Génomique, Microbiologie (GMGM), Strasbourg University-CNRS, Strasbourg, France

☯ These authors contributed equally to this work.
* n.entelis@unistra.fr

Citation: Loutre R, Heckel A-M, Jeandard D, Tarassov I, Entelis N (2018) Anti-replicative recombinant 5S rRNA molecules can modulate the mtDNA heteroplasmy in a glucose-dependent manner. PLoS ONE 13(6): e0199258. https://doi.org/10.1371/journal.pone.0199258

Editor: Johannes N. Spelbrink, Radboudumc, NETHERLANDS

Received: January 10, 2018

Accepted: June 4, 2018

Published: June 18, 2018

Data Availability Statement: All relevant data are within the paper and its Supporting Information files.

Funding: This work was supported by the CNRS, the University of Strasbourg, LIA (Laboratoire International Associé) ARN-mitocure and LabEx MitoCross (Programme Investissement Avenir, PIA). The funders had no role in study design, data collection and analysis, decision to publish, or preparation of the manuscript.

Abstract

Mutations in mitochondrial DNA are an important source of severe and incurable human diseases. The vast majority of these mutations are heteroplasmic, meaning that mutant and wild-type genomes are present simultaneously in the same cell. Only a very high proportion of mutant mitochondrial DNA (heteroplasmy level) leads to pathological consequences. We previously demonstrated that mitochondrial targeting of small RNAs designed to anneal with mutant mtDNA can decrease the heteroplasmy level by specific inhibition of mutant mtDNA replication, thus representing a potential therapy. We have also shown that 5S ribosomal RNA, partially imported into human mitochondria, can be used as a vector to deliver anti-replicative oligoribonucleotides into human mitochondria. So far, the efficiency of cellular expression of recombinant 5S rRNA molecules bearing therapeutic insertions remained very low. In the present study, we designed new versions of anti-replicative recombinant 5S rRNA targeting a large deletion in mitochondrial DNA which causes the KSS syndrome, analyzed their specific annealing to KSS mitochondrial DNA and demonstrated their import into mitochondria of cultured human cells. To obtain an increased level of the recombinant 5S rRNA stable expression, we created *trans*mitochondrial cybrid cell line bearing a site for Flp-recombinase and used this system for the recombinase-mediated integration of genes coding for the anti-replicative recombinant 5S rRNAs into nuclear genome. We demonstrated that stable expression of anti-replicative 5S rRNA versions in human *trans*mitochondrial cybrid cells can induce a shift in heteroplasmy level of KSS mutation in mtDNA. This shift was directly dependent on the level of the recombinant 5S rRNA expression and the sequence of the anti-replicative insertion. Quantification of mtDNA copy number in transfected cells revealed the absence of a non-specific effect on wild type mtDNA replication, indicating that the decreased proportion between mutant and wild type mtDNA molecules is not a consequence of a random repopulation of depleted pool of mtDNA genomes. The heteroplasmy change could be also modulated by cell growth conditions, namely increased by cells culturing in a carbohydrate-free medium, thus forcing them to use oxidative phosphorylation and providing a selective advantage for cells with improved respiration capacities. We

Competing interests: The authors have declared that no competing interests exist.

discuss the advantages and limitations of this approach and propose further development of the anti-replicative strategy based on the RNA import into human mitochondria.

Introduction

Mitochondria are essential organelles of human cells because of their fundamental roles in several critical cellular processes including energy generation, Fe-S clusters production, calcium homeostasis and apoptosis. They contain their own genome, in multiple copies per cell, allowing the synthesis of 13 polypeptides which are all essential components of the mitochondrial oxidative phosphorylation complexes in human cells. Mutations in mitochondrial DNA (mtDNA) have been associated with a wide variety of human disorders ranging from optic atrophy, deafness, diabetes to peripheral neuropathy or myopathy [1]. Most of the pathogenic mutations in human mtDNA are heteroplasmic (i.e. coexistence of mutant and wild-type genomes in a same cell) and their phenotypic expression is intimately linked to the ratio between mutant mtDNA molecules and wild-type ones (heteroplasmy level) [2]. This ratio can be variable in different tissues of the patient and even in different cells of the same tissue and can change with age [3]. Phenotypic expression of mtDNA mutations can be different for the various loads of the same mutation [4]. Typically, the biochemical defects and associated symptoms will only appear if the heteroplasmy level exceeds a given threshold generally comprised between 60% and 95% of mutant mtDNA, and subtle heteroplasmy changes can have dramatic effects on a patient's phenotype. Thus, the downshift of heteroplasmy level could potentially provide a therapeutic strategy for the mitochondrial disorders, and several laboratories work for establishing methods for removing detrimental mtDNA sequences (rev. in [5]).

For instance, the anti-genomic strategy consists in the specific cleavage of mutant mtDNA by targeted specific endonucleases [6], zinc finger nuclease [7] or transcription activator-like effector nuclease (TALEN) [8, 9]. Limitations of this strategy consist in important off-target cleavage, which leads to elimination of more than 85% of mtDNA pool thus decreasing the therapeutic potential (as it was recently demonstrated by Gammage et al. [10]), and the challenge to engineer the protein which has to recognize specific DNA sequences. MitoTALENs specificity also depends on the sequence of the DNA target site and thus not all the point mutations can be discriminated from the wild-type sequences [10].

Another approach, so-called anti-replicative strategy, consists in targeting mitochondria with small molecules able to specifically anneal with mutant mtDNA and to interfere with its replication [11, 12]. Many organisms import non-coding cytosolic RNAs into the mitochondria (rev. in [13–15]). Our team has studied the molecular mechanisms of yeast $tRNA^{Lys}$ import into yeast and human mitochondria [16, 17] and identified structural import determinants able to target oligonucleotides into mitochondria of human cells [18]. These mitochondrial RNA vectors had been applied to target anti-replicative oligonucleotides, designed to specifically anneal with mutant mtDNA, into human mitochondria. In these studies, RNA mitochondrial import induced the heteroplasmy shift in several cellular models: a) human cybrid cells and patient's fibroblasts bearing a heteroplasmic point mutation in ND5 gene [19] and b) human cybrid cell line bearing 60% of mtDNA affected by a large deletion (nucleotides 8363–15438) underlying a case of frequent mitochondrial pathology, the Kearns Sayre Syndrome (KSS) [12].

Another type of RNA mitochondrial vectors is based on 5S rRNA expressed in nucleus and partially imported into human mitochondria [20–22]. 5S rRNA is a highly conserved and

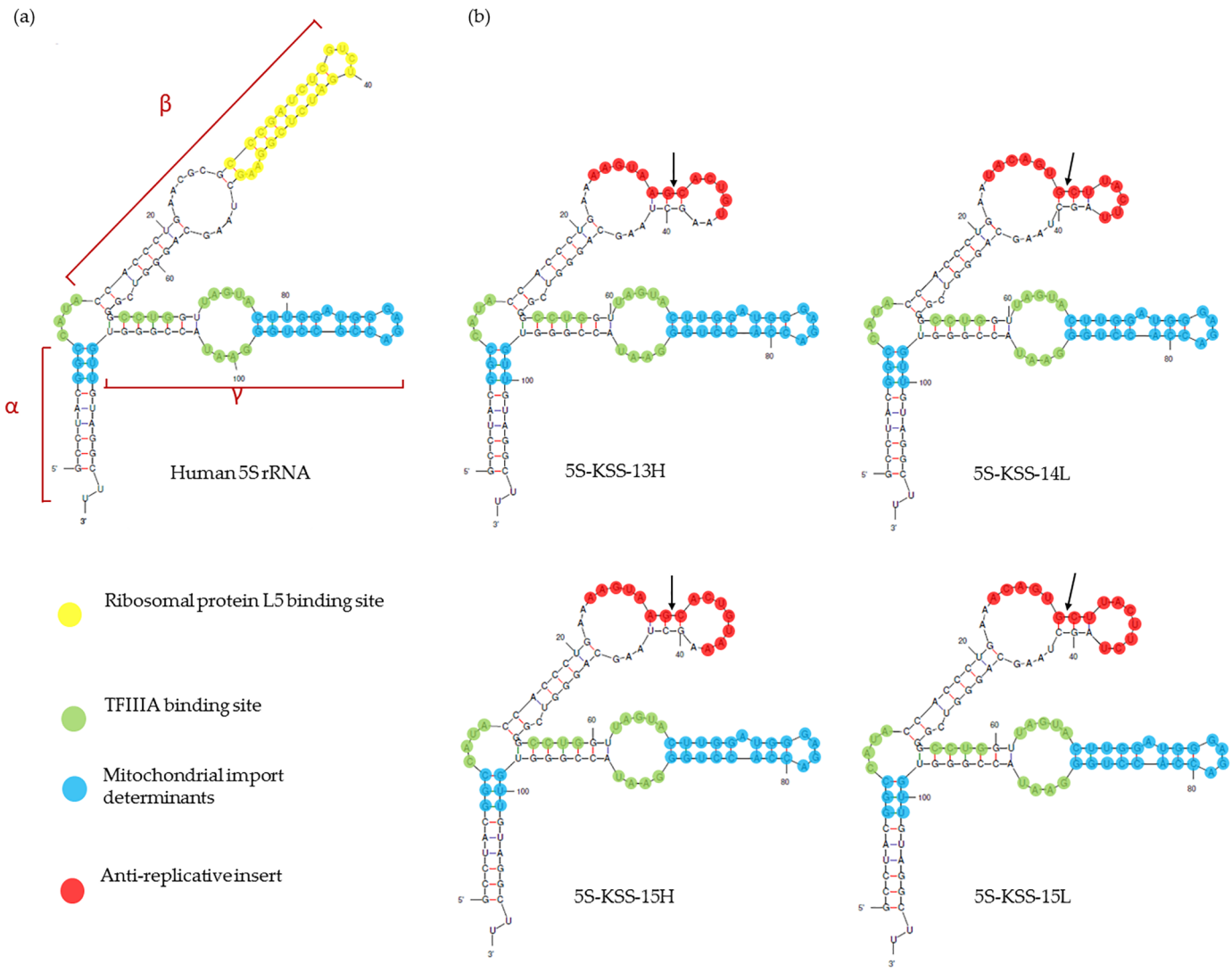

Fig 1. Secondary structure of wild type and recombinant 5S rRNAs. (a) Human 5S rRNA secondary structure, modified from [26]. (b) 2D structure of rec.5S rRNA versions, *mfold* predictions corrected manually. Sequences of the anti-replicative insertions (shown in red) correspond to boundaries of the KSS deletion in mtDNA; arrows indicate the deletion point.

https://doi.org/10.1371/journal.pone.0199258.g001

essential component of the large ribosomal subunit of all organisms, the only exceptions being mitochondrial ribosomes of yeast and mammals [23]. However, 5S rRNA seems to be the most abundantly imported RNA in mammalian mitochondria. Our studies demonstrated that 5S rRNA import mechanism relies on protein factors identified as the mitochondrial enzyme rhodanese and the precursor of mitochondrial ribosomal protein MRP-L18 [24, 25], interacting with two structural motifs located in the α and γ domains of 5S rRNA (Fig 1a), while a third motif corresponding to the distal part of the β domain and allowing the interaction with cytosolic ribosomal protein L5 may be either deleted or replaced without loss of import capacity [26]. This finding was exploited to demonstrate that 5S rRNA can function as a vector to deliver oligoribonucleotides into human mitochondria.

Our previous attempts to stably express 5S rRNA-based recombinant RNA (rec.5S rRNAs) in human cybrid cells resulted in a very weak expression level, estimated at merely 30±5 molecules per cell, though it allowed a moderate heteroplasmy shift. Moreover, variation in the

rec.5S rRNAs expression obtained in different clones of transfected cells led to diverse effects on the mitochondrial heteroplasmy level (no shifts were detected in 70% of clones) [12].

In the present study, we aimed to increase the expression level of anti-replicative rec.5S rRNAs in human cybrid cells in a stable manner, and to verify if this expression can decrease the proportion of mutant mtDNA.

Results

Design of recombinant 5S rRNA molecules

To use 5S rRNA as a mitochondrial vector targeting mtDNA molecules affected by the KSS deletion, the distal portion of the β-domain of 5S rRNA (Fig 1a) was replaced by sequences corresponding to either H- or L-strand (standard annotation of two mtDNA strands, Heavy and Light ones) of the mtDNA at the junction of the KSS deletion boundaries [12].

Previously, we designed two rec.5S rRNA versions bearing insertions corresponding to 13 nucleotides of the H-strand (5S-KSS-13H) or to 14 nucleotides of the L-strand (5S-KSS-14L) [12]. RNA 5S-KSS-13H was shown to be efficiently imported into isolated human mitochondria *in vitro* as well as *in vivo*, in cells transfected with corresponding RNA transcript [26]. In addition to these rec.5S rRNAs, we designed two new versions bearing insertions of 15 nucleotides (5S-KSS-15H and 5S-KSS-15L). For all these rec.5S rRNAs, the secondary structure predictions have been thoroughly analyzed (Fig 1b). All the versions were characterized by a classical 5S rRNA scaffold where the structure of the regions needed for interaction with transcription factor TFIIIA and the structural determinants of mitochondrial import have not been altered. *Cofold* analysis of the annealing between rec.5S rRNAs and the mutant mtDNA allowed prediction the length of the duplex region corresponding to 14 and 15 bp for 5S-KSS-14L and 5S-KSS-15L versions, and being slightly longer for 5S-KSS-13H and 5S-KSS-15H molecules (15 and 17 bp respectively, Fig 2). According to melting temperature predictions, Tm values are also different for rec.5S rRNAs targeting the L-strand of mtDNA (52.1˚C and 56.6˚C) and those targeting the H-strand (45.2˚C and 48.9˚C). Annealing of rec.5S rRNAs to wild-type mtDNA should be negligible at 37˚C. This has been directly demonstrated by *in vitro* hybridizations of labeled rec.5S rRNAs with mtDNA fragments under physiological conditions (S1 Fig); the signal can be detected only for mutant mtDNA but not for the fragments of wild type mtDNA.

Import of rec.5S rRNA molecules into human mitochondria

To evaluate the import efficiency of rec.5S rRNA variants *in vivo*, we transfected human cells with corresponding T7 transcripts as described previously [27]; RNA isolated from cells and from purified mitoplasts were analyzed by Northern blot hybridization (Fig 3 and S2 Fig).

Hybridization with a probe to mt $tRNA^{Val}$ clearly demonstrates the enrichment of mitochondrial RNA transcript in mitoplasts preparations (this is not so visible for 5S-KSS-13H transfection, since a larger amount of total RNA was loaded on gel). Comparing to this enrichment, the levels of cytosolic contamination (probe to 5.8S rRNA) in mitoplasts fractions were quite negligible (<5%), therefore the samples can be used for quantification. To estimate the import efficiencies for various rec.5S rRNA, the ratio between the signals of the rec.5S rRNA in the mitoplast fraction and in total RNA preparation was normalized to that of the mitochondrial $tRNA^{Val}$ in the same samples as described previously [26] (for details, see the Materials and methods section). Resulting import efficiencies obtained upon quantification of two transfection experiments were expressed as a percentage of the endogenous wild type 5S rRNA import efficiency (taken as 100%) estimated in control non-transfected cells (Table 1 and S2 Table).

	Annealing to KSS mtDNA	Annealing to wild-type mtDNA (5' deletion boundary)	Annealing to wild-type mtDNA (3' deletion boundary)
5S-KSS-13H 8357-8362 15438-15444	15b ; Tm = **52.1°C** 3'..UCGAAUGUCACGAAUGAAAAG..5' 5'..TCTTTACAGTGCTTACTTCTC..3	8b ; Tm = **17.3°C** 3'..UCGAAUGUCACGAAUGAAAAG..5' 5'..TCTTTACAGTGAAATGCCCC..3'	8b ; Tm = **27.3°C** 3'..UCGAAUGUCACGAAUGAAAAG..5' 5'..ACGCCCTCGGCTTACTTCTCT..3
5S-KSS-15H 8356-8362 15438-15444	17b ; Tm = **56.6°C** 3'..UCGAAAUGUCACGAAUGAAAAG..5' 5'..CTCTTTACAGTGCTTACTTCT..3	10b ; Tm = **31.7°C** 3'..UCGAAAUGUCACGAAUGAAAA..5' 5'..CTCTTTACAGTGAAATGCCCC..3'	8b ; Tm = **27.3°C** 3'..UCGAAAUGUCACGAAUGAAAA..5' 5'..AGACGCCCTCGGCTTACTTCT..3'
5S-KSS-14L 8356-8362 15438-15444	14b ; Tm = **45.2°C** 5'..GAAUACAGUGCUUACUUAG..3' 3'..GAAATGTCACGAATGAAGA..5'	7b ; Tm = **15.6°C** 5'..GAAUACAGUGCUUACUUAGC..3' 3'..GAAATGTCACTTTACGGGG..5'	8b ; Tm = **15.5°C** 5'..GAAUACAGUGCUUACUUAGC..3' 3'..TGCGGGAGCCGAATGAAGAG..5'
5S-KSS-15L 8357-8362 15438-15446	15b ; Tm = **48.9°C** 5'..AAACAGUGCUUACUUCUAG..3' 3'..AATGTCACGAATGAAGAGA..5'	6b ; Tm = **9.0°C** 5'..GAAACAGUGCUUACUUCUAGC..3' 3'..AAATGTCACTTTACGGGGTTG..5'	10b ; Tm = **27.6°C** 5'..GAAACAGUGCUUACUUCUAGC..3' 3'..CGGGAGCCGAATGAAGAGA..5'

Fig 2. Structure and melting temperatures predictions for duplexes between rec.5S rRNA and mutant or wild-type mtDNA regions. Upper part of each duplex corresponds to the anti-replicative insertion of rec.5S rRNA indicated at the left. Nucleotides complementary to the 5' boundary of the KSS deletion are shown in orange; those complementary to the 3' deletion boundary are in green. 5S-KSS-13H and 5S-KSS-15H annealed to the L-strand of mtDNA; 5S-KSS-14L and 5S-KSS-15L annealed to the H-strand of mtDNA.

https://doi.org/10.1371/journal.pone.0199258.g002

The data demonstrate that all the rec.5S rRNA molecules can be imported into human mitochondria at the levels comparable with that of endogenous 5S rRNA. Surprisingly, only one version, 5S-KSS-13H, was characterized by improved import abilities. The reasons for this are uncertain, additional studies of folding and detailed structure of this RNA molecule can help to further improvement of the recombinant RNA import into mitochondria.

Stable expression of rec.5S rRNA in human cybrid cells

Attempting to obtain an increased level of the stable expression of selected rec.5S rRNAs in human cybrid cells, we used the Flp recombinase-mediated integration of a gene of interest into specific genomic location by Flp-In™ T-Rex™ Core system (Invitrogen). To check the impact of rec.5S rRNA stable expression on the heteroplasmy level, we first had to introduce the FRT site into nuclear genome of the KSS cybrid cell line. These cells, obtained by the fusion of the patient's cytoplasts with nuclei of immortalized osteosarcoma cells, contain a heteroplasmic population of mutant and wild type mtDNA molecules and were characterized by a small decrease of oxygen consumption [12]. Zeocin-resistant clones obtained after transfection with the pFRT/*lac*Zeo plasmid were characterized by similar growth rates and by a single integrated FRT site, as determined by Southern blot hybridization (S3 Fig).

Because integration of the pFRT/*lac*Zeo plasmid into the genome occurs randomly, expression levels of the *lacZ*-Zeocin fusion gene will be dependent on the transcriptional activity of the surrounding sequences at the integration site. Thus, Zeocin-resistant clones were screened for β-galactosidase activity levels. For all of them, specific β-gal activities were 4 to 8-fold lower compared to the commercial HEK 293 T-Rex™ Flp-In ™ cells (S3 Table). Clone 5, selected for further experiments (referred to as FRT-KSS cell line), was characterized by the highest β-gal activity and by 51±5% KSS heteroplasmy level.

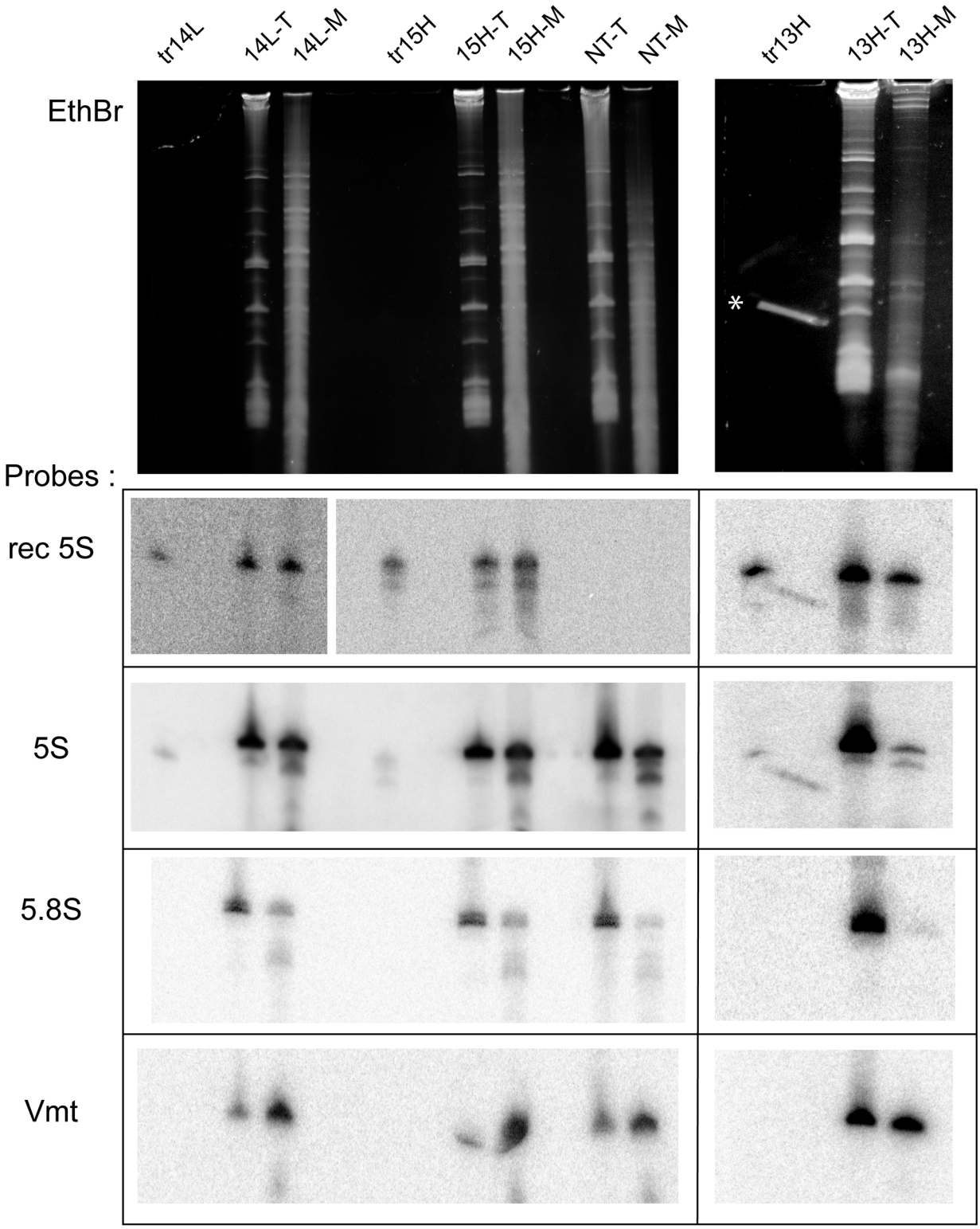

Fig 3. ***In vivo*** **test of rec.5S rRNA import into human mitochondria.** Northern blot analysis of rec.5S rRNA variants in total (T) and mitoplast (M) RNA preparations from cells transfected with various RNA, as indicated above the panels; NT, non-transfected cells; tr, 5ng of corresponding T7 transcript used for cell transfection. Gels stained with Ethidium bromide (EthBr) and hybridized with probes indicated at the left are shown. Rec 5S, probes corresponding to the insertion sequence specific for each rec.5S rRNA variant; 5.8S and Vmt, probes to cytosolic 5.8S rRNA and mitochondrial $tRNA^{Val}$. 5S, probe to 5S rRNA, can hybridize with endogenous 5S rRNA and with rec.5S rRNA versions (which are 5–8 nucleotides shorter), thus giving double bands clearly visible in 13H-M sample. The long strip marked by * on the panel "tr13H, EthBr" is due to an artifact; 5ng of the transcript (tr13H) can be visible only by probing.

https://doi.org/10.1371/journal.pone.0199258.g003

Table 1. Relative efficiencies of rec.5S rRNA mitochondrial import.

5S rRNA	Relative import efficiency, % of endogenous 5S rRNA
Endogenous 5S rRNA	100%
5S-KSS-13H	200 ± 30
5S-KSS-14L	90 ± 5
5S-KSS-15L	70*
5S-KSS-15H	90 ± 15

* Data of one transfection experiment

https://doi.org/10.1371/journal.pone.0199258.t001

Genes of rec.5S rRNA versions with natural flanking regions were cloned into pcDNA™5/FRT/TO vector and then integrated into FRT site of the nuclear genome of FRT-KSS cybrid cell line. Expression levels of rec.5S rRNAs have been assayed by semi-quantitative RT-PCR using corresponding T7-transcripts to create a calibration curve (Fig 4) and by real-time RT-qPCR (S4 Table).

We performed several independent transfections of FRT-KSS cells with pcDNA™5/FRT/TO plasmids. The first observation was that the expression of the transgenic rec.5S versions varied in different cell lines even though the FRT system is dedicated to provide a controlled level of expression directed from a given locus. Indeed, we generated lines either with high rec.5S rRNAs expression levels (referred for as 5S-KSS-13H$^{(1)}$ and 5S-KSS-14L$^{(1)}$), or those characterized by low expression for 5S-KSS-13H, 5S-KSS-14L and 5S-KSS-15L, or a medium expression level for 5S-KSS-15H (Table 2 and S4 Table). One may explain the observed variability in the expression level by multiple insertions of pcDNA™5/FRT/TO-13H and -14L plasmids into nuclear genome in the case of the best expressers 5S-KSS-13H$^{(1)}$ and 5S-KSS-14L$^{(1)}$, while single copy of rec.5S rRNA gene has been integrated in other transgenic lines. If this stands true, it can indicate that the rec.5S rRNAs expression level could be improved by integration of multiple copies of rec.5S rRNA gene in nuclear genome.

Shift of the heteroplasmy levels in transgenic cell lines

To check if the stable expression of rec.5S rRNA molecules can induce a mtDNA heteroplasmy shift in the human cybrid cells, we cultivated FRT-KSS cell lines for 8 weeks and measured the mutant mtDNA load by real-time qPCR as described previously [12]. Cells issued from independent transfections were cultivated separately, each one divided into 4 parallel cultures.

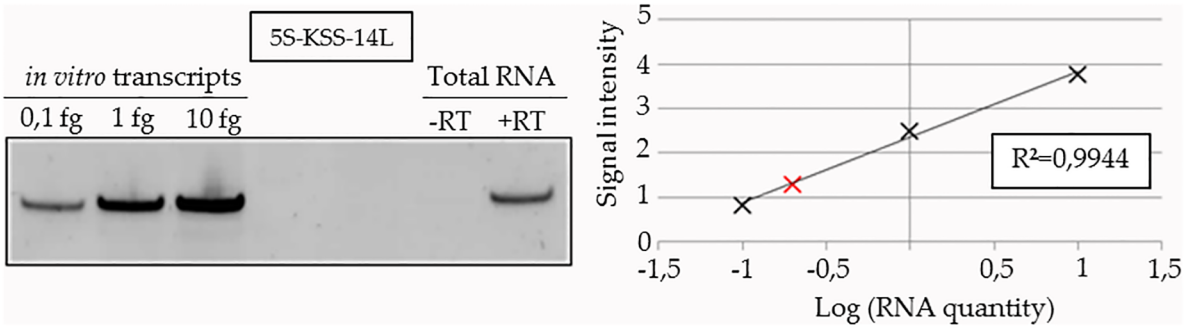

Fig 4. Quantification of 5S-KSS-14L RNA expression by semi-quantitative RT-PCR. On the left, PAGE analysis of the RT-PCR reactions performed on the total cellular RNA or known amounts of purified T7-transcripts, as indicated above the panel. On the right, an example of the calibration curve used for quantification of 5S-KSS-14L RNA (in red) in cybrid cell line.

https://doi.org/10.1371/journal.pone.0199258.g004

Table 2. Amounts of anti-replicative molecules in rec.5S rRNA expressing cell lines.

Rec.5S rRNA	Number of rec.5S rRNA/cell
5S-KSS-13H$^{(1)}$	2000±200
5S-KSS-13H	200±30
5S-KSS-14L$^{(1)}$	2000±200
5S-KSS-14L	300±50
5S-KSS-15H	1300±200
5S-KSS-15L	200±30

https://doi.org/10.1371/journal.pone.0199258.t002

Total DNA was isolated from a portion of cells every 2 weeks and analyzed by 2–3 independent qPCR experiments with each measure performed in triplicates. First, we compared the KSS heteroplasmy levels in the transgene and control cell lines after cultivation in a high glucose medium, but failed to detect any significant shift of the proportion between mutant and wild-type mtDNA molecules during 8 weeks cultivation (Fig 5a, "high glucose" samples).

To investigate if the selection for better mitochondrial respiration could create an advantage for cells with decreased heteroplasmy levels, we cultivated transgenic cells in a carbohydrate-free medium. In these conditions, only pyruvate and amino acids are available as carbon sources and cells should rely on mitochondrial oxidative phosphorylation to produce ATP.

Cybrid cells FRT-KSS were able to grow in a medium without addition of glucose and demonstrated only little heteroplasmy variations after 8 weeks of culture (Fig 5a) indicating that there were no significant random fluctuations in heteroplasmy. In all transfected cell lines with low expression of rec.5S rRNA versions, a very moderate decrease of the KSS heteroplasmy level has been observed in selective conditions. Statistically significant impact on the heteroplasmy has been detected only in 5S-KSS-15H expressing cells, where the mutation load was shifted from 51±4% to 41±2% (P-value$<$0.01) (Fig 5a). For this cell line, we obtained a tiny decrease (about 5% of heteroplasmy shift) after 4 weeks of cultivation (not shown), after 8 weeks we detected statistically significant decrease (10% of heteroplasmy shift), and this level didn't change during further cultivation up to 4 months, and remained stable after freezing-thawing of the cells.

We next applied selective conditions to the cell lines with best expression of a rec.5S rRNA, namely 5S-KSS-13H$^{(1)}$ and 5S-KSS-14L$^{(1)}$. In the case of 5S-KSS-13H$^{(1)}$, proportion of the mutant mitochondrial genomes has been significantly decreased in a clear time-dependent manner to reach 13±3% (Fig 5b). This level was thereafter stable during cell cultivation in a media either with or without glucose. Noteworthy, the 5S-KSS-13H RNA was characterized by 2 fold improved import into mitochondria (Table 1), which may explain, along with its high expression, the improved effect on the heteroplasmy load compared to the other rec.5S rRNA versions.

We suppose that the stable expression and mitochondrial import of the anti-replicative 5S rRNAs in cybrid cells can induce a shift of equilibrium between mutant and wild-type mitochondrial genomes. This shift can be more or less dramatic depending on the level of 5S rRNA expression. Thereafter, cells can adapt to a new equilibrium (may be by reprogramming of metabolic pathways, as it was demonstrated for MELAS mutation in [4]) and the obtained new heteroplasmy level remains stable during further cultivation.

On the other hand, high expression of the 5S-KSS-14L$^{(1)}$ version did not induce an important decrease of heteroplasmy. Since two rec.5S rRNA versions, 13H and 14L, are designed to target different mtDNA strands, one can hypothesize that the different anti-replication action of these rec.5S rRNA molecules may be related to the asymmetric replication mechanism specific for mammalian mtDNA (see Discussion for details).

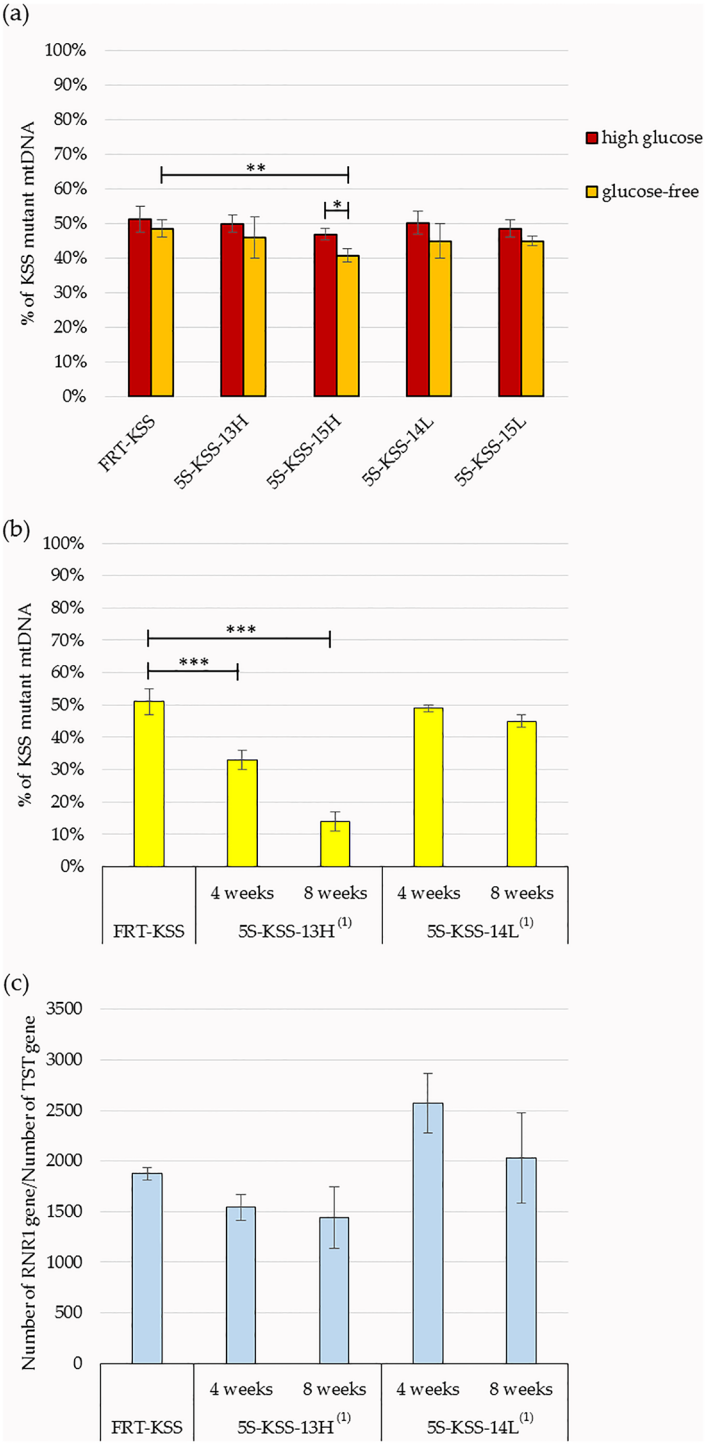

Fig 5. Effect of rec.5S rRNA expression on the heteroplasmy level of KSS mutation. (**a**) Proportion of KSS mtDNA (Y axis) in cybrids cell lines with low expression of rec.5S rRNA versions (see Table 1) after 8 weeks of cultivation in high glucose or glucose-free media, as indicated. (**b**) Time-depended decrease of KSS mutation load in cells expressing high amounts of rec.5S rRNAs 5S-KSS-13H$^{(1)}$ and 5S-KSS-14L$^{(1)}$ in glucose-free medium. (**c**) MtDNA copy numbers normalized to nuclear gene *TST1*, measured in the same cell populations as in (**b**). Cells issued from independent transfections were cultivated separately; each population was divided into 4 parallel cultures. Total DNA was isolated from a portion of each cell cultures every 2 weeks and analysed by 2–3 independent qPCR experiments, each measure performed in triplicates. Standard deviations are calculated from qPCR data obtained on the independently cultured cells (n = 4). Statistical differences were determined with a two-tailed Student's *t*-test (*, $p < 0.05$; **, $p < 0.01$; ***, $p < 0.001$).

https://doi.org/10.1371/journal.pone.0199258.g005

To ascertain the absence of a non-specific effect on replication that could reduce total mtDNA copy number in transfected cells, we estimated mtDNA amounts in FRT-KSS cybrid cell line before transfection, and in 5S-KSS-13H$^{(1)}$ and 5S-KSS-14L$^{(1)}$ cells after 4 and 8 weeks of cultivation in glucose-free medium (Fig 5c). Using real-time PCR, we measured a copy number of all mtDNA molecules (gene 12S rRNA) compared to nuclear DNA (gene of rhodanese *TST1*). We detected ≈20% decrease of mtDNA copy number in 5S-KSS-13H$^{(1)}$ cell line. In theory, inhibition of the replication of 50% of mtDNA genomes (bearing KSS mutation) should cause a 25% decrease of mtDNAcn after one round of the replication. It is difficult to build a mathematical model for the action of anti-replicative molecules, since we do not know the velocity of mtDNA replication and exact level of affected mutant genomes. Still, some small level of mtDNA copy number downshift can be anticipated. Noteworthy, in case of an unspecific effect on mitochondrial replication process, we might expect a much more important depletion of mtDNA due to replication stalling of both, mutant and wild type mitochondrial genomes. Therefore, our results indicate that no depletion effect has been caused by an eventual off-target effect on the wild-type mtDNA replication.

Obtained new data indicate that the impact of anti-replicative rec.5S rRNA molecules on the mutant mtDNA load is strongly dependent on the amount of rec.5S rRNA molecules. High levels of RNA expression and mitochondrial import seem to be necessary to affect the mutant mtDNA replication and thus change the proportion between mutant and wild-type mitochondrial genomes.

Discussion

5S rRNA as a mitochondrial RNA vector

Natural pathway of small non-coding RNA trafficking into mitochondria has been described in phylogenetic groups as diverse as protozoan, plants, fungi and animals [28, 29]. Small 5S ribosomal RNA is one of the most abundant cytosolic RNA imported into mitochondria. It had been reported that 5S rRNAs are expressed from large nuclear gene arrays (100–200 genes) and that a small portion of its cellular pool can readily be found within mitochondria in different organisms, from flies to humans [20, 21, 30]. In mammals, the mitochondrial function of 5S rRNA is not known. Cryo-electronic microscopy analysis recently demonstrated that the mitochondrial ribosomes from pig liver and human cultured cells do not contain 5S rRNA, but its place in the central protuberance of the large ribosomal subunit is occupied by mitochondrial tRNA^{Phe} or tRNA^{Val} correspondingly [31, 32]. The absence of the canonical function for 5S rRNA in human mitochondria raised some doubts concerning its mitochondrial import [33, 34]. This opinion, not supported by direct experimental data, does not make a distinction between two independent points: 1) mitochondrial localization of a small portion of the cytosolic 5S rRNA pool and 2) 5S rRNA integration into the large subunit of the mitochondrial ribosome. The absence of 5S rRNA in the large ribosomal subunit does not refute the ability of the mammalian organelle to import RNA from the cytoplasm. Moreover, the mitochondrial import of small amounts of RNA may indicate on a regulatory function of these molecules, for instance, 5S rRNA might participate in the assembly of mitochondrial ribosome (I. Tarassov, in preparation).

Even being rather inefficient compared to protein mitochondrial import, RNA targeting can be used to address into human mitochondria tRNA molecules replacing those affected by mtDNA mutation [18, 35] or the anti-replicative oligonucleotides with a therapeutic potential [12, 19, 36].

We previously demonstrated that 5S rRNA can function as a vector to deliver oligoribonucleotides into human mitochondria, and this principle has been successfully applied by three

independent laboratories [30, 37, 38]. In the present study, we analyzed mitochondrial import of four 5S rRNA molecules bearing the 14–15 bases substitutions in the distal portion of the β-domain. We detected the presence of all the rec.5S rRNA versions in purified mitoplasts, and their import efficiencies were close to that of endogenous wild type 5S rRNA.

In contrast to small artificial anti-replicative RNAs used previously for the transient transfection of human cells [19], recombinant molecules based on 5S rRNA structure can be expressed in cells in a stable manner due to the internal promoter region recognized by RNA Polymerase III, then be processed, exported from the nucleus and imported into mitochondria. Nevertheless, the discrepancy between 100–200 copies of wild-type 5S rRNA gene and a unique gene of rec.5S rRNA per genome creates a competition between 5S rRNA molecules for the transcription, maturation and export protein factors. Thus, the high expression of rec.5S rRNA molecules in human cells should be a prerequisite of their anti-replicative activity.

Expression of anti-replicative rec.5S rRNA molecules

In the present study, we used the Flp recombinase-mediated integration of a gene of interest into transcriptionally active genomic location. This approach allowed an improvement of rec.5S rRNAs expression compared to the random insertion of plasmid DNA bearing rec.5S rRNA genes [12]. Nevertheless, a significant heteroplasmy shift has been detected in cells bearing only one version of rec.5S rRNA genes, namely 5S-KSS-13H, expressed at the high level (Table 2). Lower expression of the same molecule did not affect mutant mtDNA load, indicating on an anti-replicative RNA concentration threshold. Surprisingly, 5S-KSS-15H version, which differs by 2 bp longer duplex predicted with mutant mtDNA, provided only a small heteroplasmy decrease. This can be explained by a slightly lower expression and lower mitochondrial import of this RNA. Another difference between these constructs consists in direct orientation of 5S-KSS-15H gene in respect to CMV promoter in the pcDNA™5/FRT/TO cloning vector, in contrast with the inverse orientation of 5S-KSS-13H gene. Thus, we cannot exclude possible synthesis of a longer 5S-KSS-15H transcript from external CMV promoter, which could be detected by RT-PCR therefore compromising the full-size 5S-KSS-15H RNA quantification. These considerations should be taken into account in the further studies aiming to increase the expression of anti-replicative RNA molecules in a more reproducible way by using constructs bearing only promoters for RNA polymerase III.

The mechanism of human mtDNA replication is still a subject of intense debate (rev. in [39]). The idea of anti-replicative heteroplasmy shift as a therapeutic strategy [11] was initially based on the strand-displacement mtDNA replication model [40] that suggested the existence of long single-stranded replication intermediates (S4 Fig). Discovery of RNA-DNA hybrid intermediates gave rise to RITOLS model (Ribonucleotide Incorporation Throughout the Lagging Strand) [41]. A third model proposed conventional strand-coupled DNA synthesis, initiating from sites dispersed across the broad zone named ori Z [42]. Apparently, all the three mtDNA replication mechanisms can take place in mitochondria, depending on the growth conditions and the energetic state of the cells. For instance, recent analysis of mtDNA replication in mice tissues had shown that liver and kidney cells use the asynchronous mechanism, while heart, brain and skeletal muscle employ a strand-coupled replication mode [43].

Previously, we have directly demonstrated mtDNA replication stalling induced by small anti-replicative RNA, detected as a new replication intermediate on 2D agarose gel [12]. This stalling, occurred at the site of the RNA annealing due to impairing of the replication fork progression, which can be suggested for all the three current models of mtDNA replication (S4 Fig), since the replisome helicase is unable to displace RNA from the short RNA-DNA hybrids [42]. Our present data indicate that anti-replicative RNAs 5S-KSS-13H and 5S-KSS-15H,

bearing insertions complementary to mtDNA L-strand, are able to induce a downshift of the KSS mutation load. Expression of two other rec.5S rRNA versions, 5S-KSS-14L and 5S-KSS-15L, designed to target the H-strand of mtDNA, had no significant impact on the KSS heteroplasmy level. This can be related to asymmetric strand-displacement mechanism of human mtDNA replication, supposing that at the first step, only L-strand is used as a template for DNA synthesis [40], therefore, its targeting by anti-replicative RNAs 5S-KSS-13H and 5S-KSS-15H, as shown schematically on S4 Fig, should be more efficient compared to the H-strand targeting RNAs. This is relevant to recently published data providing a strong support of the strand-displacement model of mtDNA replication in cultured cells [44].

One should also take into account that melting temperatures predicted for rec.5S rRNA-mtDNA duplexes are lower for 5S-KSS-14L and 5S-KSS-15L versions (45.2˚C and 48.9˚C) compared to 5S-KSS-13H and 5S-KSS-15H ones (52.1˚C and 56.6˚C, Fig 2). This can provide another reason for the poor anti-replicative abilities of 5S-KSS-L versions. Noteworthy, a very recent paper from the lab of Pierre Rustin [45] provided a set of evidences that human mitochondria are maintained at close to 50˚C if the respiratory chain is functional. We can hypothesize that in fully active mitochondria, 5S-KSS-14L and 5S-KSS-15L RNAs cannot anneal to mtDNA due to increased temperature in mitochondrial matrix.

All these considerations will help to optimize the anti-replicative RNA structure and to design rec.5S rRNA molecules targeting not only mtDNA deletions, but also pathogenic point mutations, as it was done for small artificial RNAs [12].

Selective cell growth conditions improved the anti-replicative RNA effect

Warburg and Crabtree effects describe the ability of rapidly proliferating cells to favor glycolysis. Recent studies suggest that cells can adapt to mitochondrial dysfunction by switching to glycolysis, despite aerobic conditions [46]. Development of *trans*mitochondrial cybrids by fusion of enucleated somatic cells harboring pathological mtDNA mutations with a cell line depleted of their mtDNA has enabled the study of consequences of mtDNA mutations [47]. However, cybrid cells cultured in media with high concentrations of glucose tend to acquire highly glycolytic phenotypes, which make them less suitable as models for studying mitochondrial dysfunction.

Attempts have been made to overcome this phenomenon, by substituting glucose with galactose, which does not support anaerobic glycolysis [48]. This is usually explained by the fact that galactose cannot be oxidized to pyruvate without prior conversion to glucose, which consumes two molecules of ATP, thus making anaerobic glycolysis useless as a source of energy [49]. Nevertheless, some cell lines cannot utilize galactose, but can grow in a carbohydrate-free media, apparently relying on the metabolism of pyruvate and amino acids, thus galactose-containing media can be replaced by carbohydrate-free ones. It was demonstrated that the activity of all respiratory chain complexes tended to be higher in the glucose-starved cells [50], since they are forced to rely on mitochondrial oxidative phosphorylation to meet their energy requirements.

Previously, few studies addressed the question of metabolically induced mtDNA heteroplasmy shifting. The ketogenic medium has been shown to shift the heteroplasmy level of cybrid cells towards the wild type [51]. Another report demonstrated that the apparently homoplasmic 100% MELAS cybrid cells kept in low-glucose medium have shifted their heteroplasmy level to 90% [52]. However, a more recent publication from the same research team demonstrated that the improvement of mitochondrial function in MELAS cybrid cells exposed to a diet combining low glucose and ketone bodies was not connected to a heteroplasmy shift, but to increase of the mtDNA copy number [53], therefore, the selective pressure alone was not capable to induce the heteroplasmy shift.

Noteworthy, in our experiments, shifts in mutant mtDNA proportion have been detected only for cells cultivated in a medium poor in glucose. These data are in accordance with the hypothesis that culturing mutant cells in a low-glucose medium and thus forcing them to use oxidative phosphorylation would create a selective advantage for cells with improved respiration capacities.

Conclusions

In the present study, we attempted to induce the heteroplasmy shifting by stable expression of anti-replicative 5S rRNA molecules capable to slow the mutant mtDNA replication in human *trans*mitochondrial cybrid cells and thus decreasing proportion between mutant and wild type mtDNA molecules. We provide the strategy of anti-replicative rec.5S rRNA selection based on the melting temperature prediction and analysis of mitochondrial import. The heteroplasmy shift, dependent on the level of the recombinant 5S rRNA expression and import, can be modulated by cell growth conditions. Applying selective conditions favorable for the cells where the mutant mtDNA proportion has been successfully decreased, allowed detection of the change in heteroplasmy load for cybrid cells bearing a large deletion in mtDNA. In contrast to recently developed engineered nuclease technology, which induced a substantial off-target effects and a significant depletion of mtDNA [10], we detected only a small decrease of mtDNA copy number, which can be caused by the stalling of the mutant KSS genomes replication. This indicates that the decreased proportion between mutant and wild type mtDNA molecules is not a consequence of a random repopulation of depleted pool of mtDNA genomes, but can be induced by the anti-replicative 5S rRNA expression.

Considering the possible therapeutic applications, the advantage of the stable rec.5S rRNA expression consists in non-reversible heteroplasmy shift, in contrast with a transient KSS mutation load decrease obtained previously by use of small anti-replicative RNAs [12]. Nevertheless, we detected the obvious limitations of the approach used: need of high level of rec.5S rRNA expression and an important variability of this level in transfected cells, influencing the impact on the heteroplasmy. Further development of the strategy can be achieved by integration of multiple copies of anti-replicative rec.5S rRNA molecules expressed from external PolIII promoter by use of plasmid or viral vectors.

In conclusion, our data demonstrate that expression of anti-replicative molecules based on 5S rRNA structure in human cybrid cells can induce a stable shift in a heteroplasmy level of pathogenic mutations in mtDNA. This shift, dependent on the rec.5S rRNA sequence and the level of its expression, can be modulated by cell growth conditions, thus opening possibility to improve models of gene therapy exploiting the anti-replicative strategy.

Materials and methods

Human cell lines and culture conditions

Human *trans*mitochondrial cybrid cells containing 65±2% of mtDNA molecules affected by KSS deletion (nucleotides 8363–15438) obtained by the team of Dr A. Lombes, Inst. Cochin, Paris [12] were cultivated in DMEM medium (Sigma) containing 4.5 g/L glucose, 0.584 g/L L-glutamine and supplemented with 50 mg/L uridine and 3.7 g/L sodium bicarbonate (for glucose-rich conditions). For glucose-free conditions, DMEM base (Sigma) was supplemented with 50 mg/L uridine, 3.7 g/L sodium bicarbonate, 0.584 g/L L-glutamine and 108 mg/L sodium pyruvate. Cybrid cells transfected with pFRT/*lacZeo* were cultivated in media containing 100 μg/mL Zeocin (Invitrogen). Cells transfected with pcDNA™5/FRT/TO were cultivated in media supplemented with 150μg/mL Hygromycin B-Gold (InvivoGen).

Design and synthesis of recombinant 5S rRNA molecules

Secondary structures of rec.5S rRNA were predicted using the *Mfold* software [54] and corrected in accordance with data on human 5S rRNA structure [55]. Analysis of the annealing between rec.5S rRNAs and the mtDNA was performed by *RNAcofold web server*, University of Vienna. To estimate melting temperatures for RNA-DNA duplexes, we used IDT Sci-Tools *OligoAnalyzer 3.1* software [56].

Rec.5S rRNAs were obtained by T7 transcription using the T7 RiboMAX Express Large-Scale RNA Production System (Promega) and gel-purified. To create PCR templates, we used a two-step protocol: PCR1 was performed on a plasmid bearing the human 5S rRNA sequence under the control of the T7 promoter [26] using forward primer n˚1 and reverse primers n˚2 to 5 (S1 Table). Resulting PCR1 product was used as forward primer for PCR2 performed on the same plasmid template with reverse primer n˚6 creating a DNA fragment containing rec.5S RNA sequence under the control of the T7 promoter. Plasmid or PCR fragment were cleaved by BglII (Fast Digest, ThermoScientific) to assure formation of the exact 5S rRNA 3' end.

Rec.5S rRNA *in vitro* hybridization and *in vivo* import test

To test specific rec.5S rRNA annealing with target mtDNA, wild-type or mutant mtDNA fragments (nucleotides 15,251–15,680 of wild-type mtDNA or 8,099–8,365/15,438–15,680 of mutant mtDNA) were amplified as described previously [12] using primers n˚7 and 8 or n˚8 and 9 respectively, separated on 1% agarose gel, blotted to Amersham Hybond-N membrane (GE Healthcare) and hybridized with ^{32}P-labeled recombinant RNA in 1X PBS at 37 ˚C. Hybridization signals were revealed by Typhoon Trio (GE Healthcare).

The *in vivo* import assay on the cells transfected with rec.5S rRNA molecules was performed as described previously [17, 26, 27]. Briefly, 40h post transfection, cells were disrupted, mitochondria were isolated by differential centrifugation, treated with RNase A (Sigma) 10 μg/ml for 10 min at 25˚C, washed three times, then treated with of 0.1% digitonin (Sigma) solution for 10 min at 25˚C to disrupt the mitochondrial outer membrane. The mitoplast pellet was washed and resuspended in TRIZol reagent (Invitrogen). RNA isolated from the mitoplasts and from an aliquot of the transfected cells were separated by 8% urea-PAGE and analysed by Northern blot hybridization with ^{32}P-labeled oligonucleotide probes (S1 Table, n˚25–29). To avoid the discrepancies caused by the loading of different amounts of material, we used the hybridization signals corresponding to the mitochondrial tRNA^{Val} as a loading control. Thus, we take into account not the absolute intensity of hybridization signals but the ratio between the signals corresponding to rec.5S rRNAs and the host mitochondrial valine tRNA either in mitoplast RNA preparations (Ratio I) or in the total cellular RNA (Ratio II). Import efficiency of each rec.5S rRNA was calculated as a quadruple ratio between Ratios I and II and expressed in the form of percentage of the efficiency thus obtained for the endogenous wild type 5S rRNA in non-transfected cells.

$$\text{Import efficiency} = \frac{\text{RI}}{\text{RII}}$$

$$\text{RI (mitoplast RNA)} = \frac{\text{rec.5S rRNA}}{\text{mt tRNA Val}}$$

$$\text{RII (total RNA)} = \frac{\text{rec.5S rRNA}}{\text{mt tRNA Val}}$$

Cytosolic contamination was checked by hybridization with a probe to 5.8S rRNA, a component of cytosolic ribosomes. The levels of cytosolic contamination were subtracted from the

import efficiency values for each rec.5S rRNA version (S2 Table). In control experiments, mitochondria were lysed before RNase treatments to demonstrate that all the RNAs were completely degraded (not shown).

Production of a human transmitochondrial cybrid cell line bearing FRT site

To generate a KSS cybrid cell line bearing an FRT site, we used the Flp-In™ T-Rex™ Core system (Invitrogen). Cybrid cells were transfected with the pFRT/*lacZeo* plasmid according to the manufacturer's protocol, and Zeocin-resistant clones were isolated.

To determine the number of FRT sites in each zeocin-resistant clone, genomic DNA was extracted, digested with HindIII (ThermoScientific), separated on a 1% agarose gel and blotted to Amersham Hybond-N membrane (GE Healthcare). To detect FRT sites, a fragment of the *lacZ* gene was amplified according to the manufacturer's protocol (Invitrogen) and ^{32}P-labelled using Prime-a-gene Labelling System (Promega). After hybridization at 65˚C and washing, signals were revealed by phosphorimaging in Typhon Trio (GE Healthcare).

Specific β-galactosidase activity in cellular lysate were determined for each clone by use of the β-gal assay kit (Invitrogen) following manufacturer's instructions and quantified as nmol of hydrolyzed substrate ONPG/30 min/mg of cellular protein.

Generation of transmitochondrial cybrid cell lines expressing rec.5S rRNA

Rec.5S rRNA genes were obtained by a two-step protocol: 1) PCR1 with partially overlapping primers: forward primers n˚10 (for 5S-KSS-15H and 5S-KSS-15L) or n˚12 (for 5S-KSS-13H and 5S-KSS-14L) and reverse primers n˚2 to 5. 2) Resulting DNA fragments were used as forward primers for PCR2 with reverse primer n˚11 (for 5S-KSS-15H and 5S-KSS-15L) or n˚13 (for 5S-KSS-13H and 5S-KSS-14L) and a plasmid containing human 5S rRNA gene with flanking regions [26] as a template.

Then, rec.5S rRNA genes were cloned into the pcDNA™5/FRT/TO plasmid vector (Invitrogen) and verified by sequence analysis. Cybrid FRT-KSS cells were co-transfected with pcDNA™5/FRT/TO-rec.5S rRNA constructs and pOG44 plasmid encoding Flp recombinase (Invitrogen) at a molar ratio 1:10 using Lipofectamine 2000 (Invitrogen). Forty-eight hours after transfection, Hygromycin B-gold (150μg/mL) (Invitrogen) was added to the medium for selection.

Rec.5S rRNA quantification

Total cellular RNA was isolated with TRIZol reagent (Invitrogen). Levels of rec.5S rRNA expression were assayed by semi-quantitative RT-PCR with forward primers specific to the anti-replicative insert (primers n˚18 to 21) (S1 Table) and reverse primer corresponding to the 3'-end of 5S rRNA (primer n˚22) using One-step RT-PCR kit (QIAGEN). For each recombinant RNA, serial dilutions of the corresponding T7-transcript were used to create a calibration curve and thus estimate the amount of rec.5S rRNA molecules per cell. Control no-RT reactions were performed for each RNA sample. RT-PCR products were PAGE separated, visualized by ethidium bromide staining and quantified using G-box Software. This approach provided reproducible data, SD = 15–20%.

RT-qPCR was performed in two steps, first by reverse transcriptase Revertaid H minus (Thermofisher) with primer n˚22, second by real-time qPCR kit Sso Advanced Universal SYBR Green Supermix (Biorad), primers n˚18 to 21 (S1 Table), in triplicates, with no-RT control reactions. Amplification cycles were performed with C1000 Touch, CFX96™ Real-Time Detection System thermocycler (BioRad). PCR was performed by initial denaturation at 95˚C

for 10 min, followed by 40 cycles of 10s at 95˚C and 45s at 55˚C. The threshold cycle (Ct) values of each sample were used in the post-PCR data analysis by BioRad CFX Manager™ software 3.0. Absolute amounts of cDNA in each reaction were estimated by use of calibration curves made with corresponding plasmid DNA.

Analysis of the heteroplasmy level and mtDNA copy number

Cells issued from independent transfections were cultivated separately, in 4 parallel cultures each one, total DNA was isolated from a portion of cells every 2 weeks and analyzed by 2–3 independent qPCR measurements in triplicates.

To isolate total DNA, cells were solubilized in 0.5 ml of buffer containing 10mM Tris–HCl pH 7.5, 10mM NaCl, 25mM Na-EDTA and 1% SDS. Then, 10 μl of proteinase K solution (20 mg/ml) was added and the mixture was incubated for 2 h at 50˚. Finally, 50 μl of 5M NaCl was added and DNA was precipitated by isopropanol.

Heteroplasmy level for KSS deletion was analyzed by real-time qPCR using SYBR Green (C1000 Touch, CFX96™ Real-Time Detection System, BioRad) as described previously [12]. This approach allows quantification of the level of KSS deletion within a sample by comparing specific amplification of two different mtDNA regions, located within and outside of the deletion, in separate reactions. To improve the accuracy of the test, we estimated absolute amounts of DNA in each reaction by use of calibration curves and thus we calculated the ratio between all mtDNA molecules (mutant and wild-type) and the wild-type ones. Differences in KSS deletion level less than 5% were not considered as significant.

Primers are listed in the S1 Table. Two pairs of primers were used: 1) n˚14 and 15 amplifying a 210bp fragment of 12S rRNA gene (nucleotides 1095–1305 in mtDNA) not affected by the KSS deletion as a value showing all mtDNA molecules, and 2) n˚16 and 17 amplifying a 164 bp fragment in the deleted region (nucleotides 11 614–11 778) as a value showing only wild-type mtDNA molecules. Nuclear DNA quantification was performed using primers to rhodanese gene *TST1* (S1 Table). All reactions were performed in a 20 μl volume in triplicates. PCR was performed by initial denaturation at 95˚C for 10 min, followed by 40 cycles of 30s at 95˚C and 30s at 60˚C. The threshold cycle (Ct) values of each sample were used in the post-PCR data analysis by BioRad CFX Manager™ software 3.0. In each experiment, absolute amount of DNA templates were determined using serial dilutions of linearized plasmid DNA bearing a corresponding sequence. The KSS heteroplasmy level was calculated using the formula: mutant mtDNA/total mtDNA = 1 − (WT mtDNA/total mtDNA). Data obtained on independently cultivated cells (n = 4) by 3–4 independent qPCR measurements were statistically processed using the two-tailed Student's *t*-test; values of $p \leq 0.05$ (*), $p \leq 0.001$ (***) were considered to be statistically significant.

Supporting information

S1 Fig. Specific annealing of rec.5S rRNAs to mutant KSS mtDNA. Southern hybridization of wild-type (WT) or KSS mtDNA fragments (Mut) with ^{32}P-labelled rec.5S rRNAs "5S-KSS-15H" and "5S-KSS-15L" (as indicated at the right) at 37˚C in 1xPBS.
(TIF)

S2 Fig. *In vivo* test of rec.5S rRNA import into human mitochondria. Northern blot analysis of rec.5S rRNA variants in total and mitoplast RNA preparations from cells transfected with various RNA (as indicated above the panels). Originals gel stained with Ethidium bromide (EthBr) and hybridized with probes indicated at the left, as on Fig 3.
(DOCX)

S3 Fig. Analysis of the FRT site copy number in isolated *trans*mitochondrial cybrid KSS-FRT cell lines. Southern blot hybridization of genomic DNA from three KSS-FRT clones (2, 5 and 8) compared to commercial HEK 293 T-Rex™ Flp-In™ cells.
(TIF)

S4 Fig. Schematic representation of three mtDNA replication models and possible effect of anti-replicative rec.5S rRNA (modified from [12]).
(TIF)

S1 Table. List of oligonucleotide primers.
(DOCX)

S2 Table. Quantification of mitochondrial import efficiencies of rec.5S rRNA.
(DOCX)

S3 Table. Characteristics of three isolated transmitochondrial cybrid KSS-FRT cell lines compared to commercial HEK 293 T-RexTM Flp-InTM.
(DOCX)

S4 Table. Quantification of anti-replicative molecules in rec.5S rRNA expressing cell lines by two approaches: Semi-quantitative one step RT-PCR and two steps real-time RT-qPCR.
(DOCX)

Acknowledgments

The authors are grateful to A. Lombès (Institut Cochin, Paris) for providing human *trans*mitochondrial KSS cybrid cells, plasmids and protocols for qPCR quantification of the KSS deletion load.

Author Contributions

Conceptualization: Ivan Tarassov, Nina Entelis.

Formal analysis: Romuald Loutre.

Funding acquisition: Ivan Tarassov.

Investigation: Romuald Loutre, Anne-Marie Heckel, Damien Jeandard.

Methodology: Romuald Loutre, Anne-Marie Heckel, Damien Jeandard.

Project administration: Nina Entelis.

Supervision: Ivan Tarassov, Nina Entelis.

Validation: Anne-Marie Heckel, Damien Jeandard, Nina Entelis.

Visualization: Romuald Loutre.

Writing – original draft: Romuald Loutre, Nina Entelis.

Writing – review & editing: Ivan Tarassov, Nina Entelis.

References

1. Gorman GS, Schaefer AM, Ng Y, Gomez N, Blakely EL, Alston CL, et al. Prevalence of nuclear and mitochondrial DNA mutations related to adult mitochondrial disease. Ann Neurol. 2015; 77(5):753–9. Epub 2015/02/06. https://doi.org/10.1002/ana.24362 PMID: 25652200.
2. Wallace DC. Mitochondrial DNA mutations in disease and aging. Environ Mol Mutagen. 2010; 51 (5):440–50. https://doi.org/10.1002/em.20586 PMID: 20544884.

3. Ozawa M, Nonaka I, Goto Y. Single muscle fiber analysis in patients with 3243 mutation in mitochondrial DNA: comparison with the phenotype and the proportion of mutant genome. Journal of the neurological sciences. 1998; 159(2):170–5. PMID: 9741403.
4. Picard M, Zhang J, Hancock S, Derbeneva O, Golhar R, Golik P, et al. Progressive increase in mtDNA 3243A>G heteroplasmy causes abrupt transcriptional reprogramming. Proceedings of the National Academy of Sciences of the United States of America. 2014; 111(38):E4033–42. https://doi.org/10.1073/pnas.1414028111 PMID: 25192935.
5. Patananan AN, Wu TH, Chiou PY, Teitell MA. Modifying the Mitochondrial Genome. Cell metabolism. 2016; 23(5):785–96. https://doi.org/10.1016/j.cmet.2016.04.004 PMID: 27166943.
6. Alexeyev MF, Venediktova N, Pastukh V, Shokolenko I, Bonilla G, Wilson GL. Selective elimination of mutant mitochondrial genomes as therapeutic strategy for the treatment of NARP and MILS syndromes. Gene Ther. 2008; 15(7):516–23. https://doi.org/10.1038/sj.gt.2008.11 PMID: 18256697.
7. Gammage PA, Rorbach J, Vincent AI, Rebar EJ, Minczuk M. Mitochondrially targeted ZFNs for selective degradation of pathogenic mitochondrial genomes bearing large-scale deletions or point mutations. EMBO molecular medicine. 2014; 6(4):458–66. https://doi.org/10.1002/emmm.201303672 PMID: 24567072.
8. Bacman SR, Williams SL, Pinto M, Peralta S, Moraes CT. Specific elimination of mutant mitochondrial genomes in patient-derived cells by mitoTALENs. Nat Med. 2012; 19(9):1111–3. https://doi.org/10.1038/nm.3261 PMID: 23913125.
9. Reddy P, Ocampo A, Suzuki K, Luo J, Bacman SR, Williams SL, et al. Selective elimination of mitochondrial mutations in the germline by genome editing. Cell. 2015; 161(3):459–69. https://doi.org/10.1016/j.cell.2015.03.051 PMID: 25910206.
10. Gammage PA, Gaude E, Van Haute L, Rebelo-Guiomar P, Jackson CB, Rorbach J, et al. Near-complete elimination of mutant mtDNA by iterative or dynamic dose-controlled treatment with mtZFNs. Nucleic Acids Res. 2016; 44(16):7804–16. https://doi.org/10.1093/nar/gkw676 PMID: 27466392.
11. Taylor RW, Chinnery PF, Turnbull DM, Lightowlers RN. Selective inhibition of mutant human mitochondrial DNA replication in vitro by peptide nucleic acids. Nat Genet. 1997; 15(2):212–5. https://doi.org/10.1038/ng0297-212 PMID: 9020853.
12. Comte C, Tonin Y, Heckel-Mager AM, Boucheham A, Smirnov A, Aure K, et al. Mitochondrial targeting of recombinant RNAs modulates the level of a heteroplasmic mutation in human mitochondrial DNA associated with Kearns Sayre Syndrome. Nucleic Acids Res. 2013; 41(1):418–33. https://doi.org/10.1093/nar/gks965 PMID: 23087375.
13. Tarassov I, Chicherin I, Tonin Y, Smirnov A, Kamenski P, Entelis N. Mitocondrial Targeting of RNA and Mitochondrial Translation. In: Duchene AM, editor. Translation in Mitochondria and Other Organels: Springer Heidelberg; 2013. p. 85–109.
14. Salinas-Giege T, Giege R, Giege P. tRNA biology in mitochondria. International journal of molecular sciences. 2015; 16(3):4518–59. https://doi.org/10.3390/ijms16034518 PMID: 25734984.
15. Kim KM, Noh JH, Abdelmohsen K, Gorospe M. Mitochondrial noncoding RNA transport. BMB reports. 2017; 50(4):164–74. https://doi.org/10.5483/BMBRep.2017.50.4.013 PMID: 28115039.
16. Kolesnikova OA, Entelis NS, Jacquin-Becker C, Goltzene F, Chrzanowska-Lightowlers ZM, Lightowlers RN, et al. Nuclear DNA-encoded tRNAs targeted into mitochondria can rescue a mitochondrial DNA mutation associated with the MERRF syndrome in cultured human cells. Human molecular genetics. 2004; 13(20):2519–34. https://doi.org/10.1093/hmg/ddh267 PMID: 15317755.
17. Gowher A, Smirnov A, Tarassov I, Entelis N. Induced tRNA import into human mitochondria: implication of a host aminoacyl-tRNA-synthetase. PloS one. 2013; 8(6):e66228. https://doi.org/10.1371/journal.pone.0066228 PMID: 23799079.
18. Kolesnikova O, Kazakova H, Comte C, Steinberg S, Kamenski P, Martin RP, et al. Selection of RNA aptamers imported into yeast and human mitochondria. Rna. 2011; 16(5):926–41. https://doi.org/10.1261/rna.1914110 PMID: 20348443.
19. Tonin Y, Heckel AM, Vysokikh M, Dovydenko I, Meschaninova M, Rotig A, et al. Modeling of antigenomic therapy of mitochondrial diseases by mitochondrially addressed RNA targeting a pathogenic point mutation in mitochondrial DNA. J Biol Chem. 2014; 289(19):13323–34. https://doi.org/10.1074/jbc.M113.528968 PMID: 24692550.
20. Magalhaes PJ, Andreu AL, Schon EA. Evidence for the presence of 5S rRNA in mammalian mitochondria. Molecular biology of the cell. 1998; 9(9):2375–82. PMID: 9725900.
21. Entelis NS, Kolesnikova OA, Dogan S, Martin RP, Tarassov IA. 5 S rRNA and tRNA import into human mitochondria. Comparison of in vitro requirements. J Biol Chem. 2001; 276(49):45642–53. https://doi.org/10.1074/jbc.M103906200 PMID: 11551911.
22. Yoshionari S, Koike T, Yokogawa T, Nishikawa K, Ueda T, Miura K, et al. Existence of nuclear-encoded 5S-rRNA in bovine mitochondria. FEBS letters. 1994; 338(2):137–42. PMID: 7508404.

23. Greber BJ, Ban N. Structure and Function of the Mitochondrial Ribosome. Annual review of biochemistry. 2016; 85:103–32. https://doi.org/10.1146/annurev-biochem-060815-014343 PMID: 27023846.

24. Smirnov A, Comte C, Mager-Heckel AM, Addis V, Krasheninnikov IA, Martin RP, et al. Mitochondrial enzyme rhodanese is essential for 5 S ribosomal RNA import into human mitochondria. J Biol Chem. 2010; 285(40):30792–803. https://doi.org/10.1074/jbc.M110.151183 PMID: 20663881.

25. Smirnov A, Entelis N, Martin RP, Tarassov I. Biological significance of 5S rRNA import into human mitochondria: role of ribosomal protein MRP-L18. Genes & development. 2011; 25(12):1289–305. https://doi.org/10.1101/gad.624711 PMID: 21685364.

26. Smirnov A, Tarassov I, Mager-Heckel AM, Letzelter M, Martin RP, Krasheninnikov IA, et al. Two distinct structural elements of 5S rRNA are needed for its import into human mitochondria. Rna. 2008; 14 (4):749–59. https://doi.org/10.1261/rna.952208 PMID: 18314502.

27. Dovydenko I, Heckel AM, Tonin Y, Gowher A, Venyaminova A, Tarassov I, et al. Mitochondrial targeting of recombinant RNA. Methods Mol Biol. 2015; 1265:209–25. https://doi.org/10.1007/978-1-4939-2288-8_16 PMID: 25634278.

28. Mercer TR, Neph S, Dinger ME, Crawford J, Smith MA, Shearwood AM, et al. The human mitochondrial transcriptome. Cell. 2011; 146(4):645–58. https://doi.org/10.1016/j.cell.2011.06.051 PMID: 21854988.

29. Schneider A. Mitochondrial tRNA import and its consequences for mitochondrial translation. Annual review of biochemistry. 2011; 80:1033–53. https://doi.org/10.1146/annurev-biochem-060109-092838 PMID: 21417719.

30. Towheed A, Markantone DM, Crain AT, Celotto AM, Palladino MJ. Small mitochondrial-targeted RNAs modulate endogenous mitochondrial protein expression in vivo. Neurobiology of disease. 2014; 69:15–22. https://doi.org/10.1016/j.nbd.2014.04.017 PMID: 24807207.

31. Amunts A, Brown A, Bai XC, Llacer JL, Hussain T, Emsley P, et al. Structure of the yeast mitochondrial large ribosomal subunit. Science. 2014; 343(6178):1485–9. https://doi.org/10.1126/science.1249410 PMID: 24675956.

32. Greber BJ, Boehringer D, Leibundgut M, Bieri P, Leitner A, Schmitz N, et al. The complete structure of the large subunit of the mammalian mitochondrial ribosome. Nature. 2014; 515(7526):283–6. https://doi.org/10.1038/nature13895 PMID: 25271403.

33. Gammage PA, Moraes CT, Minczuk M. Mitochondrial Genome Engineering: The Revolution May Not Be CRISPR-Ized. Trends in genetics: TIG. 2017. https://doi.org/10.1016/j.tig.2017.11.001 PMID: 29179920.

34. Chrzanowska-Lightowlers Z, Rorbach J, Minczuk M. Human mitochondrial ribosomes can switch structural tRNAs—but when and why? RNA Biol. 2017; 14(12):1668–71. https://doi.org/10.1080/15476286.2017.1356551 PMID: 28786741.

35. Karicheva OZ, Kolesnikova OA, Schirtz T, Vysokikh MY, Mager-Heckel AM, Lombes A, et al. Correction of the consequences of mitochondrial 3243A>G mutation in the MT-TL1 gene causing the MELAS syndrome by tRNA import into mitochondria. Nucleic Acids Res. 2011; 39(18):8173–86. https://doi.org/10.1093/nar/gkr546 PMID: 21724600.

36. Dovydenko I, Tarassov I, Venyaminova A, Entelis N. Method of carrier-free delivery of therapeutic RNA importable into human mitochondria: Lipophilic conjugates with cleavable bonds. Biomaterials. 2016; 76:408–17. https://doi.org/10.1016/j.biomaterials.2015.10.075 PMID: 26561937.

37. Zelenka J, Alan L, Jaburek M, Jezek P. Import of desired nucleic acid sequences using addressing motif of mitochondrial ribosomal 5S-rRNA for fluorescent in vivo hybridization of mitochondrial DNA and RNA. Journal of bioenergetics and biomembranes. 2014; 46(2):147–56. https://doi.org/10.1007/s10863-014-9543-2 PMID: 24562889.

38. Autour A, S CYJ, A DC, Abdolahzadeh A, Galli A, Panchapakesan SSS, et al. Fluorogenic RNA Mango aptamers for imaging small non-coding RNAs in mammalian cells. Nature communications. 2018; 9 (1):656. https://doi.org/10.1038/s41467-018-02993-8 PMID: 29440634.

39. Pohjoismaki JL, Goffart S. Of circles, forks and humanity: Topological organisation and replication of mammalian mitochondrial DNA. BioEssays: news and reviews in molecular, cellular and developmental biology. 2011; 33(4):290–9. https://doi.org/10.1002/bies.201000137 PMID: 21290399.

40. Clayton DA. Mitochondrial DNA replication: what we know. IUBMB life. 2003; 55(4–5):213–7. https://doi.org/10.1080/1521654031000134824 PMID: 12880201.

41. Yasukawa T, Reyes A, Cluett TJ, Yang MY, Bowmaker M, Jacobs HT, et al. Replication of vertebrate mitochondrial DNA entails transient ribonucleotide incorporation throughout the lagging strand. The EMBO journal. 2006; 25(22):5358–71. https://doi.org/10.1038/sj.emboj.7601392 PMID: 17066082.

42. Bowmaker M, Yang MY, Yasukawa T, Reyes A, Jacobs HT, Huberman JA, et al. Mammalian mitochondrial DNA replicates bidirectionally from an initiation zone. J Biol Chem. 2003; 278(51):50961–9. https://doi.org/10.1074/jbc.M308028200 PMID: 14506235.

43. Herbers E, Kekalainen NJ, Hangas A, Pohjoismaki JL, Goffart S. Tissue specific differences in mitochondrial DNA maintenance and expression. Mitochondrion. 2018. https://doi.org/10.1016/j.mito.2018.01.004 PMID: 29339192.

44. Phillips AF, Millet AR, Tigano M, Dubois SM, Crimmins H, Babin L, et al. Single-Molecule Analysis of mtDNA Replication Uncovers the Basis of the Common Deletion. Molecular cell. 2017; 65(3):527–38. e6. https://doi.org/10.1016/j.molcel.2016.12.014 PMID: 28111015.

45. Chretien D, Benit P, Ha HH, Keipert S, El-Khoury R, Chang YT, et al. Mitochondria are physiologically maintained at close to 50 degrees C. PLoS biology. 2018; 16(1):e2003992. https://doi.org/10.1371/journal.pbio.2003992 PMID: 29370167.

46. Marroquin LD, Hynes J, Dykens JA, Jamieson JD, Will Y. Circumventing the Crabtree effect: replacing media glucose with galactose increases susceptibility of HepG2 cells to mitochondrial toxicants. Toxicological sciences: an official journal of the Society of Toxicology. 2007; 97(2):539–47. https://doi.org/10.1093/toxsci/kfm052 PMID: 17361016.

47. King MP, Attardi G. Human cells lacking mtDNA: repopulation with exogenous mitochondria by complementation. Science. 1989; 246(4929):500–3. PMID: 2814477.

48. Dott W, Mistry P, Wright J, Cain K, Herbert KE. Modulation of mitochondrial bioenergetics in a skeletal muscle cell line model of mitochondrial toxicity. Redox biology. 2014; 2:224–33. https://doi.org/10.1016/j.redox.2013.12.028 PMID: 24494197.

49. Elkalaf M, Andel M, Trnka J. Low glucose but not galactose enhances oxidative mitochondrial metabolism in C2C12 myoblasts and myotubes. PloS one. 2013; 8(8):e70772. https://doi.org/10.1371/journal.pone.0070772 PMID: 23940640.

50. Cannino G, El-Khoury R, Pirinen M, Hutz B, Rustin P, Jacobs HT, et al. Glucose modulates respiratory complex I activity in response to acute mitochondrial dysfunction. J Biol Chem. 2012; 287(46):38729–40. https://doi.org/10.1074/jbc.M112.386060 PMID: 23007390.

51. Santra S, Gilkerson RW, Davidson M, Schon EA. Ketogenic treatment reduces deleted mitochondrial DNAs in cultured human cells. Ann Neurol. 2004; 56(5):662–9. https://doi.org/10.1002/ana.20240 PMID: 15389892.

52. Desquiret-Dumas V, Gueguen N, Barth M, Chevrollier A, Hancock S, Wallace DC, et al. Metabolically induced heteroplasmy shifting and l-arginine treatment reduce the energetic defect in a neuronal-like model of MELAS. Biochimica et biophysica acta. 2012; 1822(6):1019–29. https://doi.org/10.1016/j.bbadis.2012.01.010 PMID: 22306605.

53. Frey S, Geffroy G, Desquiret-Dumas V, Gueguen N, Bris C, Belal S, et al. The addition of ketone bodies alleviates mitochondrial dysfunction by restoring complex I assembly in a MELAS cellular model. Biochimica et biophysica acta. 2017; 1863(1):284–91. https://doi.org/10.1016/j.bbadis.2016.10.028 PMID: 27815040.

54. Markham NR, Zuker M. UNAFold: software for nucleic acid folding and hybridization. Methods Mol Biol. 2008; 453:3–31. https://doi.org/10.1007/978-1-60327-429-6_1 PMID: 18712296.

55. Szymanski M, Barciszewska MZ, Erdmann VA, Barciszewski J. 5 S rRNA: structure and interactions. The Biochemical journal. 2003; 371(Pt 3):641–51. https://doi.org/10.1042/BJ20020872 PMID: 12564956.

56. Sugimoto N, Nakano S, Katoh M, Matsumura A, Nakamuta H, Ohmichi T, et al. Thermodynamic parameters to predict stability of RNA/DNA hybrid duplexes. Biochemistry. 1995; 34(35):11211–6. PMID: 7545436.

Supplementary Materials

Anti-replicative recombinant 5S rRNA molecules can modulate the mtDNA heteroplasmy in a glucose-dependent manner

Romuald Loutre, Anne-Marie Heckel, Damien Jeandard, Ivan Tarassov and Nina Entelis

S1 Table. List of oligonucleotide primers.

N°	Name	Sequence
1	T7-prom	5' GGGATCCATAATACGACTCACTATA 3'
2	KSS-13H-rev	5’ AGGCCCGACCCTGCTTAGCTACAGTGCTTACTTTTCAGGGTGGTATGGCCGTA 3’
3	KSS-14L-rev	5’ AGGCCCGACCCTGCTTAGCTAAGTAAGCACTGTATTCAGGGTGGTATGGCCGTA 3’
4	KSS-15H-rev	5’ AGGCCCGACCCTGCTTAGCTTTACAGTGCTTACTTTTCAGGGTGGTATGGCCGTA 3’
5	KSS-15L-rev	5’ AGGCCCGACCCTGCTTAGCTAGAAGTAAGCACTGTTTCAGGGTGGTATGGCCGTA 3’
6	5S-BglII	5’ GGAGATCTAAGCCTACAACACCCGG 3’
7	Cytbwt F	5' CTTTAAAGCTTCACACGATTCTTTACCTTTC 3'
8	Cytbwt R	5' TCTTTGGAATTCGTTTGGATATATGGAGGATGG 3'
9	Lysmt F	5' TCATACAAGCTTACAGATGCAATTCCCGGACG 3'
10	5'-HindIII-5S	5' CCAAGCTTGGGCGGGGCTGGGCTCTTGGGGCAGCCAGGCGCCTCCTTCAGCGCCTACGGCCATACCACCC 3'
11	3'-BamHI-5S	5' CCGGATCCAAAGCCAAAGAAAAGCCTACAACACCCG 3'
12	5'-BamHI-5S	5'CCGGATCCGGGCGGGGCTGGGCTCTTGGGGCAGCCAGGCGCCTCCTTCAGCGCCTACGGCCATACCACCC 3'
13	3'-HindIII-5S	5' CCAAGCTTAAAGCCAAAGAAAAGCCTACAACACCCG 3'
14	1095 F	5' TAGCCCTAAACCTCAACAGT 3'
15	1305 B	5' TGCGCTTACTTTGTAGCCTTCAT 3'
16	11614 F	5' CATTGCATACTCTTCAATCAGC 3'
17	11778 B	5' CGACTGTGAGTGCGTT 3'
18	RT-5S-KSS-H	5' CACCCTGAAAAGTAAGCAC 3'
19	RT-5S-KSS-L	5' CCTGAATACAGTGCTTAC 3'
20	RT-15H-KSS	5' GAGAAGTAAGCACTGTAAAG 3'
21	RT-15L-KSS	5' CCCTGAAACAGTGCTTAC 3'
22	RT-5S-Antisens	5' AAGCCTACAACACCC 3'
23	TST1-For	5' GTGGATGTTCCGTGTGTTTGG 3'
24	TST1-Rev	5' CAGCACCTGCTCGTAGGTC 3'
25	Anti-insert 13H,15H	5' GCTTACAGTGCTTACTT 3'
26	Anti-insert 14L,15L	5' AAGTAAGCACTGTTTCAG 3'
27	Mt tRNA Valine	5' TGGGTCAGAGCGGTCAAGTTAAGTTGAAATCTCC 3'
28	Anti-5,8S rRNA	5' GGCCGCAAGTGCGTTCGAAG 3'
29	Anti-5S rRNA	5' AAAGCCTACAACACCCGGTATTCCC 3'

S2 Table. Quantification of mitochondrial import efficiencies of rec.5S rRNA.

A, data of the transfection experiment 1, see Fig. 3.

RNA	15H		13H		15L		14L		endogenous 5S rRNA	
signals ratios	rec 5S/Vmt	5,8S/Vmt	rec 5S/Vmt	5,8S/Vmt	rec 5S/Vmt	5,8S/Vmt	rec 5S/Vmt	5,8S/Vmt	5S /Val	5,8S/Vmt
Mitoplast RNA (Ratio I)	0,38	0,27	0,82	0,15	ND		0,37	0,33	1,02	0,06
Total RNA (Ratio II)	1,77	5,32	1,51	8,98			1,38	3,91	4,29	4,17
Ratio I /Ratio II	0,215	0,05	0,53	0,01			0,27	0,08	0,237	0,015
Import efficiency*	0,165		0,52				0,19		0,22	
Relative import eff.	75%		235%				86%		**100%**	

B, data of the transfection experiment 2, see S2 Figure.

RNA	15H		13H		15L		14L		endogenous 5S rRNA	
signals ratios	rec 5S/Vmt	5,8S/Vmt	rec 5S/Vmt	5,8S/Vmt	rec 5S/Vmt	5,8S/Vmt	rec 5S/Vmt	5,8S/Vmt	5S /Val	5,8S/Vmt
Mitoplast RNA (Ratio I)	0,11	0,03	0,34	0,06	0,55	0,03	0,11	0,02	0,73	0,01
Total RNA (Ratio II)	0,37	1,05	0,71	0,89	2,75	0,93	0,42	1,2	2,76	1,2
Ratio I /Ratio II	0,29	0,03	0,49	0,07	0,2	0,03	0,26	0,02	0,26	0,01
Import efficiency*	0,26		0,42		0,17		0,24		0,25	
Relative import eff.	104%		168%		68%		96%		**100%**	

* Levels of cytosolic contamination (estimated as Ratio I /Ratio II for cyt 5.8S rRNA) were subtracted from the import efficiencies (Ratio I /Ratio II for rec.5S rRNA).

Endogenous 5S rRNA import was analyzed in non-transfected cells and taken as 100%. Data on the endogenous 5S import efficiency for the individual transient transfections are not shown due to cross-hybridization of the 5S probe with rec.5S rRNA molecules.

S3 Table. Characteristics of the three isolated *trans*mitochondrial cybrid KSS-FRT cell lines compared to commercial cells HEK 293 T-Rex™ Flp-In™.

KSS pFRT cell line	KSS pFRT 2	KSS pFRT 5	KSS pFRT 8	HEK 293 T-Rex™ Flp-In™
Number of FRT site	1	1	1	1
β-gal Specific Activity (in nmol of hydrolyzed ONPG/30 min/protein mg)	23 ±10	31 ±3	15 ±6	125 ±6
KSS heteroplasmy level	52 ±5%	51 ±4%	52 ±5%	/

S4 Table. Quantification of anti-replicative molecules in rec.5S rRNA expressing cell lines by two approaches: semi-quantitative one step RT-PCR and two steps real-time RT-qPCR.

Rec.5S rRNA	Number rec.5S rRNA/cell RT-PCR semi-quant.	Number rec.5S rRNA/cell real time RT-qPCR
5S-KSS-13H[(1)]	2000±200	740±8
5S-KSS-13H	200±30	75±3
5S-KSS-14L[(1)]	2000±200	ND
5S-KSS-14L	300±50	120±5
5S-KSS-15H	1300±200	500±5
5S-KSS-15L	200±30	70±3

Values obtained by two steps RT-qPCR are ≈ three fold decreased compared to those of semi-quantitative RT-PCR. This can be explained by two factors: 1) different efficiency of cDNA synthesis, since different enzymes had been used for the One-step and for two steps RT-PCR reactions; 2) discrepancy of cell quantification mode in experiments performed now and a year ago. Despite the difference in absolute values, we obtained the same proportion of the rec.5S rRNA expression among the cell lines: the best expression for 5S-KSS-13H[(1)], lower for 5S-KSS-15H and rather small expression for other lines. Thus, we believe that new RT-qPCR data do not change the main claims of our study.

S1 Figure. Specific annealing of rec.5S rRNAs to mutant KSS mtDNA. Southern hybridization of wild-type (WT) or KSS mtDNA fragments (Mut) with ^{32}P-labelled recombinant 5S rRNAs "5S-KSS-15H" and "5S-KSS-15L" (as indicated at the right) at 37°C in 1xPBS.

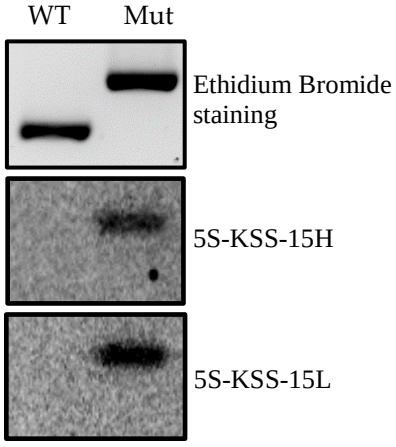

S2 Figure. *In vivo* test of rec.5S rRNA import into human mitochondria. Northern blot analysis of rec.5S rRNA variants in total and mitoplast RNA preparations from cells transfected with various RNA (as indicated above the panels). Originals gel stained with Ethidium bromide (EthBr) and hybridized with probes indicated at the right, as on Fig 3.

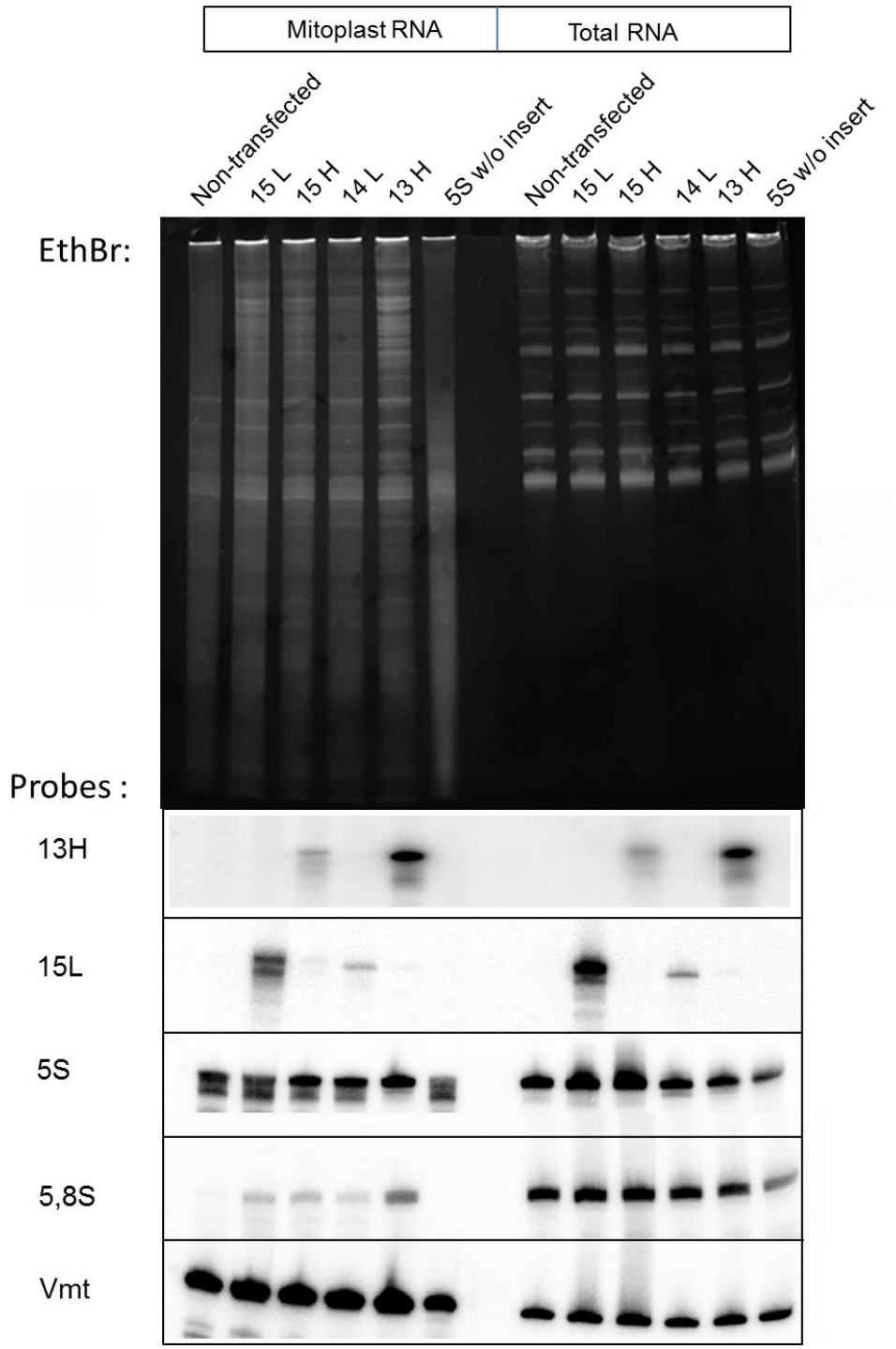

Probe 13H can hybridize with rec.5S rRNA-KSS-13H and rec.5S rRNA-KSS-15H, the signal for rec.5S rRNA-KSS-15H is much weaker due to a mismatch; the same is for the probe 15L (hybridization with rec.5S rRNA-KSS-14L is weaker than with rec.5S rRNA-KSS-15L). 5S w/o insert corresponds to cells transfected with wild type 5S rRNA transcript; in this case RNA import was not quantified due to important degradation of mitoplast RNA. Probing with 5.8S rRNA revealed that the mitoplast RNA from cells transfected with rec.5S rRNA-KSS-13H was contaminated with cytosolic RNAs, this sample could not be quantified; another transfection experiment is shown on Fig 3.

S3 Figure. Analysis of the FRT site copy number in the isolated *trans*mitochondrial cybrid KSS-FRT cell lines. Southern blot hybridization of genomic DNA from three KSS-FRT clones (2, 5 and 8) compared to commercial HEK 293 T-Rex™ Flp-In™ cells.

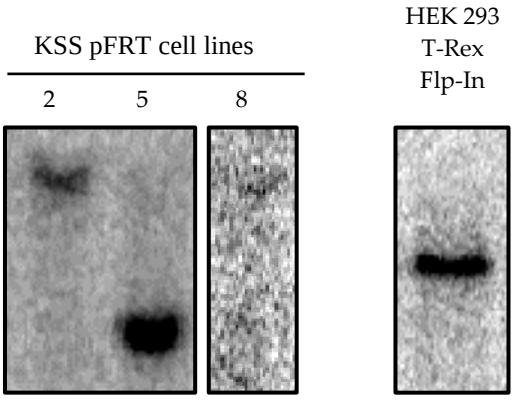

S4 Figure. Schematic representation of three mtDNA replication models (see 'Discussion' for details and references) and possible effect of anti-replicative rec.5S rRNA-KSS-13H, annealed to the L-strand of mtDNA at the KSS deletion boundaries, on the replication fork progression. OH, OL and OZ, origins of H-strand, L-strand, and strand-coupled replication, respectively. Modified from (Comte et al., 2013).

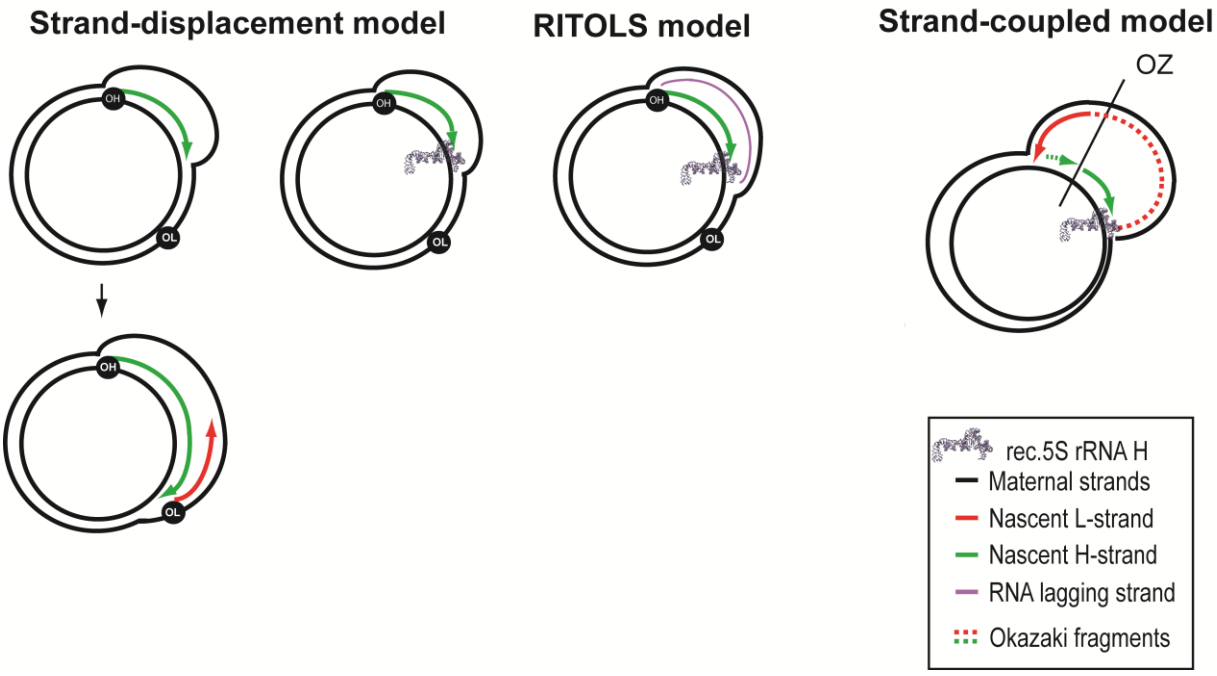

II.A.3. Application of the anti-replicative strategy to a point mtDNA mutation 13514A>G.

Contrary to mtDNA deletions, which induce the formation of a DNA sequence which highly differs from that of wild-type mtDNA, point mutation only differs by one nucleotide, thus raising the challenge for the design of specific anti-replicative molecule. Previously, small artificial RNA vectors had been applied to target anti-replicative oligonucleotides into human mitochondria. In these studies, RNA mitochondrial import induced the heteroplasmy shift in human cybrid cells and patient's fibroblasts bearing the heteroplasmic point mutation 13514 A>G in *MT-ND5* gene **(Tonin *et al.,* 2014)**. The aim of my study was to develop the rec.5S rRNA molecules targeting this point mutation. The overall methodology remains similar to the one used for the KSS mutation.

II.A.3.1. Design and selection of anti-replicative rec.5S rRNAs targeting the ND5 point mutation

II.A.3.1.1. In silico structure and melting temperature predictions

Rec.5S rRNA targeting the 13514 A>G point mutation were designed to replace a part of the β-domain (nt 24 to 49 of 5S rRNA) **(Figure 16B)** with a RNA sequence complementary to the mutated mtDNA region. The sizes of the inserted RNA sequences ranged from 15 to 17 nucleotides and target either L or H mutant mtDNA strand. As for the rec.5S rRNAs targeting the KSS deletion, the different molecules were named according to the size of the insert and the strand to which the sequence corresponds (**Figure 21A**). For example 5S-ND5-15H rec.5S rRNA contains an insert of 15 nucleotides targeting the L-strand of the mutated mtDNA.

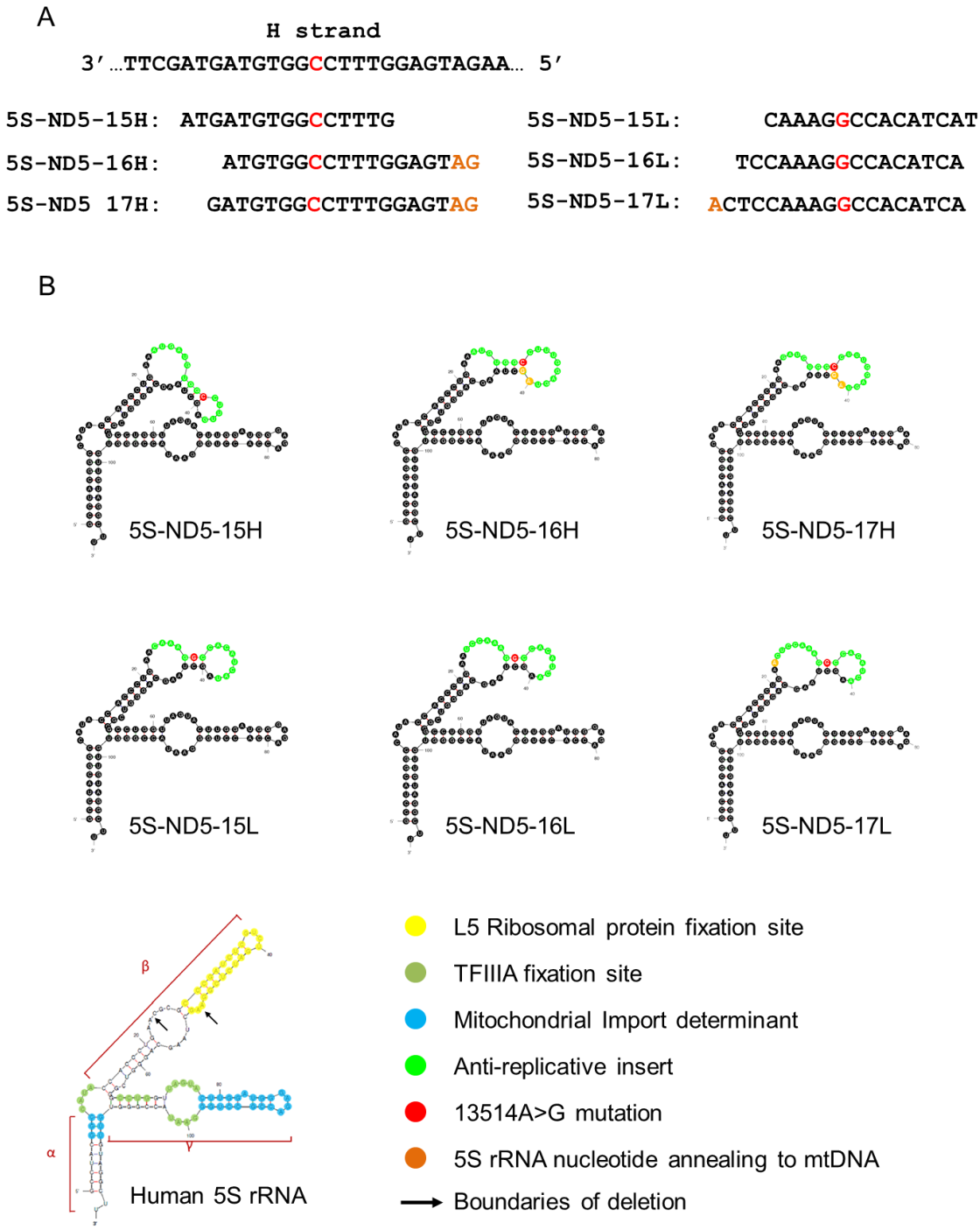

Figure 21. Anti-replicative insert sequences and secondary structure of rec.5S rRNA targeting 13514A>G ND5 point mutation.

A) Secondary structure prediction of the rec.5S rRNA molecules using the *RNA Folding form* software (Mfold). The size of the inserted RNA sequences ranged from 15 to 17 nucleotides and target either L or H-strand of mutant mtDNA. The different molecules are named according to the size of the insert, the strand to which the sequence correspond and the gene containing the mutation. The 13514A>G mutation is highlighted in red.
B) Secondary structure of the human 5S rRNA.

In silico prediction of the rec.5S rRNA secondary structure were first performed by the *RNA Folding form* software (Mfold) in order to select the molecules that retained the general secondary structure of 5S rRNA, including the structural motif of interaction with TFIIIA which mediates the nuclear export of 5S rRNA and the α et γ domain import determinants **(Figure 21B)**. Ideally, the region containing the anti-replicative insert should not be structured to ensure optimal hybridization with the target mtDNA. However, it was not possible to avoid the formation of short helices. Of note, the nucleotide discriminating wild-type from mutant mtDNA is often localized in this helix structure. The versions of rec.5S rRNAs for which many alternatives secondary structured were predicted have not been selected for further analysis.

Since mutant and wild-type mtDNA only differs by one nucleotide, it was important to select the insertion sequences with the highest discrimination ability. In this regard, melting temperatures (Tm) of the rec.5S rRNA regions annealing to target mtDNA sequence were analyzed with the OligoAnalyzer 3.1 tool (IDT-DNA) **(Table 3)**. Molecules with high predicted differences in melting temperature for each RNA-DNA duplex formed with mutant and with wild-type mtDNA molecules (ΔTm) are expected to provide more specific hybridization. Since some 5S rRNA nucleotides at the boundaries of the inserts may participate in the annealing to the target mtDNA sequence (i.e. for 5S-ND5-16H, 17H and 17L) they were also taken into account in this analysis (shown in orange in **Figure 21A)**.

Rec.5S rRNA	Insert size (nt)	Annealing to mtDNA (nt)	Tm (°C) (Mutant DNA)	Tm (°C) (Wild-type DNA)	ΔTm
5S-ND5-15H	15	15	49,2	35,4	13,8
5S-ND5-16H	16	18	55,7	45,4	10,3
5S-ND5-17H	17	19	56,6	47,6	9,2
5S-ND5-15L	15	15	49,2	40,8	8,4
5S-ND5-16L	16	16	54,3	47	7,3
5S-ND5-17L	17	18	58	52,1	5,9

Table 3. Melting temperatures prediction for duplexes between rec.5S rRNAs mutation and mutant or wild-type mtDNA regions.

These *in silico* analyses led to the selection of the 6 rec.5S rRNA presented in **Figure 21A** harboring *a priori* all the elements necessary to be correctly exported from nucleus, imported into mitochondria and specifically anneal to mutant mitochondrial genome.

II.A.3.1.2. *In vitro* selection of specific rec.5S rRNA

In order to determine which of the selected rec.5S rRNA would efficiently induce a shift in the heteroplasmy level, their capacity to specifically anneal to mutant mtDNA was tested *in vitro*. For this, we developed a test of hybridization in solution. The anti-replicative rec.5S rRNA molecules were obtained by *in vitro* transcription from PCR fragments containing the gene of rec.5S rRNA under T7 promoter. Transcripts were incubated with equimolar amounts of oligonucleotides corresponding to the mutant or wild-type mtDNA sequences in physiological conditions (1xPBS, 37°C). The formation of RNA/DNA hybrid complexes was assessed by electrophoretic mobility shift assay (EMSA) on non-denaturing polyacrylamide gel **(Figure 22).**

All the rec.5S rRNA targeting the H-strand of mtDNA (15L, 16L, 17L) showed several bands in presence or absence of mtDNA, indicating that these RNA molecule can be folded into alternative structures and/or form dimers. Only the 5S-ND5-17L version demonstrated a partial mobility shift only in presence of mutant oligonucleotide, which indicates its ability to specifically hybridize to the target mtDNA. While for this RNA the highest melting temperature of DNA/RNA duplex was predicted, the ΔTm was low, so a high specificity of its annealing to mutant mtDNA was rather unexpected **(Table 3)**. Of note, the observed EMSA signal seemed relatively low and may indicate on a weak hybridization. Concerning rec.5S rRNAs targeting the L-strand of mtDNA, both 5S-ND5-17H and, at a lesser extent, 5S-ND5-16H versions showed a prominent shift in the presence of mutant mtDNA oligonucleotide. Moreover, no shift was observed with the wild-type mtDNA indicating that the interaction with mutant mtDNA was specific. Both 5S-ND5-16H and 17H versions presented similar predicted secondary structure, Tm and ΔTm, and the difference observed may be inputted to the additional nucleotide of 5S-ND5-17H rec.5S rRNA able to anneal to mutant mtDNA **(Table 3)**. 5S-ND5-15H had a rather

low Tm that may prevent its hybridization to mtDNA in physiological conditions. Taking into account these data, 16H, 17H and 17L rec.5S rRNAs were selected for the further *in vivo* experiments and their genes were cloned into a pcDNA™5/FRT/TO plasmid for integration in ND5-cybrid-FRT cell line genome.

```
L strand 5′ TCAGAGGTTTCTACTCCAAAGACCACATCATCGAAACCGCAA 3′
Mutant L-strand 5′ TCAGAGGTTTCTACTCCAAAGGCCACATCATCGAAACCGCAA 3′
H-strand 5′ TTGCGGTTTCGATGATGTGGTCTTTGGAGTAGAAACCTGTGA 3′
Mutant H-strand 5′ TTGCGGTTTCGATGATGTGGCCTTTGGAGTAGAAACCTGTGA 3′
```

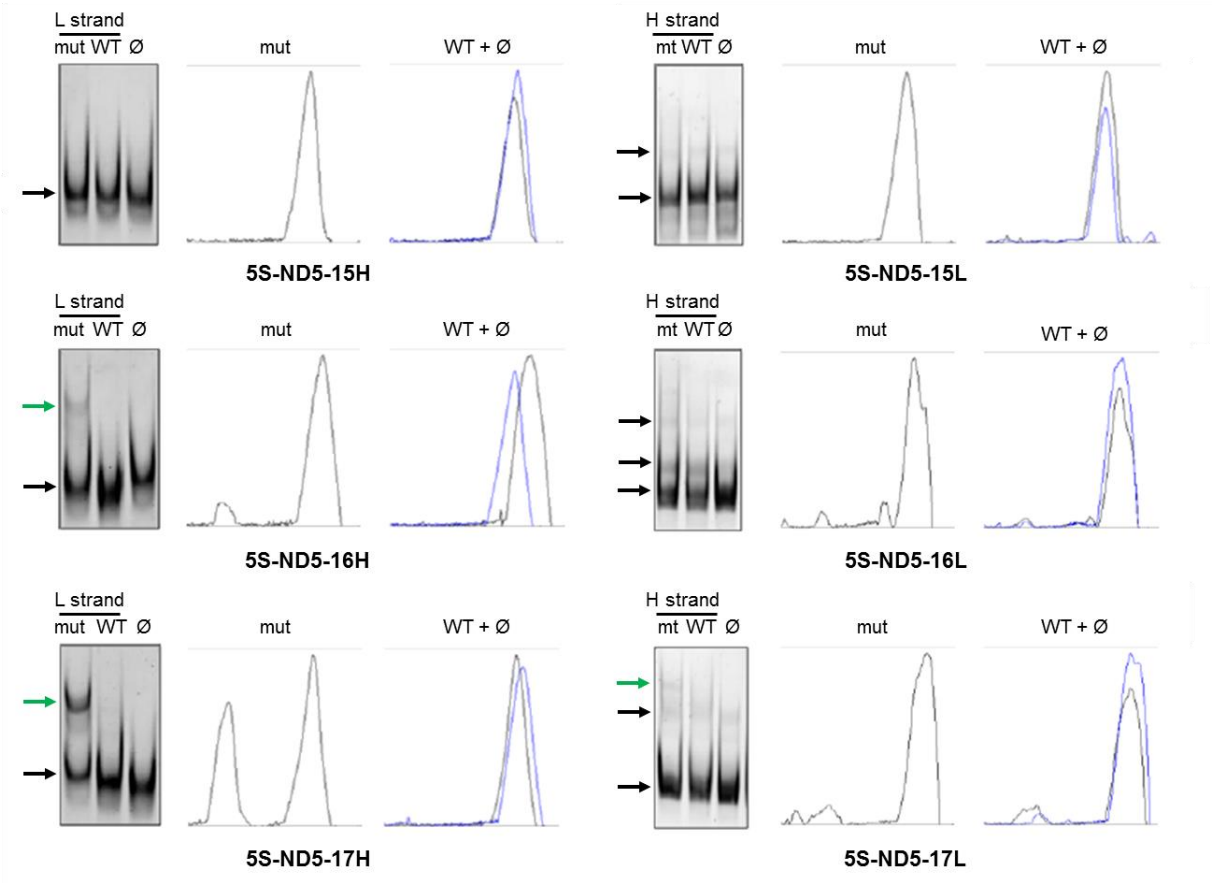

Figure 22. *In vitro* hybridization specificity assay

Rec.5S rRNAs were incubated in presence of oligonucleotides corresponding to the complementary wild-type (WT) or mutant mtDNA (mut) sequences (upper panel). The formation of RNA/DNA complex was assessed by electrophoretic mobility shift assay. For each version of rec.5S rRNA, the polyacrylamide gel stained with ethidium bromide is shown at the left and the density profiles at the right. Rec.5S rRNA transcripts alone were loaded as a control of migration (Ø) and the corresponding density profiles are represented in blue. Black arrows indicate the bands corresponding to the free rec.5S rRNAs; green arrows indicate the bands corresponding to RNA/DNA complexes.

II.A.3.2. Production of a human *trans*mitochondrial cybrid cell line bearing FRT site.

Using the Flp-In™ T-rex™ system, three Zeocin-resistant clones named ND5-cybrid-FRT were selected. As for the KSS deletion, the clone that can provide the better expression for the rec.5S rRNAs was determined by measuring the specific β-galactosidase activity **(Figure 23A)**. The commercial HEK (Human embryonic kidney) 293 T-rex™ Flp-In™, with virtually optimal insertion of the FRT-site, was used for comparison. All the obtained clones harbored at least twice less β-galactosidase activity than the commercial cells. Clone 3 showed the weakest activity up to 15 times less than HEK 293 T-rex™ Flp-In™. Clones 1 and 2 were retained for further experiments.

Several FRT sites may be introduced in nuclear genome when using the Flp-In™ T-rex™ system which could promote recombination events between the FRT sites, subsequently leading to deleterious chromosome rearrangements. In order to select clones containing only one FRT site, I performed Southern blot hybridization with total DNA extracted from the clones and digested with two restriction enzymes: XbaI and HindIII **(figure 23B)**. DNA fragments containing FRT sites were revealed with a radiolabeled probe targeting the lacZ-Zeocin gene. Two bands were observed for the clone 1, indicating that two FRT sites were integrated in the nuclear genome. On the other hand, clone 2 harbors only one FRT site and was selected for the transfection with the plasmids containing the 5S-ND5-16H, 17H or 17L rec.5S rRNAs genes. However, it is important to mention that clone 2 growth rate was reduced compared to the original cybrid cell line and that cells were fragile and showed a high mortality upon transfection.

A

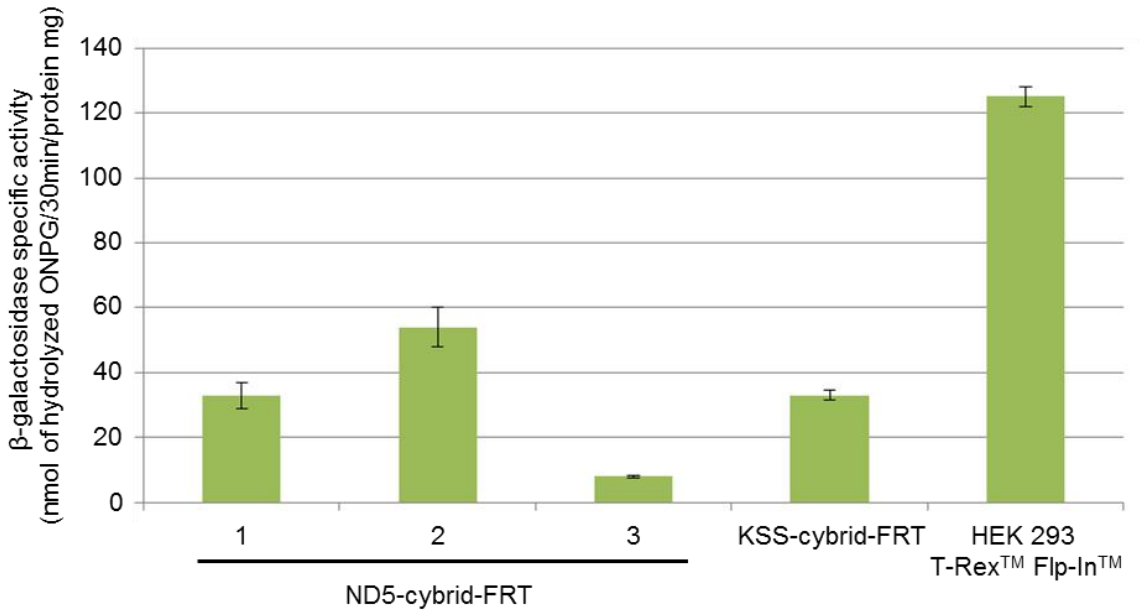

B

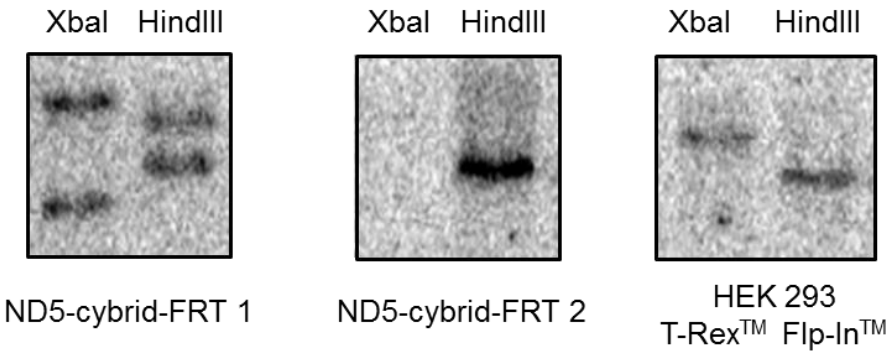

Figure 23. Characteristics of three independant *trans*mitochondrial ND5-cybrid-FRT-cell lines.

A) β-galactosidase specific activity measured in cell lysates by the « β-gal Assay kit » (Invitrogen). **B)** Number of FRT-sites introduced in nuclear genome of the ND5-cybrid-FRT clones with the highest β-galactosidase activity. DNA was digested with XbaI or HindIII restriction enzymes and the fragments containing an FRT site were revealed by southern blot with a radiolabelled DNA probe targeting the LacZ-Zeocin fusion gene. The commercial HEK 293 T-rex™ Flp-in™, bearing a unique FRT site and the KSS-cybrid-FRT cell line are shown for comparison.

II.A.3.3. Impact of the rec.5S rRNAs on the ND5-cybrid-FRT cell line heteroplasmy

Transfected cells were too fragile to be cultivated in absence of glucose, thus, they were cultivated only in standard glucose containing medium. After 1 month of culture, the mtDNA heteroplasmy was measured. The 13514A>G mutation leads to the apparition of a restriction site for the HaeIII enzyme (GGCC), absent from wild-type mtDNA, and allows the assessment of the heteroplasmy level by restriction fragment length polymorphism (RLFP). For this, the mtDNA region containing the mutation was amplified by PCR with one primer bearing a fluorophore **(Dovydenko *et al.*, 2015)**. The PCR products were then digested with HaeIII, and fragments separated on polyacrylamide gel and quantified. Heteroplasmy level was estimated by the ratio of the fluorescence intensity of the shorter band, corresponding to the mutant mtDNA, over the sum of the two bands **(Figure 24)**. Initial heteroplasmy level of clone 2 was measured in a similar way and was estimated at 73 ± 2.5%.

No decrease of heteroplasmy was observed for 5S-ND5-16H and 17L rec.5S rRNA versions. Impressively, cells transfected with 5S-ND5-17H showed an important reduction of heteroplasmy of about 55%. However, this cell line was extremely fragile and had been eventually lost, making it impossible to repeat the heteroplasmy measurement. Moreover, the fragility of the cells also made impossible the analysis of rec.5S rRNA expression and import levels. Nevertheless, the heteroplasmy decrease was observed for one version of rec.5S rRNAs, suggesting a specific effect depending on the anti-replicative molecule. These first results suggest that the anti-replicative strategy can be applied for point mutations as well as for large deletions of mtDNA. However, more experiments are required to reproduce the data and to demonstrate the direct correlation between the expression of the anti-replicative RNA molecules and the observed heteroplasmy shift.

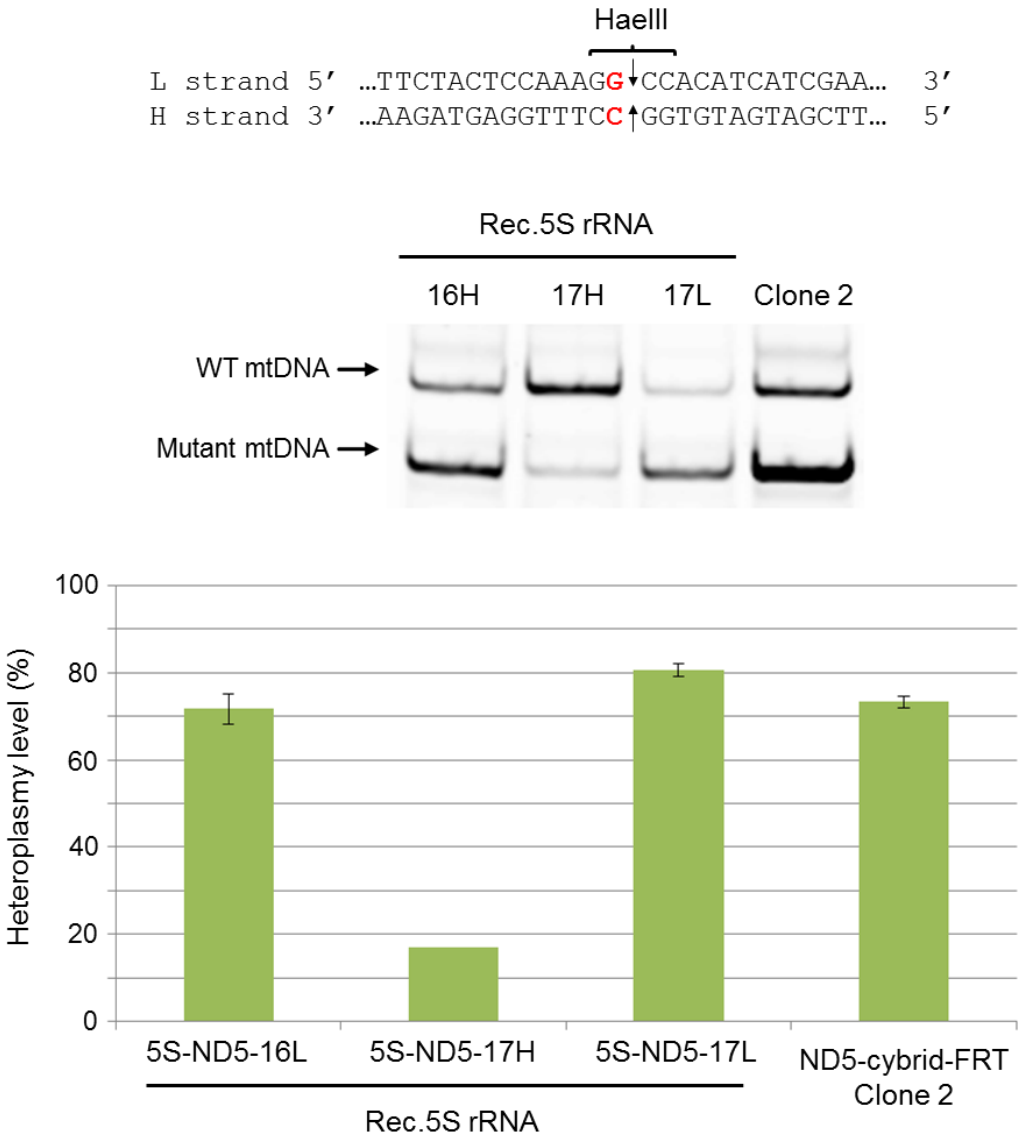

Figure 24. Heteroplasmy level of ND5-cybrid-FRT cell lines transfected with rec.5S rRNAs after 1 month of culture.

HaeIII restriction site appears in the case of the 13514 A>G mutation and allows the measure of heteroplasmy level by restriction fragment lenght polymorphism (RFLP) (Upper panel). Fluorescent PCR fragments of mtDNA were digested with HaeIII and separated on polyacrylamide gel (middle panel). The level of heteroplasmy was quantified by the ratio of the intensity of the lower band (mutant mtDNA) over the sum of the 2 bands (lower panel). Error bars correspond to 3 different measurements for cells transfected with rec.5S rRNAs and 4 different measurements for the initial clone 2.

II.B. Landscaping of human RNA importome by CoLoC-seq

Mitochondrial RNA import is actively studied, yet, little is known about mitochondrial RNA importome and the import of some RNAs often remains controversial. One of the main problems in the identification of imported RNAs is the apparent impossibility to obtain mitochondria deprived of cytosolic contaminants which confound results obtained with sensitive large scale analyses approaches (RNA deep-sequencing). Moreover, the functions of imported RNAs inside the mitochondria often remain elusive, either because of their apparent redundancy with other RNAs encoded by the mitochondrial genome or because the mitochondrial function of imported RNA can differ from the cytoplasmic one.

Nevertheless, broaden knowledge on RNA mitochondrial import may provide better tool for the development of therapies using RNA import pathways and shed light on diseases related to RNA import defects. Thus, my second project consisted in the development of a new large scale method to discriminate unequivocally imported RNA from contaminants. In this regard, my objectives were to:

i) Establish a robust approach allowing the identification of RNA present in human mitochondria

ii) Validate its ability to decipher 3 groups of RNAs: mitochondrial encoded transcripts, nuclear encoded contaminants and nuclear-encoded transcripts partially imported in mitochondria.

iii) Identify new RNA imported into human mitochondria and validate their import by other approaches.

In standard approaches for mitochondria isolation, purity of the samples is assessed by the presence or the absence of one or few cytosolic RNAs. However, RNAs can demonstrate different sensitivity to purification treatments **(Cannon *et al.*, 2015)**. While one cytosolic RNA, serving as “control”, is apparently not detected in the samples, other RNAs may persist and would only be removed with more stringent purification procedures. Thus, it is virtually impossible to be sure that the mitochondrial RNA samples are indeed deprived of cytosolic contamination. Since RNA-seq is a sensitive method able to detect even trace amounts of RNAs, large

scale analyses of mitochondrial importome are systematically confounded by the persistence of these contaminant RNAs. To address this problem, we developed a new large scale method, named “controlled level of contamination coupled with deep-sequencing” (CoLoC-seq) to distinguish unequivocally between imported RNAs and mere contaminants.

II.B.1. CoLoC-seq pilot experiment

II.B.1.1. CoLoC-seq methodology

Since the presence of contaminants cannot be neglected, CoLoC-seq aims to follow the depletion dynamic of RNA species in increasingly purified mitochondria, rather than to simply detect RNAs in partially purified mitochondria samples. One can expect that RNAs, whether they localize in mitochondria, outside mitochondria or both (partially imported RNAs) will present different pattern of depletion in progressively decontaminated mitochondrial samples. Thus, even if both cytosolic and mitochondrial RNAs persist in the samples, they could be differentiated one from another.

CoLoC-seq methodology is similar to classical mitochondrial isolation experiment followed by deep-sequencing (**Figure 18)** except that the crude mitochondria preparation is split in a series of identical samples which are then treated separately to achieve different level of purification. In order to improve accuracy and facilitate the distinction between imported RNAs and contaminant RNAs, the differential treatment must rely on a parameter that can provide quantitative, and not qualitative, analysis. Two steps of the usual mitochondrial isolation protocol, the treatment of mitochondria to remove the OMM usually performed with digitonin, and the ribonuclease treatment, rely on concentration of reagent that can be easily controlled and varied during the experiment. However, digitonin treatment may lead to the IMM rupture, limiting the range of concentrations that can be used and the efficiency of the model. Thus, RNase treatment seemed to be a convenient choice to establish CoLoC-seq procedure.

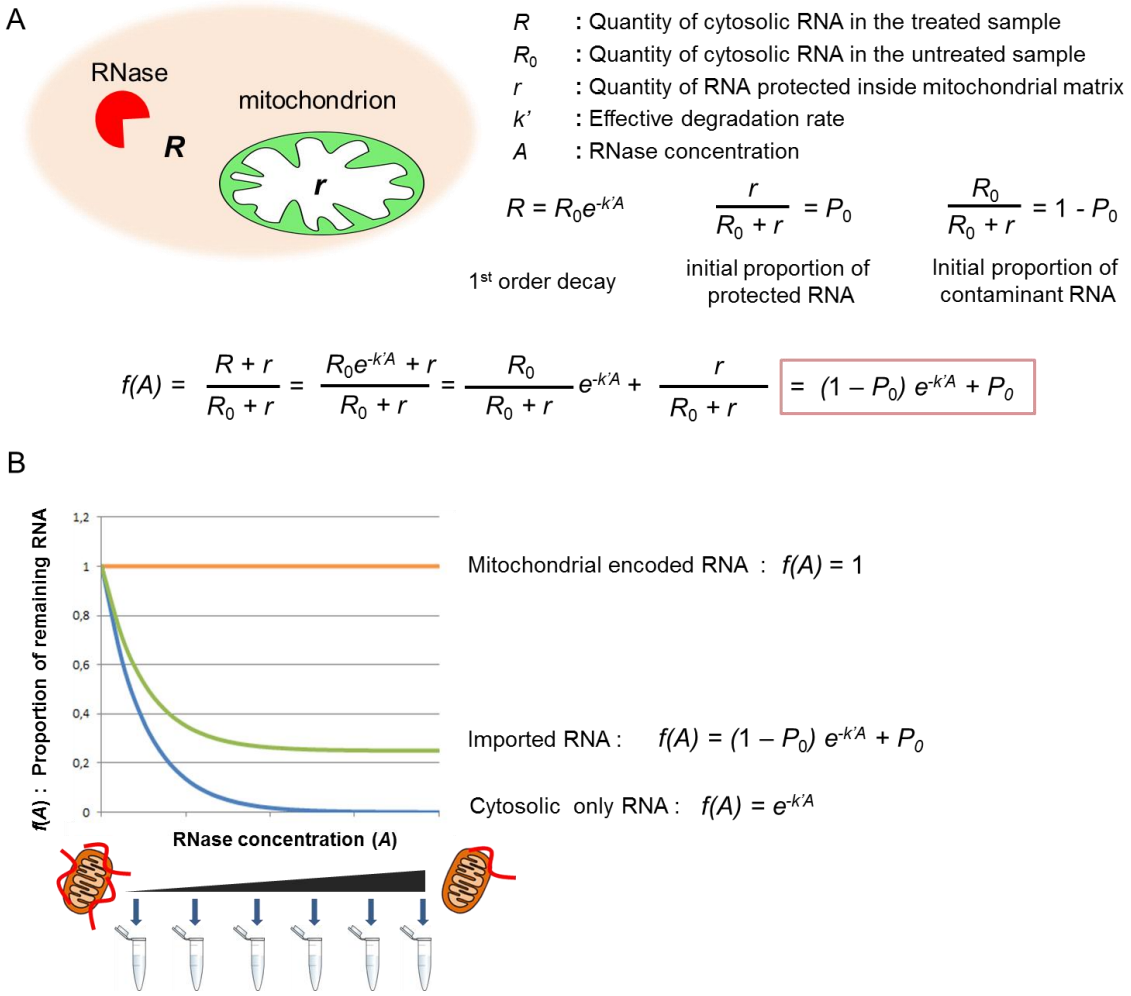

Figure 25. CoLoC-seq regression model.

A) Regression model of the RNA depletion dynamics in CoLoC experiment. RNase should exponentially degrade cytosolic RNAs but do not affect the RNA pool protected inside mitochondria. **B)** Graphical representation of the predicted RNA depletion dynamics for three types of transcripts (mt-encoded RNAs, partially imported RNAs and cytosolic only RNAs).

The depletion of RNAs can be modeled by a first-order decay regression model, where RNAs are exponentially degraded under the action of ribonucleases. The degradation rate depends on many factors, such as the sensitivity of the RNA to ribonuclease treatment, the time of incubation or the concentration of the ribonuclease. In CoLoC experiment, only the RNase concentration (*A*) varies between the samples, and other parameters, including time of incubation, are fixed and correspond to a constant specific to each RNA, termed “effective degradation rate (*k’*)” **(figure 25A)**. Thus, cytosolic RNA degradation dynamics can be simplified

to $f(A) = e^{-k'A}$. However, if a part of RNA pool resides in mitochondria, it will be protected from degradation. This initial protected proportion (P_0) is the important parameter that discriminate contaminant RNAs from imported or mitochondrial encoded RNAs. Upon RNase treatment, only the cytosolic RNA pool being exposed to RNase (1-P_0) is exponentially degraded. Hence, the depletion dynamic of dually localized RNAs can be represented by a non-linear regression model.

$f(A) = (1-P_0)e^{-k'A} + P_0$.

This model can be applied to the experimental data in order to estimate the values of P_0 and k'. Statistical significance of P_0 can be further assessed by testing the null-hypothesis that $P_0 = 0$ (the RNA is not imported) and transcripts with significant P_0 will be retained as candidates for mitochondrial import, whereas other RNAs are considered as contaminants. Of note, the complete removal of cytosolic RNAs is not required to distinguish contaminant RNA from transcripts partially present inside the mitochondria.

RNAs isolated from the samples of mitochondria treated with increasing concentrations of RNase can be then converted into cDNA library for deep-sequencing and the depletion dynamics of each transcript will be analyzed.

Using this methodology, it will be possible to distinguish the three groups of transcripts. Contaminant nuclear-encoded RNAs should be gradually degraded, mtDNA-encoded RNAs present exclusively in mitochondria will not be affected by RNase treatment and nuclear-encoded partially imported RNAs should represent an intermediate profile **(Figure 25B)**.

II.B.1.2. CoLoC proof of concept

To validate the model, I isolated mitochondria from HEK 293 cells, in conditions routinely used in the laboratory, and divided crude mitochondria into 6 identical samples for RNase treatment. Since mitoplast are more fragile than mitochondria and prolonged manipulation may induce IMM rupture, digitonin treatment was performed after the RNase treatment to avoid degradation of mitochondrial RNAs. The ribonuclease chosen for this pilot experiment was RNase A. This endoribonuclease specifically hydrolyzes RNA between the 3'-phosphate group of a pyrimidine (C or U) and the 5'-hydroxyl of the adjacent nucleotide and generates

5’-hydroxyl and 3’-phosphate groups **(Nogues *et al.,* 1995; Yang, 2011)**. Such termini are incompatible with standard ligation reactions used for RNA-seq library preparation thus preventing the sequencing of degradation products (see next section). Moreover, even if RNase A preferentially cleaves single-stranded RNAs, it can also degrade double-stranded RNAs and is commonly used to remove contaminant RNAs from mitochondrial fraction **(Mercer *et al.,* 2011; Comte *et al.,* 2013)**. Concentrations of RNase A typically used in our laboratory to eliminate contaminant RNAs range between 5 to 10 µg/mL. However, this treatment may induce disruption of mitochondrial integrity with subsequent partial degradation of mt-encoded RNAs, as we observed previously **(Loutre *et al.,* 2018a).** Thus, the aliquots of mitochondrial samples were incubated with RNase A concentrations ranging from 0.05 to 1 µg/mL then washed and treated with digitonin before RNA extraction according to the protocol established previously **(Loutre *et al.,* 2018a)**.

RNA isolated from mitochondria were separated on a denaturing polyacrylamide gel and then analyzed by Northern blothybrization to assess the depletion dynamic of specific RNA species **(Figure 26A)**. Staining of the gel with ethidium bromide revealed a clear pattern of gradually degraded RNAs. For Northern blot hybridization analyses, probes for three types of transcripts were selected: mt-encoded RNAs represented by mt-tRNA^{Val} and mt-tRNA^{Lys}, nuclear-encoded partially imported RNAs represented by 5S rRNA and cytosolic RNAs represented by 5.8S rRNA and 7SL RNA. 7SL RNA is part of the signal recognition particle (SRP) ribonucleoprotein complex which recognize the signal peptide of proteins and target the translating ribosome to the ER **(Walter and Blobel, 1982; Grudnik *et al.,* 2009)**. Since ER associates strongly with mitochondria, it is one of the main sources of contamination of mitochondrial samples. Similarly, 5.8S rRNA is a major component of the cytosolic ribosomes which were shown to be associated with OMM **(Matsumoto *et al.,* 2012; Gold *et al.,* 2017)**.

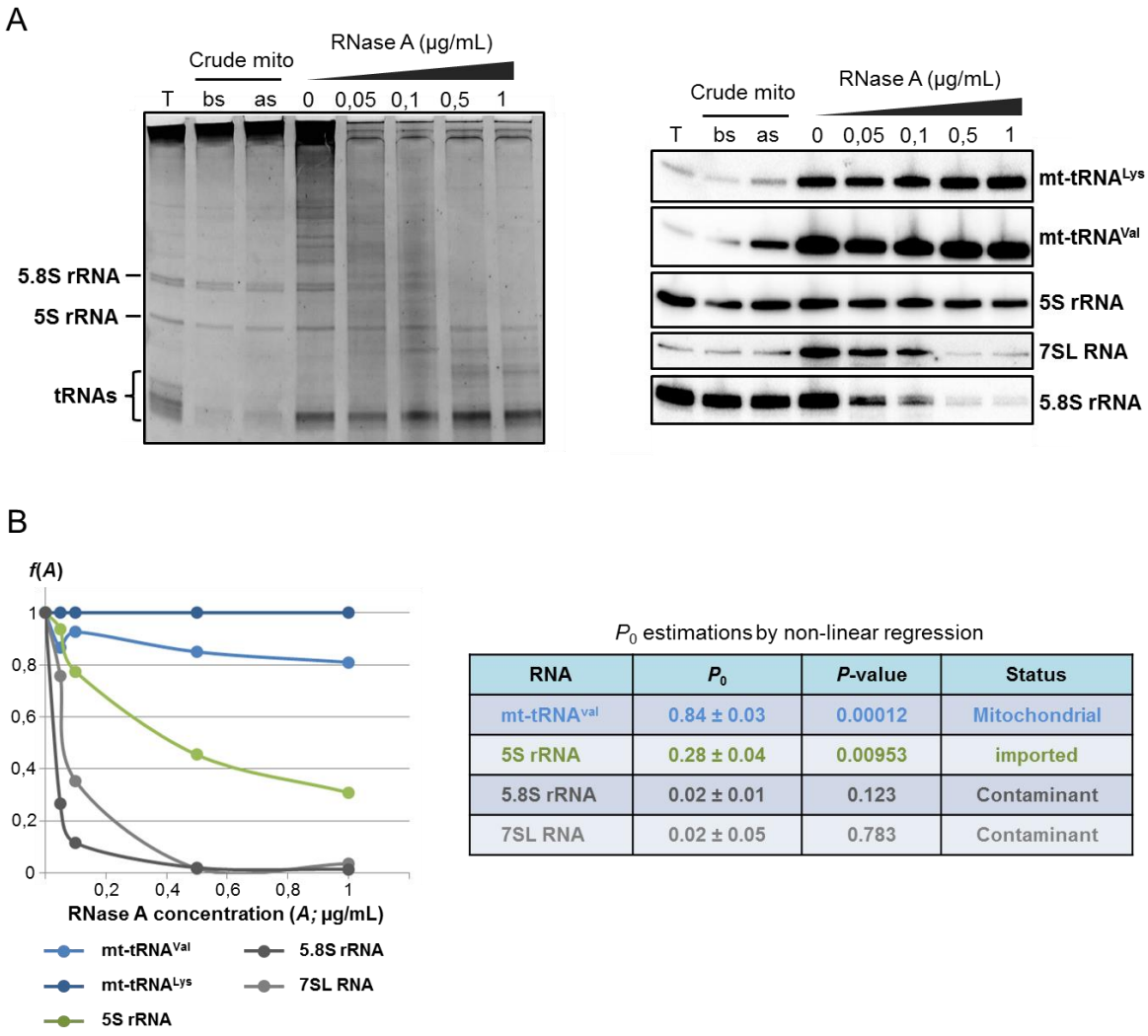

P_0 estimations by non-linear regression

RNA	P_0	*P*-value	Status
mt-tRNA^{val}	0.84 ± 0.03	0.00012	Mitochondrial
5S rRNA	0.28 ± 0.04	0.00953	imported
5.8S rRNA	0.02 ± 0.01	0.123	Contaminant
7SL RNA	0.02 ± 0.05	0.783	Contaminant

Figure 26. CoLoC procedure allows the distinction between mitochondrial RNAs and contaminant RNAs.

A) Northern blot analysis of CoLoC samples. Left panel: Ethidium bromide stained polyacrylamide gel shows the progressive degradation of RNA upon increasing RNase A treatment. Right panel: Northern blot detection of mt-encoded tRNAs (mt-tRNA^{Lys}, mt-tRNA^{Val}), partially imported RNA (5S rRNA) and cytoplasmic RNAs (7SL RNA, 5.8S rRNA). T: Total cellular RNA; bs: RNA isolated from crude mitochondrial sample before sucrose cushion purification; as: RNA from crude mitochondrial sample after sucrose cushion purification; 0: isolated mitochondria treated with digionin; 0.05 to 1: isolated mitochondria treated with the RNase A and digitonin **B)** Quantitative analysis of the Northern blot shown in panel A. Proportion of remaining RNA (f(*A*)) compared to the untreated sample (0 µg/ml of RNase A) normalized to mt-tRNA^{Lys}. At the right, table shows the P_0 values obtained by fitting the CoLoC regression model into the quantified Northern blotting data (*OriginLab* software).

To determine the proportion of remaining RNA, the signal detected by Northern blot hybridization were quantified **(Figure 26B)** as the ratio between the signal corresponding to each specific RNA observed in individual samples and the signal for the same RNA in the untreated sample (no RNase A added). To take into account the eventual difference in the loading of the samples, the ratios were normalized to the ratio calculated for a mitochondrial RNA, here mt-tRNA^{Lys}, serving as an internal control.

Three different types of depletion dynamics expected by our model were observed. First, mitochondrial RNAs, here exemplified with mt-tRNA^{val}, were virtually not degraded. However, the small decrease of mt-tRNA^{val} compared to mt-tRNA^{Lys} may indicate on a partial disruption of IMM despite the thorough efforts to maintain mitochondrial integrity during CoLoC procedure. Since similar amounts of RNA were loaded on the polyacrylamide gel (1µg of RNA for all the samples), Northern blot hybridization data shows enrichment of mitochondrial transcripts compared to other RNAs. Cytosolic RNAs (5.8S rRNA and 7SL RNA) are rapidly depleted and nearly completely disappeared in the samples treated with the high concentrations of RNase A (0.5 and 1 µg/mL). As expected, partially imported 5S rRNA demonstrated an intermediate pattern with a significant pool being protected from RNase digestion.

The regression analysis of CoLoC data shows that only mitochondrial-encoded RNAs (mt-tRNA Val) and imported RNAs (5S rRNA) present significant non-zero P_0 values. These results demonstrate the possibility to distinguish the three groups of transcripts with the CoLoC methodology and, consequently, to univocally identify mitochondrial-resident transcripts.

II.B.1.3. CoLoC-seq 1 experiment.

In order to identify imported RNAs and demonstrate the reliability of CoLoC approach at a genome-wide level, another experiment was performed with the purpose to sequence the RNA samples. A similar protocol was applied with increased number of samples (from 6 to 8) to enhance the power of analysis. At the end of the procedure, cDNA library preparation and sequencing was performed by using an original cDNA generation protocol adapted to our methodology by Vertis Biotechnologie AG (Freising, Germany) **(Figure 27)**. This protocol is based on the ligation of two adaptors that can only recognize 5'-monophosphate (5'P) and 3'-

hydroxyls (3'OH) of the RNA. Since RNase A cleavage induces the formation of 5'OH and 3'P termini, most degradation products would be removed from the analysis and thus only intact RNAs are retained for sequencing. Of note, RNA molecules can be excluded from the sequenced pool by a single RNase A cleavage, which should efficiently reduce potential biases caused by differences in RNA structure and accessibility for cleavage. Following ligation of adaptors, RNAs were transcribed into cDNA and further amplified by PCR using primers targeting the adaptors. cDNAs were then fragmented by ultrasound and specific sequencing adaptors were ligated to the fragments. A size-selection step was performed to keep sequences between 200 and 500 nt (72 and 372 nt after removal of adaptors sequences), then the cDNA library was sequenced with an Illumina next seq 500 platform giving 75 nt reads. It is important to keep in mind that because of this size-cut, our dataset did not include small RNAs such as miRNAs.

I.A.1.1.1. General analysis of CoLoC-seq data.

Sequencing data provided 6.3 to 9.8 million reads per samples mapping to 64,957 genes, although most of reads corresponded to rRNA genes since no rRNA depletion step was performed before sequencing. Initial coverage of mitochondrial genes ("0µg/mL RNase A" sample) corresponded to only 0,79% of total aligned reads, indicating the high cytosolic contamination of isolated mitochondria **(Figure 28A)**. Progressive digestion of extramitochondrial RNAs resulted in 20,3 fold enrichment of mtDNA-encoded transcripts in the sample with the highest RNase concentration, confirming the degradation of nuclear-encoded RNAs.

Reads mapped to different loci of the human genome can bias the quantitative analysis of RNA-seq data. Hence, high proportion of non-uniquely mapped reads or reads that could not be aligned to any gene may indicate low quality of samples. All the samples have shown a relatively low amount of uniquely mapped reads. However, three samples (0.05, 0.5 and 1µg/mL of RNase A), were characterized by the lowest amounts (19.19% 22.08% and 20.25% respectively) of uniquely mapped reads **(Figure 28A, left panel)**.

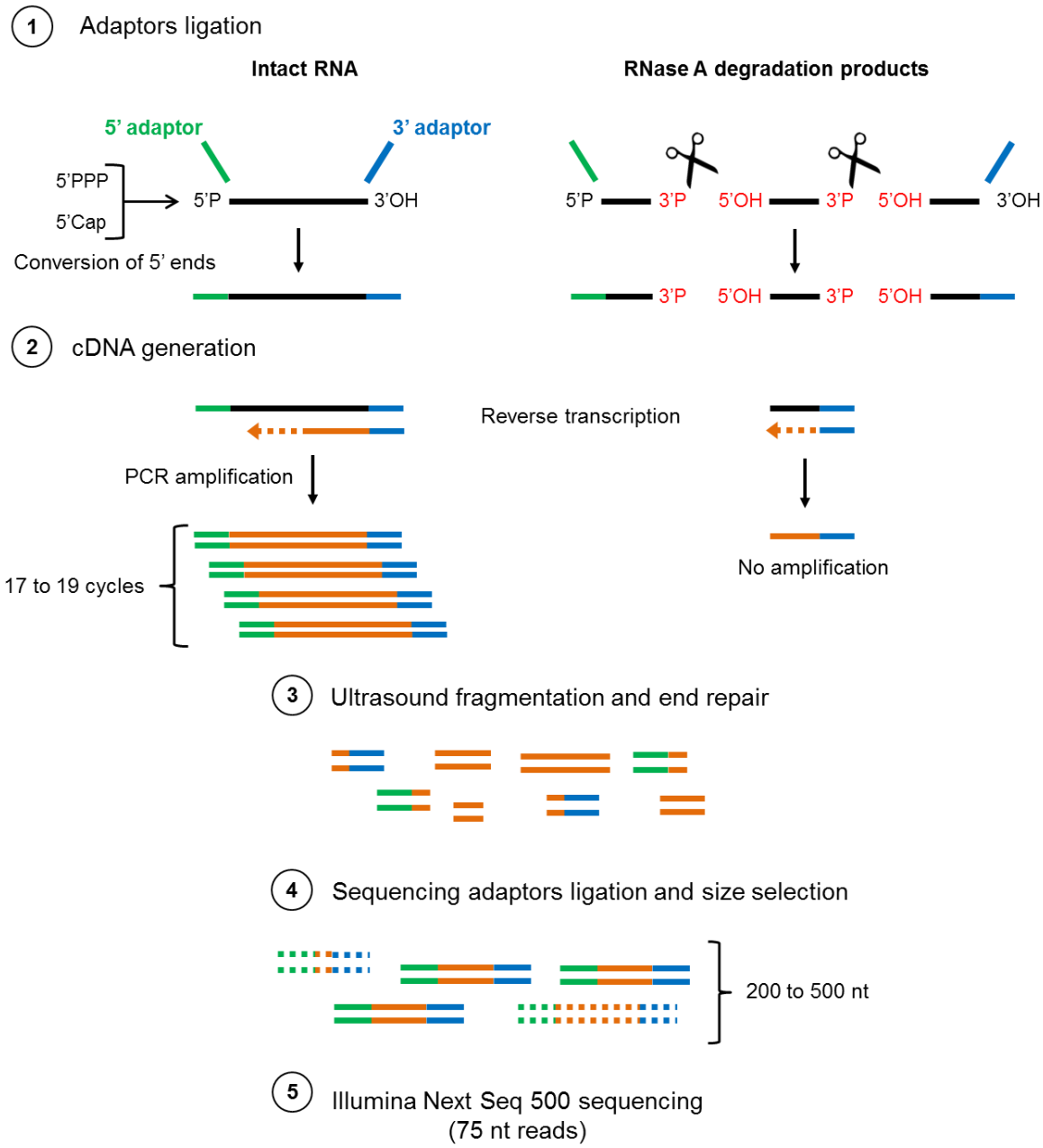

Figure 27. Pipeline of the cDNA library generation and sequencing of CoLoC RNA samples.

1. 5' Cap and 5'PPP termini are converted into 5' monophosphate by the CAP-Clip Acid Pyrophosphatase. Then, adaptor sequences are ligated specifically to the 5'P and 3'OH extremities of RNAs. Since RNase A leaves 5'OH and 3'P termini, RNA degradation products are unligatable. **2.** RNA molecules bearing adaptors are then amplified by RT-PCR. **3 and 4**. cDNAs are fragmentated by ultrasound and adaptors required for sequencing are ligated to the fragments. cDNAs are then separated on agarose gel to select fragments of 200 to 500 nt (128 nt corresponding to the sequence of adaptors). **5.** Sequencing is performed on an Illumina Next-Seq 500 platform providing reads of 75 nt.

Since mtDNA-encoded RNAs are protected from RNase A treatments, their proportion in each sample (compared to the untreated sample) were analyzed to further assess the quality of the samples **(Figure 28B)**. Interestingly, all samples demonstrated relatively high level of variability both within and between samples. The reason for this behavior remains unclear, although it may be due to the digitonin treatment, performed independently for each sample, which may affect to some extent the IMM integrity and induce partial degradation of mitochondrial RNAs. Once again, 2 samples (0.5 and 1µg/mL of RNase A) were characterized by the highest variability. Thus, the three samples (0.05, 0.5 and 1µg/mL of RNase A) of apparently low quality were removed from subsequent analyses.

2 main cut-offs were applied to the sequencing data. First, all the genes with less than 10 reads per sample have been eliminated, since so low coverage does not provide any range for analysis and is not reliable. For the second cut off, mtDNA-encoded RNAs were used as an internal reference against which all other transcripts were evaluated to assess their proportion in the different samples. Genes with less than 10% of reads remaining in the last sample compare to the untreated samples were then set aside, as they corresponded most probably to the contaminant RNAs. Strikingly, more than 99% of nuclear-encoded RNAs were rapidly depleted upon increasing RNase concentration and only 50 RNAs survived the treatment at more than 10% of their initial level. Of those, all the mtDNA-encoded (except 5 tRNAs) and 18 nuclear-encoded RNAs (see below) passed the coverage cut-off. Moreover, the extremely low coverage for mt-CO3 mRNA, known to have an unligatable 5’ terminus **(Kuznetsova *et al.*, 2017)** and for U6 snRNA which possess a 3’phosphate instead of 3’OH **(Lund and Dahlberg, 1992)** demonstrated that sequencing of RNase A degradation products was indeed avoided.

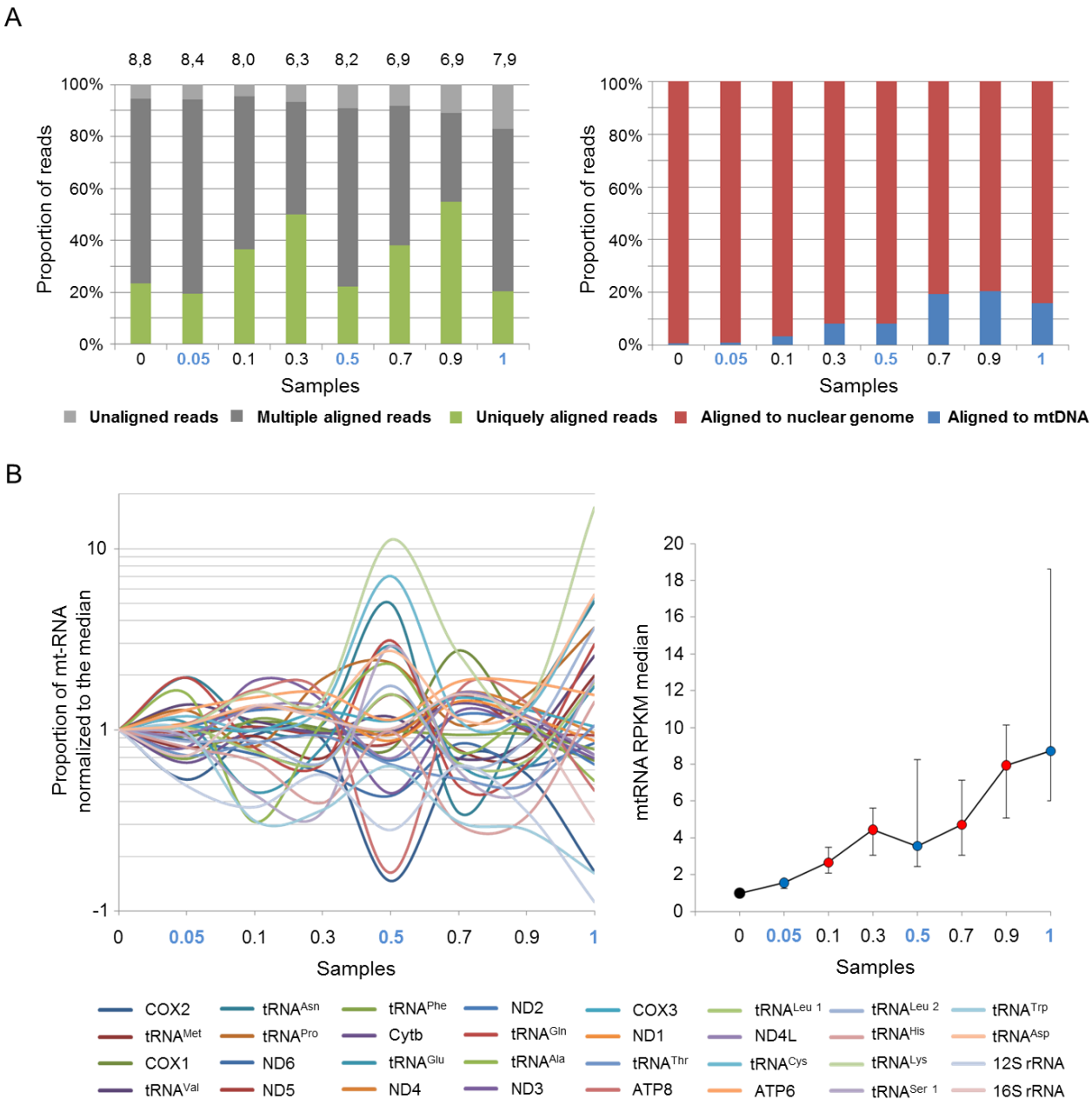

Figure 28. General quality of the pilot CoLoC-seq dataset.

A) Statistics of the reads alignment to human reference genome hg38. Left panel: proportion of uniquely aligned, multiple aligned or not aligned reads. Total amount of reads for each samples are indicated at the top of each bars (in million reads) Right panel: proportion of reads mapped to nuclear and mitochondrial human genome. **B)** Proportion of each mitochondrial transcript in all the samples compared to the untreated sample and normalized to the RPKM median of all mitochondrial transcripts (shown on the right). Samples annotated in blue presenting apparently low quality were removed from further analyses. Samples are annotated according to RNase A concentration (µg/mL) used for treatment of mitochondria. RPKM : Reads Per Kilobase Million.

II.B.1.3.3. Identification of candidates for RNA imported into mitochondria

Variability of the data did not provide the opportunity to statistically analyze the depletion dynamic of the 18 remaining cytosolic RNAs with the regression model **(Figure 29A)**. Therefore, identification of candidates for mitochondrial RNA import was achieved by taking into account, for each transcript, the general depletion dynamic and the proportion of remaining RNA in the sample treated with the highest concentration of RNase. Selected candidates were characterized by a depletion curve resembling a plateau and remaining in the range of variation of mt-encoded RNAs, in contrast with other RNAs showing constant decrease upon increasing concentrations of RNase A **(Figure 29B, Figure 30)**. Thus, six small non-coding RNAs were qualified as candidates for mitochondrial import. Surprisingly, the top-scoring nuclear-encoded RNA detected in association with mitochondria is the selenocysteine tRNA ($tRNA^{[ser]sec}$), responsible for selenocysteine incorporation during cytosolic translation **(Bulteau and Chavatte, 2015; Schoenmakers *et al.*, 2016)**. Its import, as well as putative function in mitochondria, has never been suggested before. It is even more surprising since cytosolic tRNAs are poorly covered in this dataset, which is often the case of libraries that do not include a deaminoacylation step to increase the ligatability of 3'-termini of tRNAs.

Concerning RNA species previously suggested to be imported in mitochondria, only 5S rRNA was identified at the first selection step. The RNA component of RNase P (H1 RNA), although found to be imported by some other studies **(Bartkiewicz *et al.*, 1989; Puranam and Attardi, 2001)**, behaved in this experiment as a typical contaminant undergoing a rapid degradation. This suggests that this RNA is either not imported in mitochondria or present in negligible amounts. On the other hand, MRP RNA was previously suggested to be cleaved upon import and only the 3' part of the RMRP should be protected in mitochondria **(Chang and Clayton, 1987; Noh *et al.*, 2016)**. Since the annotations of the reference genome used to analyze our data take into account the entirety of the gene, the reads corresponding to the protected part of this RNA may be hidden by the reads covering the totality of the RMRP gene, preventing its detection after the second cut-off.

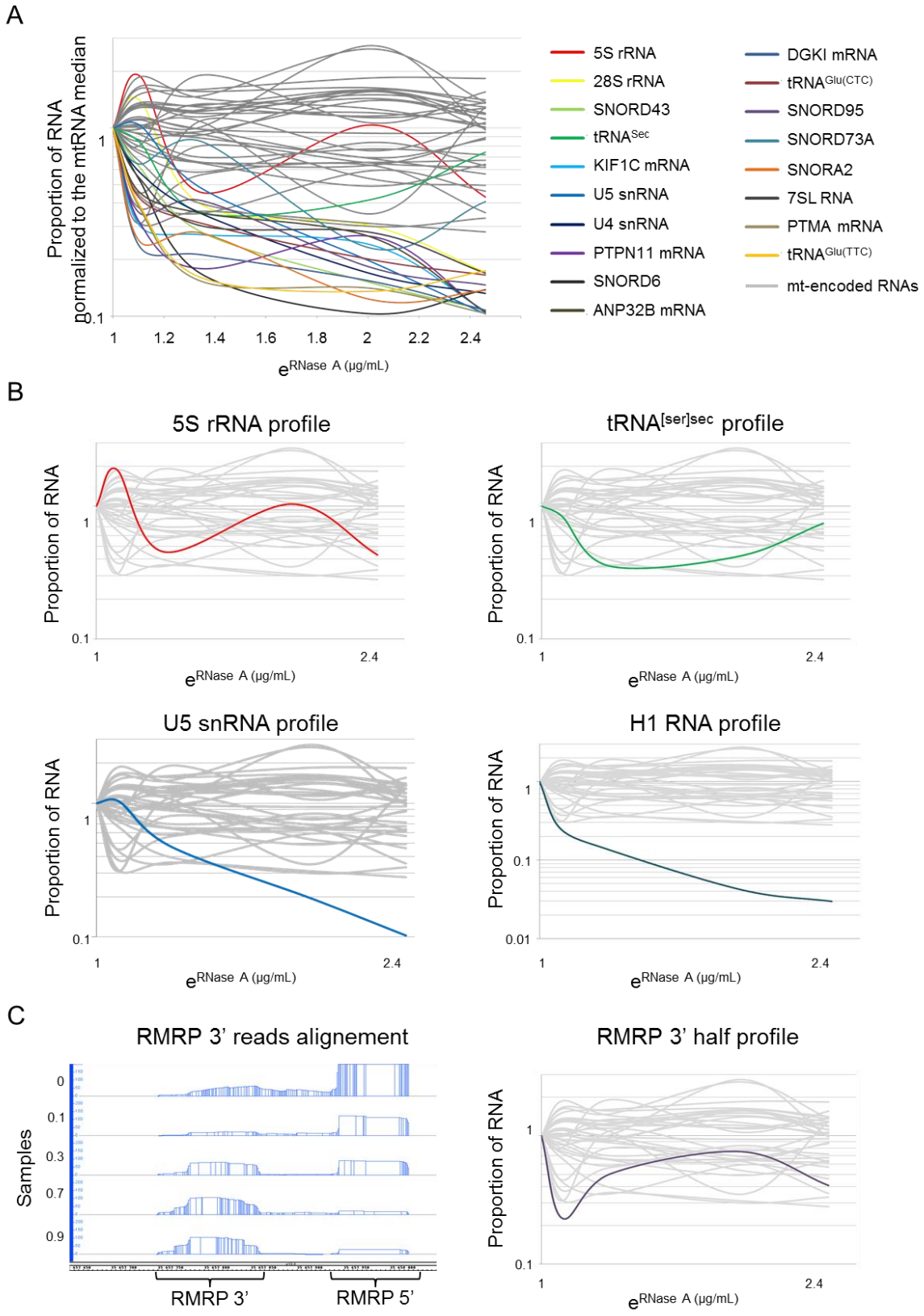

Figure 29. Depletion dynamics of nuclear-encoded RNAs.

A) Profile of the 18 nuclear-encoded RNAs that passes two main cut-offs. **B)** Depletion dynamic of 2 RNAs candidate for mitochondrial import (top panels) and 2 RNAs identified as contaminant (bottom panel). **C)** Reads alignment and profile of the imported MRP RNA. Only the 3'half of the RNA is protected from RNase treatment while the 5' half behaves as a contaminant.

Closer inspection of the reads aligned to the RMRP gene clearly revealed different patterns for the 3' and 5' regions of the gene **(Figure 29C)**. Reads mapped to the 5' half of the molecule showed a distinct depletion upon RNase treatment while the reads mapped to 3' half showed a pattern characteristic for imported RNA, in agreement with previous studies. Thereby, RMRP was also added to the list of imported RNAs identified during this pilot experiment. Of note, the telomerase RNA component TERC was also suggested to be cleaved upon mitochondrial import **(Cheng *et al.,* 2018)**, however, the gene was poorly covered in this experiment, making impossible to conclude on the RNA import.

In summary, the pilot CoLoC-seq experiment allowed to set a list of 7 RNAs potentially imported inside mitochondria **(Figure 30)**, all of them are small non-coding RNAs, among which two RNAs were already identified as imported by previous studies. However, because of the size cut-off during library preparation, the dataset did not include miRNAs. Similarly, tRNAs were poorly covered and the sequencing was performed at a the relatively low depth offered by the Illumina NextSeq platform. One can expect that increasing the depth of sequencing and switching to protocols adapted for the detection of tRNAs and miRNAs will increase the list of RNA candidates for the import.

The CoLoC experiment can also be improved by adjusting and modifying the critical steps of the mitochondria isolation procedure such as the digitonin treatment, affecting the variability between the samples, and the ribonuclease treatment. In addition, it is important to establish a control to assure that the candidates identified with the CoLoC procedure are not protected by other factors than the mitochondrial membranes. These optimizations are discussed in the next section.

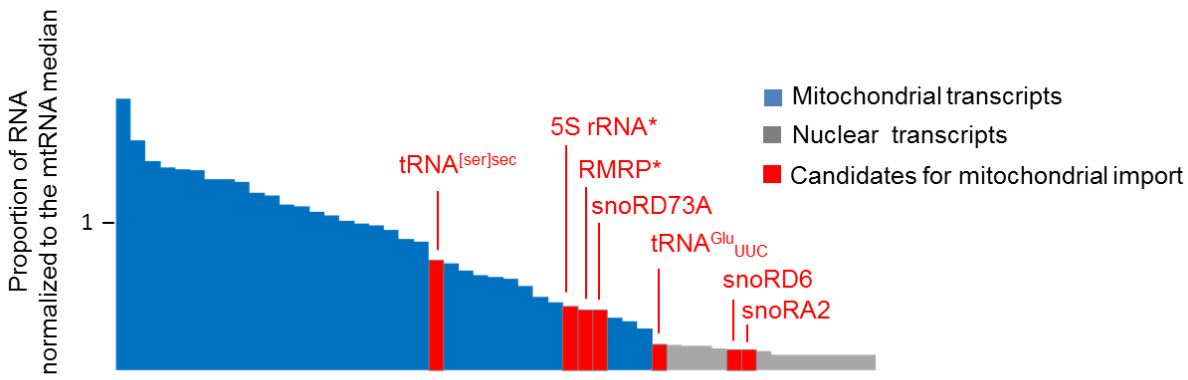

Figure 30. Overview of the 52 transcripts which remained at more than 10% at the highest RNase concentration.

RNA species are organized according to the proportion of remaining RNA in the sample treated with 0.9 µg/mL RNase A. The 7 nuclear-encoded transcripts selected as candidate are shown in red. (*) indicates RNAs previously identified as imported inside mitochondria.

II.B.2. Optimization of the CoLoC procedure

II.B.2.1. Mitoplast generation

In the protocol used in previous CoLoC experiments mitoplasts were generated after the mitochondrial samples are split and treated with RNase A. The choice to remove the OMM only after RNase treatment was initially made to avoid degradation of mt-encoded RNAs in the CoLoC procedure. However, the fact that digitonin treatment is performed independently for each sample may promote experimental variability which could be avoided by generating mitoplasts before the splitting of the samples and incubation with RNase. Moreover, performing the RNase treatment on mitoplast instead of mitochondria may facilitate the degradation of contaminant RNAs strongly associated with the OMM. To test for this hypothesis, I treated samples of mitoplasts with different concentrations of RNase A in conditions similar to the CoLoC experiment and analyzed the depletion of various RNAs by

Northern blot hybridization **(Figure 31)**. To assess for mt-RNA degradation, an artificial spike-in RNA (not present in human cells) was added to each samples before the RNA isolation step to serve as a loading reference (see IV.B.2).

The data of this experiment show that the pool of mt-tRNA^{val} remained intact in absence of digitonin treatment but was strongly depleted when mitoplasts were treated with RNase A. This demonstrates that mitoplast generation induced the partial disruption of the IMM and should not be performed before RNase treatment. As expected, cytosolic RNAs cyt-tRNA$^{Lys}_{UUU}$ and 5.8S rRNA were nearly completely eliminated in both procedure. It is important to note that the cytosolic RNA depletion was accentuated when the OMM was removed which indicates that digitonin treatment facilitates the elimination of cytosolic RNAs.

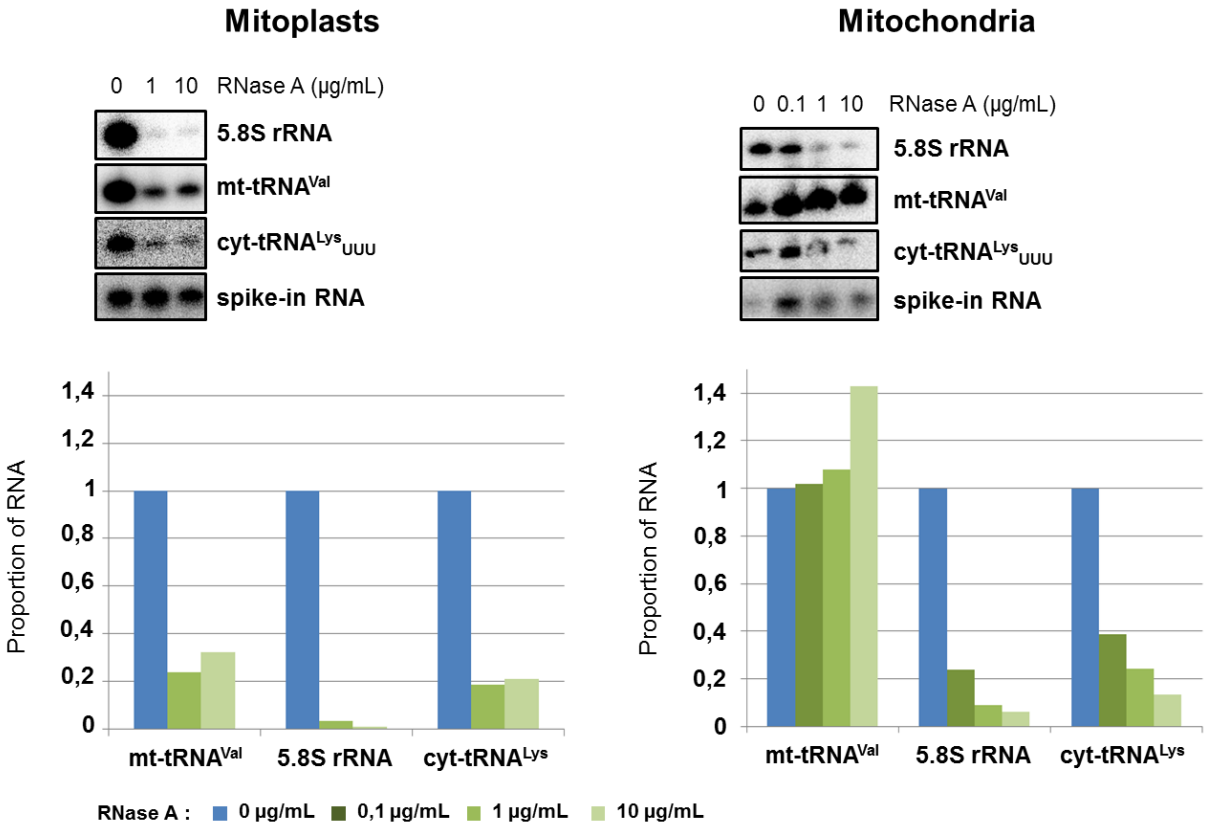

Figure 31. Impact of the digitonin treatment on the RNase A mediated degradation of RNAs associated with mitochondria.

Mitoplasts generated by digitnonin treatment (left panels) and mitochondria (right panels) were treated with different concentrations of RNase A (as indicated). RNAs samples extracted at the end of the procedure were analyzed by Northern blot. The hybridization signals were quantified as a proportion of the sample not treated by RNase A (0µg/mL) and normalized to the signal of the spike-in RNA.

II.B.2.2. Establishment of a Mock-CoLoC experiment

CoLoC-seq methodology is based on the protection of mt-resident transcripts by the integrity of the IMM, which prevents the entry of ribonuclease in the mitochondrial matrix. Using this principle, the pilot experiment allowed the identification of new RNAs candidates for mitochondrial import. However, an important control experiment should be performed to account for the possible protection of RNAs by their intrinsic structure or by the association with proteins. In this purpose, I established a “Mock-CoLoC” experiment carried out in a similar way as for standard CoLoC except that the isolated mitochondria were lysed by a detergent before RNase treatment. In such conditions all RNA molecules, including those present inside the mitochondrial matrix, should be degraded.

For the first assay of the procedure, I used only one concentration of RNase A (10µg/mL), and tested also a mix of RNase A and RNase T1 which should induce degradation of all the transcripts. RNA samples were analyzed by Northern blot and probed for different transcripts, including candidates identified during the CoLoC-seq 1 experiment, $tRNA^{[ser]sec}$ and 5S rRNA **(Figure 32A)**. The proportion of remaining RNA was quantified using the spike-in RNA, instead of mt-RNA, to normalize the quantity of RNAs loaded on the gel for each sample. The clear depletion observed for mt-encoded $tRNA^{val}$ indicates that mitochondrial RNAs are efficiently degraded and no intact mitochondria survived the procedure. Cytosolic $tRNA^{met(i)}$ was also nearly completely eliminated but, surprisingly, a proportion of 5S rRNA and $tRNA^{[ser]sec}$ persisted in the samples. The persistence of these RNAs may indicate that they are protected from degradation by other factors than the mitochondrial membrane, which confounds the imported status determined by the pilot CoLoC experiment. Nevertheless, these two RNAs were efficiently degraded by the RNase A/T1 mix which shows that they are accessible for degradation and not protected inside membrane vesicles that could be formed during the lysis procedure.

Survey of the literature on the ribonucleases activity revealed that RNase A does not require any divalent metal-cofactor to cleave RNAs **(Yang, 2011)**, however presence of 100-200mM of salt (NaCl), which was nearly absent in the buffer used in pilot CoLoC experiments, may increase the activity of RNase A **(Park and Raines, 2000, 2001)**. Thus, a modified buffer containing 100mM NaCl (see section IV.B.3.1.2)

was tested to improve the efficiency of cleavage of the persistent RNAs **(Figure 32B)**. The data showed that the salt containing buffer greatly improved the degradation of all RNAs, although a small proportion of 5S rRNA and tRNA$^{[ser]sec}$ was still observed after RNase treatment.

RNase A was initially chosen because of its property to leave termini that cannot be ligated with the adaptors used for RNA-seq library. Other RNases, such as RNase T1, RNase 1 **(Yang, 2011)** and Micrococcal Nuclease (MNase) **(Sulkowski and Laskowski, 1962)**, present similar properties. The efficiency of these various RNases was also tested on mitochondrial lysates **(Figure 33).**

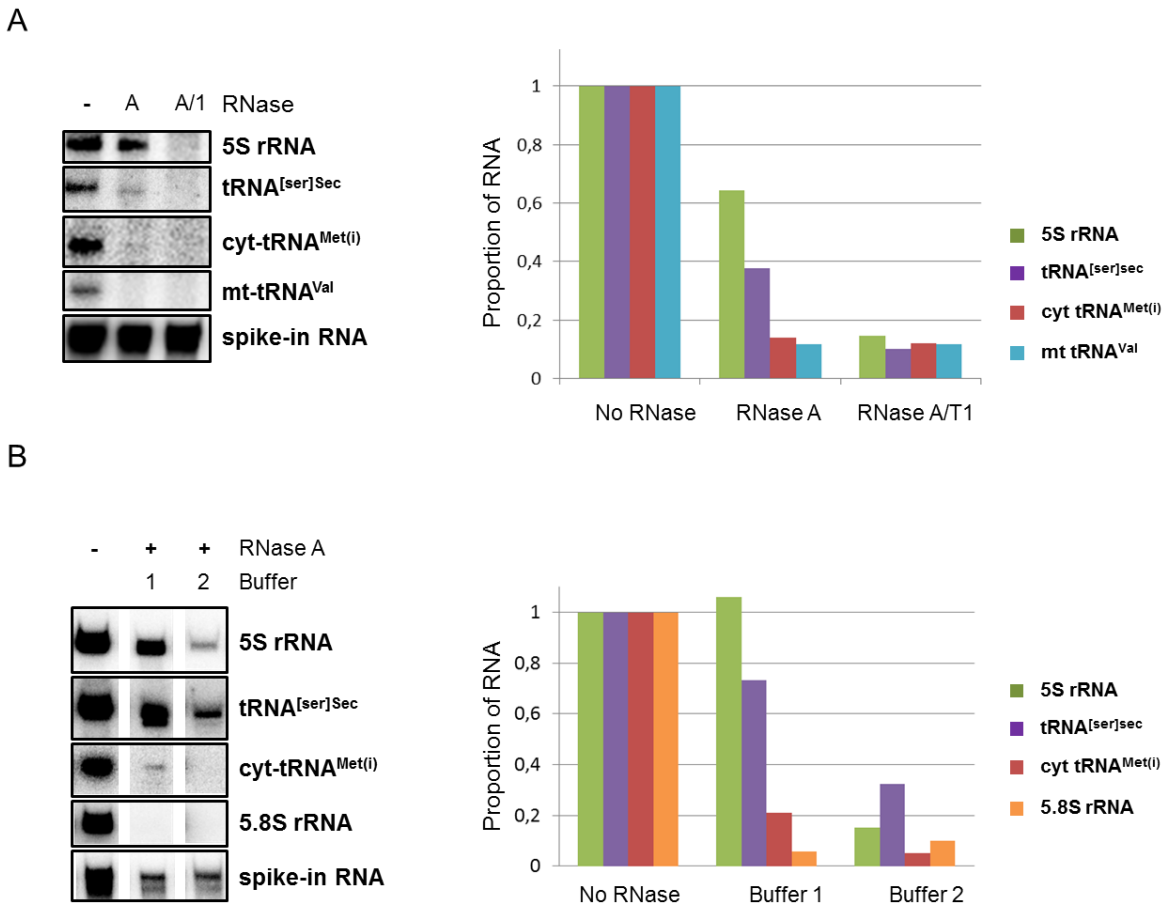

Figure 32. RNA degradation in mitochondrial lysates treated with RNase A

Isolated mitochondrial were lysed with a detergent and treated with **A)** RNase A (10µg/mL) or a mix of RNase A and RNase T1 (25U/mL)) in similar conditions as for the pilot CoLoC experiment and **B)** RNase A (10µg/mL) in standard CoLoC Buffer (Buffer 1) or improved buffer containing 200Mm NaCL (Buffer 2). RNAs were analyzed by Northern blot (left panels) and signal of each probes were quantified a in the same way as in **figure 31.**

As expected RNases showed different specificity of cleavage, for example RNase T1 was unable to cleave efficiently mt-tRNA^{Val} while other RNases induced complete elimination of this RNA. A similar case is observed with the only partial degradation of 5.8S rRNA by MNase. 5S rRNA was poorly degraded by all the RNases tested, and increasing nuclease concentration did not improve the degradation of this RNA. However, the proportion of remaining 5S rRNA depended on the RNase used. RNase A induced the best depletion of all probed RNAs, including 5S rRNA, so this nuclease has been selected for further use in CoLoC and Mock-CoLoC experiments.

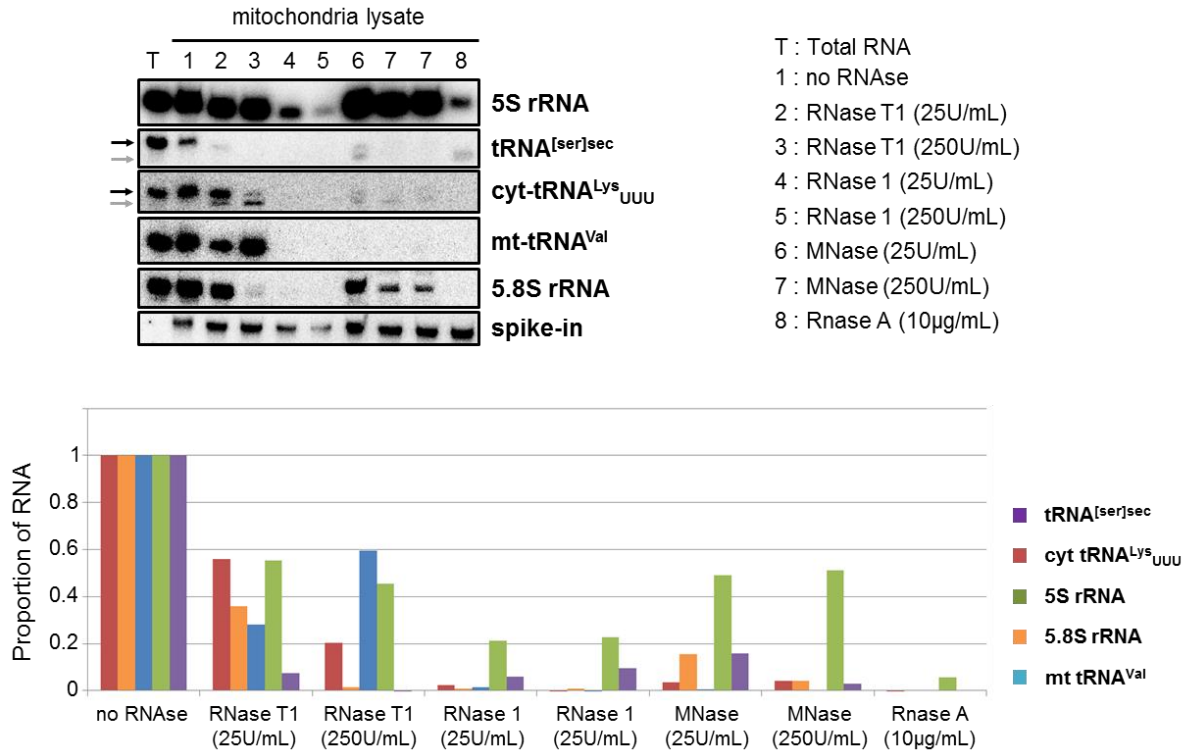

Figure 33. Degradation of mitochondria associated RNAs by different ribonucleases in Mock-CoLoC experiment.

Isolated mitochondrial were lysed with a detergent and treated with different ribonucleases in the concentrations indicated on the figure. The buffer used for RNase A corresponds to the buffer 2 in **figure 32**. Extracted RNAs were analyzed by Northern blot and signals of each probe were quantified in the same way as in **figure 31.** Black arrows indicate full length transcript and grey arrows indicate degradation products that were not take into account for the quantifications.

II.B.2.3. CoLoC and Mock-CoLoC in optimized conditions

After having determined that RNase A was indeed the best choice for our procedure and improved the conditions of treatments, a second CoLoC experiment was performed along with the corresponding Mock-CoLoC experiment. In each experiment, ten samples of mitochondria were treated with RNase A in the range of concentration from 0 to 3 µg/mL. RNase treatment was performed using the NaCl containing buffer, and the time of incubation was also increased from 5 to 7 minutes for technical convenience (see section IV.B.3.1.2). The spike-in RNA was added to the Mock-CoLoC and also to the standard CoLoC samples to assess the level of degradation of mt-encoded RNAs.

The RNA samples from both experiments were first analyzed by Northern blot and probed for two mt-encoded RNAs (mt-tRNA^{Val} and mt-tRNA^{Lys}) and five nuclear-encoded RNAs (U6 snRNA, 5.8S rRNA, 5S rRNA, tRNA$^{[ser]sec}$ and cyt-tRNA$^{Lys}_{UUU}$) as well as for the spike-in RNA **(Figure 34)**. Northern blot hybridization results confirmed that, except 5S rRNA, no full-size RNA was detected if mitochondria had been lysed with detergent before the RNase treatment **(Figure 34B)**. This demonstrates that the transcripts tested were not sufficiently protected from RNase A cleavage by particular structure or associated proteins when mitochondrial membranes are disrupted. On the other hand, 5S rRNA was only partially depleted as the RNase A concentration increased and an important proportion of 5S rRNA persisted in all samples. This can represent a case of RNA species protected from degradation by other factors than the mitochondrial membrane.

In standard CoLoC experiment **(Figure 34A)**, the proportion of mt-encoded RNAs mt-tRNA^{Val} and mt-tRNA^{Lys} remained stable as the RNase concentration increased indicating that mt-RNAs are globally not affected by RNase treatment. Of note, a moderate depletion was observed in 4 samples (1,3; 2; 2,3; and 2,6 µg/mL of RNase A) which can be explained by a partial disruption of mitochondrial membrane caused by the digitonin treatment performed independently between samples.

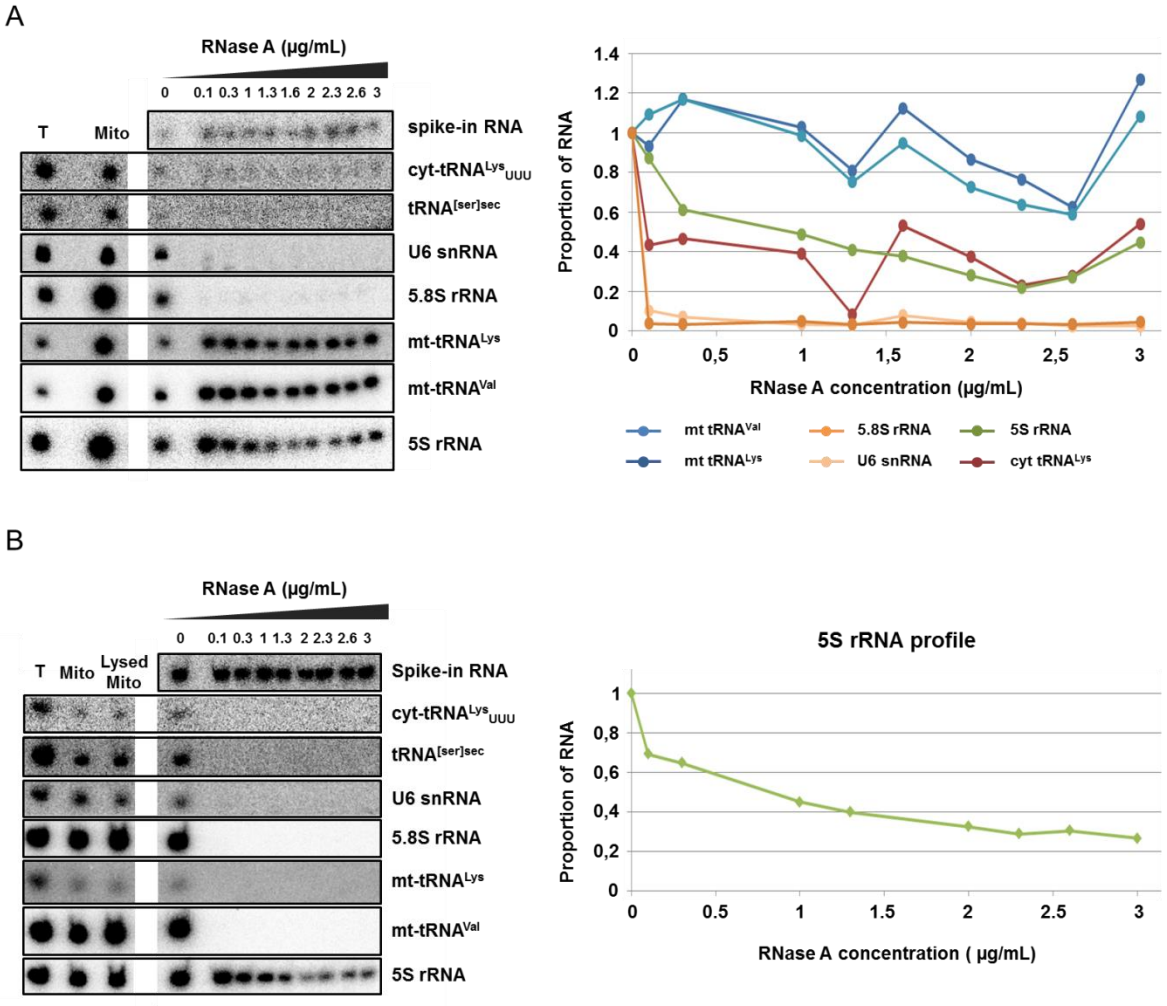

Figure 34. Northern blot analysis of the optimized CoLoC and Mock-CoLoC experiments.

A) CoLoC and **B)** mock CoLoC experiment were performed using optimized conditions and RNAs were analyzed by Northern blot. Signal of each probes were quantified a in the same way that in **figure 31**. T: total RNA; Mito: RNA extracted from crude mitochondria; Lysed Mito: RNA extracted from mitochondrial lysate.

As expected, cytosolic RNAs 5.8S rRNA and U6 snRNA were rapidly degraded upon RNase treatment. Unfortunately, hybridization signals for two cytosolic tRNAs ($tRNA^{[ser]sec}$ and $cyt\text{-}tRNA^{lys}_{UUU}$) were barely detected even in absence of RNase. Thus, quantification of the proportion of $cyt\text{-}tRNA^{Lys}_{UUU}$ may be biased since the signals were weak and close to the background level. Nevertheless, the data show that $cyt\text{-}tRNA^{Lys}_{UUU}$ was partially depleted by low concentration of RNase A but clearly reached a plateau level indicating that a proportion of this RNA had been protected from the cleavage. Since this tRNA is completely eliminated in

mitochondrial lysate samples, the protection can be provided by the integrity of mitochondrial membranes and suggests a mitochondrial import. Of note, tRNAs were generally poorly covered in the initial CoLoC-seq experiment so the import status of most cytosolic tRNAs could not be assessed. Import of cyt-tRNA$^{Lys}_{UUU}$ might be expected, since the yeast cyt-tRNA^{Lys} tRK1 is imported inside human mitochondria **(Kolesnikova *et al.*, 2000)**.

5S rRNA showed a constant and slow depletion which clearly reached a plateau level observed both in the CoLoC and in the Mock-CoLoC experiments **(Figure 34)**. This apparent protection independent on the integrity of mitochondrial membranes becomes a confounding factor that demands a careful re-visiting of the question of 5S rRNA mitochondrial import.

Northern blot analyses are limited by the detection level and number of RNA species that can be probed. Thus, we performed the sequencing of samples of CoLoC experiment performed in optimized conditions (CoLoC 2) aiming to obtain new genome-wide data and to compare them with the data of the pilot CoLoC-seq experiment (CoLoC 1).

II.B.3. Analysis of optimized CoLoC-seq data

Samples of CoLoC 2 treated with 0 – 3 µg/mL RNase A where sequenced as previously **(**Section II.B.1.3**; Figure 27)** except that no size-selection was applied allowing the sequencing of small RNAs.

Sequencing data provided a number of reads comparable to the first sequencing experiment (6.6 to 10.3 million reads per sample). Reads were mapped against the human genome and aligned to a total of 794 597 genes. However, an important proportion of the reads could not be aligned to any gene **(Figure 35A)** which can be partially inputted to the difficulty to align shorter reads retained due to the absence of size selection. On the other hand, the number of unaligned reads increased from ≈38% in the untreated sample to ≈83% in the sample treated with the highest concentration of RNase, suggesting that the treatment has affected the quality of the reads, although the reason remains unclear. In the untreated sample, 3.9% of the aligned reads mapped to the mitochondrial genome, and this proportion progressively increased up to 47.2% as the contaminant RNAs were eliminated by

RNase treatment. **(Figure 35A).** In a general manner, RNase concentration above 1µg/mL did not seem to further improve mitochondrial enrichment since the proportion of reads mapped to nuclear and mitochondrial genomes remains stable.

Reads corresponding to the spike-in RNA, although present in all samples, were not considered and mitochondrial RNAs altogether were used as an internal reference. Individual mitochondrial RNAs presented again a certain level of variability both within and between samples **(Figures 35B and 28B)**. This suggests that this variability is intrinsic to the experimental procedure and may be inputted to different factors such as the inconsistency of the digitonin treatment, the quality of the cDNA fragmentation and biais in the ligation of the adaptors. Nevertheless, no distinctive bias toward a particular sample was observed.

Identification of RNAs potentially imported inside mitochondria was conducted in the same way as for the pilot CoLoC-seq experiment (Section II.B.1.3.2). First, genes presenting a sufficient coverage (10 or more reads in each sample) were retained. Then, the proportion of reads for each transcript in RNase treated samples compared to the untreated sample (0µg/mL RNase A) was calculated and normalized to the median of mitochondrial RNAs; genes with a proportion less than 10% in the last sample were eliminated. Finally, 77 nuclear-encoded RNAs and 33 mt-encoded RNAs (all mitochondrial transcripts except $tRNA^{Asp}$, $tRNA^{Gly}$, $tRNA^{Arg}$ and $tRNA^{Trp}$) were retained **(Figure 36A).**

Remarkably, most of the identified nuclear-encoded RNAs corresponded to tRNA genes. Among them, we have found tRNAs involved in the incorporation of 14 from the 21 aminoacids. This important tRNA enrichment compared to the first experiment may be explained by the absence of size-selection which previously limited the recovering of small molecules. Interestingly, most of retained cytosolic tRNAs showed depletion dynamics resembling those of partially imported RNAs **(Figure 36B)**. Among them we identified $tRNA^{[ser]sec}$ and $tRNA^{Glu}_{UUC}$, which had been detected in the CoLoC 1 **(Figure 30)** as well as $tRNA^{Lys}_{UUU}$ which has been persistent in Northern blot experiment **(Figure 34A)**.

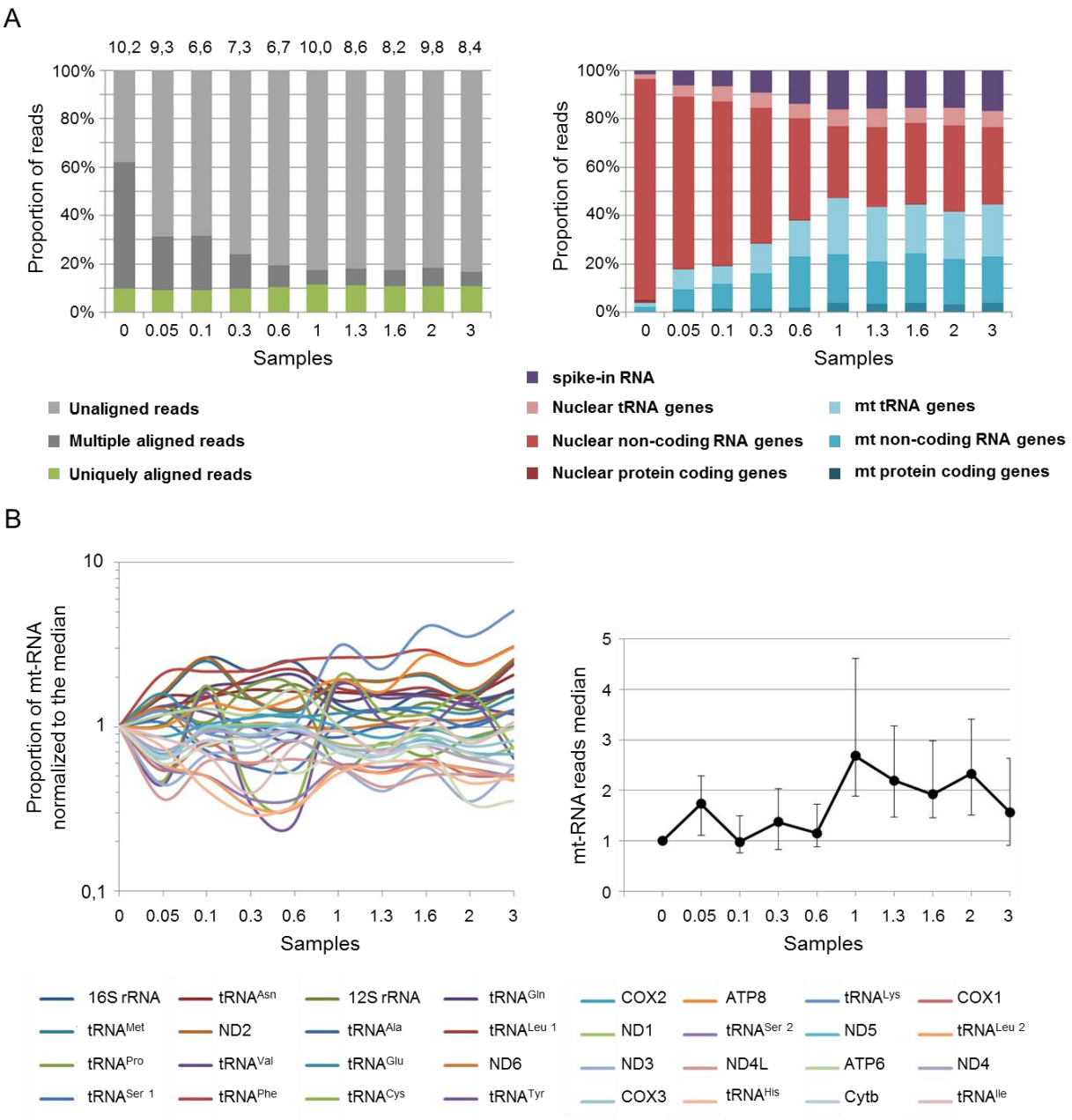

Figure 35. General dataset of the optimized CoLoC-seq experiment

A) Statistics of the reads alignment to human reference genome hg38. Left panel: proportion of uniquely aligned, multiple aligned and unaligned reads. Total amount of reads for each samples are indicated at the top of each bars (in million reads) Right panel: proportion of reads mapped to nuclear and mitochondrial human genome. **B)** Read proportion of each mitochondrial transcript in each sample compared to the untreated sample and normalized to the median of all mitochondrial transcripts (shown on the right), as in **Figure 28B**. Samples are annotated according to RNase A concentration (µg/mL) used for the treatment of mitochondria.

Unexpectedly, in this experiment five mRNAs were identified as potentially imported. However, the low number of reads compared to the size of the gene (less than 1 read per kb) suggests that the reads can result from either only a few mRNA

molecules or from an isolated small region of the gene. Further analysis is required to determine the origin of the reads mapping to these five genes.

Besides tRNAs, six other non-coding RNAs showed depletion dynamics profiles indicating on a partial protection from RNase degradation, including 5S rRNA **(Figure 36B)**. Contrary to CoLoC 1, H1 RNA was also clearly identified as protected inside mitochondria, supporting previous evidence of its import **(Bartkiewicz *et al.*, 1989; Puranam and Attardi, 2001)**.

Once again, RMRP did not survive the treatment at more than 10% read and was initially considered as a contaminant RNA. Then, the reads aligned to the RMRP gene were verified and demonstrated the same dual pattern for the two parts of the RNA as in CoLoC 1 data, supporting the import of the 3'half of the molecule **(Figure 36B)**.

Of note, snoRNAs were not detected in CoLoC 2. This discrepancy between two experiments may be explained by the changes of the CoLoC procedure, notably the composition of the buffer for RNase treatment. Yet, four RNAs (5S rRNA, RMRP, $tRNA^{[ser]sec}$ and $tRNA^{Glu}_{UUC}$) were consistently identified in the two experiments **(Figure 30 and 36A)**. In summary, the data of two independent CoLoC-seq experiments validated the new approach and allowed identification of a set of potentially imported RNAs. These results should be confirmed by sequencing of another set of independently obtained CoLoC samples and the samples issued from several Mock-CoLoC experiments. Moreover, mitochondrial import of identified RNA candidates should also be validated by orthogonal methods.

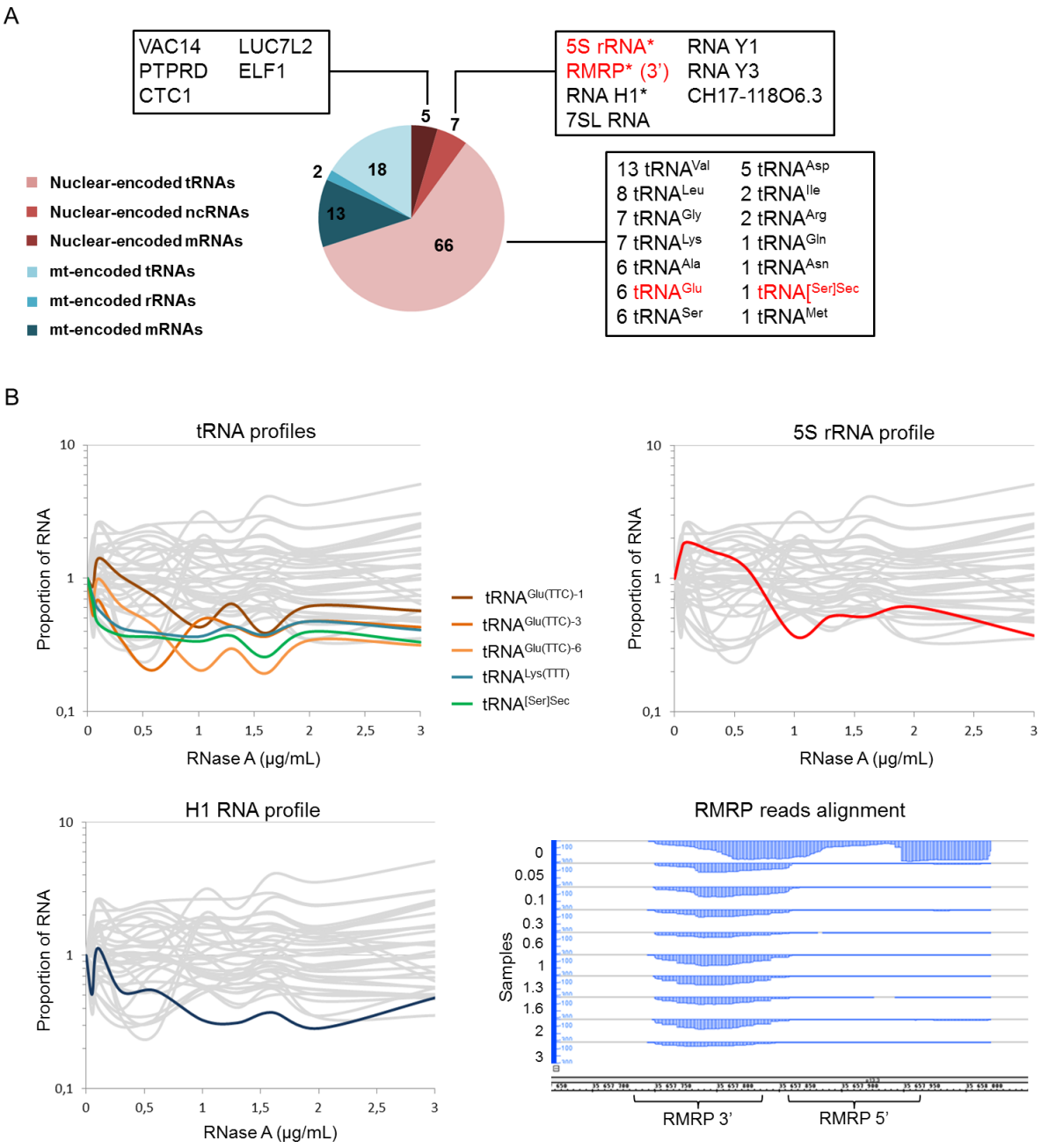

Figure 36. Selection of candidate for mitochondrial import in the second CoLoC-seq experiment.

A) Diagram representing the 110 RNAs which remained at more than 10% at the highest RNase concentration to which was added RMRP (see in the text section). RNAs highlighted in red correspond to candidates also identified in CoLoC 1 **(Figure 30)**. (*) indicates RNAs previously identified as imported inside mitochondria. **B)** Examples of the depletion dynamics of candidate RNAs. Reads aligned to the MRP RNA gene are shown to demonstrate the difference in behavior between the 3' part (imported) and 5' part of the RNA. Grey curves correspond to the depletion dynamics of the mt-encoded RNAs.

II.B.4. *In cell* confocal microscopy imaging of RNAs candidate for mitochondrial import

One of the method to study the RNA imported into mitochondria (see section I.A.4) consists in *in situ* RNA visualization by fluorescent microscopy. Single-molecule fluorescent in situ hybridization (smFISH) permits clear visualization of subcellular localization for individual RNA species **(Barrey *et al.,* 2011; Kwon, 2013; Urbanek *et al.,* 2015)** and has been successfully used for detection of mitochondrial transcripts **(Antonicka *et al.,* 2013)**. This method is currently being established in our laboratory by Dr. Anna Smirnova using branched DNA technology, which improve signal-to-noise ratio by increasing the number of fluorophore at the level of a unique target RNA molecule **(Player *et al.,* 2001; Battich *et al.,* 2013) (Figure 37A)**.

Different sets of gene-specific probe pairs designed by Affymetrix eBioscience were used to detect the following transcripts: 1) as a control for cytosolic localization, *RAN* mRNA (encoding RAN protein, a member of the RAS oncogenic proteins family); 2) for mitochondrial localization, mtDNA-encoded *MT-CO1* mRNA; 3) three RNAs candidates for mitochondrial import (5S rRNA, RMRP and $tRNA^{[ser]sec}$) **(Figure 37B and C)**. Mitochondria of HepG2 cells were labelled with either Mitotracker Red, a dye which accumulates in mitochondria **(Chazotte, 2011)**, or with fluorescent antibodies targeting the OMM protein TOM20. Images were obtained using confocal laser scanning microscopy.

The mt-encoded COI mRNA demonstrated nearly complete co-localization with the mitochondrial marker as expected for an RNA exclusively localized in mitochondrial matrix **(Figure 37B)**. In contrast, most of *RAN* mRNAs molecules anti-co-localized with mitochondria, although the limited resolution provided by conventional confocal microscopy resulted in detection of stochastic co-localization events.

Probes used to detect RMRP RNA specifically targeted the 3’ half of the molecule. As expected, most of the detected RMRP molecules were localized to the nucleus where this RNA participates in the maturation of ribosomal RNAs **(Schmitt and Clayton, 1993)**. A small proportion of the RMRP molecules were also localized in the cytosol partially associated with mitochondria.

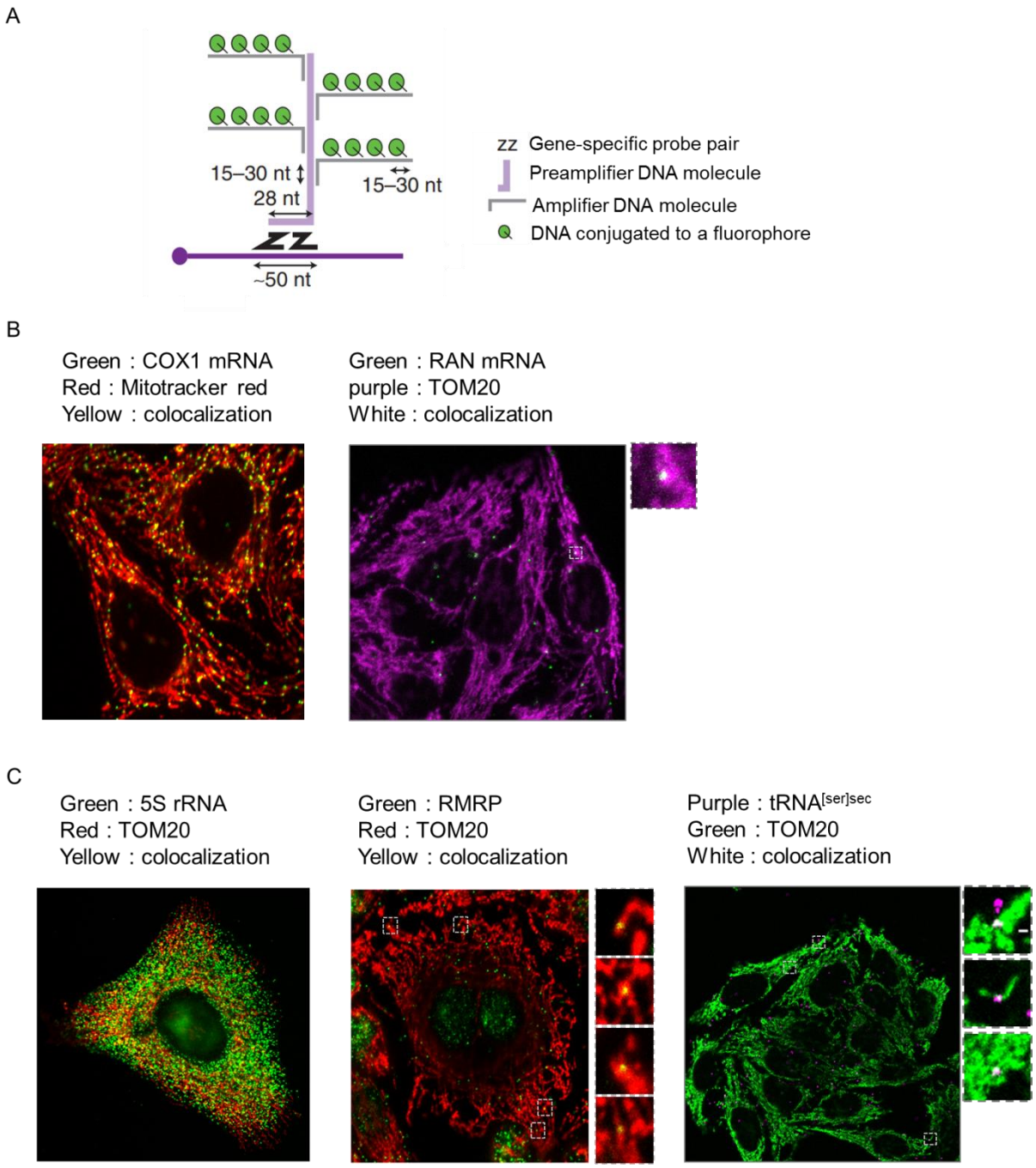

Figure 37. Imaging of mt-resident RNA in HepG2 cells by confocal microscopy using branched DNA technology.

A) The branched DNA smFISH technique. Pairs of gene-specific DNA probe anneal to the targeted RNA to allow the binding of preamplifier and amplifier DNA in a tree-like structure serving as a platform for the binding of ~400 fluorophore molecules. Adapted from **(Battich *et al.*, 2013).** **B)** Confocal microscopy imaging of mt-encoded mRNA (CO1 mRNA) and cytosolic-encoded mRNA (RAN mRNA) in HepG2cells. **C)** Confocal microscopy imaging of three nuclear-encoded RNAs candidate for the mitochondrial import in HepG2 cells. Mitochondria are visualized using either Mitotracker red or TOM20 antibodies. Nuclei are not labelled and are easily identified by the absence of mitochondria in the center of the cells. Data are kindly provided by Dr. Anna Smirnova.

tRNA$^{[ser]sec}$ was detected as a low abundant transcript (≈ 13 molecules per cells) mainly localized to the cytosol. Some molecules were clearly co-localized with mitochondria **(Figure 37C).** Further experiments and statistical analysis of the data are needed to ensure if numbers of tRNA$^{[ser]sec}$ and RMRP RNA co-localization events are significantly different from stochastic co-localization with mitochondria obtained for the cytosolic *RAN* mRNA.

5S rRNA is very abundant within the cell, and smFISH using branched DNA technology revealed that an important pool of this RNA was co-localized with mitochondria **(Figure 37C)**. By triple staining of mitochondria, 5S rRNA and 5.8S rRNA (two major RNA components of the cytosolic ribosomes) we were able to quantify and compare the mitochondrial co-localization for these two rRNAs **(Figure 38)**. Surprisingly, for both rRNAs, similar levels of co-localization with mitochondria (15±4%) have been obtained. Due to rather low level of resolution, this can be explained by the tight association of the cytosolic ribosomes with the outer mitochondrial membrane.

Data obtained by smFISH show that all the tested RNA candidates were to some extent associated with mitochondria. However, due to the diffraction of light, confocal microscopy does not provide sufficient resolution to visualize whether RNA molecules are located inside the mitochondrial matrix. Decisive evidence for the RNA import into the mitochondria can be obtained by super resolution microscopy approaches, which can provide sufficient resolution to image the sub-mitochondrial location of the RNA molecules. **(Brown *et al.,* 2011; Kuzmenko *et al.,* 2011; Jakobs and Wurm, 2014)**.

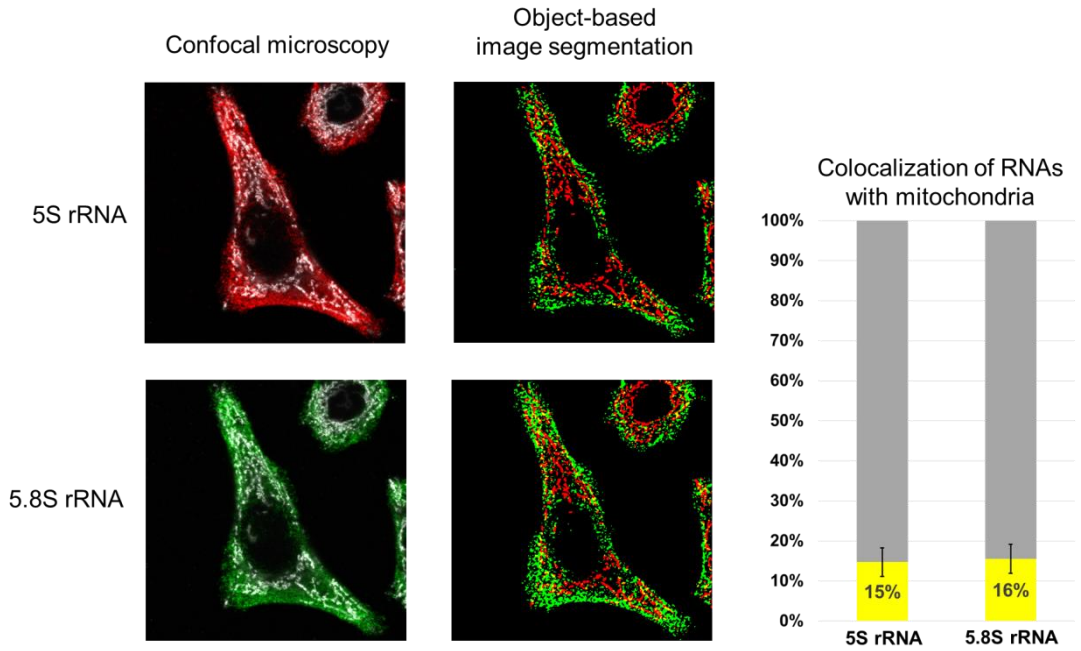

Figure 38. Imaging of 5S rRNA and 5.8S rRNA in HepG2 cells by confocal microscopy using branched DNA technology.

Left panel: Confocal microscopy imaging of 5S rRNA and 5.8S rRNA (as indicated at the left) using branched DNA smFISH technology. Red: 5S rRNA; Green: 5.8S rRNA; White: TOM20 immunofluorescent visualization. **Middle panel:** Object-based image segmentation. Fluorescent signals were transformed into delineated objects using *ImageJ* plugin « squassh » as described in **(Rizk *et al.*, 2014)**. Red: TOM20; Green: 5S rRNA or 5.8S rRNA; Yellow: overlap of the two signals. **Right panel:** Object-based quantification of the overlapping signals (% of co-localized signals shown in yellow) for 5S rRNA or 5.8S rRNA with TOM20 (presented as the mean of the quantification of 12 individual cells). Data are kindly provided by Dr. Anna Smirnova.

III. Conclusions and perspectives

In apparently all eukaryotes some nuclear-encoded RNAs are imported into the mitochondria **(Schneider, 2011; Kim *et al.,* 2017)**. In the context of human pathologies caused by mtDNA mutations, our laboratory currently work on developing therapeutic strategies based on the natural pathway of RNA import into mitochondria, by targeting tRNA molecules to replace deficient mt-encoded tRNAs **(Kolesnikova *et al.,* 2004; Karicheva *et al.,* 2011)** or by modulating mtDNA mutation load with anti-replicative oligonucleotides **(Comte *et al.,* 2013; Tonin *et al.,* 2014)** **(Figure 11)**. Better understanding of the mechanisms governing the import of RNA into mitochondria, as well as of the diversity of imported RNA species can benefit the development of therapeutic strategies. During the first part of my thesis, I continued the research performed by our laboratory on the development of an anti-replicative strategy targeting pathogenic mtDNA mutations and shed light on different factors that can be taken into account to improve the efficiency of the strategy. In the second part of my thesis I focused on the development of an original genome-wide method to identify RNA species present inside mitochondria and I identified new RNAs candidates for import into human mitochondria.

III.A. 5S rRNA mediated anti-replicative strategy

5S rRNA as a vector for the anti-replicative strategy

Most mtDNA mutations compromising mitochondrial functions are heteroplasmic and usually result in the development of mitochondrial pathology only when the heteroplasmy level reaches a pathogenic threshold. The anti-replicative strategy developed in our laboratory aim to induce the decrease of mtDNA heteroplasmy level below the pathogenic threshold by targeting RNA molecules able to slow the mutant mtDNA replication.

5S ribosomal RNA is an abundant nuclear-encoded RNA and a major component of the ribosome of most organisms **(Bogdanov *et al.,* 1995; Kouvela *et al.,* 2007; Amunts *et al.,* 2015)** except some mitochondrial ribosomes ***(Greber and Ban, 2016)***. In human cells, a subset of the 5S rRNA cellular pool is imported into mitochondria **(Entelis *et al.,* 2001; Autour *et al.,* 2018)**, although this RNA is not a

component of the mitochondrial ribosome, which contains instead the mt-tRNA^{Val} **(Rorbach *et al.*, 2016).** Our laboratory demonstrated that removing or replacing the β-domain of 5S rRNA does not affect its targeting to mitochondria **(Smirnov *et al.*, 2008).** Thus, 5S rRNA molecules can be used as a vector to import into mitochondria short RNA sequences **(Zelenka *et al.*, 2014; Autour *et al.*, 2018)**, including anti-replicative oligonucleotides targeting mutated mtDNA molecules **(Comte *et al.*, 2013)**. In contrast to the small anti-replicative RNAs based on the import determinants of the yeast tRNA^{Lys} tRK1 **(Kolesnikova *et al.*, 2010; Tonin *et al.*, 2014)**, the rec.5S rRNAs molecules conserve the internal promoter region recognized by RNA polymerase III and nuclear export signals **(Figure 21)**. Therefore, these RNA molecules can be expressed in cells in stable manner.

As it was suggested previously, replacement of the β-domain, interacting with the L5 ribosomal protein which redirects the 5S rRNA into the nucleus to be assembled into the ribosome, should increase the addressing of the RNA molecules to mitochondria **(Smirnov *et al.*, 2008)**, since 5S rRNA is not a structural component of the mitochondrial ribosome, one can expect that the anti-replicative rec.5S rRNAs would be available to anneal to mtDNA. However, 5S rRNA may interact with other factors inside mitochondria which can prevent or reduce their anti-replicative efficiency. Further investigation of 5S rRNA function in mitochondria may shed light on these factors and facilitate the design of rec.5S rRNAs free of interactions, aiming to increase their availability for annealing with mutant mtDNA.

Design of the anti-replicative 5S rRNA molecules

The rec.5S rRNA construct designed and used in this study contained different anti-replicative insertions replacing the distal portion of the β-domain and targeting either the large KSS deletion **(Comte *et al.*, 2013)** or the point mutation in the *MT-ND5* gene **(Tonin *et al.*, 2014) (Figure 19)**. The anti-replicative sequences varied in length (between 13 to 17 nt) and in sequence according to the targeted mtDNA strand (L- or H-strand). *In silico* secondary structure predictions were used to assure that the inserted sequences did not alter the 5S rRNA structural elements required for RNA expression and targeting to mitochondria.

To slow the replication of mutant mtDNA, inserted sequences should anneal to the mtDNA molecule containing the mutation but not to the wild-type mtDNA molecules. The initial expectation was that rec.5S rRNAs targeting the *MT-ND5* point mutation may also hybridize partially with the wild-type mtDNA molecule since the sequences only differs by one nucleotide. In this regard, we estimated the predicted difference in melting temperature for each RNA-DNA duplex formed with mutant and with wild-type mtDNA molecules (ΔTm). Then, hybridization of selected rec.5S rRNA versions with mutant mtDNA were tested *in vitro* by two approaches: blot-hybridization with labeled RNA probes for the KSS deletion and hybridization in solution followed by gel-shift analysis for the *MT-ND5* point mutation **(Figure 22)**. Surprisingly, rec.5S rRNAs designed to specifically anneal with the mtDNA bearing 13514 A>G point mutation, either specifically hybridized to the mutant mtDNA molecules or did not anneal to any mtDNA fragments, even for the version 5S-ND5-17L characterized by low predicted ΔTm **(Table 3)**. This may be explained by the alternative folding(s) of the rec.5S rRNA molecules which was not predicted by *RNA fold* software and could prevent their hybridization with mtDNA.

Rec.5S rRNA versions, selected by *in vitro* hybridization, were thereafter expressed in human cultured cells. Three mtDNA replication mechanisms have been suggested to take place in mitochondria and may apparently depend on the growth conditions or the energetic state of the cells **(Herbers *et al.,* 2018) (Figure 8)**. The anti-replicative strategy induces a stalling of the replication fork at the site of RNA annealing **(Comte *et al.,* 2013)** and this may take place for all three models of replication. According to the asymmetric strand displacement model, the replication of the L-strand starts after the release of the origin of replication O_L by the displacement of the H-strand. In this context, rec.5S rRNAs annealing to the L-strand of mtDNA should be more efficient compared to the H-strand targeting RNAs since they induce the stalling of the replication of H-strand mtDNA and also prevent the release of O_L. In our experiments, significant heteroplasmy shifts were effectively observed only with rec.5S rRNA versions containing insert targeting the L-strand of mtDNA (5S-KSS-13H; 5S-KSS-15H; 5S-ND5-17H), supporting the strand displacement model.

Expression and import levels of rec.5S rRNAs impact the efficiency of the anti-replicative strategy

Previously, plasmid DNAs bearing the genes of rec.5S rRNA targeting the large KSS deletion (nucleotides 8363±15438) were inserted randomly into the nuclear genome of human *trans*mitochondrial cybrid cells **(Comte *et al.,* 2013)**. This method yielded a series of clones characterized by variable and weak expression of the anti-replicative molecules and, in most cases, no detectable effect on the KSS heteroplasmy level. Nevertheless, expression of 30±5 anti-replicative molecules per cells seemed to be sufficient to induce a moderate decrease of heteoplasmy level. During my thesis, I designed similar rec.5S rRNAs containing insertions from 13 to 17 nt targeting either the KSS deletion or a point mutation in the *MT-ND5* gene (13514 A>G) **(Figure 19)** with the aim to increase the expression level of the rec.5S rRNAs and to determine whether this can enhance the heteroplasmy shift.

Transmitochondrial cybrid cell lines expressing the rec.5S rRNA were produced using the Flp-In™ T-Rex™ system (Invitrogen) which allows the Flp recombinase-mediated integration of a gene of interest into a transcriptionally active genomic location **(Figure 20)**. For these cell lines, RT-PCR quantification of the rec.5S rRNAs molecules targeting the KSS deletion demonstrated that all the rec.5S rRNAs genes were expressed 10-100 fold more efficiently (200-1000 molecules per cells) compared to the clones obtained previously. Thus, the Flp-In™ T-Rex™ system allowed an improvement of rec.5S rRNAs expression compared to the random insertion of plasmid DNA bearing rec.5S rRNA genes. However, the levels of rec.5S rRNAs expression varied between different lines of cybrid cells. A heteroplasmy shift has been detected only in cell lines with the highest expression of two rec.5S rRNA molecules (5S-KSS-13H and 5S-KSS-15H). Lower expression of the same rec.5S rRNA molecules did not induce a decrease of heteroplasmy, suggesting an anti-replicative RNA concentration threshold.

High expression of rec.5S rRNA might compensate for a low import efficiency of rec.5S rRNAs. Proportion of 5S rRNA molecules imported inside mitochondria was previously estimated at ≈1% of the cellular 5S rRNA pool in HepG2 cells **(Entelis *et al.,* 2001)**. In our experiments, all the rec.5S rRNA versions targeting the KSS deletion were detected in purified mitoplasts, and their import efficiencies were close to that of endogenous wild-type 5S rRNA. Only 5S-KSS-13H demonstrated a higher

import efficiency which can explain, along with its higher expression, the stronger effect on the heteroplasmy level compared to 5S-KSS-15H. Still, the level of rec.5S rRNAs expression remained rather weak compared to the amount of endogenous 5S rRNA molecules estimated at ≈3,2x10^6 molecules per cells **(Entelis *et al.,* 2001).** Indeed, one gene of rec.5S rRNA has been inserted into nuclear genome, while endogenous 5S rRNA molecules are expressed from 100 to 200 genes usually organized in tandem clusters of several repeats **(Sorensen and Frederiksen, 1991)**. This huge difference in expression levels and strong competition for the import factors may explain why, even if the distal part the β-domain leading to the incorporation into the cytosolic ribosome was removed, the rec.5S rRNAs did not demonstrate an improved import efficiency. Thus, high expression of rec.5S rRNA is required to ensure that anti-replicative molecules are present inside mitochondria in sufficient amounts to induce a decrease of the mutant mtDNA load.

In perspective, improved stable expression of the recombinant RNA molecules could be achieved by insertion of tandem repeats of the rec.5S rRNA genes. On the other hand, mitochondrial import of the 5S rRNA molecules could also be increased by overexpression of the protein factors involved in this pathway, namely preMRPL18 and Rhodanese **(Smirnov *et al.,* 2010; Smirnov *et al.,* 2011)** or PNPase **(Wang *et al.,* 2010; Vedrenne *et al.,* 2012)**.

Induction of the heteroplasmy shift is improved by selective cell growth condition

Multiple studies suggest that human cells in culture can compensate the energetic defects caused by mitochondrial dysfunctions through glycolysis pathway **(Marroquin *et al.,* 2007).** Thus, even harboring a high heteroplasmy level of pathogenic mtDNA mutation, cells can grow in the media containing high concentrations of glucose. In contrast, in the media deprived of glucose, cells cannot use glycolysis to meet their energy requirements and are forced to rely on mitochondrial oxidative phosphorylation. In such conditions, the cells apparently favor the metabolism of pyruvate and amino-acids and increase the activity of all respiratory chain complexes **(Cannino *et al.,* 2012)**. Therefore, culturing the cells in media deprived of glucose may create selective conditions favorable for cells with enhanced mitochondrial oxidative phosphorylation. In the context of my thesis

project, this would facilitate the detection of cells presenting a diminution of mtDNA mutation load induced by the anti-replicative action of the rec.5S rRNA molecules.

For the KSS deletion, the highest decrease of the heteroplasmy was observed in cell line expressing the 5S-KSS-13H rec.5S rRNA when cultivated in glucose-free medium. On the contrary, the same cells cultivated in high glucose medium did not show a significant reduction of the heteroplasmy. The level of the heteroplasmy in cells expressing other rec.5S rRNAs versions or not expressing any rec.5S rRNAs was not decreased in glucose-free medium indicating that the selective pressure alone was not responsible for the heteroplasmy shift. Thus, the glucose-free medium created a selective advantage for cells in which the action of the anti-replicative rec.5S rRNA successfully decreased the mutant mtDNA proportion and facilitated detection of the heteroplasmy shift.

Unfortunately, cybrids cells bearing 13514 A>G point mutation in the *MT-ND5* gene were not able to grow in the absence of glucose. Indeed the cell line demonstrated a diminished growth rate due to both the high heteroplasmy level inducing defect in cellular respiration and the insertion of an FRT site. Another cell line (clone 3, **Figure 23**), characterized by an increased vitality, can be used to reproduce the experiment. However, one can expect a reduced effect on the heteroplasmy level since this line demonstrated a low β-galactosidase activity compared to the clone 2 used in my experiments.

Optimization of the anti-replicative therapeutic strategy

The data obtained during my thesis revealed a few parameters that can be taken into account to improve the efficiency of the anti-replicative therapeutic approach based on 5S rRNA. Longer anti-replicative sequences are more efficient, although the constraint of preserving the structural elements of the 5S rRNA molecule limits the maximum length of the insertion. The effect on the heteroplasmy depends on an expression threshold, which might, as mentioned previously, be achieved by integration of multiple copies of anti-replicative rec.5S rRNA molecules and/or by the overexpression of import factors. Selective growth conditions in absence of glucose also greatly improve the effect of the anti-replicative RNA molecules and should be considered for the future application of therapeutic strategies, although the results should be confirmed for other mutations.

In this study, the anti-replicative sequences were designed to ensure that the predicted melting temperature exceeded the physiological 37°C. However, a recent paper suggested that human mitochondria may maintain the temperature close to 50°C if the respiratory chain is functional **(Chretien *et al.,* 2018)**. In this context, the annealing of our anti-replicative molecules (**Table 3; (Loutre *et al.,* 2018a))** to mtDNA may be less efficient than expected. Future design of new anti-replicative RNAs should take into account this eventual difference of temperature both for in *silico* and *in vitro* estimations of their ability to anneal to mtDNA.

To date, little is known about the diversity of RNA imported into mitochondria of human cells and the import of some RNAs often remains controversial. One can expect that therapeutic strategies based on the import of RNA into mitochondria will benefit from broaden knowledge on the RNA import and function inside mitochondria. Notably, the discovery of RNA species imported inside human mitochondria may provide new vectors for the anti-replicative strategy and shed light on the mechanisms governing RNA import.

III.B. Identification of RNA imported inside human mitochondria by CoLoC-seq

Several laboratories attempted to profile the human mitochondrial RNome by RNA deep-sequencing **(Bandiera *et al.,* 2011; Mercer *et al.,* 2011; Sripada *et al.,* 2012)**. In these studies, identification of RNA imported into mitochondria relies on the detection of nuclear-encoded RNAs in the mitochondrial fraction. Thus, due to the high contamination of mitochondria by non-resident transcripts and the apparent impossibility to obtain mitochondria deprived of cytosolic contaminants, results concerning the import of RNAs inside mitochondria often remain indecisive.

Using standard approaches of mitochondria isolation, it is virtually impossible to be sure that the mitochondrial RNA samples are indeed deprived of cytosolic contaminations. During my thesis, I developed a new strategy to unequivocally distinguish imported RNAs from mere contaminants based on their progressive depletion in isolated mitochondria treated with increasing concentration of ribonuclease, named “controlled level of contamination coupled with deep-sequencing” (CoLoC-seq).

The CoLoC regression model

CoLoC approach relies on the following of the RNA depletion dynamics in a series of progressively decontaminated mitochondrial samples. The depletion dynamics of each transcript is analyzed by fitting a simple nonlinear regression model based on modified first-order kinetic equations **(Figure 25)**. The model provides statistical estimation of two parameters, the effective degradation rate *k'* and the initial protected pool P_0 (i.e. proportion of molecules of a given transcript in principle unavailable for degradation). Transcripts with significant P0 are retained as candidates whereas all other RNAs are declared as contaminants. Noteworthy, P_0 does not represent the proportion of protected RNA *in vivo*, but in crude mitochondria preparations. One should keep in mind that the absolute P_0 values are dependent on the level of purification of isolated mitochondria, thus it can be variable from one experiment to another. The approach based on this model was tested and our experimental data demonstrated that it can be used to distinguish 3 types of transcripts: not protected (cytosolic RNAS), completely protected (mt-encoded RNAs) and partially protected (putative imported RNA) **(Figure 26)**.

In CoLoC experiments, we expect that the RNA protection from RNase treatment is provided by the integrity of the mitochondrial membrane, id est, the RNA cannot be degraded because it is protected inside the mitochondrial matrix and inaccessible to the ribonuclease. We should take into account that in crude mitochondria preparation many factors can influence the RNA cleavage by nucleases; the most important ones are the 3D RNA structure and interactions with proteins which can protect RNA from degradation. To address this question I established a control experiment, Mock-CoLoC, where mitochondrial membranes are disrupted before RNase treatment. The efficiency of lysis was demonstrated by the complete degradation of mt-encoded RNAs. Unfortunately, I have not yet obtained the data of mock-CoLoC sequencing which is absolutely necessary to conclude on the CoLoC-seq data. For instance, Northern blot data demonstrated that 5S rRNA, previously identified as imported into mitochondria RNA **(Yoshionari *et al.,* 1994; Magalhaes *et al.,* 1998; Entelis *et al.,* 2001; Smirnov *et al.,* 2011; Autour *et al.,***

2018), persisted in Mock-CoLoC experiment. The question of 5S rRNA import will be discussed below.

Regression analysis was successfully applied to Northern blot data but could not be applied to CoLoC-seq data due to great variability between the samples. This is mostly intrinsic to the bias of the RNA-seq procedure, namely fragmentation and ligation of adaptors steps. Although no statistical analyses were possible, I could analyze the characteristic depletion dynamic of the RNA species to identify candidates for mitochondrial import.

Biological significance of identified RNA candidates

Data of two independent CoLoC-seq experiments allowed identification of new potentially imported RNAs. Both experiment revealed only a few number of potentially imported RNAs suggesting that the mitochondrial RNA import in human is a highly selective process. Except for five mRNAs and one long non-coding RNA **(Figure 36A),** which deserved a more thorough analyses of the aligned reads, all the identified imported RNAs are short non-coding RNAs. This is in accordance with the results obtained by other studies **(Mercer *et al.,* 2011; Kaewsapsak *et al.,* 2017)** where no long cytosolic mRNAs were associated with mitoplasts. The differences in the data of the two CoLoC experiments can be explained by 1) the different conditions of RNase treatment which might facilitated the elimination of some RNA species such as snoRNAs and 2) the absence of size cut-off in CoLoC 2 which improved the coverage of tRNA genes. Importantly, four RNA candidates (5S rRNA, RMRP, $tRNA^{[ser]sec}$ and $tRNA^{glu}$) were identified in both experiments while several candidates were identified only in CoLoC 2 (7SL RNA, Y1 and Y3 RNAs, H1 RNA, tRNAs).

H1 RNA was previously shown to be imported into mitochondria although its mitochondrial function is not clear (see section I.B.3.1). it was suggested that this RNA cannot be completely degraded upon RNase treatments **(Cannon *et al.,* 2015)** and this may be responsible for its identification in CoLoC 2 experiment. Similarly, 7SL RNA showed a depletion profile of a cytosolic contaminant by Northern blot hybridization **(figure 26)** and its identification as an imported RNA in CoLoC 2 was surprising. The presence of this ER-associated RNA in mitochondrial fraction may be explained by the close interaction between the endoplasmic reticulum and

mitochondria **(Marchi *et al.,* 2014)**. Analyses of the depletion dynamics of these RNAs in MocK-CoLoC experiments will provide further information on their sensitivity to nuclease digestion and eventual mitochondrial import.

Non-coding Y RNAs had been discovered as components of Ro ribonucloproteins implicated in RNA quality control in eukaryotes and in several eubacteria **(Stein *et al.,* 2005; Kowalski and Krude, 2015)**. Four types of Y RNAs are present in human cells and two of them, Y1 and Y3, were fairly persistent in CoLoC 2 samples. Interestingly, in eubacteria *D. radiodurans* Y RNA can form a complex with PNPase, thus regulating the selective degradation of misfolded RNA molecules **(Chen *et al.,* 2013)**. In our laboratory, Y3 RNA had been detected in association with human mitochondria (N. Entelis, unpublished data). Since human PNPase is localized in the mitochondria (see section I.B.2.1) one can hypothesize that some Y RNAs might be partially imported into mitochondria to accomplish the same function as in eubacteria - regulation of PNPase activity and substrate specificity.

tRNAs :

Human mitochondrial genome encodes a set of 22 tRNAs sufficient for the translation. Nevertheless import of cyt-$tRNA^{Gln}$ into mammalian mitochondria has been previously reported **(Rubio *et al.,* 2008)**, Our laboratory also demonstrated that yeast $tRNA^{Lys}$ (tRK1) can be imported into mitochondria of living human cells indicating on the existence of a mechanism of tRNA mitochondrial import **(Kolesnikova *et al.,* 2004)**. Many nuclear-encoded tRNAs (66 species, **Figure 36A**) were retrieved as candidates in CoLoC 2; two of them were identified in both CoLoC experiments ($tRNA^{[ser]sec}$ and $tRNA^{glu}_{UUC}$), and $tRNA^{Lys}_{UUU}$ was also detected in mitochondria by Northern blot hybridization **(figure 34)**. Noteworthy, $tRNA^{Lys}_{UUU}$ has been previously identified as a primer used for Human Immodeficience Virus (HIV) genome replication and found in association with viral proteins and mitochondrial lysyl-tRNA synthetase **(Khoder-Agha *et al.,* 2018)**, which can also indicate on its possible interaction (not completely understood) with mitochondria.

Glutamate and lysine tRNAs decode two codon's families (AAR and GAR). In yeast, import of tRK1 into mitochondria was demonstrated to be essential for lysine AAG codon translation in stress conditions **(Kamenski *et al.,* 2007)**. One can

hypothesize that a similar mechanism may exist in human mitochondria for tRNAs Lys, Glu and Gln. Even if the import of human cytosolic tRNA into mitochondria had not been clearly demonstrated, we cannot exclude that this pathway may be required in some cell types and/or special (stress) conditions. This can be studied by applying our CoLoC approach on different cell types in various conditions.

The most exciting observation made in both CoLoC-seq experiments was the identification of selenocysteine tRNA as candidate for mitochondrial import. In human, $tRNA^{[ser]sec}$ is responsible for the selenocysteine incorporation in 25 selenoproteins, implicated in reduction-oxidation reactions **(Gromer *et al.,* 2005)**. In eukaryotes, selenocysteine biogenesis and incorporation in proteins at the level of a UGA codon required a specific pathway involved 7 proteins and a specific structure present in the 3'UTR of the mRNA, named SECIS (selenocysteine incorporation sequence) **(Bulteau and Chavatte, 2015; Schoenmakers *et al.,* 2016)**. Selenocysteine incorporation by mammalian mitoribosomes has never been hypothesized. Still, several mutations in the genes of protein factors of the selenoprotein biosynthesis cause phenotypes reminiscent of typical mitochondrial diseases **(Anttonen *et al.,* 2015; Schoenmakers *et al.,* 2016; Schweizer and Fradejas-Villar, 2016)**. Six out of seven proteins involved in translational insertion of selenocysteine in human have confirmed mitochondrial isoforms or are suspected to be mitochondrial **(Papp *et al.,* 2008; Zheng *et al.,* 2015; Calvo *et al.,* 2016)**. Thus, the system of selenocysteine incorporation might exist in mitochondria, but its mechanism may be different from the cytosolic one. Indeed, UGA triplets are not stop codons and encode tryptophan in human mitochondria **(Table 1)**. Moreover, mt-mRNAs lacks 3'UTR were SECIS elements are normally localized.

Since this hypothesis is really exiting, I have performed some preliminary experiments to verify possible localization of selenocysteine pathway in human mitochondria. I tried to verify the presence of several proteins of the selenocysteine pathway in human mitochondria by western immunodecoration. Unfortunately, antibodies used in these studies were not sufficiently specific and sensitive to detect the proteins in the mitochondrial fractions. I also performed multiple Northern blot hybridization experiments to validate the presence and to check an eventual aminoacylation of $tRNA^{[ser]sec}$ in purified mitochondria, but the data were not reproducible. Similarly, confocal microscopy data demonstrating association of tRNAsec with mitochondria **(Figure 37)** should be reproduced and statistically

analyzed. In perspective, decisive evidence of $tRNA^{sec}$ participation in mitochondrial translation may be obtained by direct incorporation of labeled selenium in mitochondrial proteins

RMRP and 5S rRNA :

RMRP and 5S rRNA were identified in both CoLoC experiment and had been previously suggested to be imported into human mitochondria. For RMRP, we needed a closer inspection of the reads aligned to the RMRP gene to clearly detect the different patterns for the 3' and 5' regions of the gene **(Figure 29C)**. Only the reads mapped to 3' half showed a characteristic pattern of imported RNA, in agreement with the previous studies **(Chang and Clayton, 1987; Noh *et al.,* 2016)**. Thus, our CoLoC experiment provided a direct evidence of the processing of RMRP and mitochondrial import of its 3' half.

5S rRNA import was described by several independent laboratories and it was demonstrated that preventing its import in the organelle impact mitochondrial functions **(Smirnov *et al.,* 2010)**. However, Northern blot hybridization analysis of Mock-CoLoC samples demonstrated that 5S rRNA was poorly degraded by RNase treatments **(Figures 32 and 33)**. This data rise a question concerning the import of 5S rRNA into human mitochondria, since many evidences of the mitochondrial localization of this RNA rely on RNase based approaches **(Yoshionari *et al.,* 1994; Magalhaes *et al.,* 1998; Entelis *et al.,* 2001)**

Nevertheless, other evidences reported by different laboratories indicate that this RNA can function as a vector to deliver RNA molecules to human mitochondria. In the first part of my thesis I developed a therapeutic strategy based on the import of anti-replicative 5S rRNA molecules. My results demonstrated that the expression of these molecules can induce a shift in mtDNA heteroplasmy level (see section II.A; **(Loutre *et al.,* 2018a)**. We also detected 5S rRNA associated with mitochondria by fluorescent microscopy **(figure 37 and 38)**. Another study has used 5S rRNA as a vector to import RNA sequences inhibiting the translation of mitochondrially-encoded proteins **(Towheed *et al.,* 2014)**. Another laboratory also developed a fluorescent *in vivo* hybridization method using 5S rRNA mediated import of nucleic acid probes targeting mitochondrial DNA or mRNAs **(Zelenka *et al.,* 2014)**. More recently, 5S

rRNA molecules bearing the mango fluorogenic aptamer were also targeted into mitochondria of living cells by fluorescent microscopy **(Autour *et al.,* 2018)**.

During my thesis I developed a new approach to identify imported RNA. This method allowed to distinguish different types of RNA localization and permitted to establish a list of RNA candidates for mitochondrial import, including previously identified imported RNAs. The data should be reproduced and supported by the sequencing of Mock-CoLoC samples. In mock-CoLoC experiment, RNA degradation may be limited by the sequence specificity of the RNase used. Therefore, a further Improvement of the CoLoC and Mock-CoLoC protocols may be achieved by the use of mix of RNases. Indeed, the best degradation was obtained using RNase A/T1 mix **(Figure 32)**.

Candidates RNA consistently identified by CoLoC-seq experiments should be validated by other methods. Confocal microscopy with smFISH already allowed the detection of candidates associated with mitochondria. Coupling smFISH with super-resolution microscopy techniques will allow the visualization of submitochondrial location of the RNA candidates.

Other approaches for genome-wide identification of subcellular localization of RNA were recently proposed **(Kaewsapsak *et al.,* 2017; Li *et al.,* 2017; Fazal, 2018; Li *et al.,* 2018)**. These 2 approaches do not rely on cellular fractionation. The method named Apex-RIP is based on the mitochondrial targeting of a protein which induces proximity biotinylation of proteins and RNAs inside the organelle. Biotinylated RNAs or RNAs interacting with biotinylated proteins can then be recovered by streptavidine enrichment. We have started to apply this approach in our laboratory to compare the results with our CoLoC-seq dataset. The second method which can be applied to mitochondria follows a similar principle and allows the modification of both proteins and RNAs (guanosine are oxidized to 8-oxoguanosine) localized to a subcellular compartment.

Identification of new RNA species imported in mitochondria in various cell types and conditions can reveal new mechanisms of the mitochondria gene expression, regulation and mitochondria-nuclear cross-talk. Identification of new RNAs through genome-wide approach can also help to uncover the general rules governing the RNA traffic to mitochondria, import determinants and protein factors.

This knowledge is a prerequisite for the development of new therapeutic strategies to cure mitochondrial diseases for which no treatment currently exists.

IV. Materials and methods

I.A. Materials

IV.A.1. Human cell lines

Cybrid cells bearing the KSS deletion :

Human *trans*mitochondrial cybrid cells obtained by the fusion of the cytoplasts generated from fibroblasts of a patient affected by the KSS deletion (nucleotides 8363 to 15438 of mtDNA) and mtDNA depleted 143B cells. Cybrid cells containing 65% mutant mtDNA used in this study were characterized by the 10±2% decrease of oxygen consumption comparing to control 143B cell line. This cell line was obtained by the team of Dr. A. Lombes (Inst. Cochin, Paris) **(Comte *et al.*, 2013).**

Cybrid cells bearing the ND5 13514A>G point mutation:

*Trans*mitochondrial cybrid cell lines obtained by the fusion of fibroblast-derived cytoplast from and 143B cells ρ0 cell line were kindly provided by M. Zeviani (National Neurological Institute “Carlo Besta” Milan, Italy) **(Corona *et al.*, 2001)**.

T-Rex™ Flp-In™ cells :

Commercial cell line derived from HEK (Human Embryonic Kidney) 293 cells containing the pFRT/LacZeo plasmid stably integrated into a transcriptionally active genomic location (*Invitrogen*). This cell line is resistant to Zeocin (100µg/mL) and blasticine (15µg/mL) antibiotics.

HepG2 cells :

Human immortalized cell line derived from a liver hepatocellular carcinoma.

IV.A.2. DNA and RNA sequences

All DNA and RNA sequences used as primers for PCR amplification are listed in **Table 4** and in supplementary material **S1 Table (Loutre *et al.*, 2018a)**. Primers used for Northern blot hybridization are listed in **Table 5**.

The sequences of the spike-in RNA added to CoLoC experiment (see II.B.2) is as followed:

5′GAGAAGTAAGCACTGTAAAGGTTTTAGAGCTAGAAATAGCAAGTTAAAATAAGGCTAGTCCGTTAT
CAACTTGAAAAAGTGGCACCGAGTCGGTGCTTGCCTTGTTGGCGCAATCGGTAGCGCGTATGACTCTT
AATCATAAGGTTAGGGGTTCGAGCCCCCTACAGGGCTCCA 3′

N°	Name	Sequence
1	T7-prom	5' GGGATCCATAATACGACTCACTATA 3'
2	KSS-13H-rev	5′ AGGCCCGACCCTGCTTAGCTACAGTGCTTACTTTTCAGGGTGGTATGGCCGTA 3′
3	KSS-14L-rev	5′ AGGCCCGACCCTGCTTAGCTAAGTAAGCACTGTATTCAGGGTGGTATGGCCGTA 3′
4	KSS-15H-rev	5′ AGGCCCGACCCTGCTTAGCTTTACAGTGCTTACTTTTCAGGGTGGTATGGCCGTA 3′
5	KSS-15L-rev	5′ AGGCCCGACCCTGCTTAGCTAGAAGTAAGCACTGTTTCAGGGTGGTATGGCCGTA 3′
6	ND5-15H-rev	5′ AGGCCCGACCCTGCTTAGCTACTCCAAAGGCCACATTCAGGGTGGTATGGCCGTA 3′
7	ND5-15L-rev	5′ AGGCCCGACCCTGCTTAGCTATGATGTGGCCTTTGTTCAGGGTGGTATGGCCGTA 3′
8	ND5-16H-rev	5′ AGGCCCGACCCTGCTTAGCTACTCCAAAGGCCACATTTCAGGGTGGTATGGCCGTA 3′
9	ND5-16L-rev	5′ AGGCCCGACCCTGCTTAGCTTGATGTGGCCTTTGGATTCAGGGTGGTATGGCCGTA 3′
10	ND5-17H-rev	5′ AGGCCCGACCCTGCTTAGCTACTCCAAAGGCCACATCTTCAGGGTGGTATGGCCGTA 3′
11	ND5-17L-rev	5′ AGGCCCGACCCTGCTTAGCTTGATGTGGCCTTTGGAGTTCAGGGTGGTATGGCCGTA 3′
12	5S-BglII	5′ GGAGATCTAAGCCTACAACACCCGG 3′
13	CRC-F	5′ CATACCTCTCACTTCAACCTCC 3′
14	CRC-R	5′ AGGCGTTTGTGTATGATATGTTTGC 3′

Table 4. List of the primers used for PCR amplification

Target RNA	Probe sequence	Hybridization temperature (°C)
5S rRNA	5' AAAGCCTACAACACCCGGTATTCCC 3'	50
5.8S rRNA	5′ GGCCGCAAGTGCGTTCGAAG 3′	50
7SL RNA	5′ AGAGACGGGGTCTCGCTATG 3′	45
U6 snRNA	5′ AAAATATGGAACGCTTCACGAATTTGC 3′	45
mt-tRNA^{Val}	5′ TGGGTCAGAGCGGTCAAGTTAAGTTGAAATCTCC 3′	45
mt-tRNA^{Lys}	5′ GGTCACTGTAAAGAGGTG 3′	42
cyt-tRNA$^{Lys}_{TTT}$	5′ ACTTGAACCCTGGACC 3′	42
cyt-tRNA$^{Met(i)}$	5′ CTTCCGCTGCGCCACTCT 3′	45
tRNA$^{[ser]sec}$	5′ TGAACCACTCTGTCGCTAGAC 3′	42
spike-in RNA	5′ TGGAGCCCTGTAGGGGGCTCGAAC 3′	45

Table 5. List of the DNA probes used for Northern blot hybridization.

IV.B. Methods

IV.B.1. Methods relative to the culture of human cell lines

IV.B.1.1. Conditions of culture

All cell lines were cultivated at 37°C with 5% of CO2. All media were supplemented with 10% FBS (Fetal Bovine Serum; *Gibco*), 100mg/L penicillin/streptomycine (Gibco) and 2.5 mg/L Fungizone (Gibco).

Cybrid cells were cultivated in DMEM (Dulbecco's Modified Eagle's Medium; *Sigma*) containing 4.5 g/L glucose and supplemented with 50 mg/L uridine (*Gibco*), 3.7 g/L sodium bicarbonate (*Sigma*). For glucose-free conditions, cells were cultivated in DMEM without glucose (*Sigma*) supplemented with 50 mg/L uridine, 3.7 g/L sodium bicarbonate, 0.584 g/L L-glutamine (*Sigma*) and 108 mg/L sodium pyruvate (*Sigma*). Cybrid cells transfected with pFRT/lacZeo plasmid (KSS-FRT and ND5-FRT) were cultivated in media containing 100 µg/mL Zeocin (*Invitrogen*). Cells transfected with pcDNA™5/FRT/TO were cultivated in media supplemented with 150µg/mL Hygromycin B-Gold (*InvivoGen*).

HepG2 cells were cultivated in MEM (Minimum Essential Medium; Sigma) containing 1g/L glucose and supplemented with 50mg/L uridine and 2.2 g/L sodium bicarbonate.

HEK 293 T-Rex^{TM} Flp-In^{TM} cells were cultivated in EMEM (Eagle's Minimum Essential Medium ; *Sigma*) containing 1g/L glucose and supplemented with 1,5g/L sodium bicarbonate and 0.11 g/L sodium pyruvate.

When cells were grown to about 80% confluency (surface of the support covered by the cells), cells were detached and divided. For this, the medium is removed by aspiration and cells are washed with 1X PBS (*Sigma*). Cells are then detached from their support by addition of Trypsine-EDTA 0.05% (*Gibco*) (0.2mL/10cm²) and incubation 5 min at 37°C. Trypsine is then inactivated by addition of 5 volume of the growth medium. Cells are then collected by centrifugation at 600g (10min, room temperature).

In order to prevent contamination with Trypsine in CoLoC and Mock-CoLoC experiments, cells were detached by addition of 1X PBS supplemented with 2.5mM EDTA and incubation 20 min at 37°C. After centrifugation, cells were washed with 1X PBS.

IV.B.1.2. Cell transfection

For transfection with plasmid DNA or with RNA, cells are cultivated until they reach 50-70% confluency. The medium is replaced with Opti-MEM (*Gibco*) pre-heated at 37°C. All the transfection were performed using Lipofectamine 2000 reagent (*Invitrogen*). DNA/lipofectamin and RNA/lipofectamin complexes are prepared according to the manufacturer's protocol and added to the cell for 6h. Opti-MEM is then replaced by the standard medium (see previous section).

IV.B.2. Methods relative to 5S rRNA anti-replicative strategy

IV.B.2.1. Design and synthesis of the recombinant 5S rRNA molecules

Secondary structure of rec.5S rRNA weas predicted *in silico* using *RNA folding form* software (Mfold) and corrected to be in agreement with the data on human 5S rRNA structure **(Szymanski *et al.*, 2003)**. Tm of the RNA/DNA duplexes was estimated using *OligoAnalyzer* software (IDT-DNA; version 3.1). The “Tm Mismatch” tool, which calculates the Tm of a DNA/DNA duplexes containing a mismatch, was used to estimate the impact of the 13514A>G point mutation.

Rec.5S rRNAs were obtained by T7 transcription using the T7 RiboMAX Express Large Scale RNA Production System (*Promega*). The template was produced by PCR with a two-step protocol using Phusion High-Fidelity DNA Polymerase (*ThermoScientific*). The first PCR step was performed on a plasmid pUC containing the sequence of human 5S rRNA under the control of the T7 promoter **(Smirnov *et al.*, 2008)** to amplify a DNA fragment containing a part of 5S rRNA

sequence and the anti-replicative insert under the control of the T7 promoter. The amplification was performed with the forward primer n°1 and one of the reverse primer n°2 to 11 containing the sequence of the anti-replicative insert **(Table 4)**. The resulting PCR products were used as forward primers, along with the reverse primer N°12, for the second PCR. The final PCR products contain the T7 promoter followed by sequence of the rec.5S rRNA and BglII restriction site. The purified PCR product is then cleaved by the BglI restriction enzyme (FastDigest BglII, *ThermoScientific*) for 1h at 37°C to yield the correct 5S rRNA 3' end.

IV.B.2.2. *In vitro* hybridization assays

IV.B.2.2.1. Hybridization assay for Rec.5S rRNA version targeting the KSS deletion

For the KSS deletion, the specific annealing of the rec.5S rRNA versions was assessed by Southern blot hybridization. The radiolabeled rec.5S rRNAs were hybridized to PCR fragments of wild-type mtDNA (nt 1521 to 15680) or mutant mtDNA (nt 8099 to 8365 and 15438 to 15680) separated on 1% agarose gel and blotted to Amersham-Hybond-N membrane (*GE Healthcare*).

Radiolabeling of rec.5S rRNAs :

2 µg of rec.5S rRNAs were dephosphorylated with 1U of alkaline phosphatase (*Roche*) at 37°C for 40 min. RNAs are then extracted by addition of 1 volume of acidic phenol. After centrifugation at 16 000g for 5 min at 4°C, the aqueous phase is collected and the RNAs are precipitated with ethanol. 0,7µg of rec.5S rRNAs are radiolabeled with 3µl γ-[^{32}P]-ATP in presence of 10U of T4 polynucleotide Kinase (*Promega*) during 45 min at 37°C. Radiollabeled rec.5S rRNAs were then purified by size exclusion chromatography on Micro Bio-Spin™ 6 Chromatography Columns (*BioRad*).

Southern blot procedure :

DNA molecules are separated by electrophoresis on agarose gel (1%) in 1X TBE buffer (Tris-borate 45Mm ; EDTA 1mM ; pH 8,3). The gel is incubated for 30 min

in a depurinization solution (0.25N HCl) followed by a 15 min incubation in a denaturation solution (1.5M NaCl, 0.5M NaOH). The gel is finally incubated twice in a neutralization solution (1.5M NaCl, 0.5M Tris-HCl, pH8.0) for 10min. DNA molecules are blotted onto Amersham Hybond N membrane by overnight capillary transfer in SSC 10X buffer. DNA molecules are finally fixed on the nitrocellulose membrane under UV exposition.

The membrane is first pre-hybridized for 1 h at 65°C in pre-hybridization buffer (6X SSC 6X; 10X Denhardt solution; 0.2% SDS). Hybridizations were performed with 10mL of hybridization buffer (1X PBS; 0.1% SDS) containing the radiolabeled rec.5S rRNA, during 6 hours at 37°C under rotation. Membranes were then washed 3 times for 10 minutes with the washing buffer (2X SSC, 0.1% SDS). Hybridization signals were revealed by Phophorimaging using Typhoon Trio scanner (*GE Healthcare*) and quantified using the *ImageQuantTL* software. To eliminate the radioactive signal, membranes were stripped with 3 x10 min incubations in stripping buffer (0.02X SSC; 0.1% SDS) at 80°C under agitation.

IV.B.2.2.2. Hybridization assay for rec.5S rRNA versions targeting the ND5 point mutation

For the 13514 A>G ND5 mutation, the specific annealing of the rec.5S rRNA versions was assessed by in solution hybridization assay in presence of oligonucleotides corresponding to the mutant and wild-type mtDNA sequences **(Figure 22)**. Rec.5S rRNAs and the olignoculeotides were unfodled at 95°C for 2 min and allowed to refold in saline physiological conditions (37°C; 1X PBS; 1mM MgCl2) for 5 min. Each rec.5S rRNA version was then mixed in equimolar amounts of either the mutant or wild-type version of the corresponding mtDNA oligonucleotide. After 30 min incubation at 37°C, formation of RNA/DNA hybrid complexes was assessed by electrophoretic mobility shift assay on 8% PAGE in 1X TAE (Tris-acetate 40mM ; EDTA 1mM ; pH 7,1) at 4°C. Nucleic acids were stained in the gel with ethidium bromide solution (0.5µg/mL) for 10 min and RNAs were visualized under UV G-Box (*Syngene*). The density profiles were obtained with the *GeneTools* software.

IV.B.2.3. RFLP quantification of heteroplasmy

To quantify the heteroplasmy level of the ND5 mutation, DNA was extracted from the cells by resupending the cell pelet in 500 µl of RSB buffer (10 mM Tris-HCl pH 7,5 ; 10 mM NaCl ; 25 mM EDTA ; 1% SDS) with 10 µl of proteinase K (20 mg/mL) and incubation 24h at 37°C. DNA was then precipitated with ethanol. A region containing the mutation was amplified by PCR using primer 13 bearing a fluorophore (FITC) at the 5' terminus and the primer 14 **(Table 4)**. The reaction was performed with 2,5mM de dNTP, 0,5U of "Phusion" DNA polymerase (Thermo Scientific) and 10 µM of each primer. PCR amplification was performed with an initial incubation at 95°C during 5 min followed by 30 cycles of 30 sec (95°C, 56°C and 72°C). The final product (125 bp) was then digested with HaeIII restriction enzyme (FastDigest, Thermo Scientific) for 1 hour at 37° leading to a fluorescent product of 80bp and a non-fluorescent product of 45bp for the mutant DNA. The PCR and digestion fragments were then separated on an 10% polyacrylamide gel and fluorescent signals were detected by the "Typhoon TRIO" (GE Healthcare) and quantified using the ImageQuantTL software. Heteroplasmy level was calculated by the ratio between the fluorescent signal of the mutant mtDNA fragment (80bp) and the total mtDNA fragments (80bp and 125bp).

Methods used for Generation of *trans*mitochondrial cybrid cell lines expressing rec.5S rRNA, *In vivo* import assay, quantification of rec.5S rRNA expression and analysis of heteroplasmy level are described in details in attached paper **(Loutre *et al.*, 2018a)**

IV.B.3. Methods relative to CoLoC-seq experiments

IV.B.3.1. CoLoC and Mock-CoLoC procedures

IV.B.3.1.1. Isolation of crude mitochondria

1125 cm² to 2250 cm² of HEK 293 T-Rex™ Flp-In™ cells (depending on the number of analyzed samples) were cultivated to reach ≈80% confluency and detached as described in section IV.B.1.1. Cells were resuspended in 30 mL of mito

buffer (10mM Tris-HCl pH 6.7; 0.6M sorbitol). All the following procedures were then perfomed at 4°C, unless mentioned otherwise. Cells were disrupted with a warring blender 3x15s at high speed. Cellular debris and intact cells were removed by 3 centrifugations 3min at 1000g. The supernatant containing mitochondria was collected and centrifuged for 30min at 21000g. The crude mitochondria pellet was resuspended in mito buffer and the suspension was loaded on two sucrose cushions (lower cushion : 10mM Tris-HCl pH6.7; 1.65M sucrose; upper cushion : 10mM Tris-HCl pH6.7, 0.6M sucrose) and centrifuged for 1 hour at 45000g. Mitochondria fraction at the interphase between the two cushions was collected, diluted with mito buffer and centrifuged for 30min at 21000g. The pellet was thoroughly resuspended and diluted in mito buffer to yield between 1.2 and 1.6 µg of protein/mL.

For Mock-CoLoC experiments, isolated mitochondria were disrupted using a dounce homogenizer with 500µL of mito buffer supplemented with 0.5% of n-dodecyl-β-D-maltoside. Intact mitochondria were eliminated by two successive centrifugations at 16000g for 10 min. The lysate was then diluted with mito buffer to yield between 1.2 and 1.6 µg of protein/mL.

IV.B.3.1.2. RNase treatment

. The suspension of mitochondria (or mitochondrial lysate) was then divided in equivalent aliquots of 80µl. One volume of buffer 1 (10mM Tris-HCl Ph6.7, 0.6M sorbitol, 5mM $MgCl_2$; CoLoC 1 procedure) or buffer 2 (10mM Tris-HCl Ph6.7, 0.6M sorbitol, 200mM NaCl; CoLoC 2 and Mock-CoLoC procedures) containing different concentrations of RNase was added to the samples. In the case of incubation with MNase, buffer 2 was supplemented with 10 mM $CaCl_2$. Samples were incubated at 25°C 5 min for CoLoC 1 procedure or 7 min for CoLoC 2 (to facilitate the manipulation of an increased number of samples). Samples were then 10 fold diluted with mito buffer supplemented with 4mM EDTA and centrifuge for 15 min at 16000g. Then, mitochondrial pellets were washed two times with mito buffer and centrifuged again. For Mock-CoLoC experiments, RNAs were directly extracted with TRIzol reagent after incubation with RNase A.

IV.B.3.1.3. Mitoplast generation

To generate mitoplasts, mitochondrial pellet were resuspended in 800µl of mito buffer supplemented with 30µg/mL of digitonin (*Sigma*) to final amount corresponding to ≈250µg digitnonin per mg of mitochondrial proteins and incubated at 25°C for 10min. Samples were then washed two times by addition of 1 mL of mito buffer and centrifugation for 15 min at 16000g at 4°C.

IV.B.3.1.4. RNA extraction

Mitoplasts were resupended in 100µl of mito buffer and RNA was extracted by TRIzol reagent. 100 ng of spike-in RNA (for CoLoC 2 and Mock-CoLoC) was added to the samples before isopropanol precipitation. RNA pellets were resuspended in 20µl of milliQ water and RNA concentration was estimated by spectrophotometry (Nanodrop).

IV.B.3.2. RNA analysis by Northern blot hybridizations

Isolated RNAs were separated by urea-PAGE (19:1 acrylamide/bisacrylamide, 8M Urea) in 1X TBE. The gel was then stained with ethidium bromide solution (0.5µg/mL) for 10 min and RNAs were visualized under UV G-box (*Syngene*). RNAs were electro-transferred to Amersham Hybond N+ membrane (*GE Healthcare*) in TBE 0.5X buffer at 200mA overnight. RNAs were then fixed to the membrane by UV.

For Northern blot hybridization, 10 pmoles of oligonucleotide probes **(Table 5)** were radiolabelled with 3µl of γATP ^{32}P (10 µCi/µl ; 3000 Ci/mmole) using 10U of T4 polynucleotide kinase (*Promega*) 45 min at 37°C. Oligonucleotides were then purified by size exclusion chromatography with Micro Bio-Spin™ 6, Chromatography Columns (*BioRad*). Membranes were pre-hybridyzed for 1 h at 65°C in hybridization buffer (6X SSC; 10X Denhardt solution 10X; 0.2% SDS) Hybridizations were performed with 10mL of hybridization buffer containing the radiolabeled probe during at least four hours under rotation. Hybridization temperatures used for each specific probe are listed in **Table 5**. Membranes were then washed 2 times for 15 minutes with the washing buffer (5X SSC, 0.1% SDS). To eliminate the radioactive signal before reprobing, membranes were stripped by 3x 15 min incubations in stripping

buffer (0.5X SSC, 0.1% SDS) at 65°C under agitation. Hybridization signals were then revealed by Phophorimager “Typhoon TRIO” (*GE Healthcare*) and quantified using the *ImageQuantTL* software. The proportion of remaining RNA in each samples was calculated by the ratio between the signals corresponding to the probed RNA in the samples treated with RNase and the signals of the same RNA in the sample not treated with RNase (0µg/mL). To avoid discrepancies caused by the loading of different amounts of materials, the ratios were normalized to the ratio calculated for a reference RNA (mt-encoded RNA or spike-in RNA). Regression analysis of CoLoC data **(Figure 26)** was performed using the *OriginLab* software.

IV.B.3.3. RNA-Sequencing of CoLoC samples

I.A.1.1.1. Sequencing procedure

Isolated RNAs were treated with DNAse I for 30 min at 37°C. Preparation of the cDNA library and sequencing was performed by Vertis Biotechnologie AG (Freising, Germany) **(figure 27)**.

First, the RNA samples were treated with CAP-Clip Acid Pyrophosphatase (*Cellscript*) in order to convert 5'PPP and CAP structures to 5' monophosphate (5'P). Then, an oligonucleotide adapter was ligated to the 5'P ends of the RNA samples. Afterwards, an oligonucleotide adapter was ligated to the 3' ends of the RNA molecules. First-strand cDNA synthesis was performed using M-MLV reverse transcriptase and the 3’ adapter as primer. The resulting full length cDNAs were amplified with PCR and purified using the Agencourt AMPure XP kit (*Beckman Coulter Genomics*). The full-length cDNA samples were treated with ultrasound (4 pulses of 30 sec at 4°C) and TruSeq sequencing adapters were ligated to the DNA fragments. Finally, the DNA was PCR-amplified, barcode sequences were attached to the 5'-ends of the DNA molecules and the samples were pooled in approximately equimolar amounts. For CoLoC 1, the cDNA pool was size fractionated in the size range of 200 – 500 bp using a preparative agarose gel. The library was sequenced on an Illumina NextSeq 500 system using 75 bp read length.

IV.B.3.3.5. Analysis of CoLoC-seq data

Reads quality was assessed using the *fastQC* software (version 0.11.4). Reads were mapped to the annotated human genome hg38 (GRCh38, Ensembl) and count using the “HISAT2” tool (version 2.0.4). Visualization of the reads alignment **(Figure 29 and 36B)** was performed using the *Integrated Genome Browser* software (IGB, version 9.0.2).

To identify candidate imported RNAs, low covered genes (less than 10 reads per gene) were first eliminated and the depletion dynamic of the transcripts corresponding to the genes passing the coverage cut-off was analyzed. For this, the proportion of remaining RNA in each sample was calculated by the ratio between the number of reads aligned in the samples treated with RNase A and in the untreated sample (0µg/mL). This ratio was normalized to the median of the ratios of the mt-encoded RNAs. For the selected candidates the proportion of corresponding reads was >10% in the last sample (highest concentration of RNase) and the depletion dynamic was characterized by the presence of a plateau.

IV.B.3.4. Microscopy analysis by smFish with branched DNA technology

All confocal microscopy analyses were generously performed by Dr. Anna Smirnova. The sets of oligonucleotide pairs annealing to the target RNAs were purchased from *Affymetrix eBioscience* **(Table 6).** SmFish imaging using branched DNA technology was performed on HepG2 cells by the View RNA® Cell plus assay (*Affymetrix eBioscience*) with oligonucleotides conjugated to Alexa Fluor 647, following the manufacturer’s instructions **(Figure 37A)**. Immaging of mitochondria was performed with mitotracker red or with primary antibodies against Tom20 and secondary antibody conjugated with Alexa Fluor 488 (*Molecular probes*, A-21246)

Quantification of of 5S rRNA and 5.8S rRNA co-localization with mitochondria had been performed with the *ImageJ* software and the plugin « squassh » as described in **(Rizk *et al.*, 2014)**.

Target RNA	Affymetrix Catalog number	Region covered by the oligonucleotide pairs	Number of pairs
CO1 mRNA	VA6-12665	5923-7254	25
RAN mRNA	VA6-3168573	1144-2520	25
RMRP	VA6-60000271	140-227	1
5S rRNA	VA6-3173307	2-118	2
5.8S rRNA	VA6-3170756	2-139	2
$tRNA^{[ser]sec}$	VA6-6000450	2-83	1

Table 6. List of the set of probes used for branched DNA technology (smFish)

The pairs of oligonucleotides (24 nt each oligonuleotide) were purchased from *Affymetrix eBioscience*. The sequences of the oligonucleotides are not revealed by the manufacturer.

References

Agaronyan, K., Morozov, Y.I., Anikin, M., and Temiakov, D. (2015). Mitochondrial biology. Replication-transcription switch in human mitochondria. Science *347*, 548-551.

Agrawal, R.K., and Sharma, M.R. (2012). Structural aspects of mitochondrial translational apparatus. Current opinion in structural biology *22*, 797-803.

Ahola-Erkkila, S., Carroll, C.J., Peltola-Mjosund, K., Tulkki, V., Mattila, I., Seppanen-Laakso, T., Oresic, M., Tyynismaa, H., and Suomalainen, A. (2010). Ketogenic diet slows down mitochondrial myopathy progression in mice. Human molecular genetics *19*, 1974-1984.

Akman, G., Desai, R., Bailey, L.J., Yasukawa, T., Dalla Rosa, I., Durigon, R., Holmes, J.B., Moss, C.F., Mennuni, M., Houlden, H.*, et al.* (2016). Pathological ribonuclease H1 causes R-loop depletion and aberrant DNA segregation in mitochondria. Proceedings of the National Academy of Sciences of the United States of America *113*, E4276-4285.

Al-Behadili, A., Uhler, J.P., Berglund, A.K., Peter, B., Doimo, M., Reyes, A., Wanrooij, S., Zeviani, M., and Falkenberg, M. (2018). A two-nuclease pathway involving RNase H1 is required for primer removal at human mitochondrial OriL. Nucleic Acids Res *46*, 9471-9483.

Amunts, A., Brown, A., Toots, J., Scheres, S.H.W., and Ramakrishnan, V. (2015). Ribosome. The structure of the human mitochondrial ribosome. Science *348*, 95-98.

Anderson, S., Bankier, A.T., Barrell, B.G., de Bruijn, M.H., Coulson, A.R., Drouin, J., Eperon, I.C., Nierlich, D.P., Roe, B.A., Sanger, F.*, et al.* (1981). Sequence and organization of the human mitochondrial genome. Nature *290*, 457-465.

Antonicka, H., Sasarman, F., Nishimura, T., Paupe, V., and Shoubridge, E.A. (2013). The mitochondrial RNA-binding protein GRSF1 localizes to RNA granules and is required for posttranscriptional mitochondrial gene expression. Cell metabolism *17*, 386-398.

Antonicka, H., and Shoubridge, E.A. (2015). Mitochondrial RNA Granules Are Centers for Posttranscriptional RNA Processing and Ribosome Biogenesis. Cell reports.

Anttonen, A.K., Hilander, T., Linnankivi, T., Isohanni, P., French, R.L., Liu, Y., Simonovic, M., Soll, D., Somer, M., Muth-Pawlak, D.*, et al.* (2015). Selenoprotein biosynthesis defect causes progressive encephalopathy with elevated lactate. Neurology *85*, 306-315.

Aravin, A.A., and Chan, D.C. (2011). piRNAs meet mitochondria. Developmental cell *20*, 287-288.

Auger, C., Alhasawi, A., Contavadoo, M., and Appanna, V.D. (2015). Dysfunctional mitochondrial bioenergetics and the pathogenesis of hepatic disorders. Frontiers in cell and developmental biology *3*, 40.

Autour, A., S, C.Y.J., A, D.C., Abdolahzadeh, A., Galli, A., Panchapakesan, S.S.S., Rueda, D., Ryckelynck, M., and Unrau, P.J. (2018). Fluorogenic RNA Mango aptamers for imaging small non-coding RNAs in mammalian cells. Nature communications *9*, 656.

Babendure, J.R., Adams, S.R., and Tsien, R.Y. (2003). Aptamers switch on fluorescence of triphenylmethane dyes. Journal of the American Chemical Society *125*, 14716-14717.

Bacman, S.R., Kauppila, J.H.K., Pereira, C.V., Nissanka, N., Miranda, M., Pinto, M., Williams, S.L., Larsson, N.G., Stewart, J.B., and Moraes, C.T. (2018). MitoTALEN reduces mutant mtDNA load and restores tRNA(Ala) levels in a mouse model of heteroplasmic mtDNA mutation. Nature medicine *24*, 1696-1700.

Baleva, M., Gowher, A., Kamenski, P., Tarassov, I., Entelis, N., and Masquida, B. (2015). A Moonlighting Human Protein Is Involved in Mitochondrial Import of tRNA. International journal of molecular sciences *16*, 9354-9367.

Bandiera, S., Ruberg, S., Girard, M., Cagnard, N., Hanein, S., Chretien, D., Munnich, A., Lyonnet, S., and Henrion-Caude, A. (2011). Nuclear outsourcing of RNA interference components to human mitochondria. PloS one *6*, e20746.

Barrey, E., Saint-Auret, G., Bonnamy, B., Damas, D., Boyer, O., and Gidrol, X. (2011). Pre-microRNA and mature microRNA in human mitochondria. PloS one *6*, e20220.

Bartkiewicz, M., Gold, H., and Altman, S. (1989). Identification and characterization of an RNA molecule that copurifies with RNase P activity from HeLa cells. Genes & development *3*, 488-499.

Bashirullah, A., Cooperstock, R.L., and Lipshitz, H.D. (1998). RNA localization in development. Annual review of biochemistry *67*, 335-394.

Battich, N., Stoeger, T., and Pelkmans, L. (2013). Image-based transcriptomics in thousands of single human cells at single-molecule resolution. Nature methods *10*, 1127-1133.

Berridge, M.V., McConnell, M.J., Grasso, C., Bajzikova, M., Kovarova, J., and Neuzil, J. (2016). Horizontal transfer of mitochondria between mammalian cells: beyond co-culture approaches. Current opinion in genetics & development *38*, 75-82.

Bertrand, E., Chartrand, P., Schaefer, M., Shenoy, S.M., Singer, R.H., and Long, R.M. (1998). Localization of ASH1 mRNA particles in living yeast. Molecular cell *2*, 437-445.

Bianchessi, V., Badi, I., Bertolotti, M., Nigro, P., D'Alessandra, Y., Capogrossi, M.C., Zanobini, M., Pompilio, G., Raucci, A., and Lauri, A. (2015). The mitochondrial lncRNA ASncmtRNA-2 is induced in aging and replicative senescence in Endothelial Cells. Journal of molecular and cellular cardiology *81*, 62-70.

Bogdanov, A.A., Dontsova, O.A., Dokudovskaya, S.S., and Lavrik, I.N. (1995). Structure and function of 5S rRNA in the ribosome. Biochemistry and cell biology = Biochimie et biologie cellulaire *73*, 869-876.

Bogenhagen, D.F. (2012). Mitochondrial DNA nucleoid structure. Biochimica et biophysica acta *1819*, 914-920.

Bogenhagen, D.F., Martin, D.W., and Koller, A. (2014). Initial steps in RNA processing and ribosome assembly occur at mitochondrial DNA nucleoids. Cell metabolism *19*, 618-629.

Bohnsack, M.T., and Sloan, K.E. (2018). The mitochondrial epitranscriptome: the roles of RNA modifications in mitochondrial translation and human disease. Cellular and molecular life sciences : CMLS *75*, 241-260.

Bohr, V.A., Stevnsner, T., and de Souza-Pinto, N.C. (2002). Mitochondrial DNA repair of oxidative damage in mammalian cells. Gene *286*, 127-134.

Boominathan, A., Vanhoozer, S., Basisty, N., Powers, K., Crampton, A.L., Wang, X., Friedricks, N., Schilling, B., Brand, M.D., and O'Connor, M.S. (2016). Stable nuclear expression of ATP8 and ATP6 genes rescues a mtDNA Complex V null mutant. Nucleic Acids Res *44*, 9342-9357.

Borowski, L.S., Dziembowski, A., Hejnowicz, M.S., Stepien, P.P., and Szczesny, R.J. (2013). Human mitochondrial RNA decay mediated by PNPase-hSuv3 complex takes place in distinct foci. Nucleic Acids Res *41*, 1223-1240.

Bouzaidi-Tiali, N., Aeby, E., Charriere, F., Pusnik, M., and Schneider, A. (2007). Elongation factor 1a mediates the specificity of mitochondrial tRNA import in T. brucei. The EMBO journal *26*, 4302-4312.

Bowmaker, M., Yang, M.Y., Yasukawa, T., Reyes, A., Jacobs, H.T., Huberman, J.A., and Holt, I.J. (2003). Mammalian mitochondrial DNA replicates bidirectionally from an initiation zone. J Biol Chem *278*, 50961-50969.

Bradshaw, E., Yoshida, M., and Ling, F. (2017). Regulation of Small Mitochondrial DNA Replicative Advantage by Ribonucleotide Reductase in Saccharomyces cerevisiae. G3 *7*, 3083-3090.

Bratic, A., and Larsson, N.G. (2013). The role of mitochondria in aging. The Journal of clinical investigation *123*, 951-957.

Brown, T.A., Tkachuk, A.N., Shtengel, G., Kopek, B.G., Bogenhagen, D.F., Hess, H.F., and Clayton, D.A. (2011). Superresolution fluorescence imaging of mitochondrial nucleoids reveals their spatial range, limits, and membrane interaction. Molecular and cellular biology *31*, 4994-5010.

Bruni, F., Lightowlers, R.N., and Chrzanowska-Lightowlers, Z.M. (2017). Human mitochondrial nucleases. The FEBS journal *284*, 1767-1777.

Brzezniak, L.K., Bijata, M., Szczesny, R.J., and Stepien, P.P. (2011). Involvement of human ELAC2 gene product in 3' end processing of mitochondrial tRNAs. RNA Biol *8*, 616-626.

Bulteau, A.L., and Chavatte, L. (2015). Update on selenoprotein biosynthesis. Antioxidants & redox signaling *23*, 775-794.

Burzio, V.A., Villota, C., Villegas, J., Landerer, E., Boccardo, E., Villa, L.L., Martinez, R., Lopez, C., Gaete, F., Toro, V.*, et al.* (2009). Expression of a family of noncoding mitochondrial RNAs distinguishes normal from cancer cells. Proceedings of the National Academy of Sciences of the United States of America *106*, 9430-9434.

Calvo, S.E., Clauser, K.R., and Mootha, V.K. (2016). MitoCarta2.0: an updated inventory of mammalian mitochondrial proteins. Nucleic Acids Res *44*, D1251-1257.

Cande, C., Vahsen, N., Metivier, D., Tourriere, H., Chebli, K., Garrido, C., Tazi, J., and Kroemer, G. (2004). Regulation of cytoplasmic stress granules by apoptosis-inducing factor. Journal of cell science *117*, 4461-4468.

Cannino, G., El-Khoury, R., Pirinen, M., Hutz, B., Rustin, P., Jacobs, H.T., and Dufour, E. (2012). Glucose modulates respiratory complex I activity in response to acute mitochondrial dysfunction. J Biol Chem *287*, 38729-38740.

Cannon, M.V., Irwin, M.H., and Pinkert, C.A. (2015). Mitochondrially-imported RNA in drug discovery. Drug development research *76*, 61-71.

Cavelier, L., Johannisson, A., and Gyllensten, U. (2000). Analysis of mtDNA copy number and composition of single mitochondrial particles using flow cytometry and PCR. Experimental cell research *259*, 79-85.

Chang, D.D., and Clayton, D.A. (1984). Precise identification of individual promoters for transcription of each strand of human mitochondrial DNA. Cell *36*, 635-643.

Chang, D.D., and Clayton, D.A. (1987). A mammalian mitochondrial RNA processing activity contains nucleus-encoded RNA. Science *235*, 1178-1184.

Chang, D.D., and Clayton, D.A. (1989). Mouse RNAase MRP RNA is encoded by a nuclear gene and contains a decamer sequence complementary to a conserved region of mitochondrial RNA substrate. Cell *56*, 131-139.

Chatterjee, K., Nostramo, R.T., Wan, Y., and Hopper, A.K. (2018). tRNA dynamics between the nucleus, cytoplasm and mitochondrial surface: Location, location, location. Biochimica et biophysica acta Gene regulatory mechanisms *1861*, 373-386.

Chazotte, B. (2011). Labeling mitochondria with MitoTracker dyes. Cold Spring Harbor protocols *2011*, 990-992.

Chen, H.W., Rainey, R.N., Balatoni, C.E., Dawson, D.W., Troke, J.J., Wasiak, S., Hong, J.S., McBride, H.M., Koehler, C.M., Teitell, M.A.*, et al.* (2006). Mammalian polynucleotide phosphorylase is an intermembrane space RNase that maintains mitochondrial homeostasis. Molecular and cellular biology *26*, 8475-8487.

Chen, X., Taylor, D.W., Fowler, C.C., Galan, J.E., Wang, H.W., and Wolin, S.L. (2013). An RNA degradation machine sculpted by Ro autoantigen and noncoding RNA. Cell *153*, 166-177.

Cheng, Y., Liu, P., Zheng, Q., Gao, G., Yuan, J., Wang, P., Huang, J., Xie, L., Lu, X., Tong, T.*, et al.* (2018). Mitochondrial Trafficking and Processing of Telomerase RNA TERC. Cell reports *24*, 2589-2595.

Chretien, D., Benit, P., Ha, H.H., Keipert, S., El-Khoury, R., Chang, Y.T., Jastroch, M., Jacobs, H.T., Rustin, P., and Rak, M. (2018). Mitochondria are physiologically maintained at close to 50 degrees C. PLoS biology *16*, e2003992.

Chujo, T., Ohira, T., Sakaguchi, Y., Goshima, N., Nomura, N., Nagao, A., and Suzuki, T. (2012). LRPPRC/SLIRP suppresses PNPase-mediated mRNA decay and promotes polyadenylation in human mitochondria. Nucleic Acids Res *40*, 8033-8047.

Claude, A. (1946). Fractionation of mammalian liver cells by differential centrifugation; experimental procedures and results. The Journal of experimental medicine *84*, 61-89.

Clayton, D.A. (2003). Mitochondrial DNA replication: what we know. IUBMB life *55*, 213-217.

Cody, N.A., Iampietro, C., and Lecuyer, E. (2013). The many functions of mRNA localization during normal development and disease: from pillar to post. Wiley interdisciplinary reviews Developmental biology *2*, 781-796.

Comte, C., Tonin, Y., Heckel-Mager, A.M., Boucheham, A., Smirnov, A., Aure, K., Lombes, A., Martin, R.P., Entelis, N., and Tarassov, I. (2013). Mitochondrial targeting of recombinant RNAs modulates the level of a heteroplasmic mutation in human mitochondrial DNA associated with Kearns Sayre Syndrome. Nucleic Acids Res *41*, 418-433.

Contreras, L., Drago, I., Zampese, E., and Pozzan, T. (2010). Mitochondria: the calcium connection. Biochimica et biophysica acta *1797*, 607-618.

Corona, P., Antozzi, C., Carrara, F., D'Incerti, L., Lamantea, E., Tiranti, V., and Zeviani, M. (2001). A novel mtDNA mutation in the ND5 subunit of complex I in two MELAS patients. Ann Neurol *49*, 106-110.

Crausaz Esseiva, A., Marechal-Drouard, L., Cosset, A., and Schneider, A. (2004). The T-stem determines the cytosolic or mitochondrial localization of trypanosomal tRNAsMet. Molecular biology of the cell *15*, 2750-2757.

Craven, L., Alston, C.L., Taylor, R.W., and Turnbull, D.M. (2017). Recent Advances in Mitochondrial Disease. Annual review of genomics and human genetics *18*, 257-275.

Cree, L.M., Samuels, D.C., de Sousa Lopes, S.C., Rajasimha, H.K., Wonnapinij, P., Mann, J.R., Dahl, H.H., and Chinnery, P.F. (2008). A reduction of mitochondrial DNA molecules during embryogenesis explains the rapid segregation of genotypes. Nat Genet *40*, 249-254.

Das, S., Ferlito, M., Kent, O.A., Fox-Talbot, K., Wang, R., Liu, D., Raghavachari, N., Yang, Y., Wheelan, S.J., Murphy, E.*, et al.* (2012). Nuclear miRNA regulates the mitochondrial genome in the heart. Circulation research *110*, 1596-1603.

Delage, L., Dietrich, A., Cosset, A., and Marechal-Drouard, L. (2003). In vitro import of a nuclearly encoded tRNA into mitochondria of Solanum tuberosum. Molecular and cellular biology *23*, 4000-4012.

Dellibovi-Ragheb, T.A., Gisselberg, J.E., and Prigge, S.T. (2013). Parasites FeS up: iron-sulfur cluster biogenesis in eukaryotic pathogens. PLoS pathogens *9*, e1003227.

Diekmann, Y., and Pereira-Leal, J.B. (2013). Evolution of intracellular compartmentalization. The Biochemical journal *449*, 319-331.

DiMauro, S., and Schon, E.A. (2003). Mitochondrial respiratory-chain diseases. The New England journal of medicine *348*, 2656-2668.

Dolgosheina, E.V., and Unrau, P.J. (2016). Fluorophore-binding RNA aptamers and their applications. Wiley interdisciplinary reviews RNA *7*, 843-851.

Dovydenko, I., Heckel, A.M., Tonin, Y., Gowher, A., Venyaminova, A., Tarassov, I., and Entelis, N. (2015). Mitochondrial targeting of recombinant RNA. Methods Mol Biol *1265*, 209-225.

Duarte, F.V., Palmeira, C.M., and Rolo, A.P. (2014). The Role of microRNAs in Mitochondria: Small Players Acting Wide. Genes *5*, 865-886.

Duchene, A.M., Pujol, C., and Marechal-Drouard, L. (2009). Import of tRNAs and aminoacyl-tRNA synthetases into mitochondria. Current genetics *55*, 1-18.

Dudek, J., Rehling, P., and van der Laan, M. (2013). Mitochondrial protein import: common principles and physiological networks. Biochimica et biophysica acta *1833*, 274-285.

Eaton, S., Bartlett, K., and Pourfarzam, M. (1996). Mammalian mitochondrial beta-oxidation. The Biochemical journal *320 (Pt 2)*, 345-357.

Efremov, R.G., Baradaran, R., and Sazanov, L.A. (2010). The architecture of respiratory complex I. Nature *465*, 441-445.

Eliyahu, E., Pnueli, L., Melamed, D., Scherrer, T., Gerber, A.P., Pines, O., Rapaport, D., and Arava, Y. (2010). Tom20 mediates localization of mRNAs to mitochondria in a translation-dependent manner. Molecular and cellular biology *30*, 284-294.

Entelis, N., Brandina, I., Kamenski, P., Krasheninnikov, I.A., Martin, R.P., and Tarassov, I. (2006). A glycolytic enzyme, enolase, is recruited as a cofactor of tRNA targeting toward mitochondria in Saccharomyces cerevisiae. Genes & development *20*, 1609-1620.

Entelis, N.S., Kolesnikova, O.A., Dogan, S., Martin, R.P., and Tarassov, I.A. (2001). 5 S rRNA and tRNA import into human mitochondria. Comparison of in vitro requirements. J Biol Chem *276*, 45642-45653.

Esakova, O., and Krasilnikov, A.S. (2010). Of proteins and RNA: the RNase P/MRP family. Rna *16*, 1725-1747.

Estaquier, J., Vallette, F., Vayssiere, J.L., and Mignotte, B. (2012). The mitochondrial pathways of apoptosis. Advances in experimental medicine and biology *942*, 157-183.

Fabian, M.R., Sonenberg, N., and Filipowicz, W. (2010). Regulation of mRNA translation and stability by microRNAs. Annual review of biochemistry *79*, 351-379.

Fakruddin, M., Wei, F.Y., Emura, S., Matsuda, S., Yasukawa, T., Kang, D., and Tomizawa, K. (2017). Cdk5rap1-mediated 2-methylthio-N6-isopentenyladenosine modification is absent from nuclear-derived RNA species. Nucleic Acids Res *45*, 11954-11961.

Falkenberg, M., Gaspari, M., Rantanen, A., Trifunovic, A., Larsson, N.G., and Gustafsson, C.M. (2002). Mitochondrial transcription factors B1 and B2 activate transcription of human mtDNA. Nat Genet *31*, 289-294.

Fazal, F.M.H., S.; Kaewsapsak, P; Parker, K.R.; Xu, J.; Boettiger, A.N.; Chang, H.Y. Chang; Ting, A.Y. (2018). Atlas of subcellular RNA localization revealed by APEX-seq. preprint on bioRxiv.

Fearnley, I.M., and Walker, J.E. (1987). Initiation codons in mammalian mitochondria: differences in genetic code in the organelle. Biochemistry *26*, 8247-8251.

Fiedler, M., Rossmanith, W., Wahle, E., and Rammelt, C. (2015). Mitochondrial poly(A) polymerase is involved in tRNA repair. Nucleic Acids Res *43*, 9937-9949.

Filonov, G.S., Moon, J.D., Svensen, N., and Jaffrey, S.R. (2014). Broccoli: rapid selection of an RNA mimic of green fluorescent protein by fluorescence-based selection and directed evolution. Journal of the American Chemical Society *136*, 16299-16308.

Filosto, M., and Mancuso, M. (2007). Mitochondrial diseases: a nosological update. Acta neurologica Scandinavica *115*, 211-221.

Filosto, M., Scarpelli, M., Cotelli, M.S., Vielmi, V., Todeschini, A., Gregorelli, V., Tonin, P., Tomelleri, G., and Padovani, A. (2011). The role of mitochondria in neurodegenerative diseases. Journal of neurology *258*, 1763-1774.

Frey, S., Geffroy, G., Desquiret-Dumas, V., Gueguen, N., Bris, C., Belal, S., Amati-Bonneau, P., Chevrollier, A., Barth, M., Henrion, D.*, et al.* (2017). The addition of ketone bodies alleviates mitochondrial dysfunction by restoring complex I assembly in a MELAS cellular model. Biochimica et biophysica acta Molecular basis of disease *1863*, 284-291.

Fuller, K.M., and Arriaga, E.A. (2004). Capillary electrophoresis monitors changes in the electrophoretic behavior of mitochondrial preparations. Journal of chromatography B, Analytical technologies in the biomedical and life sciences *806*, 151-159.

Gall, J.G. (1990). Telomerase RNA: tying up the loose ends. Nature *344*, 108-109.

Gammage, P.A., Moraes, C.T., and Minczuk, M. (2017). Mitochondrial Genome Engineering: The Revolution May Not Be CRISPR-Ized. Trends in genetics : TIG *34*, 101-110.

Gammage, P.A., Viscomi, C., Simard, M.L., Costa, A.S.H., Gaude, E., Powell, C.A., Van Haute, L., McCann, B.J., Rebelo-Guiomar, P., Cerutti, R.*, et al.* (2018). Genome editing in mitochondria corrects a pathogenic mtDNA mutation in vivo. Nature medicine *24*, 1691-1695.

Gao, F., Wesolowska, M., Agami, R., Rooijers, K., Loayza-Puch, F., Lawless, C., Lightowlers, R.N., and Chrzanowska-Lightowlers, Z.M.A. (2017). Using mitoribosomal profiling to investigate human mitochondrial translation. Wellcome open research *2*, 116.

Garalde, D.R., Snell, E.A., Jachimowicz, D., Sipos, B., Lloyd, J.H., Bruce, M., Pantic, N., Admassu, T., James, P., Warland, A.*, et al.* (2018). Highly parallel direct RNA sequencing on an array of nanopores. Nature methods *15*, 201-206.

Geiger, J., and Dalgaard, L.T. (2017). Interplay of mitochondrial metabolism and microRNAs. Cellular and molecular life sciences : CMLS *74*, 631-646.

Geisler, S., and Coller, J. (2013). RNA in unexpected places: long non-coding RNA functions in diverse cellular contexts. Nature reviews Molecular cell biology *14*, 699-712.

Gill, T., Cai, T., Aulds, J., Wierzbicki, S., and Schmitt, M.E. (2004). RNase MRP cleaves the CLB2 mRNA to promote cell cycle progression: novel method of mRNA degradation. Molecular and cellular biology *24*, 945-953.

Gold, V.A., Chroscicki, P., Bragoszewski, P., and Chacinska, A. (2017). Visualization of cytosolic ribosomes on the surface of mitochondria by electron cryo-tomography. EMBO reports *18*, 1786-1800.

Golzarroshan, B., Lin, C.L., Li, C.L., Yang, W.Z., Chu, L.Y., Agrawal, S., and Yuan, H.S. (2018). Crystal structure of dimeric human PNPase reveals why disease-linked mutants suffer from low RNA import and degradation activities. Nucleic Acids Res *46*, 8630-8640.

Gorman, G.S., Chinnery, P.F., DiMauro, S., Hirano, M., Koga, Y., McFarland, R., Suomalainen, A., Thorburn, D.R., Zeviani, M., and Turnbull, D.M. (2016). Mitochondrial diseases. Nature reviews Disease primers *2*, 16080.

Gorman, G.S., Schaefer, A.M., Ng, Y., Gomez, N., Blakely, E.L., Alston, C.L., Feeney, C., Horvath, R., Yu-Wai-Man, P., Chinnery, P.F.*, et al.* (2015). Prevalence of nuclear and

mitochondrial DNA mutations related to adult mitochondrial disease. Ann Neurol *77*, 753-759.

Gowher, A., Smirnov, A., Tarassov, I., and Entelis, N. (2013). Induced tRNA import into human mitochondria: implication of a host aminoacyl-tRNA-synthetase. PloS one *8*, e66228.

Gray, M.W., Burger, G., and Lang, B.F. (1999). Mitochondrial evolution. Science *283*, 1476-1481.

Greber, B.J., and Ban, N. (2016). Structure and Function of the Mitochondrial Ribosome. Annual review of biochemistry *85*, 103-132.

Greber, B.J., Bieri, P., Leibundgut, M., Leitner, A., Aebersold, R., Boehringer, D., and Ban, N. (2015). Ribosome. The complete structure of the 55S mammalian mitochondrial ribosome. Science *348*, 303-308.

Gromer, S., Eubel, J.K., Lee, B.L., and Jacob, J. (2005). Human selenoproteins at a glance. Cellular and molecular life sciences : CMLS *62*, 2414-2437.

Grudnik, P., Bange, G., and Sinning, I. (2009). Protein targeting by the signal recognition particle. Biological chemistry *390*, 775-782.

Gustafsson, C.M., Falkenberg, M., and Larsson, N.G. (2016). Maintenance and Expression of Mammalian Mitochondrial DNA. Annual review of biochemistry *85*, 133-160.

Haag, S., Sloan, K.E., Ranjan, N., Warda, A.S., Kretschmer, J., Blessing, C., Hubner, B., Seikowski, J., Dennerlein, S., Rehling, P.*, et al.* (2016). NSUN3 and ABH1 modify the wobble position of mt-tRNAMet to expand codon recognition in mitochondrial translation. The EMBO journal *35*, 2104-2119.

Hallberg, B.M., and Larsson, N.G. (2014). Making proteins in the powerhouse. Cell metabolism *20*, 226-240.

Hancock, K., and Hajduk, S.L. (1990). The mitochondrial tRNAs of Trypanosoma brucei are nuclear encoded. J Biol Chem *265*, 19208-19215.

He, J., Cooper, H.M., Reyes, A., Di Re, M., Sembongi, H., Litwin, T.R., Gao, J., Neuman, K.C., Fearnley, I.M., Spinazzola, A.*, et al.* (2012). Mitochondrial nucleoid interacting proteins support mitochondrial protein synthesis. Nucleic Acids Res *40*, 6109-6121.

Herbers, E., Kekalainen, N.J., Hangas, A., Pohjoismaki, J.L., and Goffart, S. (2018). Tissue specific differences in mitochondrial DNA maintenance and expression. Mitochondrion.

Hillen, H.S., Temiakov, D., and Cramer, P. (2018). Structural basis of mitochondrial transcription. Nature structural & molecular biology *25*, 754-765.

Holzmann, J., Frank, P., Loffler, E., Bennett, K.L., Gerner, C., and Rossmanith, W. (2008). RNase P without RNA: identification and functional reconstitution of the human mitochondrial tRNA processing enzyme. Cell *135*, 462-474.

Hopper, A.K., Pai, D.A., and Engelke, D.R. (2010). Cellular dynamics of tRNAs and their genes. FEBS letters *584*, 310-317.

Hrdlickova, R., Toloue, M., and Tian, B. (2017). RNA-Seq methods for transcriptome analysis. Wiley interdisciplinary reviews RNA *8*.

Huang, B., Bates, M., and Zhuang, X. (2009). Super-resolution fluorescence microscopy. Annual review of biochemistry *78*, 993-1016.

Huang, H., Suslov, N.B., Li, N.S., Shelke, S.A., Evans, M.E., Koldobskaya, Y., Rice, P.A., and Piccirilli, J.A. (2014). A G-quadruplex-containing RNA activates fluorescence in a GFP-like fluorophore. Nature chemical biology *10*, 686-691.

Huang, L., Mollet, S., Souquere, S., Le Roy, F., Ernoult-Lange, M., Pierron, G., Dautry, F., and Weil, D. (2011). Mitochondria associate with P-bodies and modulate microRNA-mediated RNA interference. J Biol Chem *286*, 24219-24230.

Huntzinger, E., and Izaurralde, E. (2011). Gene silencing by microRNAs: contributions of translational repression and mRNA decay. Nature reviews Genetics *12*, 99-110.

Jain, I.H., Zazzeron, L., Goli, R., Alexa, K., Schatzman-Bone, S., Dhillon, H., Goldberger, O., Peng, J., Shalem, O., Sanjana, N.E.*, et al.* (2016). Hypoxia as a therapy for mitochondrial disease. Science *352*, 54-61.

Jakobs, S., and Wurm, C.A. (2014). Super-resolution microscopy of mitochondria. Current opinion in chemical biology *20*, 9-15.

Jemt, E., Persson, O., Shi, Y., Mehmedovic, M., Uhler, J.P., Davila Lopez, M., Freyer, C., Gustafsson, C.M., Samuelsson, T., and Falkenberg, M. (2015). Regulation of DNA replication at the end of the mitochondrial D-loop involves the helicase TWINKLE and a conserved sequence element. Nucleic Acids Res *43*, 9262-9275.

Jinek, M., Chylinski, K., Fonfara, I., Hauer, M., Doudna, J.A., and Charpentier, E. (2012). A programmable dual-RNA-guided DNA endonuclease in adaptive bacterial immunity. Science *337*, 816-821.

Jo, A., Ham, S., Lee, G.H., Lee, Y.I., Kim, S., Lee, Y.S., Shin, J.H., and Lee, Y. (2015). Efficient Mitochondrial Genome Editing by CRISPR/Cas9. BioMed research international *2015*, 305716.

Joshi, A.S., Zhou, J., Gohil, V.M., Chen, S., and Greenberg, M.L. (2009). Cellular functions of cardiolipin in yeast. Biochimica et biophysica acta *1793*, 212-218.

Jourdain, A.A., Koppen, M., Wydro, M., Rodley, C.D., Lightowlers, R.N., Chrzanowska-Lightowlers, Z.M., and Martinou, J.C. (2013). GRSF1 regulates RNA processing in mitochondrial RNA granules. Cell metabolism *17*, 399-410.

Jung, H., Gkogkas, C.G., Sonenberg, N., and Holt, C.E. (2014). Remote control of gene function by local translation. Cell *157*, 26-40.

Kaewsapsak, P., Shechner, D.M., Mallard, W., Rinn, J.L., and Ting, A.Y. (2017). Live-cell mapping of organelle-associated RNAs via proximity biotinylation combined with protein-RNA crosslinking. eLife *6*.

Kamenski, P., Kolesnikova, O., Jubenot, V., Entelis, N., Krasheninnikov, I.A., Martin, R.P., and Tarassov, I. (2007). Evidence for an adaptation mechanism of mitochondrial translation via tRNA import from the cytosol. Molecular cell *26*, 625-637.

Kamenski, P., Smirnova, E., Kolesnikova, O., Krasheninnikov, I.A., Martin, R.P., Entelis, N., and Tarassov, I. (2010). tRNA mitochondrial import in yeast: Mapping of the import

determinants in the carrier protein, the precursor of mitochondrial lysyl-tRNA synthetase. Mitochondrion *10*, 284-293.

Karicheva, O.Z., Kolesnikova, O.A., Schirtz, T., Vysokikh, M.Y., Mager-Heckel, A.M., Lombes, A., Boucheham, A., Krasheninnikov, I.A., Martin, R.P., Entelis, N.*, et al.* (2011). Correction of the consequences of mitochondrial 3243A>G mutation in the MT-TL1 gene causing the MELAS syndrome by tRNA import into mitochondria. Nucleic Acids Res *39*, 8173-8186.

Karnkowska, A., Vacek, V., Zubacova, Z., Treitli, S.C., Petrzelkova, R., Eme, L., Novak, L., Zarsky, V., Barlow, L.D., Herman, E.K.*, et al.* (2016). A Eukaryote without a Mitochondrial Organelle. Current biology : CB *26*, 1274-1284.

Kazakova, H.A., Entelis, N.S., Martin, R.P., and Tarassov, I.A. (1999). The aminoacceptor stem of the yeast tRNA(Lys) contains determinants of mitochondrial import selectivity. FEBS letters *442*, 193-197.

Khoder-Agha, F., Dias, J.M., Comisso, M., and Mirande, M. (2018). Characterization of association of human mitochondrial lysyl-tRNA synthetase with HIV-1 Pol and tRNA3(Lys). BMC biochemistry *19*, 2.

Kim, D.H., and Hwang, I. (2013). Direct targeting of proteins from the cytosol to organelles: the ER versus endosymbiotic organelles. Traffic *14*, 613-621.

Kim, K.M., Noh, J.H., Abdelmohsen, K., and Gorospe, M. (2017). Mitochondrial noncoding RNA transport. BMB reports *50*, 164-174.

Klemm, B.P., Wu, N., Chen, Y., Liu, X., Kaitany, K.J., Howard, M.J., and Fierke, C.A. (2016). The Diversity of Ribonuclease P: Protein and RNA Catalysts with Analogous Biological Functions. Biomolecules *6*.

Koehler, C.M., Jarosch, E., Tokatlidis, K., Schmid, K., Schweyen, R.J., and Schatz, G. (1998). Import of mitochondrial carriers mediated by essential proteins of the intermembrane space. Science *279*, 369-373.

Kolesnikova, O., Kazakova, H., Comte, C., Steinberg, S., Kamenski, P., Martin, R.P., Tarassov, I., and Entelis, N. (2010). Selection of RNA aptamers imported into yeast and human mitochondria. Rna *16*, 926-941.

Kolesnikova, O.A., Entelis, N.S., Jacquin-Becker, C., Goltzene, F., Chrzanowska-Lightowlers, Z.M., Lightowlers, R.N., Martin, R.P., and Tarassov, I. (2004). Nuclear DNA-encoded tRNAs targeted into mitochondria can rescue a mitochondrial DNA mutation associated with the MERRF syndrome in cultured human cells. Human molecular genetics *13*, 2519-2534.

Kolesnikova, O.A., Entelis, N.S., Mireau, H., Fox, T.D., Martin, R.P., and Tarassov, I.A. (2000). Suppression of mutations in mitochondrial DNA by tRNAs imported from the cytoplasm. Science *289*, 1931-1933.

Kouvela, E.C., Gerbanas, G.V., Xaplanteri, M.A., Petropoulos, A.D., Dinos, G.P., and Kalpaxis, D.L. (2007). Changes in the conformation of 5S rRNA cause alterations in principal functions of the ribosomal nanomachine. Nucleic Acids Res *35*, 5108-5119.

Kowalski, M.P., and Krude, T. (2015). Functional roles of non-coding Y RNAs. The international journal of biochemistry & cell biology *66*, 20-29.

Kruse, B., Narasimhan, N., and Attardi, G. (1989). Termination of transcription in human mitochondria: identification and purification of a DNA binding protein factor that promotes termination. Cell *58*, 391-397.

Kuhl, I., Miranda, M., Posse, V., Milenkovic, D., Mourier, A., Siira, S.J., Bonekamp, N.A., Neumann, U., Filipovska, A., Polosa, P.L.*, et al.* (2016). POLRMT regulates the switch between replication primer formation and gene expression of mammalian mtDNA. Science advances *2*, e1600963.

Kukat, C., Davies, K.M., Wurm, C.A., Spahr, H., Bonekamp, N.A., Kuhl, I., Joos, F., Polosa, P.L., Park, C.B., Posse, V.*, et al.* (2015). Cross-strand binding of TFAM to a single mtDNA molecule forms the mitochondrial nucleoid. Proceedings of the National Academy of Sciences of the United States of America *112*, 11288-11293.

Kumarswamy, R., Bauters, C., Volkmann, I., Maury, F., Fetisch, J., Holzmann, A., Lemesle, G., de Groote, P., Pinet, F., and Thum, T. (2014). Circulating long noncoding RNA, LIPCAR, predicts survival in patients with heart failure. Circulation research *114*, 1569-1575.

Kutik, S., Stojanovski, D., Becker, L., Becker, T., Meinecke, M., Kruger, V., Prinz, C., Meisinger, C., Guiard, B., Wagner, R.*, et al.* (2008). Dissecting membrane insertion of mitochondrial beta-barrel proteins. Cell *132*, 1011-1024.

Kuzmenko, A., Tankov, S., English, B.P., Tarassov, I., Tenson, T., Kamenski, P., Elf, J., and Hauryliuk, V. (2011). Single molecule tracking fluorescence microscopy in mitochondria reveals highly dynamic but confined movement of Tom40. Scientific reports *1*, 195.

Kuznetsova, I., Siira, S.J., Shearwood, A.J., Ermer, J.A., Filipovska, A., and Rackham, O. (2017). Simultaneous processing and degradation of mitochondrial RNAs revealed by circularized RNA sequencing. Nucleic Acids Res *45*, 5487-5500.

Kwon, S. (2013). Single-molecule fluorescence in situ hybridization: quantitative imaging of single RNA molecules. BMB reports *46*, 65-72.

Landerer, E., Villegas, J., Burzio, V.A., Oliveira, L., Villota, C., Lopez, C., Restovic, F., Martinez, R., Castillo, O., and Burzio, L.O. (2011). Nuclear localization of the mitochondrial ncRNAs in normal and cancer cells. Cellular oncology *34*, 297-305.

Lecuyer, E., Yoshida, H., Parthasarathy, N., Alm, C., Babak, T., Cerovina, T., Hughes, T.R., Tomancak, P., and Krause, H.M. (2007). Global analysis of mRNA localization reveals a prominent role in organizing cellular architecture and function. Cell *131*, 174-187.

Leucci, E., Vendramin, R., Spinazzi, M., Laurette, P., Fiers, M., Wouters, J., Radaelli, E., Eyckerman, S., Leonelli, C., Vanderheyden, K.*, et al.* (2016). Melanoma addiction to the long non-coding RNA SAMMSON. Nature *531*, 518-522.

Levy, S., Allerston, C.K., Liveanu, V., Habib, M.R., Gileadi, O., and Schuster, G. (2016). Identification of LACTB2, a metallo-beta-lactamase protein, as a human mitochondrial endoribonuclease. Nucleic Acids Res *44*, 1813-1832.

Li, Y., Aggarwal, M.B., Ke, K., Nguyen, K., and Spitale, R.C. (2018). Improved Analysis of RNA Localization by Spatially Restricted Oxidation of RNA-Protein Complexes. Biochemistry *57*, 1577-1581.

Li, Y., Aggarwal, M.B., Nguyen, K., Ke, K., and Spitale, R.C. (2017). Assaying RNA Localization in Situ with Spatially Restricted Nucleobase Oxidation. ACS chemical biology *12*, 2709-2714.

Lill, R., and Muhlenhoff, U. (2005). Iron-sulfur-protein biogenesis in eukaryotes. Trends in biochemical sciences *30*, 133-141.

Lin, C.L., Wang, Y.T., Yang, W.Z., Hsiao, Y.Y., and Yuan, H.S. (2012). Crystal structure of human polynucleotide phosphorylase: insights into its domain function in RNA binding and degradation. Nucleic Acids Res *40*, 4146-4157.

Litonin, D., Sologub, M., Shi, Y., Savkina, M., Anikin, M., Falkenberg, M., Gustafsson, C.M., and Temiakov, D. (2010). Human mitochondrial transcription revisited: only TFAM and TFB2M are required for transcription of the mitochondrial genes in vitro. J Biol Chem *285*, 18129-18133.

Liu, X., Fu, R., Pan, Y., Meza-Sosa, K.F., Zhang, Z., and Lieberman, J. (2018). PNPT1 Release from Mitochondria during Apoptosis Triggers Decay of Poly(A) RNAs. Cell *174*, 187-201 e112.

Lodeiro, M.F., Uchida, A., Bestwick, M., Moustafa, I.M., Arnold, J.J., Shadel, G.S., and Cameron, C.E. (2012). Transcription from the second heavy-strand promoter of human mtDNA is repressed by transcription factor A in vitro. Proceedings of the National Academy of Sciences of the United States of America *109*, 6513-6518.

Longen, S., Woellhaf, M.W., Petrungaro, C., Riemer, J., and Herrmann, J.M. (2014). The disulfide relay of the intermembrane space oxidizes the ribosomal subunit mrp10 on its transit into the mitochondrial matrix. Developmental cell *28*, 30-42.

Loutre, R., Heckel, A.M., Jeandard, D., Tarassov, I., and Entelis, N. (2018a). Anti-replicative recombinant 5S rRNA molecules can modulate the mtDNA heteroplasmy in a glucose-dependent manner. PloS one *13*, e0199258.

Loutre, R., Heckel, A.M., Smirnova, A., Entelis, N., and Tarassov, I. (2018b). Can Mitochondrial DNA be CRISPRized: Pro and Contra. IUBMB life.

Lund, E., and Dahlberg, J.E. (1992). Cyclic 2',3'-phosphates and nontemplated nucleotides at the 3' end of spliceosomal U6 small nuclear RNA's. Science *255*, 327-330.

Luo, S., Valencia, C.A., Zhang, J., Lee, N.C., Slone, J., Gui, B., Wang, X., Li, Z., Dell, S., Brown, J.*, et al.* (2018a). Biparental Inheritance of Mitochondrial DNA in Humans. Proceedings of the National Academy of Sciences of the United States of America *115*, 13039-13044.

Luo, Y., Na, Z., and Slavoff, S.A. (2018b). P-Bodies: Composition, Properties, and Functions. Biochemistry *57*, 2424-2431.

Magalhaes, P.J., Andreu, A.L., and Schon, E.A. (1998). Evidence for the presence of 5S rRNA in mammalian mitochondria. Molecular biology of the cell *9*, 2375-2382.

Mager-Heckel, A.M., Entelis, N., Brandina, I., Kamenski, P., Krasheninnikov, I.A., Martin, R.P., and Tarassov, I. (2007). The analysis of tRNA import into mammalian mitochondria. Methods Mol Biol *372*, 235-253.

Maida, Y., Yasukawa, M., Furuuchi, M., Lassmann, T., Possemato, R., Okamoto, N., Kasim, V., Hayashizaki, Y., Hahn, W.C., and Masutomi, K. (2009). An RNA-dependent RNA polymerase formed by TERT and the RMRP RNA. Nature *461*, 230-235.

Malarkey, C.S., Bestwick, M., Kuhlwilm, J.E., Shadel, G.S., and Churchill, M.E. (2012). Transcriptional activation by mitochondrial transcription factor A involves preferential distortion of promoter DNA. Nucleic Acids Res *40*, 614-624.

Manwaring, N., Jones, M.M., Wang, J.J., Rochtchina, E., Howard, C., Mitchell, P., and Sue, C.M. (2007). Population prevalence of the MELAS A3243G mutation. Mitochondrion *7*, 230-233.

Marchi, S., Patergnani, S., and Pinton, P. (2014). The endoplasmic reticulum-mitochondria connection: one touch, multiple functions. Biochimica et biophysica acta *1837*, 461-469.

Marroquin, L.D., Hynes, J., Dykens, J.A., Jamieson, J.D., and Will, Y. (2007). Circumventing the Crabtree effect: replacing media glucose with galactose increases susceptibility of HepG2 cells to mitochondrial toxicants. Toxicological sciences : an official journal of the Society of Toxicology *97*, 539-547.

Martin, R.P., Schneller, J.M., Stahl, A.J., and Dirheimer, G. (1979). Import of nuclear deoxyribonucleic acid coded lysine-accepting transfer ribonucleic acid (anticodon C-U-U) into yeast mitochondria. Biochemistry *18*, 4600-4605.

Martin, W., and Koonin, E.V. (2006). Introns and the origin of nucleus-cytosol compartmentalization. Nature *440*, 41-45.

Matilainen, S., Carroll, C.J., Richter, U., Euro, L., Pohjanpelto, M., Paetau, A., Isohanni, P., and Suomalainen, A. (2017). Defective mitochondrial RNA processing due to PNPT1 variants causes Leigh syndrome. Human molecular genetics *26*, 3352-3361.

Matsumoto, S., Uchiumi, T., Saito, T., Yagi, M., Takazaki, S., Kanki, T., and Kang, D. (2012). Localization of mRNAs encoding human mitochondrial oxidative phosphorylation proteins. Mitochondrion *12*, 391-398.

Mercer, T.R., Neph, S., Dinger, M.E., Crawford, J., Smith, M.A., Shearwood, A.M., Haugen, E., Bracken, C.P., Rackham, O., Stamatoyannopoulos, J.A.*, et al.* (2011). The human mitochondrial transcriptome. Cell *146*, 645-658.

Miralles Fuste, J., Shi, Y., Wanrooij, S., Zhu, X., Jemt, E., Persson, O., Sabouri, N., Gustafsson, C.M., and Falkenberg, M. (2014). In vivo occupancy of mitochondrial single-stranded DNA binding protein supports the strand displacement mode of DNA replication. PLoS Genet *10*, e1004832.

Montoya, J., Christianson, T., Levens, D., Rabinowitz, M., and Attardi, G. (1982). Identification of initiation sites for heavy-strand and light-strand transcription in human mitochondrial DNA. Proceedings of the National Academy of Sciences of the United States of America *79*, 7195-7199.

Montoya, J., Ojala, D., and Attardi, G. (1981). Distinctive features of the 5'-terminal sequences of the human mitochondrial mRNAs. Nature *290*, 465-470.

Moretton, A., Morel, F., Macao, B., Lachaume, P., Ishak, L., Lefebvre, M., Garreau-Balandier, I., Vernet, P., Falkenberg, M., and Farge, G. (2017). Selective mitochondrial DNA degradation following double-strand breaks. PloS one *12*, e0176795.

Nagaike, T., Suzuki, T., Katoh, T., and Ueda, T. (2005). Human mitochondrial mRNAs are stabilized with polyadenylation regulated by mitochondria-specific poly(A) polymerase and polynucleotide phosphorylase. J Biol Chem *280*, 19721-19727.

Nagaike, T., Suzuki, T., Tomari, Y., Takemoto-Hori, C., Negayama, F., Watanabe, K., and Ueda, T. (2001). Identification and characterization of mammalian mitochondrial tRNA nucleotidyltransferases. J Biol Chem *276*, 40041-40049.

Nickel, A.I., Waber, N.B., Gossringer, M., Lechner, M., Linne, U., Toth, U., Rossmanith, W., and Hartmann, R.K. (2017). Minimal and RNA-free RNase P in Aquifex aeolicus. Proceedings of the National Academy of Sciences of the United States of America *114*, 11121-11126.

Niemann, M., Harsman, A., Mani, J., Peikert, C.D., Oeljeklaus, S., Warscheid, B., Wagner, R., and Schneider, A. (2017). tRNAs and proteins use the same import channel for translocation across the mitochondrial outer membrane of trypanosomes. Proceedings of the National Academy of Sciences of the United States of America *114*, E7679-E7687.

Nissanka, N., Bacman, S.R., Plastini, M.J., and Moraes, C.T. (2018). The mitochondrial DNA polymerase gamma degrades linear DNA fragments precluding the formation of deletions. Nature communications *9*, 2491.

Nogues, M.V., Vilanova, M., and Cuchillo, C.M. (1995). Bovine pancreatic ribonuclease A as a model of an enzyme with multiple substrate binding sites. Biochimica et biophysica acta *1253*, 16-24.

Noh, J.H., Kim, K.M., Abdelmohsen, K., Yoon, J.H., Panda, A.C., Munk, R., Kim, J., Curtis, J., Moad, C.A., Wohler, C.M.*, et al.* (2016). HuR and GRSF1 modulate the nuclear export and mitochondrial localization of the lncRNA RMRP. Genes & development *30*, 1224-1239.

Ojala, D., Crews, S., Montoya, J., Gelfand, R., and Attardi, G. (1981a). A small polyadenylated RNA (7 S RNA), containing a putative ribosome attachment site, maps near the origin of human mitochondrial DNA replication. Journal of molecular biology *150*, 303-314.

Ojala, D., Montoya, J., and Attardi, G. (1981b). tRNA punctuation model of RNA processing in human mitochondria. Nature *290*, 470-474.

Osellame, L.D., Blacker, T.S., and Duchen, M.R. (2012). Cellular and molecular mechanisms of mitochondrial function. Best practice & research Clinical endocrinology & metabolism *26*, 711-723.

Paige, J.S., Wu, K.Y., and Jaffrey, S.R. (2011). RNA mimics of green fluorescent protein. Science *333*, 642-646.

Palade, G.E. (1953). An electron microscope study of the mitochondrial structure. The journal of histochemistry and cytochemistry : official journal of the Histochemistry Society *1*, 188-211.

Palmieri, F., and Pierri, C.L. (2010). Mitochondrial metabolite transport. Essays in biochemistry *47*, 37-52.

Papp, L.V., Wang, J., Kennedy, D., Boucher, D., Zhang, Y., Gladyshev, V.N., Singh, R.N., and Khanna, K.K. (2008). Functional characterization of alternatively spliced human SECISBP2 transcript variants. Nucleic Acids Res *36*, 7192-7206.

Park, C., and Raines, R.T. (2000). Origin of the 'inactivation' of ribonuclease A at low salt concentration. FEBS letters *468*, 199-202.

Park, C., and Raines, R.T. (2001). Quantitative analysis of the effect of salt concentration on enzymatic catalysis. Journal of the American Chemical Society *123*, 11472-11479.

Petit, P.X., Goubern, M., Diolez, P., Susin, S.A., Zamzami, N., and Kroemer, G. (1998). Disruption of the outer mitochondrial membrane as a result of large amplitude swelling: the impact of irreversible permeability transition. FEBS letters *426*, 111-116.

Picard, M., Zhang, J., Hancock, S., Derbeneva, O., Golhar, R., Golik, P., O'Hearn, S., Levy, S., Potluri, P., Lvova, M.*, et al.* (2014). Progressive increase in mtDNA 3243A>G heteroplasmy causes abrupt transcriptional reprogramming. Proceedings of the National Academy of Sciences of the United States of America *111*, E4033-4042.

Pietras, Z., Wojcik, M.A., Borowski, L.S., Szewczyk, M., Kulinski, T.M., Cysewski, D., Stepien, P.P., Dziembowski, A., and Szczesny, R.J. (2018). Dedicated surveillance mechanism controls G-quadruplex forming non-coding RNAs in human mitochondria. Nature communications *9*, 2558.

Player, A.N., Shen, L.P., Kenny, D., Antao, V.P., and Kolberg, J.A. (2001). Single-copy gene detection using branched DNA (bDNA) in situ hybridization. The journal of histochemistry and cytochemistry : official journal of the Histochemistry Society *49*, 603-612.

Pohjoismaki, J.L., and Goffart, S. (2011). Of circles, forks and humanity: Topological organisation and replication of mammalian mitochondrial DNA. BioEssays : news and reviews in molecular, cellular and developmental biology *33*, 290-299.

Popow, J., Alleaume, A.M., Curk, T., Schwarzl, T., Sauer, S., and Hentze, M.W. (2015). FASTKD2 is an RNA-binding protein required for mitochondrial RNA processing and translation. Rna *21*, 1873-1884.

Posse, V., Shahzad, S., Falkenberg, M., Hallberg, B.M., and Gustafsson, C.M. (2015). TEFM is a potent stimulator of mitochondrial transcription elongation in vitro. Nucleic Acids Res *43*, 2615-2624.

Puranam, R.S., and Attardi, G. (2001). The RNase P associated with HeLa cell mitochondria contains an essential RNA component identical in sequence to that of the nuclear RNase P. Molecular and cellular biology *21*, 548-561.

Rackham, O., and Filipovska, A. (2014). Analysis of the human mitochondrial transcriptome using directional deep sequencing and parallel analysis of RNA ends. Methods Mol Biol *1125*, 263-275.

Rackham, O., Shearwood, A.M., Mercer, T.R., Davies, S.M., Mattick, J.S., and Filipovska, A. (2011). Long noncoding RNAs are generated from the mitochondrial genome and regulated by nuclear-encoded proteins. Rna *17*, 2085-2093.

Reid, D.W., and Nicchitta, C.V. (2015). Diversity and selectivity in mRNA translation on the endoplasmic reticulum. Nature reviews Molecular cell biology *16*, 221-231.

Reinhard, L., Sridhara, S., and Hallberg, B.M. (2017). The MRPP1/MRPP2 complex is a tRNA-maturation platform in human mitochondria. Nucleic Acids Res *45*, 12469-12480.

Repp, B.M., Mastantuono, E., Alston, C.L., Schiff, M., Haack, T.B., Rotig, A., Ardissone, A., Lombes, A., Catarino, C.B., Diodato, D.*, et al.* (2018). Clinical, biochemical and genetic spectrum of 70 patients with ACAD9 deficiency: is riboflavin supplementation effective? Orphanet journal of rare diseases *13*, 120.

Rhee, H.W., Zou, P., Udeshi, N.D., Martell, J.D., Mootha, V.K., Carr, S.A., and Ting, A.Y. (2013). Proteomic mapping of mitochondria in living cells via spatially restricted enzymatic tagging. Science *339*, 1328-1331.

Rich, P.R., and Marechal, A. (2010). The mitochondrial respiratory chain. Essays in biochemistry *47*, 1-23.

Rinehart, J., Krett, B., Rubio, M.A., Alfonzo, J.D., and Soll, D. (2005). Saccharomyces cerevisiae imports the cytosolic pathway for Gln-tRNA synthesis into the mitochondrion. Genes & development *19*, 583-592.

Rinn, J., and Guttman, M. (2014). RNA Function. RNA and dynamic nuclear organization. Science *345*, 1240-1241.

Rizk, A., Paul, G., Incardona, P., Bugarski, M., Mansouri, M., Niemann, A., Ziegler, U., Berger, P., and Sbalzarini, I.F. (2014). Segmentation and quantification of subcellular structures in fluorescence microscopy images using Squassh. Nature protocols *9*, 586-596.

Rorbach, J., Gao, F., Powell, C.A., D'Souza, A., Lightowlers, R.N., Minczuk, M., and Chrzanowska-Lightowlers, Z.M. (2016). Human mitochondrial ribosomes can switch their structural RNA composition. Proceedings of the National Academy of Sciences of the United States of America *113*, 12198-12201.

Rorbach, J., Nicholls, T.J., and Minczuk, M. (2011). PDE12 removes mitochondrial RNA poly(A) tails and controls translation in human mitochondria. Nucleic Acids Res *39*, 7750-7763.

Rossmanith, W., Tullo, A., Potuschak, T., Karwan, R., and Sbisa, E. (1995). Human mitochondrial tRNA processing. J Biol Chem *270*, 12885-12891.

Rother, S., and Meister, G. (2011). Small RNAs derived from longer non-coding RNAs. Biochimie *93*, 1905-1915.

Rothman, J.E., and Wieland, F.T. (1996). Protein sorting by transport vesicles. Science *272*, 227-234.

Rubio, M.A., and Hopper, A.K. (2011). Transfer RNA travels from the cytoplasm to organelles. Wiley interdisciplinary reviews RNA *2*, 802-817.

Rubio, M.A., Rinehart, J.J., Krett, B., Duvezin-Caubet, S., Reichert, A.S., Soll, D., and Alfonzo, J.D. (2008). Mammalian mitochondria have the innate ability to import tRNAs by a mechanism distinct from protein import. Proceedings of the National Academy of Sciences of the United States of America *105*, 9186-9191.

Rusecka, J., Kaliszewska, M., Bartnik, E., and Tonska, K. (2018). Nuclear genes involved in mitochondrial diseases caused by instability of mitochondrial DNA. Journal of applied genetics *59*, 43-57.

Salinas-Giege, T., Giege, R., and Giege, P. (2015). tRNA biology in mitochondria. International journal of molecular sciences *16*, 4518-4559.

Salinas, T., Duchene, A.M., Delage, L., Nilsson, S., Glaser, E., Zaepfel, M., and Marechal-Drouard, L. (2006). The voltage-dependent anion channel, a major component of the tRNA import machinery in plant mitochondria. Proceedings of the National Academy of Sciences of the United States of America *103*, 18362-18367.

Salinas, T., Farouk-Ameqrane, S.E., Ubrig, E., Sauter, C., Duchene, A.M., and Marechal-Drouard, L. (2018). Molecular basis for the differential interaction of plant mitochondrial VDAC proteins with tRNAs. Nucleic Acids Res.

Schmitt, M.E., and Clayton, D.A. (1993). Nuclear RNase MRP is required for correct processing of pre-5.8S rRNA in Saccharomyces cerevisiae. Molecular and cellular biology *13*, 7935-7941.

Schneider, A. (2011). Mitochondrial tRNA import and its consequences for mitochondrial translation. Annual review of biochemistry *80*, 1033-1053.

Schoenmakers, E., Carlson, B., Agostini, M., Moran, C., Rajanayagam, O., Bochukova, E., Tobe, R., Peat, R., Gevers, E., Muntoni, F.*, et al.* (2016). Mutation in human selenocysteine transfer RNA selectively disrupts selenoprotein synthesis. The Journal of clinical investigation *126*, 992-996.

Schweizer, U., and Fradejas-Villar, N. (2016). Why 21? The significance of selenoproteins for human health revealed by inborn errors of metabolism. FASEB journal : official publication of the Federation of American Societies for Experimental Biology *30*, 3669-3681.

Scorrano, L. (2013). Keeping mitochondria in shape: a matter of life and death. European journal of clinical investigation *43*, 886-893.

Shi, Y., Dierckx, A., Wanrooij, P.H., Wanrooij, S., Larsson, N.G., Wilhelmsson, L.M., Falkenberg, M., and Gustafsson, C.M. (2012). Mammalian transcription factor A is a core component of the mitochondrial transcription machinery. Proceedings of the National Academy of Sciences of the United States of America *109*, 16510-16515.

Sieber, F., Duchene, A.M., and Marechal-Drouard, L. (2011a). Mitochondrial RNA import: from diversity of natural mechanisms to potential applications. International review of cell and molecular biology *287*, 145-190.

Sieber, F., Placido, A., El Farouk-Ameqrane, S., Duchene, A.M., and Marechal-Drouard, L. (2011b). A protein shuttle system to target RNA into mitochondria. Nucleic Acids Res *39*, e96.

Simpson, L., and Shaw, J. (1989). RNA editing and the mitochondrial cryptogenes of kinetoplastid protozoa. Cell *57*, 355-366.

Sinha, P., Islam, M.N., Bhattacharya, S., and Bhattacharya, J. (2016). Intercellular mitochondrial transfer: bioenergetic crosstalk between cells. Current opinion in genetics & development *38*, 97-101.

Sjostrand, F.S. (1953). Electron microscopy of mitochondria and cytoplasmic double membranes. Nature *171*, 30-32.

Smirnov, A., Comte, C., Mager-Heckel, A.M., Addis, V., Krasheninnikov, I.A., Martin, R.P., Entelis, N., and Tarassov, I. (2010). Mitochondrial enzyme rhodanese is essential for 5 S ribosomal RNA import into human mitochondria. J Biol Chem *285*, 30792-30803.

Smirnov, A., Entelis, N., Martin, R.P., and Tarassov, I. (2011). Biological significance of 5S rRNA import into human mitochondria: role of ribosomal protein MRP-L18. Genes & development *25*, 1289-1305.

Smirnov, A., Tarassov, I., Mager-Heckel, A.M., Letzelter, M., Martin, R.P., Krasheninnikov, I.A., and Entelis, N. (2008). Two distinct structural elements of 5S rRNA are needed for its import into human mitochondria. Rna *14*, 749-759.

Sologub, M., Litonin, D., Anikin, M., Mustaev, A., and Temiakov, D. (2009). TFB2 is a transient component of the catalytic site of the human mitochondrial RNA polymerase. Cell *139*, 934-944.

Sorensen, P.D., and Frederiksen, S. (1991). Characterization of human 5S rRNA genes. Nucleic Acids Res *19*, 4147-4151.

Spinelli, J.B., and Haigis, M.C. (2018). The multifaceted contributions of mitochondria to cellular metabolism. Nature cell biology *20*, 745-754.

Sripada, L., Singh, K., Lipatova, A.V., Singh, A., Prajapati, P., Tomar, D., Bhatelia, K., Roy, M., Singh, R., Godbole, M.M*., et al.* (2017). hsa-miR-4485 regulates mitochondrial functions and inhibits the tumorigenicity of breast cancer cells. Journal of molecular medicine *95*, 641-651.

Sripada, L., Tomar, D., Prajapati, P., Singh, R., Singh, A.K., and Singh, R. (2012). Systematic analysis of small RNAs associated with human mitochondria by deep sequencing: detailed analysis of mitochondrial associated miRNA. PloS one *7*, e44873.

Stein, A.J., Fuchs, G., Fu, C., Wolin, S.L., and Reinisch, K.M. (2005). Structural insights into RNA quality control: the Ro autoantigen binds misfolded RNAs via its central cavity. Cell *121*, 529-539.

Steitz, J.A., Berg, C., Hendrick, J.P., La Branche-Chabot, H., Metspalu, A., Rinke, J., and Yario, T. (1988). A 5S rRNA/L5 complex is a precursor to ribosome assembly in mammalian cells. The Journal of cell biology *106*, 545-556.

Sulkowski, E., and Laskowski, M., Sr. (1962). Mechanism of action of micrococcal nuclease on deoxyribonucleic acid. J Biol Chem *237*, 2620-2625.

Suzuki, T., Nagao, A., and Suzuki, T. (2011). Human mitochondrial tRNAs: biogenesis, function, structural aspects, and diseases. Annual review of genetics *45*, 299-329.

Szymanski, M., Barciszewska, M.Z., Erdmann, V.A., and Barciszewski, J. (2003). 5 S rRNA: structure and interactions. The Biochemical journal *371*, 641-651.

Szymanski, M., and Barciszewski, J. (2007). The genetic code--40 years on. Acta biochimica Polonica *54*, 51-54.

Tadi, S.K., Sebastian, R., Dahal, S., Babu, R.K., Choudhary, B., and Raghavan, S.C. (2016). Microhomology-mediated end joining is the principal mediator of double-strand break repair during mitochondrial DNA lesions. Molecular biology of the cell *27*, 223-235.

Taivassalo, T., and Haller, R.G. (2005). Exercise and training in mitochondrial myopathies. Medicine and science in sports and exercise *37*, 2094-2101.

Tanaka, M., Borgeld, H.J., Zhang, J., Muramatsu, S., Gong, J.S., Yoneda, M., Maruyama, W., Naoi, M., Ibi, T., Sahashi, K.*, et al.* (2002). Gene therapy for mitochondrial disease by delivering restriction endonuclease SmaI into mitochondria. Journal of biomedical science *9*, 534-541.

Tarassov, I., Entelis, N., and Martin, R.P. (1995). An intact protein translocating machinery is required for mitochondrial import of a yeast cytoplasmic tRNA. Journal of molecular biology *245*, 315-323.

Temperley, R., Richter, R., Dennerlein, S., Lightowlers, R.N., and Chrzanowska-Lightowlers, Z.M. (2010a). Hungry codons promote frameshifting in human mitochondrial ribosomes. Science *327*, 301.

Temperley, R.J., Wydro, M., Lightowlers, R.N., and Chrzanowska-Lightowlers, Z.M. (2010b). Human mitochondrial mRNAs--like members of all families, similar but different. Biochimica et biophysica acta *1797*, 1081-1085.

Terzioglu, M., Ruzzenente, B., Harmel, J., Mourier, A., Jemt, E., Lopez, M.D., Kukat, C., Stewart, J.B., Wibom, R., Meharg, C.*, et al.* (2013). MTERF1 binds mtDNA to prevent transcriptional interference at the light-strand promoter but is dispensable for rRNA gene transcription regulation. Cell metabolism *17*, 618-626.

Tilokani, L., Nagashima, S., Paupe, V., and Prudent, J. (2018). Mitochondrial dynamics: overview of molecular mechanisms. Essays in biochemistry *62*, 341-360.

Timmis, J.N., Ayliffe, M.A., Huang, C.Y., and Martin, W. (2004). Endosymbiotic gene transfer: organelle genomes forge eukaryotic chromosomes. Nature reviews Genetics *5*, 123-135.

Tonin, Y., Heckel, A.M., Vysokikh, M., Dovydenko, I., Meschaninova, M., Rotig, A., Munnich, A., Venyaminova, A., Tarassov, I., and Entelis, N. (2014). Modeling of antigenomic therapy of mitochondrial diseases by mitochondrially addressed RNA targeting a pathogenic point mutation in mitochondrial DNA. J Biol Chem *289*, 13323-13334.

Toompuu, M., Tuomela, T., Laine, P., Paulin, L., Dufour, E., and Jacobs, H.T. (2018). Polyadenylation and degradation of structurally abnormal mitochondrial tRNAs in human cells. Nucleic Acids Res *46*, 5209-5226.

Towheed, A., Markantone, D.M., Crain, A.T., Celotto, A.M., and Palladino, M.J. (2014). Small mitochondrial-targeted RNAs modulate endogenous mitochondrial protein expression in vivo. Neurobiology of disease *69*, 15-22.

Ule, J., Jensen, K.B., Ruggiu, M., Mele, A., Ule, A., and Darnell, R.B. (2003). CLIP identifies Nova-regulated RNA networks in the brain. Science *302*, 1212-1215.

Urbanek, M.O., Nawrocka, A.U., and Krzyzosiak, W.J. (2015). Small RNA Detection by in Situ Hybridization Methods. International journal of molecular sciences *16*, 13259-13286.

van der Laan, M., Meinecke, M., Dudek, J., Hutu, D.P., Lind, M., Perschil, I., Guiard, B., Wagner, R., Pfanner, N., and Rehling, P. (2007). Motor-free mitochondrial presequence translocase drives membrane integration of preproteins. Nature cell biology *9*, 1152-1159.

Vedrenne, V., Gowher, A., De Lonlay, P., Nitschke, P., Serre, V., Boddaert, N., Altuzarra, C., Mager-Heckel, A.M., Chretien, F., Entelis, N.*, et al.* (2012). Mutation in PNPT1, which encodes a polyribonucleotide nucleotidyltransferase, impairs RNA import into mitochondria and causes respiratory-chain deficiency. American journal of human genetics *91*, 912-918.

Vendramin, R., Verheyden, Y., Ishikawa, H., Goedert, L., Nicolas, E., Saraf, K., Armaos, A., Delli Ponti, R., Izumikawa, K., Mestdagh, P.*, et al.* (2018). SAMMSON fosters cancer cell fitness by concertedly enhancing mitochondrial and cytosolic translation. Nature structural & molecular biology *25*, 1035-1046.

Verechshagina, N., Nikitchina, N., Yamada, Y., Harashima, H., Tanaka, M., Orishchenko, K., and Mazunin, I. (2018). Future of human mitochondrial DNA editing technologies. Mitochondrial DNA Part A, 1-8.

Villegas, J., Burzio, V., Villota, C., Landerer, E., Martinez, R., Santander, M., Martinez, R., Pinto, R., Vera, M.I., Boccardo, E.*, et al.* (2007). Expression of a novel non-coding mitochondrial RNA in human proliferating cells. Nucleic Acids Res *35*, 7336-7347.

Vogtle, F.N., Wortelkamp, S., Zahedi, R.P., Becker, D., Leidhold, C., Gevaert, K., Kellermann, J., Voos, W., Sickmann, A., Pfanner, N.*, et al.* (2009). Global analysis of the mitochondrial N-proteome identifies a processing peptidase critical for protein stability. Cell *139*, 428-439.

von Ameln, S., Wang, G., Boulouiz, R., Rutherford, M.A., Smith, G.M., Li, Y., Pogoda, H.M., Nurnberg, G., Stiller, B., Volk, A.E.*, et al.* (2012). A mutation in PNPT1, encoding mitochondrial-RNA-import protein PNPase, causes hereditary hearing loss. American journal of human genetics *91*, 919-927.

Walker, M.A., Volpi, S., Sims, K.B., Walter, J.E., and Traggiai, E. (2014). Powering the immune system: mitochondria in immune function and deficiency. Journal of immunology research *2014*, 164309.

Walter, P., and Blobel, G. (1982). Signal recognition particle contains a 7S RNA essential for protein translocation across the endoplasmic reticulum. Nature *299*, 691-698.

Wang, D.D., Guo, X.E., Modrek, A.S., Chen, C.F., Chen, P.L., and Lee, W.H. (2014). Helicase SUV3, polynucleotide phosphorylase, and mitochondrial polyadenylation polymerase form a transient complex to modulate mitochondrial mRNA polyadenylated tail lengths in response to energetic changes. J Biol Chem *289*, 16727-16735.

Wang, G., Chen, H.W., Oktay, Y., Zhang, J., Allen, E.L., Smith, G.M., Fan, K.C., Hong, J.S., French, S.W., McCaffery, J.M.*, et al.* (2010). PNPASE regulates RNA import into mitochondria. Cell *142*, 456-467.

Wang, G., Shimada, E., Nili, M., Koehler, C.M., and Teitell, M.A. (2015). Mitochondria-targeted RNA import. Methods Mol Biol *1264*, 107-116.

Wanrooij, P.H., Uhler, J.P., Simonsson, T., Falkenberg, M., and Gustafsson, C.M. (2010). G-quadruplex structures in RNA stimulate mitochondrial transcription termination and primer formation. Proceedings of the National Academy of Sciences of the United States of America *107*, 16072-16077.

Weis, B.L., Schleiff, E., and Zerges, W. (2013). Protein targeting to subcellular organelles via MRNA localization. Biochimica et biophysica acta *1833*, 260-273.

Westermann, B. (2010). Mitochondrial fusion and fission in cell life and death. Nature reviews Molecular cell biology *11*, 872-884.

Wiedemann, N., and Pfanner, N. (2017). Mitochondrial Machineries for Protein Import and Assembly. Annual review of biochemistry *86*, 685-714.

Williams, C.C., Jan, C.H., and Weissman, J.S. (2014). Targeting and plasticity of mitochondrial proteins revealed by proximity-specific ribosome profiling. Science *346*, 748-751.

Wrobel, L., Trojanowska, A., Sztolsztener, M.E., and Chacinska, A. (2013). Mitochondrial protein import: Mia40 facilitates Tim22 translocation into the inner membrane of mitochondria. Molecular biology of the cell *24*, 543-554.

Xu, F., Ackerley, C., Maj, M.C., Addis, J.B., Levandovskiy, V., Lee, J., Mackay, N., Cameron, J.M., and Robinson, B.H. (2008). Disruption of a mitochondrial RNA-binding protein gene results in decreased cytochrome b expression and a marked reduction in ubiquinol-cytochrome c reductase activity in mouse heart mitochondria. The Biochemical journal *416*, 15-26.

Yakubovskaya, E., Chen, Z., Carrodeguas, J.A., Kisker, C., and Bogenhagen, D.F. (2006). Functional human mitochondrial DNA polymerase gamma forms a heterotrimer. J Biol Chem *281*, 374-382.

Yang, D., Oyaizu, Y., Oyaizu, H., Olsen, G.J., and Woese, C.R. (1985). Mitochondrial origins. Proceedings of the National Academy of Sciences of the United States of America *82*, 4443-4447.

Yang, W. (2011). Nucleases: diversity of structure, function and mechanism. Quarterly reviews of biophysics *44*, 1-93.

Yang, W., Wu, J.M., Bi, A.D., Ou-Yang, Y.C., Shen, H.H., Chirn, G.W., Zhou, J.H., Weiss, E., Holman, E.P., and Liao, D.J. (2013). Possible formation of mitochondrial-RNA containing chimeric or trimeric RNA implies a post-transcriptional and post-splicing mechanism for RNA fusion. PloS one *8*, e77016.

Yarham, J.W., Lamichhane, T.N., Pyle, A., Mattijssen, S., Baruffini, E., Bruni, F., Donnini, C., Vassilev, A., He, L., Blakely, E.L.*, et al.* (2014). Defective i6A37 modification of mitochondrial and cytosolic tRNAs results from pathogenic mutations in TRIT1 and its substrate tRNA. PLoS Genet *10*, e1004424.

Yasukawa, T., Reyes, A., Cluett, T.J., Yang, M.Y., Bowmaker, M., Jacobs, H.T., and Holt, I.J. (2006). Replication of vertebrate mitochondrial DNA entails transient ribonucleotide incorporation throughout the lagging strand. The EMBO journal *25*, 5358-5371.

Yoshionari, S., Koike, T., Yokogawa, T., Nishikawa, K., Ueda, T., Miura, K., and Watanabe, K. (1994). Existence of nuclear-encoded 5S-rRNA in bovine mitochondria. FEBS letters *338*, 137-142.

Zelenka, J., Alan, L., Jaburek, M., and Jezek, P. (2014). Import of desired nucleic acid sequences using addressing motif of mitochondrial ribosomal 5S-rRNA for fluorescent in vivo hybridization of mitochondrial DNA and RNA. Journal of bioenergetics and biomembranes *46*, 147-156.

Zeviani, M., and Di Donato, S. (2004). Mitochondrial disorders. Brain : a journal of neurology *127*, 2153-2172.

Zhang, X., Zuo, X., Yang, B., Li, Z., Xue, Y., Zhou, Y., Huang, J., Zhao, X., Zhou, J., Yan, Y.*, et al.* (2014). MicroRNA directly enhances mitochondrial translation during muscle differentiation. Cell *158*, 607-619.

Zheng, D., Li, C., Wang, S., Cang, Y., Song, Y., Liu, X., Li, X., Mohan, C., Wu, T., Hu, D.*, et al.* (2015). PSTK is a novel gene associated with early lung injury in Paraquat Poisoning. Life sciences *123*, 9-17.

Zhou, Q., Li, H., Li, H., Nakagawa, A., Lin, J.L., Lee, E.S., Harry, B.L., Skeen-Gaar, R.R., Suehiro, Y., William, D.*, et al.* (2016). Mitochondrial endonuclease G mediates breakdown of paternal mitochondria upon fertilization. Science *353*, 394-399.

Zimorski, V., Ku, C., Martin, W.F., and Gould, S.B. (2014). Endosymbiotic theory for organelle origins. Current opinion in microbiology *22*, 38-48.

Zischka, H., Larochette, N., Hoffmann, F., Hamoller, D., Jagemann, N., Lichtmannegger, J., Jennen, L., Muller-Hocker, J., Roggel, F., Gottlicher, M.*, et al.* (2008). Electrophoretic analysis of the mitochondrial outer membrane rupture induced by permeability transition. Analytical chemistry *80*, 5051-5058.

Zollo, O., and Sondheimer, N. (2017). Topological requirements of the mitochondrial heavy-strand promoters. Transcription *8*, 307-312.

Zollo, O., Tiranti, V., and Sondheimer, N. (2012). Transcriptional requirements of the distal heavy-strand promoter of mtDNA. Proceedings of the National Academy of Sciences of the United States of America *109*, 6508-6512.

Zong, W.X., Rabinowitz, J.D., and White, E. (2016). Mitochondria and Cancer. Molecular cell *61*, 667-676.

Résumé de Thèse

Introduction :

Les mitochondries sont des organites essentiels impliquées dans de nombreuses fonctions des cellules eucaryotes telles que la formation des centres fer-soufre, la β-oxidation des acides gras ou l'apoptose. Ces organites possèdent deux membranes les délimitant du reste du cytoplasme et abritant la chaîne respiratoire, qui permet la production de l'énergie nécessaire aux cellules grâce à la phosphorylation oxidative. Les mitochondries ont aussi la particularité de posséder leur propre génome qui, chez l'homme, est double brin, circulaire et présent en plusieurs copies au sein d'une même cellule. La répartition des gènes entre les deux brins est inégale. Le brin lourd (brin H) contient la plupart des gènes codant pour des protéines, 14 ARNt ainsi que les deux gènes codant pour des ARN ribosomiques. Le brin de léger (brin L) ne contient qu'un seul gène codant pour une protéine et quelques gènes d'ARNt. Ce génome rudimentaire ne contient donc que des gènes nécessaires à la synthèse de 13 protéines de la chaine respiratoire et est donc largement insuffisant pour permettre aux mitochondries de réaliser toutes leurs fonctions. Ainsi, la majorité des protéines et certains ARN sont encodés par le génome nucléaire puis importés dans les mitochondries.

De manière générale, l'import mitochondrial d'ARN répond à trois critères: 1) la présence de signaux sélectifs, ou déterminants d'import, au sein de l'ARN, 2) l'existence d'un mécanisme permettant de détourner l'ARN de sa fonction cytosolique et de le rediriger vers la surface mitochondriale, et 3) l'utilisation d'une voie permettant de transférer l'ARN à travers les membranes mitochondriales. Cependant, les mécanismes moléculaire d'import, ainsi que la diversité des ARN importés dans les mitochondries des cellules humaines, sont encore peu connus et jusqu'à présent, seul l'import mitochondrial de deux ARN, l'ARNr 5S et l'ARNt^{Lys} de levure (tRK1), a été étudiée en détail pour les cellules humaines. Cela est principalement dû aux limitations méthodologiques qui ne permettent pas de distinguer sans ambiguïté un ARN partiellement importés dans les mitochondries d'un ARN cytosolique simplement associés aux membranes mitochondriales. En effet, les mitochondries sont fortement associées à d'autres composants cellulaires tels que le réticulum endoplasmique, l'appareil de Golgi, les endosomes, ou les ribosomes cytosoliques engagés dans la traduction à la surface des mitochondries.

Le développement de techniques expérimentales adéquates pour détecter et confirmer l'import d'ARN dans les mitochondries est donc essentiel.

Les mutations du génome mitochondrial peuvent affecter le bon fonctionnement de la chaine respiratoire et la production d'énergie. Ces dysfonctionnements sont à l'origine de pathologies mitochondriales variées, souvent neuromusculaires car elles concernent principalement les organes les plus demandeurs en énergie tel que les muscles, le cœur et le cerveau. Les symptômes apparaissent généralement tôt dans la vie, avec une aggravation progressive conduisant souvent à la mort.

Les molécules d'ADN mitochondrial sauvages et mutés peuvent coexister au sein d'une même cellule, ce que l'on appelle hétéroplasmie. Les symptômes dus aux mutations de l'ADN mitochondrial n'apparaissent souvent que lorsque le ratio d'ADN muté par rapport au sauvage (niveau d'hétéroplasmie) excède un certain seuil dit pathogénique, généralement 60 à 90% de l'ADNmt muté, en fonction de la mutation, du tissu et de l'âge du patient. Des taux de mutation de l'ADN mitochondrial plus élevés sont souvent associés à des symptômes plus graves.

Jusqu'à présent, il n'existe aucun traitement efficace pour guérir les maladies mitochondriales et, dans la majorité des cas, les traitements sont uniquement palliatifs. Cependant, de nombreuses approches de thérapie géniques sont en cours de développement. La plupart des stratégies envisagées se basent alors sur l'import de protéines et d'ARN afin de compenser la perte d'une fonction (stratégie allotopique) ou de réduire le niveau d'hétéroplasmie sous le seuil pathogénique en agissant sur l'intégrité (stratégie anti-génomique) ou la réplication (stratégie anti-réplicative) du génome mitochondrial muté.

Objectifs de thèse :

I. Le laboratoire « Trafic intracellulaire et pathologies mitochondriales » où j'ai réalisé ma thèse utilise les voies d'import d'ARN afin de développer des stratégies thérapeutiques. La première partie de ma thèse consistait à poursuivre le projet d'utilisation de l'import de l'ARNr 5S afin d'adresser des séquences anti-réplicatives dans les mitochondries. Mes objectifs étaient de :

1) Générer des lignées cellulaires hétéroplasmiques pour deux types de mutations du génome mitochondrial exprimant de manière stable des ARNr 5S recombinants anti-réplicatifs ;

2) Vérifier l'expression et l'import de ces ARN *in vivo* ;

3) Mesurer leur effet sur l'hétéroplasmie dans différentes conditions de croissance des cellules.

II.

La seconde partie de ma thèse a été de développer une nouvelle méthode d'identification des ARN importés dans les mitochondries permettant de différencier sans équivoque un ARN réellement importé d'un simple contaminant persistant après purification des organites. Dans cet optique, mes objectifs étaient de :

1) Développer une approche robuste pour identifier les ARN résidant dans les mitochondries des cellules humaines ;

2) Valider l'approche sur la possibilité de différentier les 3 groupes de transcrits : les transcrits encodés par le génome mitochondrial, les transcrits contaminants encodés par le génome nucléaire et les transcrits partiellement importés ;

3) Utiliser l'approche pour identifier de nouveaux ARN importés dans les mitochondries et valider leur import par d'autres techniques.

Résultats :

I. Mon laboratoire d'accueil a précédemment identifié les déterminants d'import de l'ARNr 5S dans les mitochondries de cellules humaines. Ces recherches ont montré qu'une partie de cet ARN, le domaine β, pouvait être remplacé par une séquence complémentaire de l'ADN mitochondrial muté sans affecter l'import de l'ARN. Mon laboratoire d'accueil a aussi montré que ces ARNr 5S recombinants exprimés de façon stable dans des cellules humaines pouvaient s'hybrider à l'ADN mitochondrial et conduire à une baisse du niveau d'hétéroplasmie en gênant spécifiquement la réplication du génome muté. Lors de la première partie de mon projet de thèse j'ai poursuivi les travaux de l'équipe sur l'adressage de ces ARN anti-réplicatifs dans les mitochondries. Deux mutations ont été utilisées comme modèles,

une large délétion de 7075 pb (nucleotides 8363 à 15438) du génome mitochondrial associé au syndrome de Kearn-Sayre (KSS) qui entraîne la disparition de 9 gènes codant pour des protéines et de 6 gènes d'ARNt ainsi que une mutation ponctuelle dans le gène *MT-ND5* (13514 A>G) associée au syndrome MELAS (mitochondrial encephalopathy, lactic acidosis and stroke-like episodes).

En premier lieux j'ai conçu de nouvelles versions d'ARNr 5S recombinants contenant différentes séquences anti-réplicatives remplaçant la partie distale du domaine β et ciblant soit la délétion KSS, soit la mutation ponctuelle du gène *MT-ND5*. Les séquences anti-réplicatives variaient en longueur (entre 13 et 17 nucléotides) et en séquence en fonction du brin de l'ADN mitochondrial ciblé (brin L ou brin H). La structure secondaire des ARNr 5S recombinants a été prédite *in silico* afin de s'assurer que les séquences insérées ne modifiaient pas les éléments structurels de l'ARNr 5S nécessaires à l'expression et à l'adressage mitochondrial des ARN.

Pour ralentir la réplication de l'ADN mitochondrial muté, les séquences insérées doivent s'hybrider uniquement aux molécules d'ADN mitochondrial contenant la mutation. Les molécules capables de s'hybrider spécifiquement aux génomes mutés et non aux génomes normaux ont été sélectionnées sur les prédictions de températures de fusion des duplex ARN/ADN muté et ARN/ADN sauvage *in silico et* par des tests d'hybridation *in vitro.*

La deuxième étape a consisté à générer, à la base de cellules *trans*mitochondriales cybrides humaines portant les mutations d'ADN mitochondrial, des lignées stables exprimant fortement les ARNr 5S recombinants dans le but d'accroitre l'effet sur l'hétéroplasmie. Les cellules cybrides ont été précédemment créées par la fusion de cellules de patients énucléés portant une mutation dans l'ADN mitochondrial avec des cellules immortalisées dépourvues d'ADN mitochondrial afin de pouvoir les cultivées presque indéfiniment. Afin d'exprimer fortement et de manière stable les ARNr 5S recombinants dans ces cellules, j'ai utilisé le système Flp-In™ T-rex™ qui permet l'intégration d'un site de recombinaison au sein du génome nucléaire de ces cellules. Parmi les différents clones obtenus, j'ai sélectionné ceux pour lesquels le site de recombinaison FRT se trouve dans une région transcriptionellement active du génome et n'impacte pas la croissance cellulaire. En intégrant les différents plasmides contenant les gènes des

ARN anti-réplicatifs au niveau du site FRT, j'ai pu obtenir différentes lignées cellulaires exprimant stablement les versions d'ARNr 5S recombinants.

Les cellules ont ensuite été cultivées dans différents milieux et l'expression, l'import et l'effet sur l'hétéroplasmie des ARNr 5S recombinants ont été mesuré pour chaque condition de culture. Des baisses significatives du niveau d'hétéroplasmie, liées à l'expression des ARN recombinants anti-réplicatifs, ont été obtenues lorsque les cellules étaient cultivées en absence de glucose. Cette diminution était plus importante pour les cellules avec le plus fort taux d'expression des ARN anti-réplicatifs. Ainsi les résultats obtenus durant ma thèse ont permis de confirmer l'effet anti-réplicatifs des ARNr 5S recombinants et d'identifier des conditions pouvant améliorer leur effet thérapeutique. Ces résultats ont donnés lieux à une publication.

II. Les méthodes employées jusqu'à présent pour identifier les ARN mitochondriaux à l'échelle globale se basent sur le séquençage des ARN (RNA-seq) extraits de mitochondries isolées. Les résultats des séquençages ont révélé une importante proportion d'ARN cytosoliques associés aux mitochondries. Cependant, d'après des études sur plusieurs modèles, l'import mitochondrial d'ARN est un phénomène hautement sélectif et la grande variabilité des données obtenues entre les expériences réalisées par différents laboratoires suggère que la majorité des ARN retrouvés ne sont pas importés dans les mitochondries. En effet, il semble pratiquement impossible d'obtenir des mitochondries complètement pures par les méthodes d'isolation conventionnelles et il est difficile de déterminer dans quelle proportion les ARN cystosoliques sont présent dans les échantillons mitochondriaux. De plus, les techniques de RNA-seq sont particulièrement sensible et permette de détecter les plus petites quantités d'ARN contaminant. La présence de ces ARN contaminants complique l'identification des ARN réellement importés dans les mitochondries et, dans l'ensemble, les études d'ARN-seq sur le RNome mitochondrial n'ont pas permis de mieux comprendre l'import mitochondrial des ARN. Cependant, à ce jour, la méthode de RNA-seq reste la seule stratégie permettant l'identification à grande échelle des ARN. La méthodologie doit donc être adaptée afin d'établir une liste précise des ARN importés dans les mitochondries.

La seconde partie des travaux que j'ai réalisés durant ma thèse a donc consistée au développement d'une nouvelle stratégie, nommée « Controlled Level of Contamination coupled with deep sequencing » (CoLoC-seq), permettant

l'identification à grande échelle des ARN importés dans les mitochondries des cellules humaines. Lors du processus de purification des mitochondries, celles-ci sont généralement traitées avec une ribonucléase (RNase), incapable de traverser les membranes mitochondriales, afin de dégrader les ARN contaminants. Néanmoins, ce traitement ne suffit pas à éliminer de manière sûre la totalité des ARN présent à l'extérieur des mitochondries. Afin de pouvoir différencier les ARN contaminants des ARN partiellement importés, CoLoC-seq se base non pas sur des échantillons « statiques », traité avec une concentration unique de RNase, mais sur la dynamique de déplétion des ARN en présence de concentrations croissantes de RNase. Les ARN importés auront une dynamique de déplétion différente de celle des ARN contaminant grâce à la présence d'une population des molécules protégées de la dégradation par les membranes mitochondriales, ce qui peut être établie par des analyses cinétiques quantitatives.

J'ai réalisé différentes variantes du protocole d'isolement et de traitement des mitochondries de cellules humaines et testé différentes RNases, ce qui m'a permis de déterminer les conditions optimales pour différencier un ARN contaminant d'un ARN importé dans les mitochondries. La dynamique de déplétion d'un ARN par une ribonucléase est une décroissance exponentielle qui peut être facilement modélisée. Afin de vérifier si le modèle élaboré était cohérent avec les données obtenues, et ainsi valider la méthode, les ARN extraits à l'issue de mes expériences ont d'abord été analysés par hybridation sur membrane pour observer la dynamique de déplétion d'ARN de localisation connue (cytosolique, mitochondrial ou partiellement importé). Les données que j'ai obtenues ont montré une nette corrélation entre les 3 différentes localisations des ARN et leur dynamique de déplétion.

Dans les expériences CoLoC, la protection des ARN contre le traitement à la RNase devrait être assurée par l'intégrité des membranes mitochondriales. Cependant, il faut tenir compte, du fait que de nombreux facteurs peuvent influer sur le clivage de l'ARN par les nucléases, les plus importants étant la structure tridimensionnelle des ARN et les interactions avec les protéines pouvant protéger l'ARN de la dégradation. Pour répondre à cette question, j'ai mis en place une expérience de contrôle, Mock-CoLoC, qui consiste à lyser les mitochondries avant la digestion des ARN par la RNase. L'efficacité de la lyse a été démontrée par la dégradation complète des ARN codés par le génome mitochondrial. Mes résultats

préliminaires semblent confirmer que la majorité des ARN sont complètement digérés par la RNase en absence de membranes mitochondriales.

Les ARN obtenus après la réalisation de la méthode CoLoC ont ensuite été séquencés à haut débit. L'analyse des résultats de deux expériences indépendantes de CoLoC-seq a permis de retrouver la totalité des ARN mitochondriaux ainsi que différents ARN encodés par le génome nucléaire fortement associés aux mitochondries. En appliquant notre modèle cinétique sur le profil de déplétion de ses ARN, j'ai pu déterminer que seulement un petit nombre d'ARN non-codant étaient potentiellement importés dans les mitochondries, dont deux, l'ARNr 5S et l'ARN de la RNase MRP, déjà identifiés auparavant. Mes résultats ont ainsi corroboré les données publiées précédemment sur l'import mitochondrial des ARN dans les cellules humaines et il a été possible d'établir pour la première fois une liste des ARN candidats pour l'import mitochondrial. L'import de certains ARN candidats a ensuite été vérifié par microscopie à fluorescence (hybridation *in situ*) ce qui m'a permis de constater leur co-localisation avec les mitochondries, validant ainsi les résultats obtenus avec la méthode CoLoC.

Discussion et perspectives :

Lors de ma thèse j'ai poursuivi le projet de mon équipe sur le développement d'ARN adressés aux mitochondries à visés thérapeutiques et j'ai pu confirmer que des ARN anti-réplicatifs basés sur l'ARNr 5S pouvaient diminuer le niveau d'hétéroplasmie de deux mutations pathogéniques différentes.

Mes résultats ont aussi montré que leur effet est augmenté lorsque les cellules sont cultivées en absence de glucose. Dans ces conditions la production d'énergie par la phosphorylation oxidative mitochondriale devient essentielle pour la croissance des cellules, ce qui permet de donner un avantage sélectifs aux cellules présentant une amélioration des fonctions mitochondriales due à une baisse du niveau d'hétéroplasmie. De plus, le taux d'hétéroplasmie des cellules cultivées dans un milieu sans glucose mais n'exprimant pas les ARN anti-réplicatifs reste inchangé. Ceci démontre que la pression de sélection seule n'est pas responsable de la diminution du niveau d'hétéroplasmie.

L'utilisation du système Flp-In^{TM} T-rex^{TM} pour produire les lignées cellulaires cybrides exprimant les molécules d'ARNr 5S anti-réplicatives a permis une amélioration de l'expression des ARN anti-réplicatives de 10 à 100 fois par rapport à

l'insertion aléatoire des plasmides portant les gènes d'ARNr 5S recombinants réalisé précédemment par notre équipe.

J'ai aussi pu mettre en avant un effet de seuil d'expression des ARN anti-réplicatif puisque les diminutions d'hétéroplasmie les plus importantes ont été obtenues pour les ARNr 5S recombinants fortement exprimés tandis qu'une expression plus faible des mêmes molécules n'affectait pas le niveau d'hétéroplasmie. Les ARN recombinants sont exprimés à partir d'un seul gène et leur import mitochondrial doit se faire en compétition avec les molécules d'ARNr 5S endogène, exprimées à partir de plus d'une centaine de gènes. Une expression forte des gènes peut alors favoriser l'import des ARN anti-réplicatifs et permette d'obtenir une diminution d'hétéroplasmie plus importante. Intégrer plus de gènes d'ARN recombinants ou surexprimer les facteurs protéiques d'import mitochondrial pourrait améliorer l'effet anti-réplicatif. D'autre part, les ARNr 5S recombinants peuvent interagir avec différents facteurs protéiques présent dans la matrice mitochondrial ce qui peut empêcher ou réduire leur efficacité anti-réplicative. Des études plus approfondie de la fonction de l'ARNr 5S endogène dans les mitochondries pourront être réalisées afin de faciliter la conception d'ARN anti-réplicatif échappant à ses interactions. Les conditions de croissance sélective en l'absence de glucose, qui améliorent considérablement l'effet des molécules d'ARN anti-réplicatives, devraient aussi être considérées pour l'application future de stratégies thérapeutiques.

À ce jour, on en sait peu sur la diversité des ARN importés dans les mitochondries des cellules humaines et l'import de certains ARN reste souvent controversé. La découverte de nouveaux ARN adressés dans les mitochondries de cellules humaines pourrait fournir de nouveaux vecteurs pour la stratégie anti-réplicative et éclairer les mécanismes régissant leur import.

Au cours de ma thèse j'ai aussi pu développer une nouvelle méthode, nommée CoLoC-seq, permettant de déterminer les ARN importés dans les mitochondries. Mes résultats issus de deux expériences indépendantes m'ont permis d'identifier de nouveaux ARN potentiellement importés dans les mitochondries des cellules humaines et de confirmer l'import de deux ARN déjà connus, l'ARNr 5S et l'ARN de la RNase MRP. L'ARN de la RNase P, dont l'import a aussi été suggéré par différentes études, n'a cependant put être validée que par une seule des deux expériences réalisées. Les variations entre les données des deux expériences

CoLoC peuvent être expliquées par les différences des conditions expérimentales et de la méthodologie de séquençage. De manière générale, les deux expériences ont révélé que seulement un petit nombre d'ARN non-codant était importés dans les mitochondries de cellules humaines suggérant que, chez l'homme, ce processus est hautement sélectif. Le séquençage des échantillons obtenus avec l'expérience contrôle,Mock-CoLoC, devra bien entendu être réalisé pour s'assurer de la validité des résultats obtenus.

Des protocoles adaptés pour le séquençage de certains types d'ARN pourront aussi être réalisés afin d'élargir la liste des ARN criblés. Les ARNt notamment sont très structurés, présentent de nombreuses modifications de nucléotides et sont amino-acylés, ce qui rend difficile leur séquençage. Mes résultats suggèrent en effet que certains ARNt pourraient être importés dans les mitochondries de cellules humaines. Même si, chez l'homme, l'import d'ARNt cytosoliques n'a pas été clairement démontré, il est possible que cette voie puisse être nécessaire dans certains types de cellules et/ou dans des conditions particulière de stress. Cela pourra être étudié en appliquant l'approche CoLoC-seq à différents types de cellules et dans diverses conditions de culture.

Les ARN identifiés par la méthode CoLoC-seq devront être validés par d'autres méthodes. L'ARNt sélénocystéine par exemple, l'un des candidats à l'import révélé au cours de mes expériences, a pu être détecté par microscopie confocale associé aux mitochondries bien que sa fonction mitochondriale reste pour le moment inconnue. La présence de ses candidats au sein de la matrice mitochondriale pourrait être confirmée par l'utilisation de techniques de microscopie à super-résolution.

Afin de corroborer les résultats obtenus avec la méthode CoLoC-seq, une autre approche à grande échelle pourra être mise en œuvre. Lors de ma thèse, j'ai donc commencé à optimiser une méthode initialement utilisée pour l'identification de la localisation subcellulaire des protéines et qui a récemment été adaptée pour les transcrits mitochondriaux. Cette méthode permet la biotinylation localisée des protéines mitochondriales au moyen d'une peroxidase (Apex2) adressée dans l'organite et la co-purification des ARN cross-linkés à ces protéines *in vivo*.

Les résultats obtenus au moyen de ces deux méthodes permettront d'une part de compléter la liste des ARN importés connus mais aussi de mieux comprendre leurs mécanismes d'import. L'application de ces méthodes sur différents modèles

cellulaires permettra de mieux comprendre le rôle de l'import d'ARN au sein des mitochondries et d'identifier les mécanismes moléculaires des pathologies associées aux défauts de cette voie. Ces connaissances seront mises à profit lors du développement de nouvelles stratégies thérapeutiques pour soigner les maladies mitochondriales pour lesquelles aucun traitement n'existe actuellement.

Communications :

Publication scientifique :

- R. Loutre*, AM. Heckel*, D. Jeandard*, I. Tarassov and N. Entelis (2018). Anti-replicative recombinant 5S rRNA molecules can modulate the mtDNA heteroplasmy in a glucose-dependent manner. PLoS ONE , 13(6) : e0199258
*co-premier auteurs

Communication orale :

-Landscaping of the human mitochondrial RNome by CoLoC-Seq. Damien JEANDARD, Ivan TARASSOV, Nina ENTELIS et Alexandre SMIRNOV. 7th World Congress on Targeting Mitochondria (Berlin, Allemagne). Octobre 2016

Communications par affiche :

- Exploitation of the natural mitochondrial import pathways to modulate the heteroplasmy level of pathogenic mutations in the mtDNA. Anne-Marie Heckel, Romuald Loutre, Damien Jeandard, Nina Entelis et Ivan Tarassov. Targeting Mitochondria (Berlin, Allemagne). Octobre 2015.

- CoLoC-seq, a new genome-wide approach to profile organellar RNA importome. Damien JEANDARD, Ivan TARASSOV, Nina ENTELIS et Alexandre SMIRNOV. 22nd annual meeting of the RNA society (Prague, République Tchèque). Mai-juin 2017

- CoLoC-seq, a new genome-wide approach to profile organellar RNA importome. Damien JEANDARD, Ivan TARASSOV, Nina ENTELIS et Alexandre SMIRNOV. 8th World Congress on Targeting Mitochondria (Berlin, Allemagne). Octobre 2017

- Anti-replicative recombinant 5S rRNA molecules can modulate the mtDNA heteroplasmy in a glucose-dependent manner. Anne-Marie HECKEL, Romuald LOUTRE, Damien JEANDARD, Ivan TARASSOV et Nina ENTELIS. 7th World Congress on Targeting Mitochondria (Berlin, Allemagne). Octobre 2017

- Application of anti-replicative RNA strategy to mouse models containing different mtDNA haplotypes. Anne-Marie HECKEL, Anna SMIRNOVA, Damien JEANDARD, Lars ZIMMERMANN, Thomas KOLBE, Joerg BURGSTALLER, Ivan TARASSOV et Nina ENTELIS. 10e Colloque Meeto*O*chondrie (Pornichet, France). Mai 2018

- Profiling organellar RNA importomes by CoLoC-seq. Damien JEANDARD, Ivan TARASSOV, Nina ENTELIS et Alexandre SMIRNOV. 27th tRNA Conference : tRNA at the crossroad (Strasbourg, France). Septembre 2018

Université de Strasbourg

École Doctorale des Sciences de la Vie et de la Santé STRASBOURG

Damien JEANDARD

Import d'ARN dans les mitochondries de cellules humaines : identification à grande échelle et applications thérapeutiques

Résumé

Les mutations dans le génome mitochondrial humain sont souvent associées à de graves maladies neuromusculaires. Mon projet de thèse a consisté tout d'abord au développement d'une stratégie thérapeutique basée sur l'import mitochondrial de molécules d'ARN. J'ai pu démontrer que l'expression stable de molécules d'ARN recombinantes dans les cellules humaines permet de diminuer le taux de mutations pathogéniques de l'ADN mitochondrial.

Dans une seconde partie, j'ai élaboré une nouvelle méthode, CoLoC-seq, permettant l'identification à grande échelle des ARN localisés dans les mitochondries. En appliquant cette méthode sur des cellules humaines, j'ai pu confirmer l'adressage mitochondrial de certains ARN cytosoliques non-codant et identifier de nouveaux ARN potentiellement importés. Ces données permettront d'élargir les connaissances sur les voies d'adressage mitochondrial des ARN, leurs mécanismes et leur régulation, et d'optimiser les stratégies thérapeutiques basées sur l'import d'ARN.

Mitochondrie, RNome mitochondrial, Import d'ARN, Stratégie thérapeutique, Séquençage d'ARN.

Résumé en anglais

Mutations in the human mitochondrial genome are often associated with severe neuromuscular disorders. The first part of my thesis project consisted in the development of a therapeutic strategy based on the mitochondrial import of RNA molecules. I demonstrated that the stable expression of recombinant RNA molecules in human cells induced the decrease of the pathogenic mutation load in mitochondrial DNA.

In the second part, I developed a new method, CoLoC-seq, for the large-scale identification of RNA species localized in the mitochondria. By applying this method to human cells, I confirmed the mitochondrial targeting of some non-coding cytosolic RNAs and identified new potentially imported RNAs. These data will broaden the knowledge on the pathway of RNA targeting into the mitochondria, its mechanisms and regulation, and will allow optimization of the therapeutic strategies based on RNA import.

Mitochondria, Mitochondrial RNome, RNA import, Therapeutic strategy, RNA sequencing.